COALESCENCE MECHANISMS OF DISPERSIONS IN GLASS FIBRE BEDS

by

GHOLAM REZA ATTARZADEH

A thesis submitted to the University of Aston in Birmingham for the degree of Doctor of Philosophy

DEPARTMENT OF CHEMICAL ENGINEERING,
THE UNIVERSITY OF ASTON IN BIRMINGHAM.

February 1979.

TO MY MOTHER AND FATHER

SUMMARY

COALESCENCE MECHANISMS OF DISPERSIONS IN GLASS FIBRE BEDS

GHOLAM REZA ATTARZADEH Ph.D. 1979

The separation of secondary liquid-liquid dispersions in fibrous glass packing has been investigated.

A novel technique was developed to study drops within the packing by matching the refractive indices of the packing, its holder and the continuous and dispersed phases. This rendered the packing transparent and a soluble phototropic dye was used to colour the drops by illumination with ultraviolet light. A second technique developed was the use of ultrasonic probes, to detect drop collection and coalescence within the packing.

Observation of droplet collection, coalescence and travel within the packing indicated that captured drops moved along the fibres and coalesced at intersections. Droplets exceeding the equilibrium size moved in a tortuous path with velocities far greater than the continuous phase superficial velocity.

A novel knit-fibre glass packing was subsequently selected and utilized to collect and coalesce droplets in the range of 1-100 μm with both oil/water and water/oil dispersions. This packing proved to be 100% efficient for superficial velocities substantially higher than critical velocities for other packings. Four different oil/water and water/oil dispersion systems were studied giving an interfacial tension range of $8.6 \times 10^{-3} Nm^{-1}$ to $29.2 \times 10^{-3} Nm^{-1}$. Reproducible results were obtained from coalescers made-up from different numbers of layers. Single and two phase flow pressure drops across the packing were correlated by modified Blake-Kozeny type equations.

Six different mechanisms of droplet release were identified viz drip-point, jetting, pointing, graping, foaming and chaining.

KEY WORDS

Dispersions
Coalescence
Glass fibrous packings

ACKNOWLEDGEMENTS

The author wishes to thank the following:

Professor G.V. Jeffreys,

for his encouragement and supervision.

Dr. C. J. Mumford,

for his continual help, supervision and constructive criticism.

Members of the Technical and Photographic Staff of the Department of Chemical Engineering in particular Mr. M. Lee for his assistance in devising the electronic circuit for the ultrasonic probes, and Mr. M. Pitt for his assistance in preparing the phototropic dye.

The author is especially grateful to his wife, Mrs. N. Attarzadeh for her encouragement and for her patience in typing this Thesis.

LIST OF CONTENTS

LIST OF CONTENTS (contd)

LIST OF CONTENTS (contd)

LIST OF CONTENTS (contd)

LIST OF CONTENTS (contd)

CHAPTER 1

INTRODUCTION

CHAPTER 1
INTRODUCTION

Droplet dispersions resulting from agitation or mixing of one liquid in a continuum of the other, are encountered in many engineering fields. In liquid-liquid extraction, two liquid streams are contacted to facilitate transfer of solute from one phase to the other and a high interfacial area is needed to accelerate the process of mass transfer. This is achieved by forming droplets of one phase in the other.

While the formation of a dispersion is a necessary part of any liquid-liquid extraction process, there are numerous other industrial situations where liquid-liquid dispersions are inadvertantly created and are in fact an undesirable feature. Examples are contamination of aviation fuel by water and problems in the management of waste water contaminated by oil.

The separation of liquid-liquid dispersions is of considerable importance in present day technology whether the dispersion is purposely created, as in liquid-liquid extraction, or is brought about as a result of unwanted contamination. In all these operations rapid and efficient separation of the two phases is advantageous. The type and design of separation for any given duty depends upon the efficiency of separation required and particularly on the characteristics of the dispersion.

Generally dispersions are characterised as 'primary' or 'secondary' depending on the mean drop size of the dispersed phase. Primary dispersions are characterised by droplets of mean diameter greater than 100×10^{-6}m. These dispersions

separate under gravity due to bouyancy forces. They collect at a phase boundary where drop/drop and drop/interface coalescence take place. Although there is no clear division between primary and secondary dispersions in terms of drop size, most workers conventionally refer to dispersions of mean droplet diameter less than 100μm as secondary dispersions. Dispersions containing droplets below this size are easily created either as a result of pumping or high turbulence or in a variety of other ways, e.g. condensation of super saturated vapour or alternate heating and cooling. Gravity separation becomes proportionately less effective as droplet size reduces and conventional settler designs become very inefficient when the droplet diameter falls below 100μm. For example, on the basis of Stokes Law,

$$u = \frac{gd^2(\rho_1 - \rho_2)}{18\mu_c} \qquad \ldots\ldots\ldots\ldots 1.1$$

$$\text{or} \qquad u \propto d^2 \qquad \ldots\ldots\ldots\ldots\ldots\ldots\ldots\ldots 1.2$$

Hence the settling velocity u is proportional to the square of the drop diameter so that a 10μm drop settles 400 times slower than a 200μm drop (the sign of u, and hence the direction in which the drop will move, depends on the relative values of the densities). Therefore to increase the settling rate it is necessary to increase the diameter of the drop. The basic requirement is to promote inter drop coalescence. One of the most effective methods involves coalescence by flow through a fibrous bed, in which droplets are held and

grow by coalescence until the surface forces are overcome by other forces acting in the opposite direction and they are released. However, due to the difficulty of observing events within a fibrous bed, no quantitative models exist to assist the design and the selection of optimum fibre diameter and voidage for specific dispersions. Therefore in this study techniques have been developed, and used, to study collection/coalescence of droplets within packings. In addition a novel packing, comprising knitted fibrous glass and permitting an ordered reproducible arrangement, has been investigated for the separation of both oil-in-water and water-in-oil dispersions. The essential processes of collection and drop growth are followed by drop release, either within or at the outlet from the coalescer. The mechanisms involved in this, and the manner in which it determines exit drop size, have also been considered.

CHAPTER 2

The nature, formation, occurrence and separation of secondary dispersions

CHAPTER 2
THE NATURE, FORMATION, OCCURRENCE AND SEPARATION OF SECONDARY DISPERSIONS

Emulsions, or liquid-liquid dispersions, and foams are disperse systems comprising a discrete inner phase dispersed in a continuous outer liquid. The inner phase is liquid in emulsions and gaseous in foams. The term dispersion does not generally imply any range of ratios between two phases. However foams always contain a large volume of gas in a small volume of liquid which is present as thin films separating gas from gas; dispersions in which the total gas volume is markedly smaller than the total liquid volume are known as gas emulsions.

The present work is concerned with secondary liquid-liquid dispersions and only their characteristics will be reviewed in detail.

2.1. NATURE OF SECONDARY DISPERSIONS

A secondary liquid-liquid dispersion, or emulsion, containing droplets of dispersed phase less than 100μm is generally cloudy in appearance and is often referred to as a haze. Small droplets of one liquid are suspended in a second immiscible liquid and, since almost invariably one of them is aqueous, the two common type of emulsions are oil-in-water (o/w) and water-in-oil (w/o), i.e. the term "oil" is used as a generic term for the water-insoluble fluid.

It is not usually difficult to determine which phase is continuous and which dispersed. One method consists of adding a small amount of one phase; the emulsion should be readily diluted if it is the continuous phase that has been added. Alternatively, a dye may be added which is soluble in only one of the phases; the dye will diffuse readily to give a general colour if it is the continuous phase in which it is soluble. Also o/w dispersions tend to have much higher electrical conductivities than w/o dispersions. Finally breaking the emulsion and observing which phase has the lowest hold-up and coalesces at the interface will show which phase is dispersed.

2.2. FORMATION

Emulsions may be produced intentionally or as a result of materials transfer, mixing or change of parameters (e.g. temperature) during a liquid-liquid process.

It is useful to review the parameters affecting formation of emulsions for several reasons. Firstly to evaluate the performance of a fibrous bed coalescer a means must be provided to generate a reproducible secondary dispersion. Secondly in the design of a coalescer care must be taken to avoid reformation of a secondary dispersion. Finally the operations yielding secondary despersions give some indication of where fibrous bed coalescers are likely to be applicable. In the present section the main mechanisms of formation by the introduction of one liquid into another by means of orifices, high shear, or ultrasonic techniques

will be discussed.

2.2.1. ORIFICE MIXING

Orifice mixing involves acceleration of one liquid, to form the dispersed phase, into a continuum of the other. Either a nozzle or a perforated plate may be used for liquid injection.

Richardson (1) has considered preparation of an emulsion by injection of one liquid phase into another. Under these circumstances the velocity of flow is extremely important, and break up of the liquid jet is controlled by inertial and viscous forces. The critical velocity v_o from a nozzle of diameter d_n is defined by

$$\frac{\mu_1}{(\rho_1 \gamma\ d_n)^{\frac{1}{2}}} = 2000 \left(\frac{\mu_1}{v_o\ \rho_1 d_n}\right)^{4/3} \quad \ldots\ldots\ldots 2.1$$

In figure 2.1. the upper distribution curve relates to super-critical conditions in which the velocity is so high that a jet is not formed and the outlet is in the form of droplets; the lower curve relates to sub-critical conditions in which a jet is formed with subsequent disruption to droplets. The mean droplet diameter can be read from the 50 percent intercept on each curve. When the Reynolds number $\frac{\rho_1 v d}{\mu_1}$ is plotted logarithmically against the ratio $\frac{\mu_c \rho_1}{\mu_1 \rho_c}$, a straight line relationship is obtained for a number of systems. The data are correlated by the empirical formula (2).

$$\left(\frac{vd\rho_1}{100\ \mu_1}\right)^{5/4} = 100\ \left(\frac{\mu_c\rho_1}{\mu_1\rho_c}\right) \quad \ldots\ldots\ldots\ldots 2.2.$$

Equation 2.2. can be used to calculate the velocity of injection which should be used, to produce an emulsion of a given mean drop size, if the viscosities of the two components are known (2). However this method is not used in practice.

2.2.2. HIGH SHEAR

Formation at high shear involves flow of the liquid-liquid system through a narrow gap between a high speed rotor or rotors, for example in a centrifugal pump or a colloid mill.

Taylor (3) deduced a relationship between the radii of droplets formed under conditions of high shear and such parameters as rate of shear, interfacial tension, and the viscosities of the two phases. At low speeds, the drop size is given by the approximate expression,

$$\frac{L - B}{L + B} = D \quad \ldots\ldots\ldots\ldots\ldots\ldots\ldots\ldots 2.3$$

where L is the radius of the largest droplet which can exist under the conditions of shear, B the radius of the corresponding smallest droplet. D is a dimensionless quantity proportional to the speed of flow, and also involves the interfacial tension, viscosity, and droplet radius. Under shear, a

droplet undergoes distortion, elongates into threadlike filaments, and subsequently breaks up into smaller drops. This is evidenced by photographic studies of oil drops suspended in syrup under stress (4).

Mechanisms of break up under shear shown in Figure 2.2. are based on the work of Rumscherdt and Mason (4). Taylor's deformation equation, based on the definition of deformation of equation 2.3 was used to show that,

$$D = F f(\delta) = A \quad \ldots\ldots\ldots\ldots\ldots 2.4$$

where A is the ratio of the viscous to surface tension forces and:

$$F = \frac{Gb\,\mu_c}{\gamma} \; ; \quad f(\delta) = \frac{(19\delta + 16)}{(16\delta + 16)} \quad \ldots\ldots 2.5$$

and $$A = F f(\delta)$$

where $$\delta = \frac{\mu_1}{\mu_c}$$

When the pressure drop due to shear across the droplet interface is greater than the surface tension forces which hold the drop together, it will rupture. It was also shown that in both shear and hyperbolic flow, the critical deformation above which the droplet will rupture is given by

$$D_R = A_R = \tfrac{1}{2} \quad \ldots\ldots\ldots\ldots\ldots 2.6$$

An interesting aspect of this work was the observation that depending upon the system parameters the 'breakage' pattern of droplets assumed a variety of forms.

In Figure 2.2. break up patterns are shown as a function of the viscosity ratio, δ, with values ranging from $\delta = 2 \times 10^{-4}$ to 6.0 and increasing G up to break up. These are tabulated in Table 2.1.

Figure No.	Viscosity Ratio	Comment
2.3 a	$\delta = 2 \times 10^{-4}$	No neck formed
2.3 b	$\delta = 1.0$	Neck formed (Picture 4) disintegrated into three satellite droplets
2.3 c	$\delta = 0.7$	Drops drawn out into long cylindrical threads (Picture 4)
2.3 d	$\delta = 6.0$	No rupture observed

Table 2.1 Mechanisms of deformation of droplets for systems with different viscosity ratios under shear.

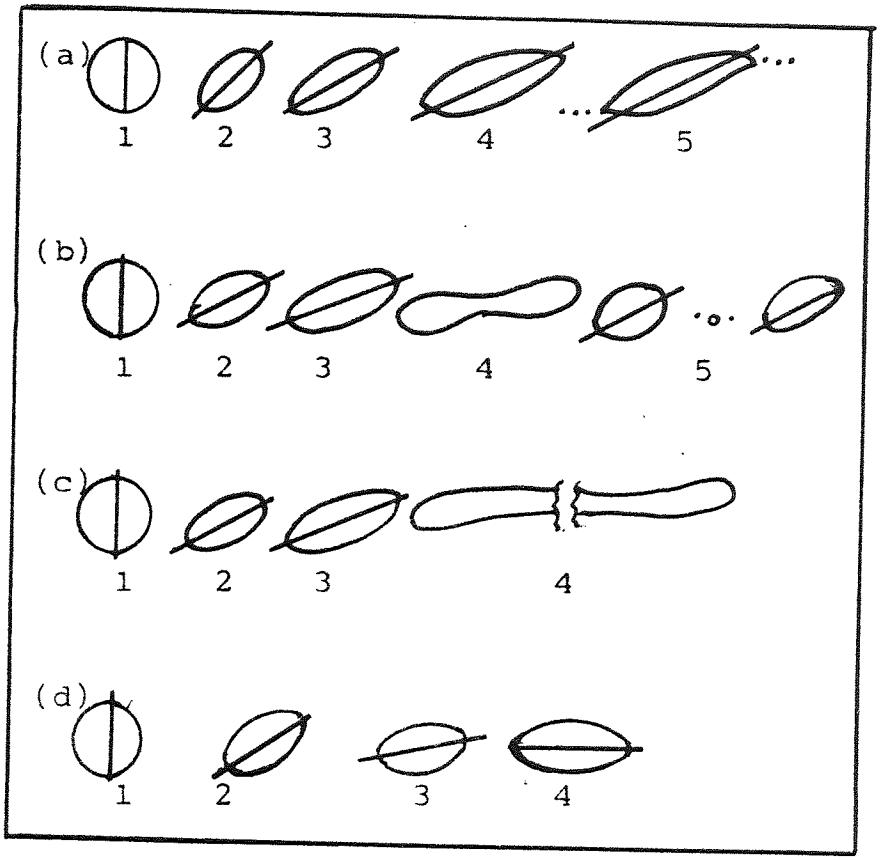

Figure 2.2. Mechanisms of droplet breakage in shear flow (4)

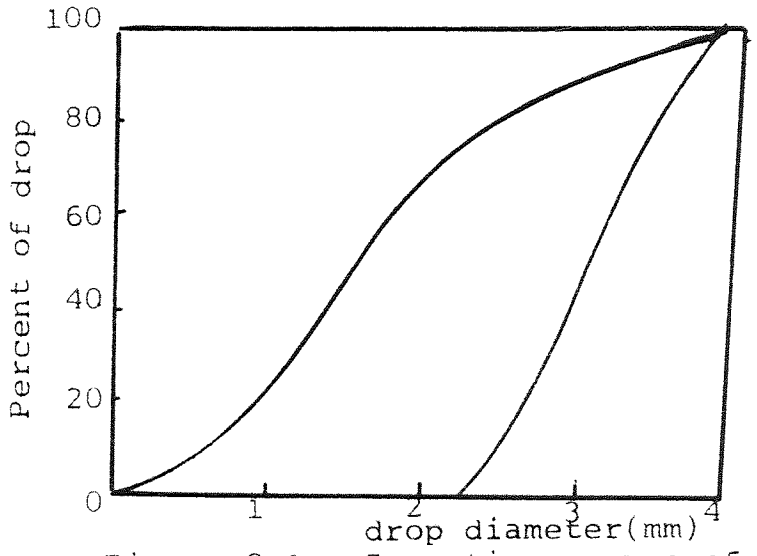

Figure 2.1. Summation curves of drop distributions from an oil-water jet (1)

2.2.3 ULTRASONIC EMULSIFICATION

Emulsions may be produced by passage of sound waves through a liquid-liquid mixture. Wood and Loomis (5) were among the first workers to produce emulsions by the use of ultrasonic vibrations, i.e. acoustic waves of such high frequency as to be inaudible. Vibrations of a frequency of about 200,000 cycles/s were employed compared with the audible limit, for persons of average hearing of about 15,000 cycles/s.

Conversely, in addition to increasing the tendency for break-up, the intense agitation which is brought on by these effects also increases the number of collisions between the dispersed droplets, and hence increases the possibility of coalescence. The process therefore represents a competition between these opposing effects, and it is necessary to choose operating conditions, and frequencies, in which the disruptive effect predominates (6). Conditions can be found favouring coalescence, and ultrasonic devices can be employed for this purpose.

2.3. SEPARATION

The separation of unwanted dispersions represents a problem of considerable complexity. The following discussion of separation is therefore sub-divided into two parts w/o and o/w, concerned with the 'breaking' of w/o and o/w dispersions respectively. However some of the techniques are common to both.

2.3.1 WATER-IN-OIL DISPERSIONS

The majority of literature on the separation of dispersions relates to w/o emulsions since the industrially important, oil-field emulsions fall into this class. As crude petroleum rises from the fissures of the earth, its passage through narrow openings, accompanied by water, gases and agitation by pumping, gives rise to conditions favourable to the formation of a w/o emulsion via the high shear mechanisms explained in Section 2.2.2. These emulsions cannot be processed without first removing the majority of the oil. There are seven basic methods available for dehydration (7).

1. Use of chemicals
2. Electrical dehydration
3. Heating or distillation at atmospheric pressure
4. Heating or distillation at elevated pressures
5. Settling
6. Centrifugation
7. Use of coalescers

All of these methods, and combinations of them, are currently in extensive use.

In general, the chemical methods are based on the introduction of an agent which counteracts the influence of the protective films that surround the dispersed drops due to the presence of natural emulsifying agents. Carbon disulphide and carbon tetrachloride are, for example, good solvents for the materials forming the protective film, albeit of limited practical value. Some break the film by phase inversion of

o/w emulsions into w/o emulsions, or vice versa. In modern techniques complex organic surface-active agents are used. One application of chemical demulsifiers is the "down-the-hole" method, in which the demulsifying chemicals are pumped down into the well, to prevent emulsification taking place (8).

A specific demulsifier will produce optimum results, and the choice must be made after a careful study of the physical and chemical properties and drop size distribution of the emulsion. Some indication of the wide variety of compounds proposed as demulsifiers is given in Table 2.3.1.

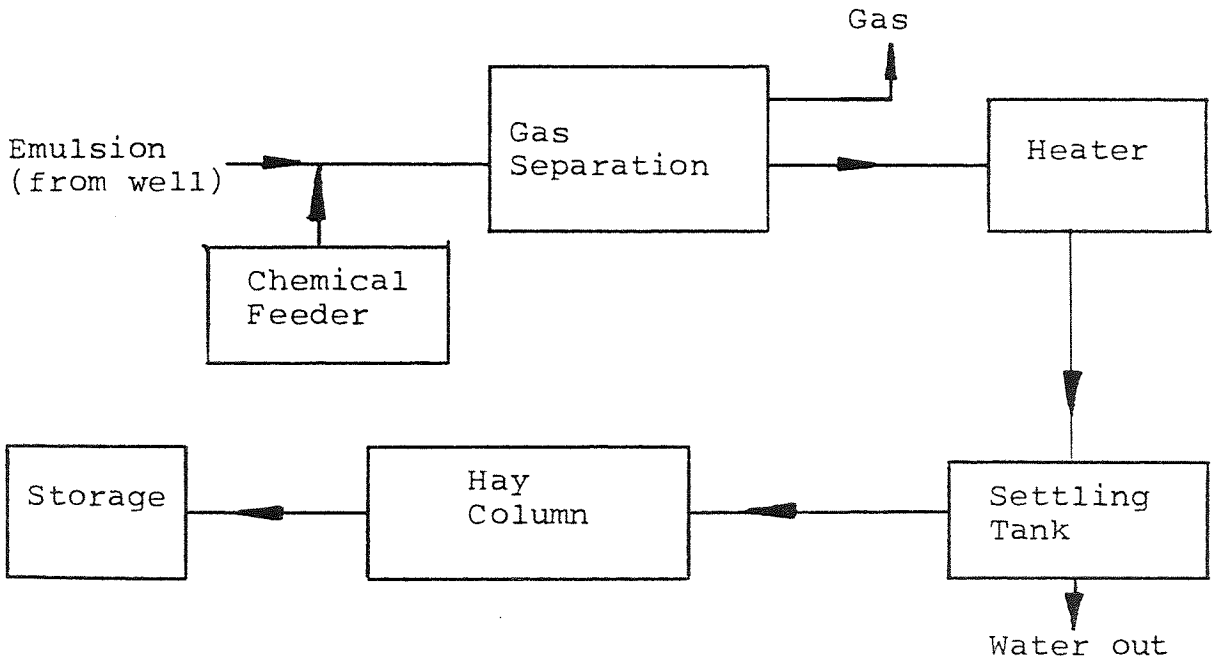

FIGURE 2.3.1.

Flow diagram for separation of w/o emulsion from oil well (30)

TABLE 2.3.1.

LIST OF DEMULSIFICATION CHEMICALS

CHEMICALS	REF.	CONTENTS
Nitrosophenols or nitrosoaromatic carboxylic acids	9	Used in oil field
Picric acid or other nitro compounds	10	Used in oil field
Acetone in combination with sulfonated fatty acid	11	Used in oil field
Sodium silicate and sodium hydroxide in ratio Na_2O to SiO_2 larger than 0.7	12	Used in oil field
Alkali metal hexametaphosphates or pyrophosphate	13	For emulsions which contain appreciable calcium ions
Water soluble, oil insoluble mahogany sulfonate, preferrably the sodium salt	14	Used in oil field emulsions
Nitrogen derivaties hydroxylamine and diamine compounds	15 16	Used in oil field emulsions
Black petroleum sulfonaphthenic acids	17	Used in certain Russian oil fields to bring the water content down to 0.5 percent

Electrostatic coalescers work on the principle of applying an electric field to dispersions of water in a non-conductive continuous phase stabilized by ions. The droplets are polarised and align into chains along the line of force. The increased collision rate as the chains make contact enhances coalescence rate.

Magaril (18) studied the coalescence of transformer oil-in-water emulsions under varying electrical gradients using a microscopic technique. No demulsification was observed until the electrical field reached a gradient of 200 v/cm. No change was observed in the behaviour of the emulsions when the current frequency was increased from 50 to 200,000 cycles. It was concluded that the effectiveness of an electric field in demulsification is enhanced by increasing the non-uniformity of the field.

Small (19) has described the use of high frequency vibration in conjunction with an electrical discharge maintained at the point of maximum compression. In this method, the voltage and current requirements are dependant on the specific gravity of the oil. Passler (20) has described a technique of electrical dehydration; the energy requirements for twenty four hour operation of a plant to demulsify 80 to 100 cubic meters of an emulsion containing 40% water were estimated as 15 to 20 KW- hours. In operation, an original mean droplet size of about 1 μm increased to 10 μm after four minutes and to 50 μm after eight minutes of treatment. This resulted in an increase in settling velocity by a factor of 2.5×10^3 after eight minutes.

Other methods such as centrifugation and filtration are

less commonly employed. For example centrifugation at very high rates (i.e. 17,000 to 40,000 rpm) will usually break emulsions. Materials containing 70 to 80 percent of water may often be reduced to a water concentration of 0.5 percent. Passage of emulsions through a suitable packing in which droplets grow to a size which can be removed by gravity separation, is discussed fully in Chapter 5.

Combinations of the methods may be used, as for example in the flow diagram shown in Figure 2.3.1 (21). In this plant the chemical demulsifier is metered into the flow line immediately at the feed point. The liquid passes into a gas separator for the removal of dissolved or occluded gases; it then flows through a heating unit, which presumably accelerates the chemical action as well as raising the temperature which will increase the rate of coalescence. (A great many such emulsions are in fact separable by no more that heating followed by settling). The emulsion is then passed to a settling tank in which the major separation takes place, and then through a column packed with hay or excelsior in which further separation may take place. A petroleum emulsion subjected to such treatment will contain less than 1 percent of water; therefore it will require additional treatment.

Undesirable water-in-oil emulsions frequently arise in industrial practice; examples occur in liquid-liquid extraction, and contamination of aviation fuel with water. An important type is the so-called gas-tar emulsion which arises in the thermal cracking of illuminating gas, the emulsions forming in wash-boxes and scrubbers of the plant.

The techniques used for separation are similar to those employed for oil field emulsions. A similar problem arises with emulsions containing water in fuel oil, which are sometimes encountered on ships. These emulsions are also amenable to treatments of the type used for oil-field emulsions. Preventive measures are often used, e.g. involving addition of a demulsifying agent in the oil prior to pumping to the fuel tanks.

2.3.2. OIL-IN-WATER EMULSIONS

Oil-in-water emulsions arise in various industrial processes, e.g. waste water from petroleum refineries, petrochemical plants, steel mills, wool scouring wastes and other industrial facilities may contain significant quantities of free and emulsified oils. Petroleum refineries invariably have to remove small amounts of oil from effluents. However, the quantity of material to be treated is much less than with w/o emulsions and there is less variety in the treatments used.

Gravity separation to remove oil is usually the first process step in the treatment of oily wastes. While gravity separators are effective in removing most of the free oil, soluble oil and a large portion of the emulsified oil containing mostly droplets less than 150 μm in diameter will remain in the separator effluent. The effluents from these treatment devices, when operated properly, may contain 30 to 150 g/m^3 of oil.

Secondary de-oiling processes such as acid cracking, centrifugal separation and dissolved air flotation are commonly

used to supplement gravity separation. In acid cracking the liquid is filtered first and sulphuric acid is then added to reduce the pH (initially 9 to 10.5) to 4, and the grease is allowed to settle in the form of sludge or "magna", which still contains about 90% water. This is pumped to heated storage tanks.

Acidification can also be carried out by passage of the liquor through a bed of an ion-exchange resin, resulting in exchange of sodium ions of the soap with hydrogen ions of the resin. Addition of various heavy metals salts, e.g. of magnesium and calcium, has been proposed. Although careful control of the relative concentrations of cations should make this a satisfactory method, this is difficult to achieve in practice. However, the combination of acid-cracking with such chemical treatment has proven satisfactory.

Centrifugation may be used for separation of the wool-scouring waste emulsion, by taking advantage of the fact that the maximum difference in density between the wool wax and water occurs at 70^{o}c. Numerous types of high speed centrifugal separators are used for this purpose (22).

The other mechanical technique which may be employed is dissolved air flotation. This technique involves the use of jets of air, or other gas, in the form of a stream of fine bubbles. This results in the formation of an extremely active froth, and highly efficient separations are possible (22). These secondary de-oiling steps will generally reduce oil content in the waste water to as low as 20 g/m^3 under optimum conditions. When effluent limits demandan oil concentration of less than 5 g/m^3, the above treatment methods are

inadequate (23). Further de-oiling could be carried out by carbon adsorption, but excessive oil tends to rapidly exhaust the adsorptive capacity of activated carbon. Therefore the high costs of the process make this technique less attractive unless adequate pretreatment is employed to reduce the emulsified oil content. Which separation method is selected clearly depends upon system properties, the drop size distribution, the efficiency of separation required and the end uses of both phases.

2.3.3. DISADVANTAGES OF SEPARATION METHODS

All the above methods suffer from certain disadvantages. With chemical additions the disadvantages are a high cost and technical and practical limitations in their application; there is also the possibility of the liquid system becoming contaminated. Care is therefore needed in the choice of chemical(s) and levels of addition. In most cases filtration and coagulation are subsequently necessary to achieve a separation and the chemical additive could harm the filter or coalescer element by forming surface coatings on them. Reproducibility of breaking rate can only be obtained with a high degree of control. Results have been found to vary dependent upon traces of impurities, the quantity of air bubbles drawn into the system during agitation, and with the variation of intensity of agiation. Clearly it would be difficult to control all these variables in industrial scale operation.

There is a great interest in electrostatic coalescers capable of coalescing water droplets; however

these involve high capital and high operating costs.

Centrifugation also suffers from high capital and operating costs. Consequently the use of centrifuges has been restricted to military applications such as the purification of jet fuel or where space is at a premium e.g. on ships. They are used in ordinary chemical processes only when low residence time is essential or when phase separation is difficult; examples therefore arise in pharmaceutical and radiological processes.

Recently, fibrous bed coalescers have received more consideration as efficient and economical emulsion breaking devices. These are discussed in detail in Chapter 5.

CHAPTER 3

Droplet coalescence

CHAPTER 3

DROPLET COALESCENCE

Coalescence involves two or more drops not only touching but flowing together to form a large drop or finally, a macroscopic liquid layer. There are two distinct modes of coalescence namely drop-interface coalescence and drop-drop coalescence. The basic mechanism in both cases involves the approach of a drop to an interface followed by entrapment of a film of continuous phase between the drop and interface; this film eventually drains away leading to rupture of the film and subsequent fusion of the drop with the homophase. Both mechanisms are assumed to occur when primary dispersions are coalesced in packings. This work is not directly involved with the separation of primary dispersions but, since during separation in a fibrous bed the droplets of a secondary dispersion grow at some stage within the packing to the size in a primary dispersion, i.e. >100 μm, a review of the literature on the coalescence of primary droplets is of some relevance.

3.1. DROP-INTERFACE COALESCENCE

This mechanism is assumed to take place in dispersed phase wetted packings used in the separation of primary dispersions.

All investigators (24, 25, 26) studying the coalescence mechanisms of a droplet at plane interface have found that the time interval between the arrival of a droplet at the interface and its final disappearance into its parent phase is not constant.

There is rather a distribution of times - the distribution being approximately Gaussian. Furthermore it is established that the coalescence process takes place via five consecutive stages:

(a) the arrival of the drop at the interface and the subsequent deformation of both the drop and the interface;

(b) damping of oscillations caused by the drops arrival at the interface;

(c) the formation and subsequent drainage of a continuous film between the drop and its bulk interface;

(d) rupture of the continuous film and the expansion of the resultant hole until the remaining film has been removed;

(e) transfer of the contents of the drop, partially or wholly, into its bulk phase.

Most of the time required for the coalescence of a drop is taken up by the drainage time i.e. stage (c). The time required for deformation and damping out of the oscillation of the drop, stages (a) and (b), have been defined as the pre-drainage time, and occupies a relatively short period, viz 0.1 seconds. High speed cine-photography of stage (e) has shown that the deposition time is of the order of 0.05 seconds. The stages (c) and (d), named respectively the "drainage time" and the "film removal time", are of the order of several seconds.

Attempts have been made to reduce the number of samples required to obtain a reproducible mean coalescence time. For a specific pure liquid-liquid system at constant temperature

and a drop of given diameter Gillespie and Rideal (27) obtained their results from observation of 100 to 200 drops. Jeffreys and Hawksley (28) used a carefully controlled, all glass apparatus to obtain reproducible mean results from 70-100 drops; the technique was refined later (29) and the number of measurements reduced to 30. Hodgson and Lee (30) improved the technique further and demonstrated that the rest times of droplets coalescing at an interface are very sensitive to the presence and accumulation of impurities at the interface.

The coalescence time has been expressed as a mean rest time t_m or the half-life rest time $t_{½}$. Generally $t_{½}$ has been more reproducible than t_m and the ratio $(t_m/t_{½})$ is always in the range 1.01-1.27 (31).

Correlations for coalescence times have been evaluated using pure systems (28) but in other studies surfactants (32) or electrolytes (33) were present which are known to change the interfacial tension and surface viscosity.

One important phenomenon is step-wise coalescence in which, under some circumstances, a drop residing at the interface coalesces partially leaving behind a smaller drop which in turn coalesces and produces an even smaller drop. Charles and Mason (34) have reported eight stages. Secondary dispersions formation in certain types of settling equipment is due to this phenomenon and the satellite drops generated may undergo entrainment resulting in loss of efficiency. This seems particularly likely to occur with low interfacial tension systems.

3.2. FACTORS AFFECTING COALESCENCE

Since coalescence of a drop at an interface is accomplished through drainage and rupture of the trapped film of the continuous phase the factors that most affect the drainage and rupture control the coalescence process. These factors are summarised in Table 3.2. (35).

There is general agreement between investigators regarding the effects of temperature, vibration, surfactants, mass transfer and electrical field upon coalescence. Disagreement arises however as to the effect of density difference, interfacial tension, and distance of fall. This may have arisen either because the effect of a particular parameter was not constant for all the immiscible liquid-liquid systems studied or because of the variety of experimental conditions under which the variable was investigated.

Although the above studies concern drop-interface coalescence, similar considerations apply in packed beds and fibrous bed coalescers. These are discussed in Chapters 4 and 5.

3.3. DROP-DROP COALESCENCE

A study of drop-drop coalescence is important for full analysis of all the design parameters for separation equipment. Indeed, in non-wetted packing, it is generally assumed that the coalescence of primary dispersions proceeds solely via the drop-drop mechanism. In contrast to the experimental work carried out on drop-interface coalescence, relatively little

FACTORS AFFECTING COALESCENCE TIME

No.	Variable (increasing)	Effect on coalescence time	Explanation in terms of effect on continuous film drainage rate	Reference	comments
(1)	Drop size	(i) Increases $t_{\frac{1}{2}} \propto d^n$ n varied with conditions (ii) Independent of drop size	More of the continuous phase film	27,32,33, 34,35,42, 68,69,70. 71,72	In stepwise coalescence smaller size daughter drops have a longer life at the interface than the original larger drops. (24,42,68)
(2)	Distance of fall	(i) Increases $t \propto H^n$ where n is const. depending upon drop size or $n = 11 \times 10^{-5} (\frac{\gamma^2}{\mu_c 0.5})^{0.91}$ (ii) Independent of distance travelled (iii) Either increases or decreases.	Drop 'bounces' and film is replaced. Depending on thermal or mechanical disturbances produced	28,35 69 71	Discrepancy of results was due to apparatus dimensions and particularly the dimensions of the cup that receives the drop. (25,35)
(3)	Interfacial tension	Decreases	More rigid drop, force causing drainage acts on smaller area.	42,71	

(4)	Curvature of interface towards drop: (a) concave (b) convex	Increases Decreases	More continuous phase in film Less continuous phase in film.	25,69,73	
(5)	Viscosity Ratio $\frac{\mu_c}{\mu_d}$	Decreases	Either less continuous phase film or higher drainage rate.	32,33,34, 71	
(6)	Phase $\Delta\rho$	Increases $\Delta\rho^n$ n = 1.2,0.32,0.25	More drop deformation, more continuous phase film.	24,34,68, 71,73	
(7)	Temperature	Decreases $t_{\frac{1}{2}} = (\frac{T}{25})^{-0.7} \mu_d^{0.5}$	Increases μ ratio.	27,28,32, 34,68,69, 79	Overall coalescence time, however, as distinct from first step time, may on occasions show an increase in temperature because of transition from single step to stepwise coalescence.
(8)	Temperature gradients	Decrease	Film distorts.	32,69	
(9)	Vibrational effects	Decreases	Assists in film rupture	27,32,69, 71	

Table 3.2 continued

(10)	Electrostatic effects	Decreases	Assists in film rupture.	27,32,33, 34	Causes formation of twin secondary drops (35,68).
(11)	Applied electric field	(i) Decreases (ii) Independent	Increase in effective gravitational field.	42,74, 75	The efficiencies of electrostatic coalescers are dependent on this fact.
(12)	Presence of a third component (a) Surfactants	Increases $t_m \propto c_1^n$ $0.3 < n < 0.45$	'Skin' formation around the drop, film drainage inhibited.	69,76	
	(b) Mass transfer into drop	Increases	Sets up interfacial tension gradients which oppose film flow	24,34,35, 68,77,78	Coalescence times are almost independent of solute concentration only primary step being affected for transfer from the drop. (24)
	(c) Mass transfer out of drop	Decreases	Sets up interfacial tension gradients which assist flow of film.	24,34,35, 68,77,78	
(13)	Impurities	Varies in an unpredictable way.		31	All researchers found it necessary to clean the interface, otherwise reproducible results were unobtainable.

work has been undertaken on drop-drop coalescence. This is due to difficulties in controlling collisions between two drops and because the randomness with which drops rebound and coalesce makes analysis inherently difficult. In spite of these difficulties a few techniques have been developed to study drop-drop coalescence (36,37,38,39,40). It is worth noting that factors governing drop-drop coalescence are relative drop sizes, terminal velocities and position of contact during collision of the droplets.

Scheele and Leng (36) carried out an experimental study to determine whether two colliding drops would coalesce or rebound. For approach velocities within the range 1.9×10^{-2} to $11.2 \times 10^{-2} ms^{-1}$ and a controlled drop size and collision angle they concluded that:

(a) There were no obvious relations between coalescence probability and impact velocity.

(b) Coalescence phenomena appeared to be very sensitive to the phase of oscillation at the point of contact.

(c) A model based upon consideration of a parallel disc and immobile interface, describing film thinning, failed by several orders of magnitude to predict fast enough rates of thinning to enable rupture to occur within the apparent time of contact.

Hence it was concluded that the controlling mechanism in drop-drop coalescence is film thinning. This is in agreement with the findings of Mackay (40). Most of the models for drop-drop coalescence are based on the criteria that the two drops approach each other, and squeeze out the continuous phase film separating them; when the film is thin enough, disturbances of a random nature rupture it and coalescence follows.

Various models have been derived based on the idea of film thinning; some of these are summarized in Table 3.3. However, the mechanisms of drop-drop coalescence are still not fully understood, and models are generally theoretically based. A considerable amount of additional experimental investigation appears necessary before it is fully understood.

3.4. BEHAVIOUR AND COALESCENCE OF DROPLETS ON SOLID SURFACES

The behaviour of droplets on solid surfaces is fundamental to the coalescence of dispersions using a solid packing. The simplest case to study is the behaviour of a single drop on a plane surface. The effect of surface energy of the solid material, equations of wetting and effects of material intersection on the coalescence of droplets will now be considered.

3.4.1. SURFACE ENERGY AND CONTACT ANGLE CONSIDERATIONS

An index of the relationship between the solid surface energy and the overall coalescence mechanism is provided by the contact angle of a sessile drop at the liquid-liquid-solid interface. The contact angle of a liquid drop on a solid surface, defined as the angle between the tangent to the drop and the solid surface measured into the drop, is a direct measure of the 'wettability'. If the contact angle is zero, then the surface is completely wetted by the dispersed phase. At the other extreme a contact angle of 180^{o} corresponds to complete non-wetting. The mechanisms of coalescence of both primary and secondary dispersions differ for wetted and

TABLE 3.3

RATE OF FILM THINNING

		Ref.
Rate of film thinning for two equal size spheres immobile interface	$t = \frac{3\pi \mu_c}{F}\left(\frac{d^2}{4} \ln \left(\frac{h_1}{h_2}\right)\right)$	41
Two rigid drops not equal size approaching a rigid plane interface; immobile interface	$\frac{dh}{dt} = -\frac{Fh}{6\pi \mu}\left(\frac{2}{d_1} + \frac{2}{d_2}\right)^2$	25
Deformable drop resulting in a non uniform film immobile interface	$\frac{dh}{dt}\min = \frac{2.78\pi\gamma^2}{\frac{d^2}{4}\mu_c F} h^3\min$ $\frac{dh}{dt}\max = \frac{13.0\pi^3\gamma^4}{\mu\frac{d^2}{4}F^3} h^5\max$	43
The rate of drainage of film between equal size drops mobile film	$h = \frac{h_o}{1 + Kh_oJ_o}$ where $J = \int_o^t \frac{F}{R^4} dt$ and $K = \frac{8R_d}{\pi \mu_d}$	44

non-wetted packings. These are discussed in Chapters 4 and 5.

Contact angle provides information about solid surface energies, surface roughness, the surface heterogenity and it is also a sensitive measure of surface contamination. From a study of the importance of solid surface energetics, particularly contact angle, upon the macroscopic motion of liquids under the influence of their own surface and interfacial forces (45) it was concluded that when flow is extensive, as in wicking and blotting or in capillary imbibing systems, consideration must be taken not only of the fluid dynamics, but also of the surface energetics. Unfortunately however, due to difficulty in observing the events within the packing, previous investigations have been limited to observations of the inlet and outlet drop sizes.

3.4.2. EQUATIONS OF WETTING

The following equation, correlating the work of adhesion, i.e. the work required to effect separation of a liquid from a surface, and the surface tension is attributed to Dupre (46).

$$W_A = \gamma_a + \gamma_b - \gamma_{ab} \quad \ldots\ldots\ldots\ldots\ldots\ldots 3.1.$$

where W_A is the work of adhesion

γ_{ab} is the interfacial adhesion

γ_a and γ_b are the surface tensions of the two liquids a and b.

Harkins (48) modified Dupre's equation to cover the spreading of liquids. The spreading coefficient S is given in terms of the surface tension by the equation:

$$S = \gamma_a - (\gamma_b + \gamma_{ab}) \quad \ldots\ldots\ldots\ldots\ldots\ldots 3.2$$

Harkin's equation implies that liquid b will not spread on liquid a unless

$$(\gamma_b + \gamma_{ab}) < \gamma_a \quad \ldots\ldots\ldots\ldots\ldots\ldots 3.3$$

i.e. the spreading coefficient S is positive. This reasoning has been extended further to relate the contact angle to the surface free energies of the liquid-liquid and liquid-solid interfaces by the equation

$$\gamma_{sc} = \gamma_{sL} + \gamma_L \cos \sigma \quad \ldots\ldots\ldots\ldots\ldots\ldots 3.4$$

where γ_{sc} is the surface tension of the solid covered with an absorbed film from the liquid. This equation is generally ascribed to Young (47).

Modifications have been made to Young's equation. To account for the influence of surface roughness of the solid, Wenzel (66) introduced the concept of actual and geometrical surface areas. Thus the factor r is defined as the ratio of actual surface area to geometrical surface area and Young's equation becomes

$$r\,(\gamma_{sc} - \gamma_{sL}) = \gamma_L \cos\sigma^1_c \quad \ldots\ldots\ldots\ldots\ldots 3.5$$

where σ^1_c is the contact angle on the roughened surface. Thus the contact angle measured on a smooth surface is related to that observed on a roughened surface by the equation

$$r \cos\sigma = \cos \sigma^1_c$$

Furthermore the contact angle may vary depending on how the droplet is formed on the surface. Thus the concept of advancing and receding contact angles (Figure 3.5) is used

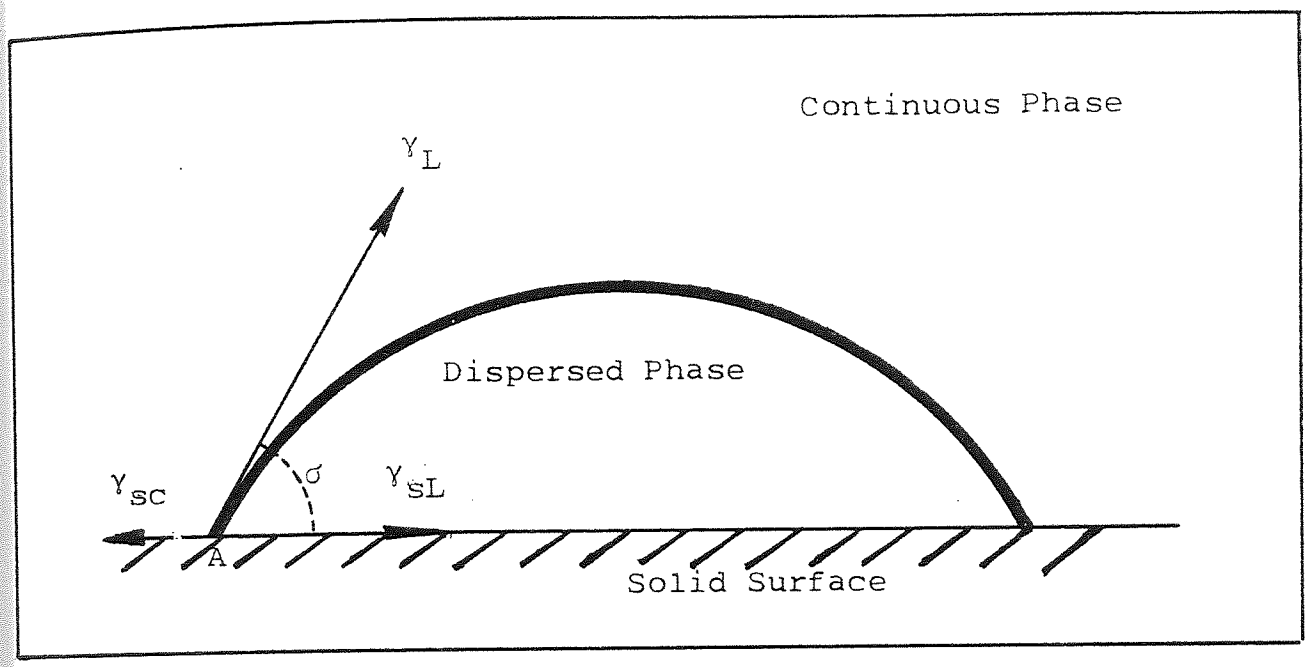

Figure 3.4 Sessile drop at solid/liquid/liquid boundary

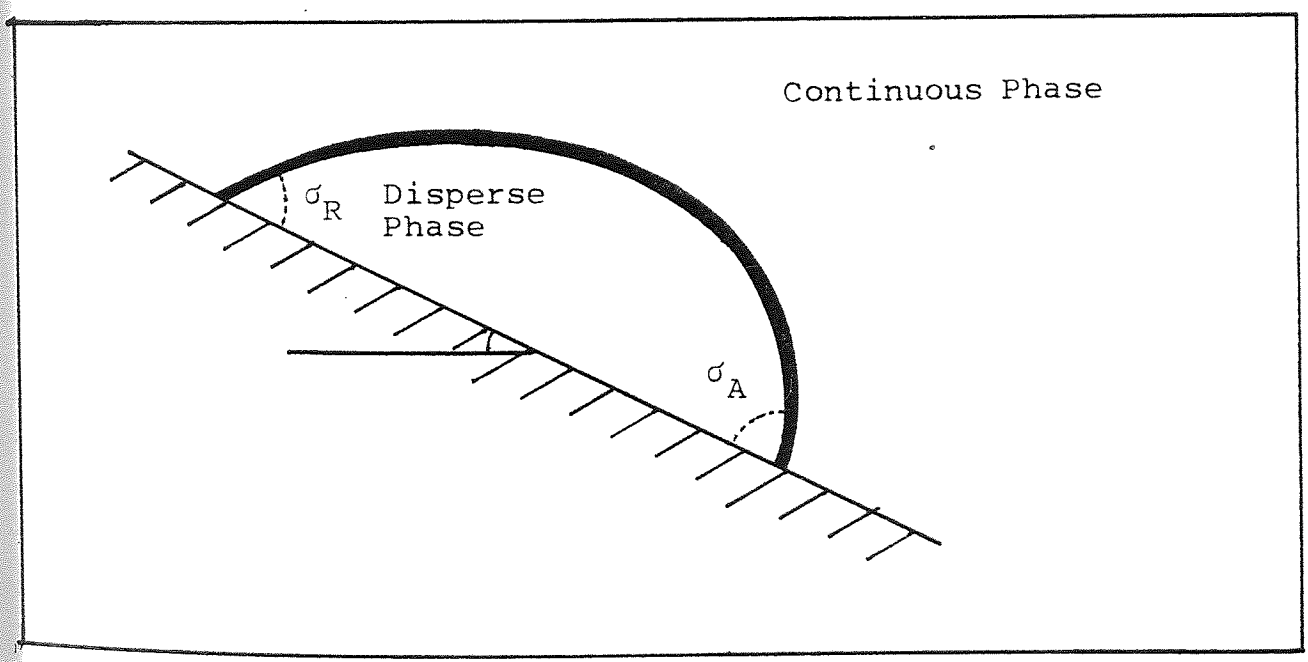

Figure 3.5 Advancing and receding contact angles demonstrated by the form of a drop on a tilted solid surface.

by most research workers (46,48).

Attempts have been made to take into account the dynamic behaviour of droplets during coalescence. The concept of "Dynamic Contact Angle" was used by Elliot and Riddiford (67) to show that the advancing angle was independent of interfacial velocity up to a value of 1mm min^{-1}. Above this value σ_A is increased to a limiting value. Conversely the receding angle was found to decrease continuously with increasing velocity.

However the equilibrium contact angle σ_c, which does not take into consideration any dynamic behaviour, is easier to measure and has been used by Davies and Jeffreys (49) to characterise coalescence on various solid surfaces.

3.4.3 JUNCTION EFFECT

A 'junction' is defined as an intersection between two solids with different surface energies e.g. p.t.f.e. (low surface energy) and stainless steel (high surface energy).

The practical importance of a junction has been observed in knitted mesh packings consisting of high and low energy filaments (50). This packing is claimed to be superior in performance to similar single material packings for distillation and phase separation of primary dispersions, with both higher efficiencies and higher throughputs being obtained. It is also claimed to be universal in application, i.e. to efficiently coalesce both o/w and w/o primary dispersions. No clear reasons have been given for this phenomena, but it has recently been studied (51) for primary droplets using different solid surface energies.

When droplets were allowed to coalesce on low surface energy solid surfaces, they tended to coalesce to form a "pool". Droplets deposited on top of this "pool" rarely coalesced on the surface of the "pool" itself; if they did, the coalescence time tended to be fairly long and the process was usually step-wise. However, the usual course was for the droplet to roll off until it arrived at the edge of the liquid pool. With a junction of p.t.f.e. and stainless steel "instantaneous" coalescence in one step was observed at the junction. This behaviour was also true for any other high surface energy and low surface energy junctions.

It was observed that (51) for junctions:

(a) No bouncing occurred i.e. the droplet adhered to the junction the first time it touched it.

(b) The total mean coalescence time from the moment the droplet touched the junction was about 0.037 seconds and no daughter droplets were released.

By comparison for a droplet coalescing on a low surface energy material the time was about 0.585 second to the end of first step coalescence with the formation of a daughter drop.

There is no model yet to explain the reason for this effect. However it could be due partly or wholly to the junction causing deformation of the drop resulting in an unstable shape and hence assisting rupture.

No studies have yet been reported regarding the junction effect with secondary dispersions.

CHAPTER 4

Coalescence of primary dispersions in packed beds

CHAPTER 4

COALESCENCE OF PRIMARY DISPERSIONS IN PACKED BEDS

Because of the sphericity and stability of droplets in secondary dispersions, most investigators have postulated different mechanisms of coalescence for primary and secondary dispersions (49). The present work is concerned with droplets in the mean size range 8×10^{-6} to 40×10^{-6}m termed secondary dispersions. However, since the smaller drops grow to primary drops in the range above 1×10^{-4}m within the bed, and the mechanism of release following a successful coalescence involves primary drops, it is worthwhile to review the literature concerning primary dispersions separation.

Phase separation of a primary dispersion is possible by gravity forces alone. However, when the drops are small and the density difference between the phases is also small phase separation through buoyancy will be very slow. Therefore in the design of a continuous process, where a rapid separation is required, a coalescing device is always necessary.

4.1 FUNDAMENTALS

There are two basic mechanisms for coalescence dependent upon the 'wetting' situation prevailing (49). For packings wetted by the continuous phase, drop-drop coalescence occurs between moving drops and drops retained in the interstices of the packing. For a packing wetted by the dispersed phase drops form a film on the packing and subsequent coalescence into this film takes place via a drop interface mechanism. This film

eventually drains through the bed when the buoyancy force exceeds the solid adhesion force.

A packing wetted by the dispersed phase enhances coalescence and hence has an improved separation efficiency. However, the adhesion force holding the dispersed phase to the packing tends to increase the hold up and hence the pressure drop, which can reduce maximum throughput before flooding for a wetted packing.

Therefore design and composition of a coalescing bed depends largely on the type of dispersion to be treated. Among the materials used are fibrous beds consisting of glass-wool, cotton, metal and polymer strands, knitted mesh packings formed by interlocking loops of metals and polymeric material, ballotini beads, pebbles and gravel composites. The more conventional packings, such as ceramic Raschig Rings and Berl Saddles may also be used.

Several prerequisites have been proposed for successful operation, viz the coalescer materials should be preferentially wetted by the dispersed phase; they should possess a large surface to volume ratio; the interstices should be small enough to cover the range of droplet size encountered; and they should cause as low a pressure drop as possible.

4.2. COALESCENCE OF PRIMARY DISPERSIONS IN CONVENTIONAL AND SPHERICAL PACKINGS

Pratt et al (52,53) studied droplet behaviour using nine different liquid-liquid systems in conventional packings (different size Raschig Rings and Berl Saddles) packed in a 4.9×10^{-2}m diameter, 0.91m column height. The packings were

preferentially wetted by the continuous phase. Their results showed that the mean diameter of the droplets leaving the column was independent of the mean diameter of droplets entering the column provided the latter were above a certain minimum value below which growth was very slow. There was a critical size of packing, depending upon the equilibrium droplet, above which the latter was independent of the packing size and shape. This critical packing size was defined as:-

$$d_c = 2.42 \left(\frac{\gamma}{\Delta\rho g}\right)^{0.5} \quad \text{.....4.2.1.}$$

For packings larger than the critical packing size (d_c) the exit drop size was independent of the packing size and flow rate until the onset of flooding. This was explained by the fact that a droplet larger than its equilibrium size, would break by impact with the packing element, whilst small drops coalesced until the equilibrium size was attained. The following correlation was derived for the exit Sauter mean diameter (54).

$$\frac{d_{vs}\,\Delta\rho\,\gamma}{\mu_c^2} = 1.42 \left(\frac{\Delta\rho\,\gamma^3}{\mu_c^4\, g}\right)^{0.475} \left(\frac{\bar{v}_o EX}{v_d}\right) \text{.....4.2.2.}$$

By changing the exponent to .5 equation, 4.2.2. reduces to equation 4.2.3. with some reduction in accuracy.

$$d_{vs} = 0.92 \left(\frac{\gamma}{\Delta\rho\, g}\right)^{\frac{1}{2}} \left(\frac{\bar{v}_o EX}{v_d}\right) \text{.....4.2.3.}$$

At substantially zero flow rates:

$$d^{o}_{vs} = 0.92 \left(\frac{\gamma}{\Delta\rho g}\right)^{0.5} \quad \ldots\ldots\ldots\ldots\ldots\ldots 4.2.4$$

The concept of a critical drop size was developed further for a number of aqueous hydrocarbon systems by Ramshaw and Thornton (55,56). They found that the equilibrium drop size was achieved after a certain height and the change in drop diameter with packing height was represented by:

$$d_{vs} = d_{vs\ (eq)} + 0.27 \exp - (0.157\ h) \quad \ldots\ldots\ldots\ldots 4.2.5.$$

Thornton suggested that the droplets travelled at 80% of this terminal velocity within the packing while Thomas claimed 50% to be a more realistic velocity (57). However due to the difficulty of observing droplets within the packing no data are available to substantiate these claims. Wilkinson et al (58) studied coalescence and phase separation of primary dispersion swarms in coalescer cells packed with glass ballotini and, with single nozzles, with a layer of ballotini packing. A two dimensional mathematical model was proposed to predict the upper and lower limits of the size of drop that would be retained by a given packing. The model was presented in graphical form in terms of drop size and packing interstice size with the group ($\Delta\rho g/2\gamma$) characterizing the physical properties of the system as parameter. Statistical treatment of the experimental results indicated that depth of packing in the bed, the superficial velocity of dispersed phase, preferential surface

treatment, and inlet drop size had only minor effects on the drop size in the effluent dispersion. However in this work continuous phase was stationary and, since this is not usual in separation processes, a minor modification would be necessary to apply the model in practical packing coalescers.

4.3. KNITTED MESH COALESCERS FOR PRIMARY DISPERSIONS

Knitted mesh packed beds have been widely used to coalesce primary dispersions. They are also inserted into Scheibel extraction columns which comprise a series of mixed compartments. Under certain conditions, the packed sections, coalesce the dispersion formed by the turbines (59), but more often they serve to isolate the mixing sections and prevent back-mixing within the column (60). A study of coalescence of a methyl isobutyl ketone and water system has been performed in a Scheibel column (61). It was concluded that the mean exit drop size was dependent upon packing height, but independent of the inlet drop size and the dispersed or continuous phase flow rate. A 'characteristic' drop size was produced similar to that found in conventional packings greater than the critical size.

Piper (62) studied limiting flow phenomena in knitted mesh packings, wetted by the continuous phase and covering voidages in the range of 97.5 - 98.75%. The working range of the packings increased with increasing voidage, a conclusion also reached by Slatter (63), and the limiting flow was dependent upon the inlet droplet size.

4.3.1. MECHANISM OF COALESCENCE IN KNITTED PACKINGS

Primary droplet coalescence in packings has been shown to be more efficient if the dispersed phase wets the packing surface (64). Jeffreys and Davies (65) identified two distinct mechanisms of coalescence dependent upon the 'wetting' situation in the packing. For packings wetted by the dispersed phase, drops formed a film on the packing and subequent coalescence into this film took place via a drop-interface mechanism. When the buoyancy forces were greater than the solid-liquid adhesion forces film drainage occurred. The exit drops thus formed left by a drip-point mechanism.

When dispersed phase did not wet the packings, drop-drop coalescence occurred between moving drops and drops held up in the interstices of the packing. It was concluded that the surface properties of the packing in relation to the liquid-liquid system determined the mechanism of coalescence. This fact was investigated further by observing drops leaving a perforated plate under different conditions. In the case of non-wetting conditions, when $d_n/d_{vs} < 0.4$, the drops did not pass through the perforation. However, when $0.4 < \frac{d_n}{d_{vs}} < 0.8$ the drops deformed and passed through. A force balance, suggested the relationship:

$$V = \pi d_n \left(\frac{\gamma}{\Delta\rho g}\right) \quad \ldots\ldots\ldots\ldots\ldots\ldots 4.3.1$$

However, when the dispersed phase wetted the plate, a ten fold increase in exit drop diameter was observed.

In the same study, the above approach was extended to packings. A selection of knitted packings made from p.t.f.e.,

nylon and stainless steel, was used. From the study using the toluene-acetone-water system it was concluded that the performance of the packing was in agreement with the results of contact angle measurements. Therefore for the organic phase dispersed p.t.f.e. and nylon packings were more efficient than stainless steel; of the two nylon was marginally better. This was expected since the contact angle of the drop on the nylon was greater than on p.t.f.e. It was also concluded that the most important factor in the design of coalescers for primary dispersions was the correct selection of packing material considering wettability by dispersed phase and the surface roughness. However the study did not cover the release mechanisms which could in fact determine the exit size of droplets and hence the efficiency of coalescence.

Thomas et al (57) studied the coalescence of primary dispersions in knitted packings 'wet' by the dispersed phase and observed the mechanisms of release. With high voidage packings (95.0-99.0%) at low flow rates the exit droplet detachment mechanism was by 'drip-point' formation. At higher flow rates and with lower voidages 'jetting' occurred, and the dispersed phase left the packing in the form of a continuous stream. Discrete droplets were formed due to Rayleigh-type instabilities (65) in this stream, leading to exit droplets smaller than those produced by 'drip-point' mechanism. For packing operated within the drip-point region the exit drop size at low disperse flow rate was correlated with the physical properties of the systems separated. Using dimensional analysis and a limited amount of data, correlations were produced (57):

$$\frac{d^{o}_{vs}\ (\text{'wetted' knitted mesh})}{d^{o}_{vs}\ (\text{'non wetted' Raschig rings})} = \frac{2.44\ (\frac{\gamma}{\Delta\rho\, g})^{0.5}}{0.92\ (\frac{\gamma}{\Delta\rho g})^{0.5}} = 2.65....4.3.2$$

$$\frac{d^{o}_{vs}\ (\text{'wetted' knitted mesh})}{d^{o}_{vs}\ (\text{'non wetted' knitted mesh})} = \frac{2.44\ (\frac{\gamma}{\Delta\rho\, g})^{0.5}}{0.92\ (\frac{\gamma}{\Delta\rho g})^{0.5}} = 2.65...4.3.3$$

Equations 4.3.2 and 4.3.3 indicate the improved coalescing performance of packings wetted by the dispersed phase. However both equations assume 'drip-point' mechanism, which is not the most efficient case of coalescer performance. The most efficient performance with 'wetted' packings the maximum flow rate of dispersed phase corresponds to transition between 'drip-point' detachment and 'jet' formation (57).

CHAPTER 5

Secondary dispersions separation in fibrous beds

CHAPTER 5

SECONDARY DISPERSIONS SEPARATION IN FIBROUS BEDS

The various methods for the separation of secondary dispersions are discussed in Chapter 2. Coalescence in packings of appropriate porous materials is especially attractive since, in the absence of particulate matter, it can be conducted continuously with a high separation efficiency. Secondary dispersion droplets can be coalesced from micron sizes to millimeter sizes which are then readily separated via gravity settling. Some of the variety of materials used as coalescing media, are described in Table 5.1.

This study is restricted to fibrous bed coalescers and in particular glass fibre beds.

5.1. BASIC REQUIREMENTS OF A COALESCER ELEMENT

The requirements of a coalescer with regard to operating and packing characteristics are as follows.

(a) The bed should possess a high surface to volume ratio and be closely packed (100).

(b) The bed should, on balance, be preferably wetted by the dispersed phase and should, if practicable, be presoaked before operation. This is contradicted by some authors and is discussed in Section 5.1.1.

(c) Coalescence is more complete as fibre diameter is decreased (81,120). Surface roughness is an important factor affecting drop collection, fine fibres with high surface roughness being most efficient.

TABLE 5.1

COALESCER PACKING MATERIALS AND THEIR APPLICATIONS

BED	APPLICATION	REF.
6 webs of polypropylene micro-fibres (av. dia. 2 μ, 6oz/yd^2) and 5 webs of resin-bonded glass fibres (diam.4.2 μ, 1 lb/ft^3).	Water containing petroleum 394 p.p.m. reduced to 1.2 p.p.m.	119
Aluminium fibres with average length 10-20mm, deposited with silica gel binder on ceramic support.	Kerosene drops of (3-15 μm) were coalesced to resulting drops of 0.05-0.5mm mostly 0.1-0.2mm.	123
Polyster, polypropylene, knitted steel, fibre glass, polytetrafluoroethylene felt. Also a mixed bed of fibre glass and polyster felt.	Separation of 1000 ppm water-in-gasoil emulsion, droplet size 5×10^{-6}m in diameter. The mixed bed proved most efficient.	90
Steel Wool	Separation of traces of caustic soda dispersed in gasoline after the Sweetening Process. (Extraction of mercaptans by sodium or potassium hydroxide solution).	114
'Alundum', or glass wool	Water-in-oil emulsion. Bed must be preferentially water wetted in the presence of oil.	117
A pebble bed filter, 5×10^{-2}m in diameter, 18×10^{-2} deep using 0.16×10^{-2} to 0.32×10^{-2}m pebbles.	Separation of 1000 ppm fuel oil-water emulsion, 80% of which was finer than 254×10^{-6}m in diameter. Only 20 ppm escaped in the treated effluent.	115 116
A granular mixture of dissimilar metals such as iron and aluminium or of carbon with a metal.	Separation of 1100 ppm oil-in-water as well as water-in-oil emulsions. Only 50 ppm escaped in the effluent.	118

(d) The fibres should be chemically inert and mechanically strong.

(e) The presence of surfactants or high viscosities of either phase tend to significantly reduce coalescence but the latter may be alleviated by operation at higher temperatures (101). As would be expected, a high interfacial tension system is more easily coalesced than one of low interfacial tension.

(f) The superficial velocity should be maintained between certain minima and maxima; a typical range reported is 0.1 to 2.5 x 10^{-2} m/s (81). The minimum velocity places a practical limitation on coalescer area whereas the permissible maximum velocity increases with bed depth, as does capture efficiency (120). However, there is an optimum thickness for each application as excessive bed depth causes redispersion of the coalesced drops. Also, operation at high velocities is associated with high pressure drops and a reduction in exit drop sizes. If the critical separation velocity is exceeded, break-through of the secondary dispersion occurs. This is discussed in more detail in Section 5.1.2.

(g) For more efficient separation, mixed beds of high and low energy surface materials have proved successful (90,102). Examples of the fibrous packing materials employed as coalescence media are shown in Table 5.2, together with their performance under typical operating conditions. Table 5.3 shows the main uses of fibrous coalescers.

5.1.1. WETTABILITY

The significance of packing wettability, and indeed

TABLE 5.2.

TYPICAL PERFORMANCE OF PACKINGS USED IN SECONDARY DISPERSION COALESCENCE

PACKING TYPE	BED THICKNESS m x 10^{-2}	MAX. OPERATING VELOCITY m/s x 10^{-2}	PRESSURE DROP BAR
Reticulated ceramic (124)	1.5	1.0	0.25
Cotton/Glass fibre (cartridge) (125)	5.0	0.45	0.75
Glass fibre (compressed) (101)	0.2	2.0	1.5
Carbon/Metal (102)	15.2	0.5	0.05
Glass fibre (93)	4.0	2.0	0.8
Glass fibre (woven)	0.35	0.5	0.25
Glass fibre mats (100)	0.3	1.5	0.06
Stainless steel meshes (126)	0.25	2.5	0.08

Fibre diameters	3 - 35 μm
Voidages	0.4 - 0.95
Phase ratio	0.07 - 7% $^{v}/_{v}$

TABLE 5.3.

FIBROUS BEDS FOR WATER OR OIL REMOVAL

a) Water Removal Aircraft Jet Fuel	Water removal to avoid ice crystal formation at high altitude causing filter/ passages blockage. Solid contaminants also removed (97,113).
Diesel Engine Fuel	To reduce corrosion. Solid contaminants also removed to reduce abrasion.
Steam Turbine Lubricating Oil	Water separation in addition to sludge removal.
Crude Oil	Desalting of crude petroleum, e.g. 80% removal of natural salts in aqueous solution (127).
Process Streams	Water removal from chlorinated hydrocarbons. Sodium hydroxide solution separation from butadiene (128). Water removal to prevent catalyst poisoning
Naptha, Kerosene, Petroleum spirits, L.P.G.'s	Removal of trace water.
b) Oil Removal Cleaning of oil tanks at sea. Ballasting.	To meet International Standards of 100 p.p.m. in the discharge (85).
Oily effluents from ships at sea.	Causes additional to cleaning.
Trade Wastes.	To rivers - usual limit 5 p.p.m. Discharge of petroleum spirit to sewers prohibited but e.g. 500/mg/1 combined limit may be imposed on grease/oil.
Wool scouring wastes	Recovery of grease.
Refrigerants	Removal of compressor oil, Freon 12 or liquid ammonia(96).

whether 'wetting' , as discussed in Section 3.4 occurs to any extent has been the subject of some controversy.

Voyutskii et al (80) studied water-in-oil emulsions separation using fibrous materials. By varying relative wettability, they observed that an intermediate wettability gave the most effective separation and concluded that for the best performance the coalescer should be sufficiently water-wetted to coalesce the water, but not so saturated as to produce extensive clogging by accumulated water. Jeffreys and Davies (49) stated that, since micron sized droplets do not wet the surface, the wetting properties of the packing in relation to the liquid-liquid system used should be of little importance.

Sareen et al (81), in their study using photomicrography, showed that in most cases the droplets which adhered to the cotton fibres did not actually wet the fibres. From this they concluded that preferential wetting was not the controlling factor which made cotton a more efficient coalescer than the other fibres.

Conversely, Burtis and Kirkbride (82) stated that the packing must be preferentially wetted by the dispersed phase. Hazlett (83), who agreed with the theoretical considerations of fibre wettability, considered wetting important at the drop release point. Langdon et al (84) considered the separation performance of a packing to be mainly determined by its wetting properties. An improved element with well defined and stable wetting characteristics could be achieved by using a packed bed composed of two materials, one essentially hydrophobic and the other essentially hydrophilic. For separation of oil from water Farley et al (85) concluded that water wetted packings were far superior to oil wetted ones. This was due to the fact

the oil wetted packing held the coalesced drops too tightly and did not allow coalesced drops to leave the packing; this resulted in redispersion to small drops. Chieu et al (99) studied the significance of wetting properties using polyester felt, and glass mats. Keeping the flow rate, influent oil concentration and coalescer depth constant they found that removal efficiency increased as the fibrous bed became saturated with captured oil. They also obtained a better removal efficiency by polyester and polypropylene felt which indicated that preferential oil-wet media were more effective for separation of an oil-water emulsion. Several investigators have studied mixed packings containing different fibre materials (82,112). Voyutskii et al(121) observed that mixtures of viscose and wool fibres resulted in improved coalescence performance over single fibrous materials.

The above studies involved analysis of the performance of packings and/or single drop studies. As described in Chapter 4 wettability is recognized as important in coalescence of primary dispersions. Therefore since secondary dispersion drops coalesce to primary sized drops at some stage within the packing, consideration of wetting properties of the packing for secondary dispersions alone could be misleading. In the case of single fibre studies the shadow of the fibre on the drop, and the lens effect of the fibre, could be misleading when finding the contact angle by microphotography.

5.1.2. SUPERFICIAL VELOCITY

This is defined as the volumetric flow rate of the complete dispersion divided by the surface area across the empty coalescer cell. (86).

The performance of a coalescer is usually assessed both by its efficiency in coalescing small drops and its ability to operate at a high superficial velocity with the lowest possible pressure drop. An investigation into desalting crude oils by fibrous glass packing showed that the effluent salt content increased with increasing flow velocity (82). Voyutskii et al (80) studied water-in-oil emulsions coalescence using fibrous materials and found that separation occurred only below a certain critical velocity. Below this velocity coalescence depended on total fibre contacting surface rather than on pore size. Investigation of the coalescence of w/o dispersions induced by beds of glass fibres with subsequent gravity settling showed that (87,88), effluent water content steadily decreased with increased superficial velocity. Gudesen (89) using a mixed fibrous bed of cotton and glass wool investigated the coalescence of petroleum fractions dispersed in water by turbulent mixing. Coalescence performance was judged visually from exit drops. Again a flow velocity was identified below which complete coalescence was achieved; this velocity passed through a maximum with changing bed depth, and a minimum with changing bed composition. Superficial velocities ranging from 0.1×10^{-2} to $1.8 \times 10^{-2} ms^{-1}$ were studied by Sareen et al (81). Several liquid-liquid systems were used with various physical properties; they were separated in a mixed packing made of cotton and a supporting fibre (p.t.f.e, glass, Dynel). It was concluded that for a mixed fibre bed, with a specific ratio of fibre species, there is an optimum bed depth for best performance Coalescence performance increased with decrease in fibre diameter.

Although the above work gave useful, practical information concerning superficial velocities and other packing variables, it provided no clear understanding of the phenomena of break-through and "critical" velocity. For example micron sized drops in the exit stream could be caused either by drops passing through unchanged or by redispersion in the bed/ at the outlet.

5.1.3. PRESSURE DROP

For a given packing material, the pressure drop across a coalescer is a function of the dispersed phase hold-up, or bed saturation, prevailing at the operating velocity.

Phenol-formaldehyde coated glass fibres of 3.2×10^{-6}m diameter were used by Langdon et al (89) to separate effluent oil content. They claimed 100% efficiency at a superficial velocity of $1 \times 10^{-2} ms^{-1}$. The pressure drop during the run increased from 13.8×10^{3} to $172.4 \times 10^{3} Nm^{-2}$. This was considered to be due to oil accumulation within the bed and, to a lesser extent, to mechanical degradation of the fibre.

Euzen et al (90) used a composite packing of thin fibre glass wool followed by a coarse packing of polyester felt for the removal of water from oil. Packing pressure drop was accurately predicted by:

$$\Delta P = K' \times (L \times V')^{0.86} \quad \ldots\ldots\ldots\ldots 5.4$$

However this correlation applies only to the specific system studied and is hence of limited use.

The regeneration of fibrous bed coalescers operating on

secondary oil-in-water emulsions was studied by Shah et al (91). Unstabilized or commercially available glass fibres were used and the latter fibres were either bound together into a rigid structure or stabilized by application of isobutyl methacrylate resin and subsequent heat treatment. The efficiency of these coalescers was claimed to be 100% for several hours but then fell off rapidly. The cycle life was defined as the time when concentration of the effluent emulsion reached 5 ppm, and was found to be of the order of 6 hours. Pressure drop increased gradually during the operation. Their study was therefore under unsteady conditions which is not the usual mode of operation of coalescers.

5.1.4 SYSTEM PROPERTIES

Due to the important effect of system interfacial tension upon coalescence, many investigators have studied the effect of variations in interfacial tension on packing performance. Vinson, (104) observed little effect, when it was varied above 30 x 10^{-3} Nm^{-1}, but when it was decreased below 11 x 10^{-3} Nm^{-1} the performance of the packing element was found to decrease. Bartel (96) suggests that systems with values as low as 20 x 10^{-3} Nm^{-1} can be separated satisfactorily, but below this value separation becomes increasingly difficult. This was later confirmed from a study involving nine different water-organic dispersions (105).

When interfacial tension was lowered incrementaly by using surfactant during separation of oil in water emulsions, incomplete coalescence was observed for an interfacial tension value of

$20 \times 10^{-3} Nm^{-1}$ for water soluble surfactants; coalescence was complete with oil soluble surfactants for values as low as $3.52 \times 10^{-3} Nm^{-1}$(81). However, none of the investigators report different critical interfacial values for different systems. Hazlett and Carhart (97) and Bitten (92) have stressed the importance of interfacial tension, but report many instances in which emulsions have been separated by coalescers in spite of low interfacial tensions. Langdon et al (84) have reported similar data and instances where coalescer performance seemingly improves in the presence of some additives. Beatty (106) concludes that the effect of surface-active fuel components cannot be predicted from contact angle and interfacial data alone. Wasan and co-workers (107,108) have shown that interfacial viscosity and the rigidity of the interface critically affect coalescence. From emulsion stability studies using crude oil, they reported good coalescence with interfacial tensions as low as 0.01 dynes/cm. Jaisinghani (109) studied the effect of six commercial fuel oil additives on the water removal performance of a fibre glass coalescer with a low surface energy coating; it was concluded that interfacial tension was not the most important property determining the separation-ability of coalescers. Normal coalescer performance was possible under extremely low interfacial tensions i.e. 0.5 dynes cm^{-1}. The performance of the pleated paper element was lowered by an additive which had no effect on the fibre glass coalescer. However, these experiments were based on techniques for changing the interfacial tension of the system by addition of surface active additives which are known to change the performance of a packing. Beatty and Wallcutt(110) have shown that cellulose paper and uncoated fibre glass have

high surfactant adsorption compared with the negligible adsorption observed with fibre glass coated with polymeric materials (low surface energy). Osterman (111) suggested there was adherence of the surfactant to the media thus allowing the emulsion to pass through unaffected due to the change in fibre wettability. Lindenhofen (112) did not agree with the above theories and suggested that, with water dispersed, a surfactant film at the water-oil interface may present a mechanical or electrical barrier to the coalescence of water droplets in the media.

It is apparent from the above review that due to the ambiguity associated with effects of surfactant on the packing and its performance, it is not good practice to study variation of interfacial tensions using surfactive additives. It is preferable to use pure systems. Interfacial viscosity, pH and specific gravity must also be considered to test a particular packing.

Continuous phase viscosity is known to influence coalescence. In the impingement mechanism of coalescence discussed in Section 5.2.c the viscous drag forces will increase with increase in viscosity so that lower droplet sizes will break away from the fibres attracting them (96). Viscosity will also affect the settling velocity according to the Stokes Equation discussed in Chapter 1. Vinson (104) investigated the coalescence of oil-water dispersions, using a fine mesh screen to simulate layers of fibres. A slight increase in coalescence was observed over a 30 fold increase in droplet viscosity. Sareen et al (81) observed that at velocities greater than 1.3×10^{-2} m/s and less than 0.6×10^{-2} m/s viscosity had no effect on the critical separation velocity. Their results were

based on one particular system i.e. mixtures of LF-1584 oil and No.10 base oil in various proportions to give different viscosity values. Davies and Jeffreys (49) observed a decrease in the "critical" velocity and thus the capacity of their glass fibrous coalescer as the viscosity of the dispersed phase was increased. However, before any firm conclusions can be made more experimental data, is needed.

pH value and specific gravity are of less importance with regard to coalescence mechanism. However in choosing a coalescer element the pH value must be considered i.e. the packing material must be resistant to the liquid-liquid system. Specific gravity difference is important in positioning the coalescer element and in the design of the after settler, i.e. the higher the difference in specific gravity between the phases the higher the rate of settling and hence the smaller the settler.

5.2. MECHANISMS OF COALESCENCE

There are several proposed mechanisms regarding the manner in which micron sized droplets in secondary dispersions coalesce within a packing. However these are all theoretically based and are not universally accepted. These mechanisms, which contain many similarities, are summarized below.

Voyutskii et al (80) suggested the following steps:

(a) Collision of the droplets with fibres in the bed

(b) Adhesion of the droplets to the fibres

(c) Coalescence of the micron sized droplets

(d) Adhesion of the coalesced drops to the fibre surface

(e) Trickling of the coalesced drops through the bed

Bartle (96) proposed three other possible mechanisms:

(a) Pore catchment:

Any drops larger than the pore diameter are held up. Subsequent drops coalesce with the captured drop as shown in Figure 5.2.1a. This behaviour could be encountered at a screen or wire gauze.

(b) Flow path intersections:

Droplets of dispersed phase are considered to travel in a tortuous path. When changing direction, large droplets will not follow the streamlines as readily as small ones, owing to inertial forces. Flow paths of different size droplets will therefore intersect with the possibility of collision and subsequent interdrop coalescence at each path intersection. This type of collision, which is likely to occur in fibrous bed coalescers, is shown in Figure 5.2.1b.

(c) Impingement:

For a hydrophilic packing, a droplet will impinge upon fibres, cling to them, and then move along the fibres in the direction of the overall pressure gradient until it arrives at either a fibre intersection, or a pore too small to pass through. The next drop, arriving in a similar manner, will coalesce with it until a sufficient drop size is reached to break away from its site under the influence of viscous drag caused by the continuous phase flowing round it. Curtis (113) also proposed this mechanism for the separation of water from oil as shown in Figure 5.2.1c.

Sareen et al (81) proposed the following mechanisms:

(a) Inertial impaction:

Droplets with the same relative mass as the continuous

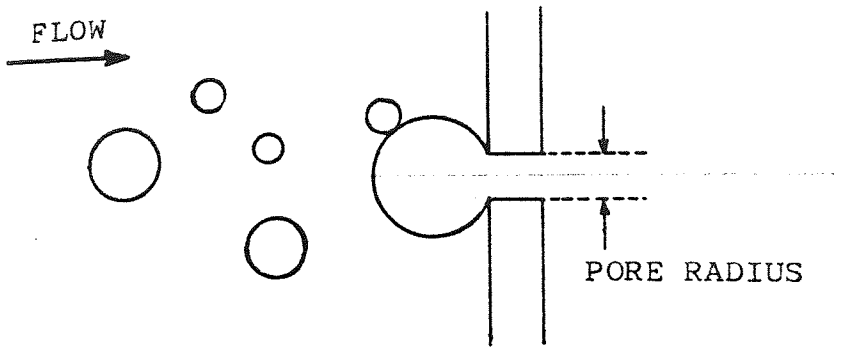

(a) PORE CATCHMENT

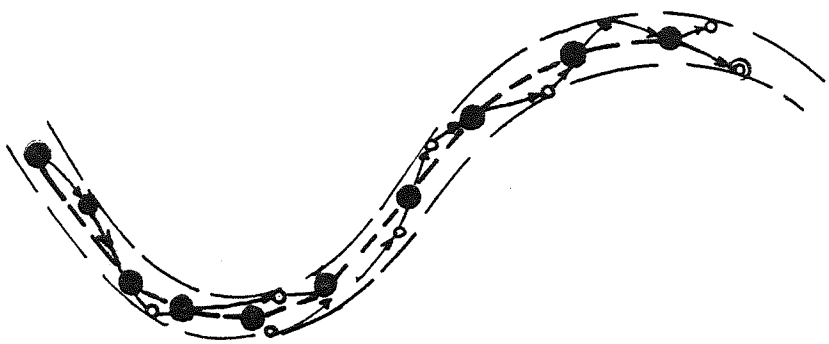

(b) FLOW PATH INTERSECTIONS

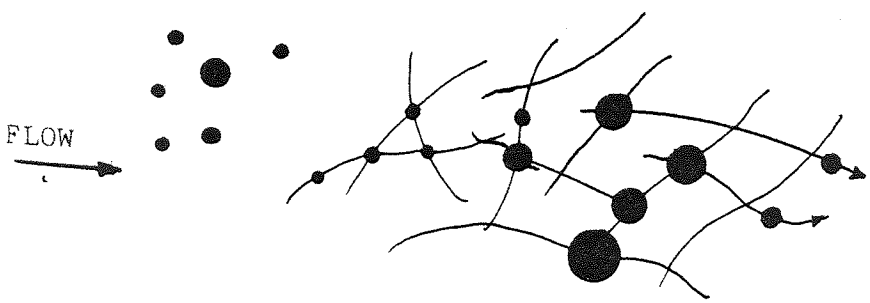

(c) IMPINGEMENT

Figure 5.2.1. MECHANISMS OF COALESCENCE (96)

phase follow the streamlines around any obstructions in the stream. When flow is turbulent and vortices occur, the drops can be brought to a fluid interface even though the density difference is low. If the drop density is less than that of the continuous liquid, this mechanism should act to prevent drops approaching the fibre or other drops.

(b) Direct interception:

Finite diameter droplets tend to touch the fibre at a distance $\frac{d}{2}$ from the packing surface; drops outside this distance will not be collected.

(c) Brownian movement:

Submicron size range droplets can reach each other and other wetted surfaces due to Brownian motion.

(d) Electrostatic movement:

Droplets which carry opposite electrostatic charges can attract each other. Like Brownian movement, this mechanism is only effective with very small droplets.

(e) Rupture in capillaries:

When a dispersion is passed through the packing, there is a tendency for the droplets to be forced together as they move through the passages. Film thinning would then occur and the drops would coalesce together while moving. However photomicrographic studies have shown that little or no coalescence occurs between two freely moving droplets which come into contact as they are carried through the bed.

Hazlett (83) has suggested the mechanism in a fibrous bed as a sum of several processes. The major steps were finally divided into three steps as follows:

(a) Collection of droplets:

This includes approach, film drainage and film rupture.

The diffusion process may contribute to the overall approach efficiency for droplets less than one micron.

(b) Passage through the bed:

Droplets collected by the bed from the continuous phase are not released immediately. They are collected until their equilibrium value is reached dependent upon phase ratio, flow velocity and surfactant content. Distribution of droplets throughout the packing is not constant, and most of them are held at the entry zone; this is in agreement with the results obtained by Shahloub (93) and Bitten et al (92). Once the equilibrium value is exceeded, droplets move into the flow channels and pass through the remainder of the bed (92).

(c) Release:

In an ideal situation, one thread feeds a droplet at the downstream face of the bed. A balloon-shaped drop formed in this way continues to grow in size until the hydrodynamic forces exceed the interfacial forces. The rupture occurs at the balloon's neck, the size of the released drop being dependent upon flow velocity and interfacial tension. Two other types of release mechanism are "pointing" and "graping". In "pointing", fingers taper to a point, vibrate and kick small drops from the tip. "Graping" mechanism has been reported by a number of observers (84,98). This behaviour is found at high dispersed phase concentrations or with certain additives. An exit surface preferentially wetted by the dispersed phase encourages "graping". The various droplet release patterns observed by previous workers are shown in Figure 5.2.2.

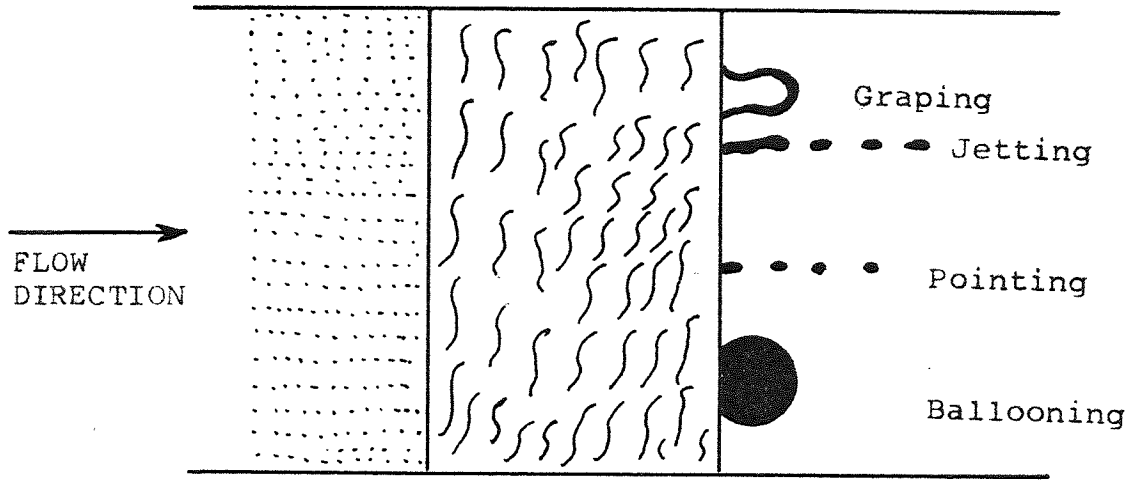

Figure 5.2.2. TYPES OF DROPLET RELEASE MECHANISM (97)

5.3. MODELS OF FIBROUS BED COALESCERS

Models developed by previous workers (49,117,120,134) were based on assumptions of coalescence mechanisms within the packing and/or observations of drop coalescence on a single fibre. However, as discussed in Section 5.3.2. the extrapolation of mechanisms of coalescence on a single fibre to those within a complete packing could be misleading. Therefore there is no acceptable mathematical model based upon the actual mechanisms of coalescence within a packing.

The more important mathematical models which have nevertheless been derived to assist in the design of fibrous bed coalescers are reviewed below.

5.3.1. SHERONY AND KINTERS' MODEL:

Using a combination of aerosol filtration models and the kinetic theory of gases a model of a fibrous bed coalescer was presented which relates the collision frequency between droplets and fibres to the overall coalescence frequency (120). The basic assumption is that there is a population of drops adhering to the fibres and that this size distribution of drops is some subset of the size distribution in the main stream. Therefore, this model is confined to a sufficiently small concentration of dispersed phase in the entering emulsion, that it does not form a continuum in the bed.

The model took into account coalescence by the following mechanisms:

(a) Impaction:

This method of coalescence occurs when a drop in the

stream collides with a drop attached to a fibre and a coalescence results.

(b) Brownian diffusion:

Collision by Brownian motion can occur between two drops in the stream or between a drop in the stream and a drop on the fibre.

(c) Coagulation in a turbulent field. In this mechanism, drops which are associated in pairs as they are squeezed through the capillary passages of the bed eventually coalesce.

As a first order of magnitude they calculated that the collision frequency due to the impaction mechanism was about 150 times higher than turbulent collision and 10,000 times higher than diffusion. Thus only the impaction mechanism was considered. This lead to their final equations where filtration coefficient for a coalescer λ_c is given as:

$$\lambda_c = \frac{3}{4} \frac{S}{(1-S)} \frac{(1-E)\ (1+{}^{d}10/{}^{d}f)}{d_f} \eta_c \quad \ldots\ldots\ldots\ldots 5.3.1.1$$

for S and η_c constant over the bed length

$$Y = \frac{\mu_o(L)}{\mu_o(0)} = \exp\ (-\lambda_c L) \quad \ldots\ldots\ldots\ldots\ldots\ldots 5.3.1.2$$

This model shows that the performance of a coalescer will increase with (a) decrease in fibre diameter (b) larger mean inlet drop size, and (c) increase in packing thickness, in agreement with experimental results (120).

In the model, in order to keep the study of coalescence in a fibrous bed in perspective with aerosol filtration, the

overall fibre efficiency was defined as:

$$\eta_c = \alpha \beta$$

Calculations indicated that η_c increased with increase in velocity, in agreement with aerosol theory and Hazlett's model(93) but contrary to experimental results with fibrous bed coalescers (82,85,94,95). Clearly therefore the coalescence efficiency predicted from aerosol filtration theory is not applicable to fibrous bed coalescence and a more accurate theory is needed for predicting efficiency.

5.3.2. HAZLETT'S MODEL

Hazlett (83) based his model on three major steps:

(a) Approach of a dispersed water droplet to a fibre,

(b) Attachment of the droplet,

and (c) Release.

The approach process was subdivided into direct interception, diffusion and inertial impaction. Direct interception was the most important step. Diffusion may assist direct interception for submicron drops but inertial impaction was insignificant.

Direct Interception:

Under the laminar flow conditions generally existing in a fibrous bed coalescer fluid will flow past a glass fibre, analogous to a submerged cylinder, in streamlines. The droplets which follow streamlines close to the fibre centre will be intercepted. Using Langmuir's (122) equation to evaluate the interception process:

$$E_s = \frac{1}{2(2 - \ell n R_e)} \left(2 (1 + R) \ell n (1 + R) + \frac{1}{1 + R}\right) \ldots\ldots 5.3.2.1$$

This equation predicts an increase in efficiency with increase in velocity, which is contrary to experimental observations (82,85,94,95). In any case it is misleading to relate bed efficiency to single fibre efficiency because packed bed fibres are orientated at different angles to the flow, and there are many intersections, causing different collection efficiencies; there is also hold up within the bed which alters the effective voidage. With a single fibre in a fixed position there is no significant hold up and there is no variation in collection efficiencies.

The release mechanism was considered to involve coalesced droplets forming threads through the bed until released as individual drops from the exit face. Drop release occurs when the hydrodynamic force exceeds the adhesive force between the drop and the fibre or fibres. The size of the released drop depends upon flow velocity, surfactant content and fibre diameter. Three possible release mechanisms are presented:

(a) Drop-Volume Rupture:

This equates the drag force exerted on the drop with the restraining forces due to interfacial tension. This yields:

$$\frac{C \rho_c V'^2 \pi (\frac{1}{4} (d)^2 - a^2)}{2} = 2\pi a \gamma \ldots\ldots\ldots\ldots 5.3.2.2$$

(b) Drop Elongation Rupture:

This release is due to the effect of the moving fluid

surrounding a drop. For the viscosity ratio of the drop to the continuous phase frequently encountered, 0.5 to 1.0, the elongation at small distortions is proportional to a dimensionless number F:

$$F = \frac{2G\ u_2\ (\frac{1}{2})d}{\gamma} \qquad \text{.....5.3.2.3.}$$

(c) Jet Rupture:

This is the rupture of an extended jet due to Rayleigh instability producing a series of uniform but smaller drops whose size is governed by interfacial tension and nozzle size. Whilst this is a common release mechanism, no equation is presented to describe this process. Thus Hazlett's model is of limited use for designing a fibrous bed coalescer.

5.3.3. ROSENFELD AND WASANS' MODEL

This model (129) is based on the following mechanisms: Droplets impact upon the fibres and adhere; a distribution of retained drops is thus created. Other drops from the main stream impact upon the retained drops and coalesce. Coalescence proceeds until an equilibrium drop size is reached at which the drop is pulled away from the fibre due to the fluid drag.

A design equation was derived based on the following assumptions:

(a) The dispersed phase is dilute and the droplets are small i.e. dispersed phase droplets do not affect the flow of the continuous phase. This is in agreement with observations of

Spielman and Goren (100).

(b) The saturation in the bed is sufficiently small that a continuum of the dispersed phase does not exist.

(c) Approach to a fibre is mainly by the interception mechanism. London Van-der-Waals forces have been shown to be negligible (130). This has been accepted by a number of investigators (81,120,128,131).

(d) When a drop strikes a fibre or a retained drop the probability that it will remain on the fibre, or coalesce with the drop, is a constant for one particular system.

(e) Drops grow by coalescence of a retained drop with drops from the free stream. There is essentially no coalescence between two drops in the field stream, which is in agreement with the experimental results of Sareen et al (81) and Bitten(132)

(f) The drop detaches from the fibre after reaching a critical size. This has been observed in single fibre studies (81,147).

(g) Each drop can be considered independently of the overall distribution. Spielman and Goren (134) found that for dilute emulsions, e.g. 0.1% concentration, provided the dispersed phase viscosity is not too large compared with the continuous phase viscosity, the coalescence efficiency for any given drop size is independent of the size distribution.

A set of equations were formulated and solved to give a final theoretical design equation as follows:

$$\lambda = \frac{8\beta\ (1 - E)d}{\pi^2 E\ (1-S)d_f^2} \times \frac{2d_{fe} + d}{d_{fe} + d} \quad \ldots\ldots\ldots\ldots\ldots\ldots 5.3.3.1$$

Comparison of equation 5.3.3.1 with Spielman's experimental data (95,129,133), showed that it is only valid at low velocities of less than $1.5 \times 10^{-3} ms^{-1}$ for $\beta = 0.24$, when the turbulence in the bed is insignificant. At larger velocities, the effect of turbulence grows until the equation is no longer valid. A purely empirical extension of the above equation is made to fit this data. This leads to:

$$\lambda = \frac{8\beta\ (1 - E)d}{\pi^2 E\ (1 - S)\ d_f^2} \times \left(\frac{V'_{cr}}{V'}\right)^{0.5} \times \left(\frac{2d_{fe} + d}{d_{fe} + d}\right) \quad \ldots\ldots 5.3.3.2$$

Although this theoretical model is an improved version of the Sherony et al (120) model described in Section 5.3.1, various workers (82,95,104,148) have obtained results showing that it is inadequate for velocities > $0.5 \times 10^{-2} ms^{-1}$.

CHAPTER 6

Experimental techniques

CHAPTER 6

EXPERIMENTAL TECHNIQUES

All previous proposals regarding mechanisms of coalescence of secondary dispersions within packings, the effective sites in the packing and the hold up throughout the packing, are theoretically based because of the difficulty of visual observation through the bed.

Information based on behaviour observed near a transparent wall may be misleading since the packing voidage and orientation of the fibres may be different to those within the bed proper. Furthermore the transparent wall has generally been of a different material to the packing and the different surface energies may therefore have created junction effects of the type discribed in Section 3.4.3.

Shahloub's (93) proposals for the mechanisms were based on studies using a conductivity measurement technique. This made use of the principle that for single flow conditions all the pores of the packing were occupied by water; the bed then had a certain conductivity value. When operated under two phase flow conditions, some of the pores were occupied by the oil, thus changing its conductivity. Since the water existed as a film surrounding the fibres, joining them together and thus increasing the conductivity of the whole, the packing conductivity was greater the higher the proportion of water in the pores. Thus the difference between the single phase flow conductivity and

the two phase flow conductivity was related qualitatively to the quantity of oil held up within the pores of the bed. However the study involved different materials such as copper meshes, and p.t.f.e. rings between layers of the packing hence changing the construction and possibly the mechanism of the coalescence, from those for the packing alone i.e. with the same surface energy throughout. The technique enabled the relative amount of the hold-up of the droplets within layers of the packing to be determined, but no real observations could be made of the way that the small droplets coalesced.

To overcome the above difficulties two different techniques were developed in the present investigation to study drop collection/coalescence mechanisms within the bed. The first method involved matching the refractive indices of the packing, its holder and the continuous and dispersed phases. The second technique involved the use of ultrasonic probes to detect the hold-up, the effective collection sites and the droplet growth within the packing.

6.1. REFRACTIVE INDEX MATCHING TECHNIQUE

Under normal conditions the opacity of the packing and of the secondary dispersions, due to the difference in the refractive indices of the packing and the phases under study, make observation through the packing impossible. If however the refractive indices of the packing, its holder and the continuous and dispersed phases are matched the system becomes transparent, and events within the cell will be visible when the dispersed phase is coloured. This is explained in

Section 6.1.3. In such an iso-optic system, distortion of an image by refraction is eliminated.

Several investigators have used iso-optic systems for flow visualisation of simpler systems. De Jong (135) used an aniline dye in crushed optical glass saturated with an ammonia salt solution to study molecular diffusion in porous media. Heller (136) suggested the use of crystalline calcium fluoride for the solid component because of its low refractive index (n = 1.4338) making accessible a large assortment of matching liquids. Calcium fluoride is also relatively insoluble, chemically inert and nontoxic. Cloupean and Klarsfeld (137) used several organic components for the liquid phase with various types of commonly used glasses in the form of microballs, filters or powder for the study of two dimensional thermal phenomena in saturated porous media. The refractive index matching enabled the visualization of a certain number of isotherms as bright lines of different colours. Handley (138) studied the motion of tracer marked fluid and particles in a fluidised bed using the iso-optic system methyl benzoate/Soda glass. Hummel et al (139) studied fluidised bed behaviour with the iso-optic system naphthalene in decalin/methyl methacrylate. Vignes (140) refers to the work of Viglecca (141) in which an attempt was made to produce an iso-optic system for packed column liquid-liquid extraction studies; success was limited to the matching of a liquid phase to a solid packing. Davies et al (142) investigated coalescence in close packed dispersion bands of primary sized drops in spray columns and gravity settlers using two liquid phases of matched refractive

index.

All these investigators used iso-optic systems consisting of a solid packing and a liquid phase, and also systems consisting of two liquid phases. As part of the present study this was extended to produce an iso-optic system consisting of two liquid phases and an efficient coalescing media.

6.1.1. THE PACKING

The choice of system was constrained by the packing material because any specific solid has a fixed refractive index. The packing must be an efficient coalescer for secondary dispersions with the lowest possible refractive index. It must also be inert to chemicals, non-absorbant and possess the tendency to become transparent in the liquid-liquid system. Therefore the choice was limited. There are many plastics with refractive indices ranges from 1.37 to 1.60 which could be used for the packing and made transparent provided that they are either in an amorphous state or have a crystalline structure smaller than the wave length of the incident light. Of synthetic rubbers only silicone rubber (RI=1.42) is transparent.

Only one plastic, methyl methacrylate (RI=1.49) is normally manufactured in the transparent amorphous state. However, crystalline polymers may be rendered transparent by heating above the melt temperature, at which there is transition to the amorphous state, followed by rapid quenching to room temperature. Polypropylene RI=1.49 may be prepared in thin transparent films in this manner. Further polytetrafluoroethylene (p.t.f.e.) (RI=1.376), Polychlorotrifluoro-ethylene (p.c.t.f.e.) (RI=1.43)

tetrafluoroethylene (RI=1.338) or polyformaldehyde (RI=1.41) could be useful if they were either made in an amorphous state or the quenching technique could be applied to them to prepare an amorphous state. However, neither the packing nor the holder could be manufactured in an amorphous form; with the possible exception of silicone rubber which is manufactured in an amorphous form but which is not inert to most solvents.

Fibrous glass coalescers have very favourable properties for the separation of secondary dispersions. Glass fibres from glass with refractive indices ranging from 1.48 to 1.60, are manufactured in several diameters from 2 μm upward. Further the packing could be placed in a glass holder to eliminate extraneous coalescence effects due to junctions between two different energy surfaces. In practice the packing was matched in refractive index to that of the liquid system; the container was hence matched automatically which eliminated the lens effect of the holder.

Several fibrous glass materials were considered and the one with the lowest refractive index, about 1.50, was selected. This was pure soda lime silicate type of about 10 μm diameter. This packing is described further in Section 8.1.2.

6.1.2. LIQUID-LIQUID SYSTEMS

Due to the relatively high refractive indices of fibrous glass materials few immiscible liquid-liquid systems were available which could be matched in refractive indices to those of fibrous glass. Although there are several suitable liquid packing systems (i.e. one liquid matched with packing) not

many liquid-liquid packing system could be found. However after an intensive literature survey a few liquid-liquid systems were considered to possess the same refractive indices and for one liquid a mixture of Analar grade potassium thiocyanate and formamide was used and for the other O-xylene plus Analar xylene were used. The concentrations and the physical properties of this system and all other systems considered are given in Tables 8.1 and 8.2.

6.1.3. DISPERSED PHASE VISUALIZATION

Having made the packing and the flow transparent by matching the refractive indices the dispersed phase could be made coloured by an ordinary dye or a phototropic dye.

A phototropic dye is one that changes from a colourless to a coloured form by exposure to light. After the irradiation source is removed the dye reverts to its original colour. Generally the forward reaction is instantaneous but the reverse reaction is slower and depends on the concentration of the dye and the intensity of irradiation. Most dyes were found to be activated by light in the region of ultraviolet. Some dyes are phototropic in the solid state only and others are phototropic when dissolved in a solvent. A survey by Exelby and Grnter (143) lists various types of dye, properties and their phototropic behaviour.

Hummel et al (144) claimed to have utilized the phototropic properties of 2- (2',4'-dinitrobenzyl) pyridine (DNBP) to measure the mean velocity profiles in a vertical glass tube of 1.226 cm^2 cross section. The dye was dissolved in 95% alcohol and was activated using a pulsed ruby laser with a second harmonic

generator to reduce the wave length of the laser light from 6943A to 3471A. A still camera was used to record the event.

Zolotrofe and Scheele (145) used an ultra violet sensitive photochromic spiropyran to measure the velocity profiles of organic liquids in pipes using high speed photography.

6.2. MEASUREMENT OF DROP SIZE IN LIQUID-LIQUID DISPERSIONS BY ULTRASONICS

A further method used to detect the hold-up sites and the droplet growth within the packing, made use of ultrasonic probes. Measurement of drop size in liquid-liquid dispersions by means of acoustics depends upon the difference in elastic properties between the continuous and dispersed liquid phases and upon the consequent difference in the velocities of transmission of longitudinal acoustic waves (146). The relationship between acoustic velocity and liquid properties is $v^2 = \frac{1}{\rho K}$ where ρ is the mass density and K is the elastic modulus. A longitudinal acoustic wave tranversing a region in which the droplets of dispersed phase are large in size compared with the length of the wave passes through regions of each fluid successively. Its velocity of transmission is given by:

$$\frac{1}{v} = \frac{c}{v_1} + \frac{1 - c}{v_2} \qquad \text{.....6.2.1.}$$

where v_1 and v_2 are the velocities in the pure dispersed phase

and pure continuous phase respectively and c is the volume fraction of dispersed phase in the mixture. When droplets are small in size compared with the length of the acoustic wave, a more complex relationship is appropriate. Based on the assumption that the dispersion behaves as a homogeneous fluid with the combined properties of both liquid phases, the velocity of the acoustic wave is defined by:

$$\frac{1}{v^2} = c\rho_1 + (1-c)\rho_2 \quad \frac{c}{\rho_1 v_1^2} + \frac{1-c}{\rho_2 v_2^2} \quad \ldots 6.2.2.$$

The composition of a mixture can be deduced from the acoustic velocity in it if the velocities in the two pure components are known. Acoustic velocity can be measured by finding the wave length at a fixed frequency.

By choosing a separation of several wavelengths between transmitter and receiver, readily measurable changes in phase angle and good resolution of concentration can be obtained. Accepting the linear relationship between composition and phase angle, the concentration is given by:

$$c = \frac{\theta_2 - \theta}{\theta_2 - \theta_1} \quad \ldots\ldots\ldots\ldots\ldots\ldots\ldots 6.2.3.$$

where θ_1 and θ_2 are the measured phase angle for pure dispersed liquid and pure continuous liquid respectively.

Drop size:- As flow of the disperse system sweeps the space between the faces of the transducers, drops of dispersed liquid enter and leave this sample volume, there follow appreciable

variations in the composition of the sample space. A variance in composition dependent upon the sizes of the droplets of the dispersed liquid, is superimposed on the time-averaged composition. If the sample space is occupied by droplets of dispersed phase and segments of continuous phase of the same size as the droplets, a binomial probability mechanism for occupation of the volume gives the composition variance as:

$$S^2 = c(1 - c)/n \quad \text{.....6.2.4.}$$

where n is the number of droplets and segments required to fill the sample volume.

Measurement of this composition variance allows the average drop volume to be deduced from the relationship:

$$\frac{\pi d^3}{6} = \frac{\pi D^2}{4} \times \frac{1}{n} \quad \text{.....6.2.5.}$$

where d is the droplet diameter and D is the diameter of the transducer disc and X is separation of transducer faces.

Linearity of phase angle with composition of the dispersion has been confirmed (146) in the systems kerosene-water and tetrachloroethene-water with droplet size ranging down to below 1mm in diameter.

In this work the above technique was developed further to detect droplets captured and/or passing through the bed. The experimental procedure and observations are given in Section 8.2.

CHAPTER 7

Experimental investigation

CHAPTER 7

EXPERIMENTAL INVESTIGATION

Most experiments in the study of coalescence of secondary dispersions in glass fibrous beds have been conducted using packings of loose chemically-bonded glass fibres (81,93). These proved efficient but, due to the difficulty of obtaining reproducible voidage and pore size distributions across the cell for different heights, the correlations obtained were of limited accuracy. Furthermore the distribution of resin through the bed, and its effect on individual fibre performance, was not studied.

A novel knit fibrous glass packing was used in the present study. It was placed in a specially designed glass holder. Equipment was then constructed to produce both oil-in-water and water-in-oil dispersions to pump through the packing vertically in either direction.

7.1. EXPERIMENTAL EQUIPMENT

To minimize contamination to the liquid-liquid system, the materials of construction were restricted to glass, stainless steel, p.t.f.e., and a very small amount of Viton for pump glands.

7.2. GENERAL ARRANGEMENT

The equipment is shown schematically in Figure 7.1. and the general arrangement is illustrated in Figure 7.2.

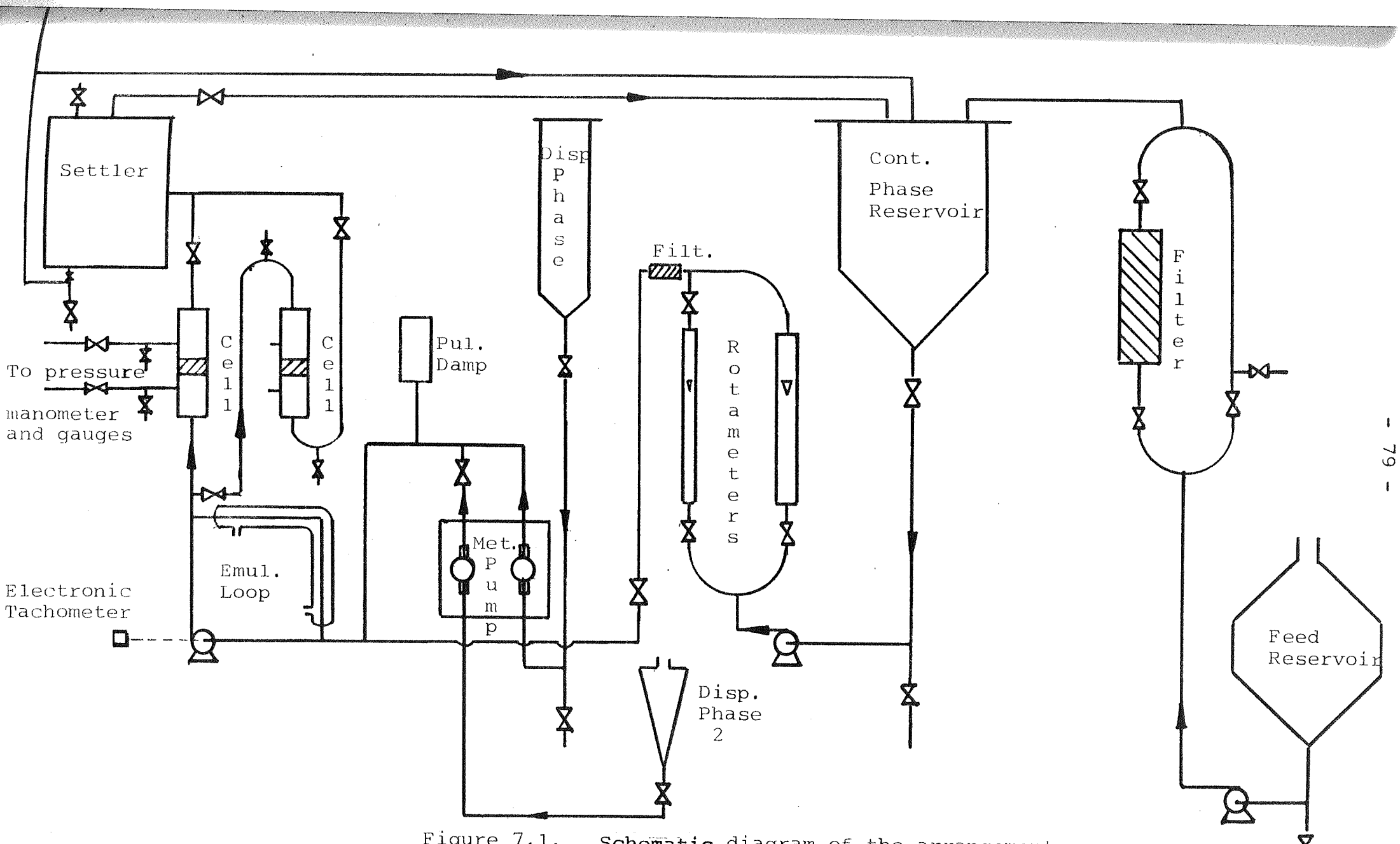

Figure 7.1. Schematic diagram of the arrangement

Feed section and continuous phase section situated on the right, dispersed phase section in the middle. Emulsification loop, packings and settler on the left of the diagram. Pressure gauges and manometers are not shown.

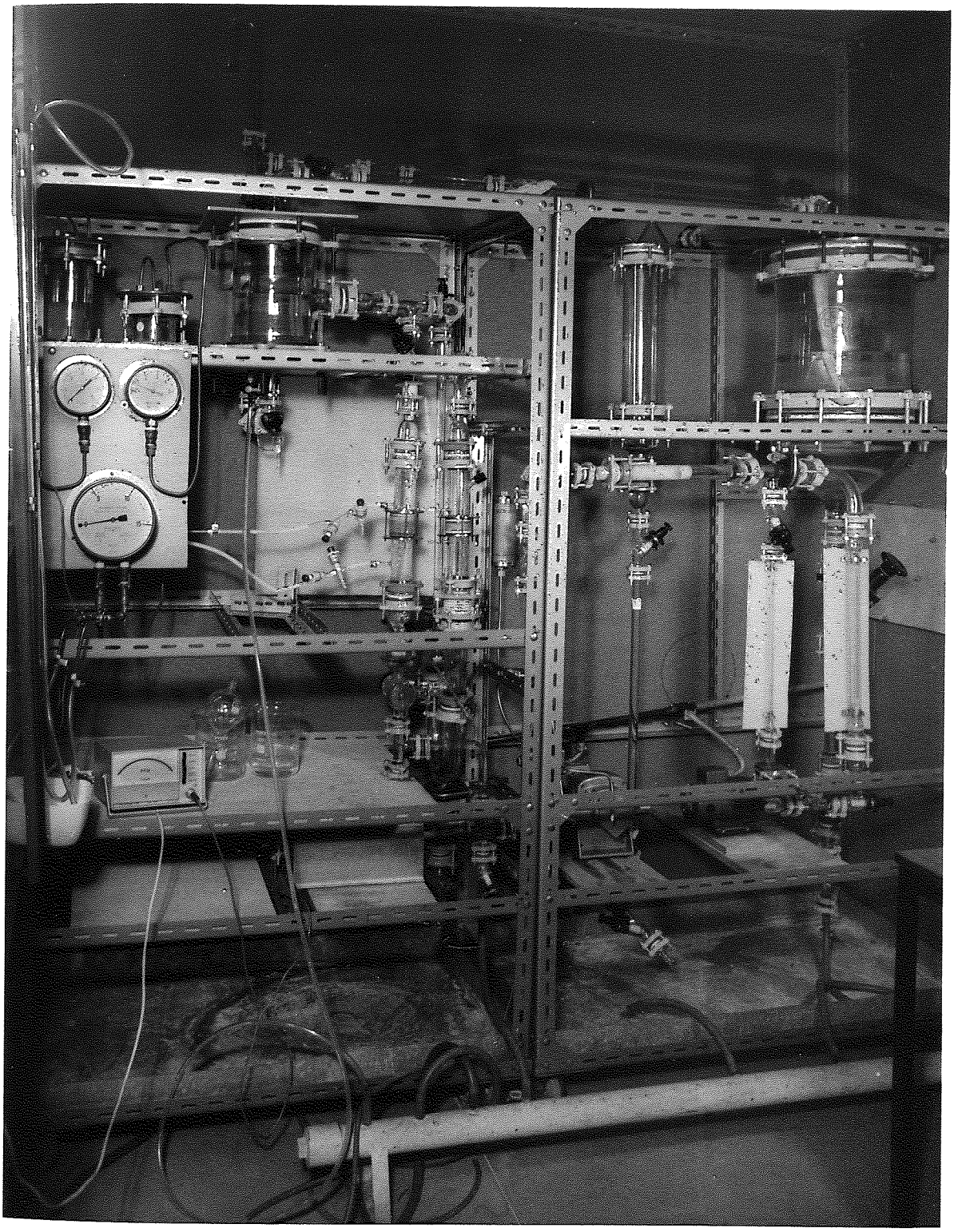

Figure 7.2. General arrangement of equipment

Phase reservoirs and transfer pumps are on the right. Dispersion generating loop and coalescer cells are mounted in the middle.

The equipment was installed in a hardboard cabinet to exclude draughts and light. This limited any deterioration of the liquid-liquid system due to the effect of light. Darkness was also necessary for the refractive index matching experimentation discussed in Chapter 8. Temperature control, by cooling was found to be necessary because of the energy imput from the centrifugal pumps. The temperature was controlled by a parallel tube heat exchanger in the emulsification loop shown in Figure 7.4. This method of temperature control was found to be very effective and controlled the temperature within $\pm$ 0.5^{o}C.

Pressure drop across the packing was determined using two interchangeable 1m long U tube manometers; one was filled with water, for low pressure drops and the other with mercury for higher pressure drops. Manometer readings were checked using two pressure gauges in the range 0 to 2.1 x 10^{5} Nm^{-2} at the high pressure end, and 0 to 3.4 x 10^{4} Nm^{-2}, at the low pressure end. A further check was made using a differential pressure gauge in the range 0 to 1.03 x 10^{5} Nm^{-2}. These instruments were connected via two reservoirs which prevented the process liquids entering the manometer and/or gauges and also acted as 'shock absorbers', that is, to damp out minor fluctuations and give stable readings.

7.2.1. FEED SECTION

The feed section, Figure 7.3., consisted of a 1.5 x 10^{-2} m^{3} capacity container, constructed from two QVF industrial glass reducers, connected to a Stuart Turner No.12 centrifugal pump. This pumped the feed through a fibrous glass cartridge filter

Figure 7.7. Feed section arrangement

Two flame proof lights are mounted to provide rear illumination.

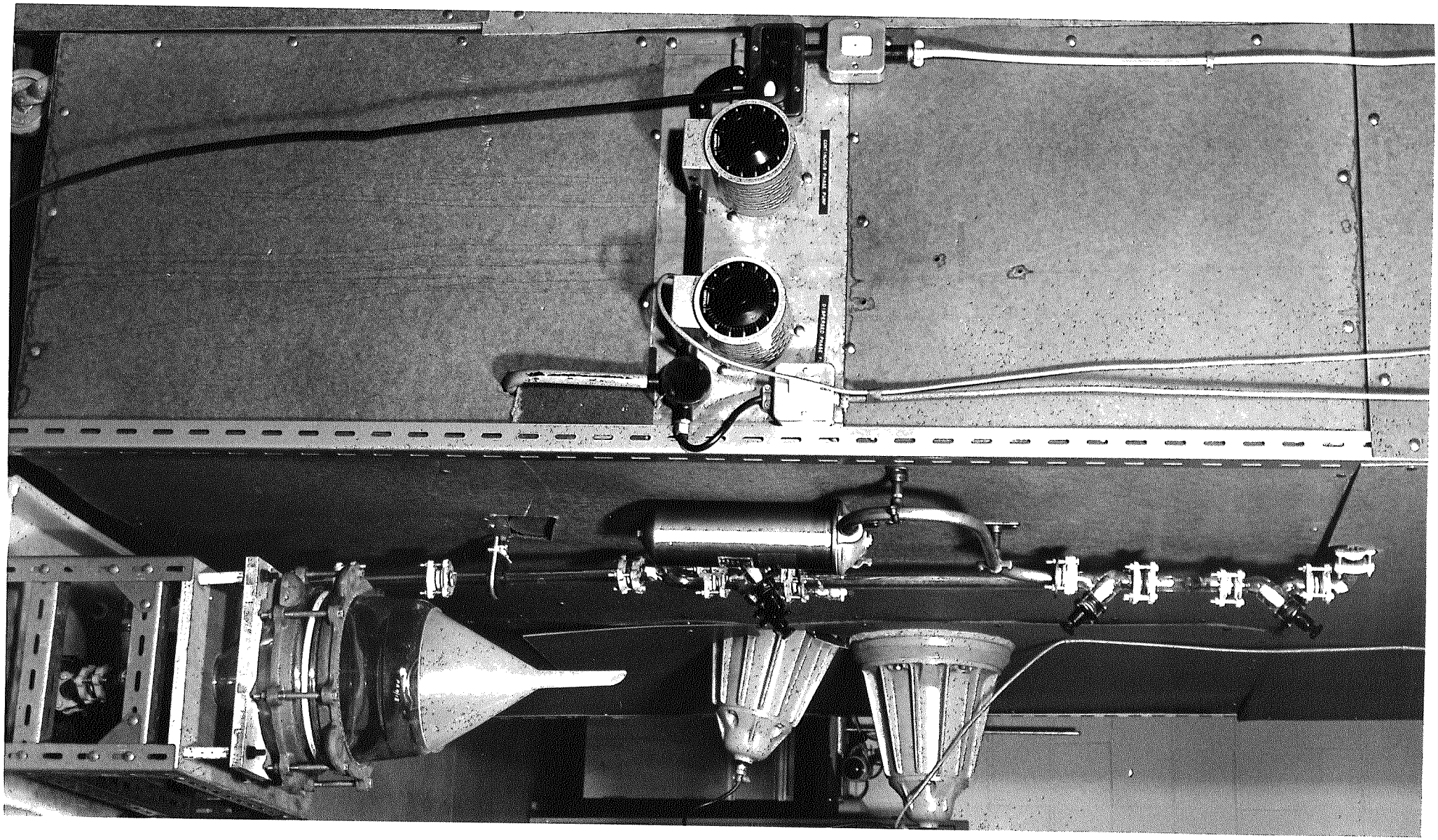

with a stainless steel jacket which retained any solid particles larger than 1 μm in diameter.

7.2.2. CONTINUOUS PHASE SECTION

The continuous phase reservoir consisted of a 30 x 10^{-2}m diameter QVF glass column with stainless steel end plates. This had a capacity of 50 litres. Continuous phase was pumped via a Stuart Turner No.12 stainless steel centrifugal pump with Viton seals. This was capable of transferring a maximum flow rate of 54.5 l/min against a head of 3.0m or a flow rate of 11.4 l/min against a maximum head of 13.7m. The rate was controlled by two QVF industrial glass valves and flow was measured by two K14 and K7 rotameters with Koronite and stainless steel floats respectively; these covered a range of 0 to 56 x $10^{-6}m^3s^{-1}$. As well as earlier filter discussed in Secion 7.2.1. the continuous phase was filtered further by passage through a specially designed pure fibrous glass packing, made of 10 layers of the knitted fibrous glass placed in a 2.5 x 10^{-2}m i.d. glass pipe section. This filter eliminated any residual particulate matter which could have caused blockage of the pores of the coalescer and hence affect reproducibility of the results.

7.2.3. DISPERSED PHASE SECTION

The dispersed phase reservoirs comprised one 5 x $10^{-3}m^3$ and one 5 x $10^{-4}m^3$ capacity glass containers. Each reservoir was provided with a glass fibre filter to retain particulate

matter > 0.1 μm in diameter. The dispersed phase was metered by a Micro Metering Pump series II type manufactured by Metering Pumps Ltd. This had two units, one long-stroke and one short-stroke, both having stainless steel pump heads. The ranges of flow rate were 0 to 8.7 x $10^{-7} m^3 s^{-1}$ and 0 to 2.6 x $10^{-7} m^3 s^{-1}$ respectively. These ranges were reduced in the ratio of 5 to 1 by means of a reduction capsule gear when required. The pump delivery lines were also provided with,

1. A pulsation damper (type PD 25).
2. Two stainless steel back pressure valves, one for each pump head.
3. A safety relief valve set to 25p.s.i.g.
4. Two outlet points to facilitate direct calibration of flow rate versus vernier setting on the pump stroke.

Each of the dispersed and continuous phase reservoirs were connected via a QVF 'T' piece to the emulsification loop.

7.2.4. THE EMULSIFICATION LOOP

The formation of an emulsion by the application of high shear was discussed in Section 2.2.2. Previous work (93,125) proved the practicability and reliability of emulsion production by circulation in a loop using a centrifugal pump. Therefore this technique was adopted in this work.

The emulsification loop is shown in Figure 7.4. It consisted of a Stuart Turner No.12 stainless steel centrifugal pump fitted with an electronic tachometer; this tachometer was activated by reflection of light from a line painted on the pump shaft. The pump speed was varied in the range of 16 to 83 revs s^{-1} and

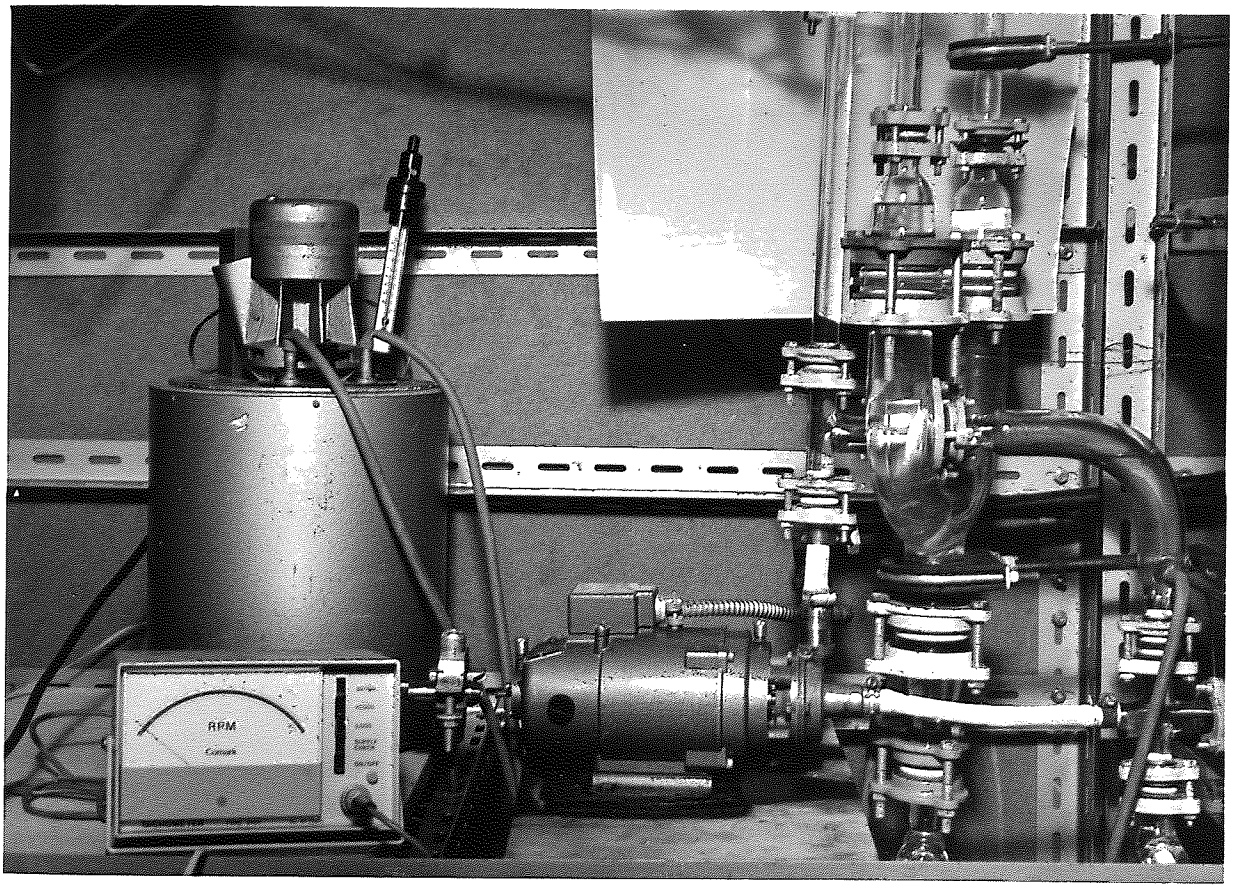

Figure 7.4. Arrangement of the emulsification loop

Pump with loop. Electronic tachometer for pump speed measurement. Heat transfer reservoir for temperature control (left background).

the drop size distribution was found to vary with pump speed as described in Section 9.2.

7.2.5. PACKING SECTION AND SETTLER

Provision was made for the dispersion from the emulsion loop to flow through the packing vertically upwards or downwards depending upon whether the dispersed phase was the heavier or lighter phase. The settler comprised a 6 inch diameter QVF industrial glass T-piece with stainless steel end plates. Provision was made for continuous phase recycle from either the top or the bottom dependent upon its relative density.

7.3. COALESCER CELL/HOLDER

During preliminary experiments it was observed that a junction between two different surface energy materials had a significant effect upon coalescence of the secondary dispersion droplets. Hence the junction between the glass section and the p.t.f.e. gasket inserted before the coalescer was found to act as a coalescer. To eliminate such extraneous junction effects, and to observe coalescence in the packing only, a glass packing holder was therefore designed. This comprised a 5×10^{-2}m i.d. glass section cut to the appropriate height and placed between two pieces of 4×10^{-2}m glass piping having platforms and side arms. A pair of split flanges were designed to hold the pieces together using a very thin layer of non-reactive, non-surfactive Adhesive AV138 and HV998. The coalescer cell/holder arrangement is shown in operation in Figure 7.5.

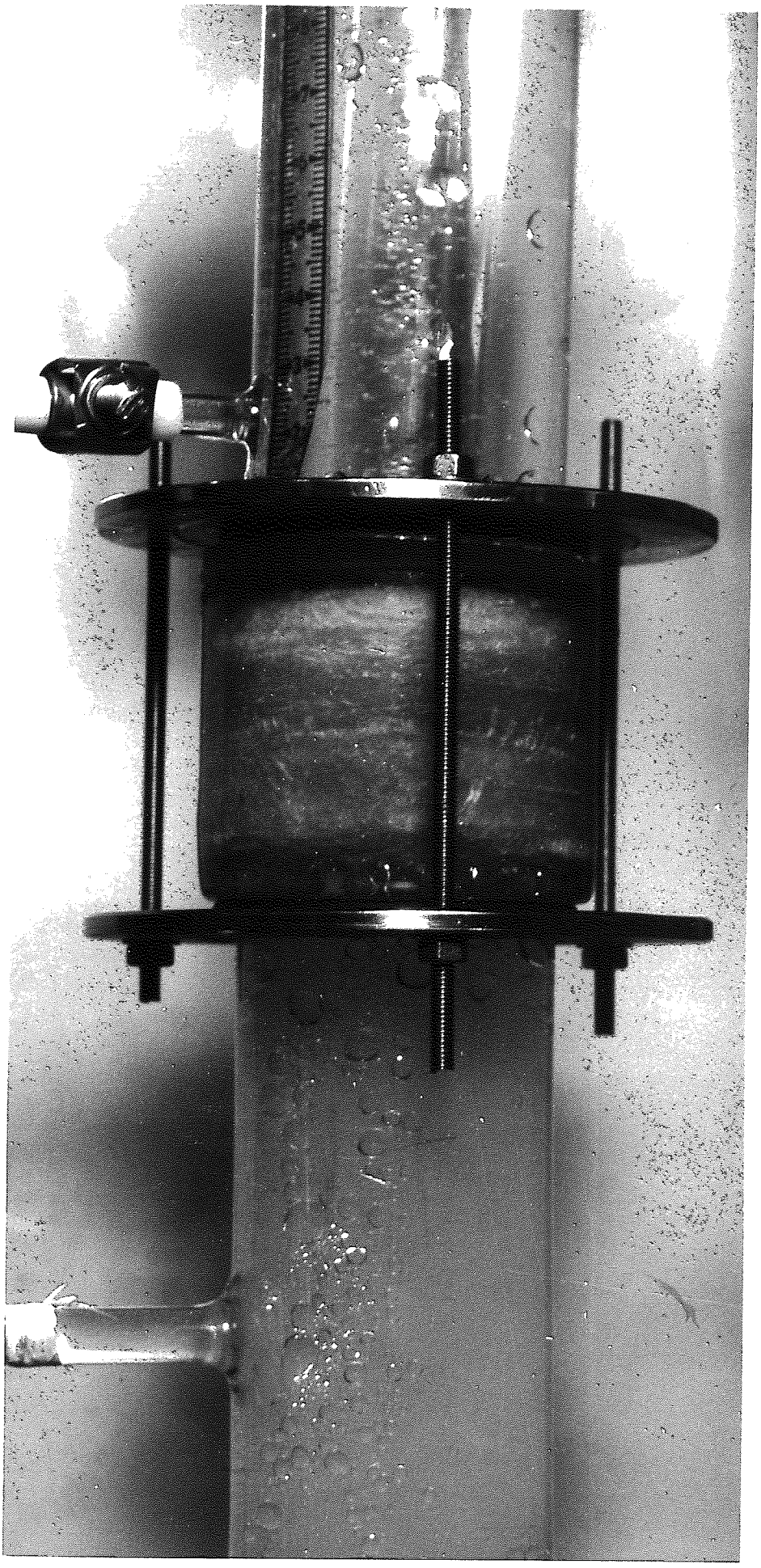

Figure 7.5. Arrangement of the coalescer cell/holder Secondary dispersion entering from below and coalesced drops leaving the upper face under gravity.

7.3.1. PACKING SELECTION

The coalescence cells comprised texturised pure glass fibre manufactured by Mar Glass. It had a thickness of 1mm ±10% and a weight of 390g/m^2 ±10%. The strength was of 242 kgf/5 cms/warp and 89 kgf/5cm/weft. The mean fibre diameter was 6 μm.

This material was selected because the large number of intersections between fibres was expected to provide numerous coalescence sites and hence a high efficiency. It also had a constant voidage and pore size, an essential requirement for reproducibility of results. Figure 7.7. shows a Stereoscan of the material used. Unlike the resin bonded fibre glass used by earlier workers (81,93) this packing was unbonded which eliminated potential contamination of the liquid-liquid system. Variation of surface energy across the bed, due to the difference between glass fibre and resin was also eliminated. Figure 7.6 is a Stereoscan photograph of bonded glass fibre; the presence of bonding resin is clear from this photograph by comparison with Figure 7.7.

7.3.2. PREPARATION OF COALESCER CELL

Each layer of packing was punched out from a sheet of the material using a 5 x 10^{-2}m diameter hardened, carbon steel punch specially made to cut circular pieces to fit the packing holder. The layers were pressed together to give the required height. The cell was then placed between the two pieces of 4 x 10^{-2}m i.d. QVF glass as described in detail in Section 7.3. The thickness

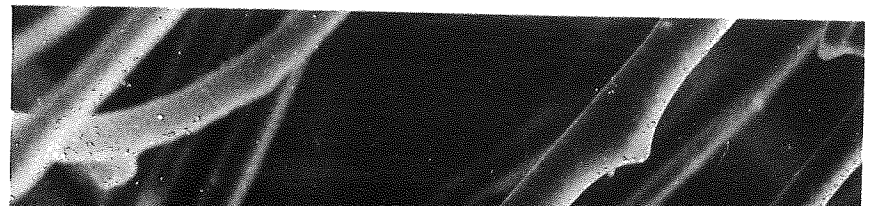

Figure 7.6. Stereoscan of resin bonded loose glass fibres, the fibres are covered with an irregular film of resin and there are random deposits throughout the packing.
Magnification: 1400x

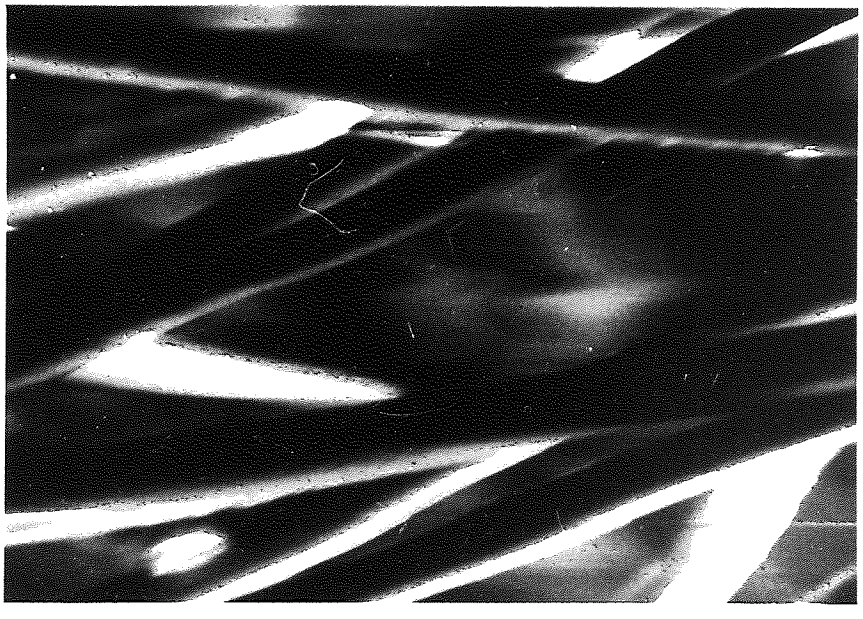

Figure 7.7. Stereoscan of the texturised glass fibres used in this work.

Magnification: 1400x

of each circular piece was about 1mm; therefore packings were made by placing each layer in 1mm height i.e. 40 layers in a 40mm height holder. This arrangement was found to perform better than when packings were compressed further to give 40 layers in a 20mm packed height.

During experimentation, droplet release mechanisms of the type described in Chapter 5 were found to be a major factor affecting outlet drop size. The outlet surface played an important role in the release mechanism and hence in the sizes of exit droplets. To study the effect of changes in the outlet surface upon the release mechanisms, the pores on the surface were carefully shaved off using an electric shaver to give a smooth surface. In a subsequent experiment they were further roughened using a brush.

7.4. SELECTION, HANDLING AND PREPARATION OF LIQUID-LIQUID SYSTEMS

The organic systems selected covered a range of relevant physical properties. Interfacial tension values were in the range 8×10^{-3} to $35 \times 10^{-3} Nm^{-1}$ viscosity values were in the range of 0.5×10^{-3} to $7.6 \times 10^{-3} Kgs^{-1}m^{-1}$ and density difference values were in the range 0.8×10^{3} to 1×10^{3} Kgm^{-3}. In one set of experiments filtered, de-ionized, distilled water was used as dispersed phase; in all other experiments it was the continuous phase.

The organic liquids and their physical properties are listed in Appendix C. These systems were all convenient to use; all being relatively non-toxic, non-corrosive and available to a fixed specification at low cost.

Prior to use, the organic phase was distilled with a distillation cut of $\pm$ 1°C around its theoretical boiling point and stored in clean, sealed dark-glass containers to eliminate the possibility of deterioration due to exposure to sunlight.

Coulter Counter Analysis of distilled water produced by a standard laboratory distillation column showed that it contained a small amount of particles larger than 1 μm. These could have entered the water from the atmosphere. This distilled water was considered unsuitable since on passage through the packing the particles would have been captured and hence change the pore size and pressure drop characteristics. Great care was therefore taken to obtain pure, uncontaminated water. Mains water was continuously passed through a filter to retain all particles > 10 μm; it was then de-ionized and distilled. Distillation was at a rate of 8 litres per hour with collection in a special sealed container of 40 litre capacity.

Periodic checks of phase purity were carried out using a 'Du Nuoy Tensiometer' to determine interfacial tension values.

7.5. CLEANING PROCEDURE

The following procedure was adopted to clean all parts of the equipment in contact with the liquid phases.

Before each set of experiments the equipment was flushed through with hot distilled water. It was then filled with a 2% solution of Decon 90 in distilled water and allowed to soak for two days with periodic recirculation of the cleaning solution. After soaking the equipment was drained and rinsed with distilled water several times to eliminate any residual surface active

compounds which could affect coalescence behaviour as discussed in Chapter 2.

7.6. OPERATING PROCEDURE

On start-up the continuous phase was first pumped through the coalescence cell at a superficial velocity of $7 \times 10^{-2} ms^{-1}$ and allowed to recirculate for thirty minutes. This removed any air bubbles trapped in the bed. The continuous phase flow rate was then varied and single phase pressure drops across the packing were determined for incremental increases in flow rate.

The continuous phase flow rate was then adjusted to a set value and the dispersed phase was metered in at a rate to give the required phase ratio. The mixture passed into the emulsification, temperature-control loop containing the variable speed centrifugal pump. For each value of phase ratio the emulsification pump speed was increased incrementally and a sample of the dispersion collected for inlet drop size analysis as described in Section 7.7. This procedure was repeated for several phase ratios between 0.1% - 3% and for a constant phase ratio at different flow rates.

Each dispersion, produced by operating the recirculation pump at a speed preset to achieve the required drop size distribution, was passed through the coalescence cell until steady state was attained. Steady state conditions were judged to have been achieved when the pressure drop and mean exit drop size remained constant with time. Photographs were taken of droplets leaving the exit side of the bed for size analysis, as described in Section 7.8. Samples were also taken from the outlet to determine whether any secondary dispersion was present;

this is fully discussed in Section 7.7. The pressure drop across the packing was also recorded. Experiments were repeated for different flow rates at a constant phase ratio and constant inlet drop size distribution.

The same operating procedure was used with cells having different packing heights but with a constant voidage. Four different liquid-liquid systems were used. The flooding characteristics of the packing were investigated in each case by increasing the dispersed phase up to 50% phase ratio.

The mechanisms of outlet droplet release with each packing and liquid-liquid system were carefully observed and photographed over the complete range of operating parameters.

7.7. INLET DROP SIZE ANALYSIS

The distribution of drop size in a secondary dispersion is of particular relevance to the study of the performance of any coalescer element. The various methods for particle size analysis; are reviewed elsewhere (93); in this work a Coulter Counter and microscopy were used. The use of the Coulter Counter and its reliability for micro-size drop analysis has been demonstrated earlier (93). The Counter (Figure 7.8) was a model ZB, ex Coulter Electronics Ltd., and had an access for a model M2 volume converter which eliminated up to 90% of operator responsibility for computation; this facilitated particle size analysis over the range 0.6×10^{-6} to 300×10^{-6}m.

The correct operation of the Coulter Counter and its application for drop size analysis are fully discussed in

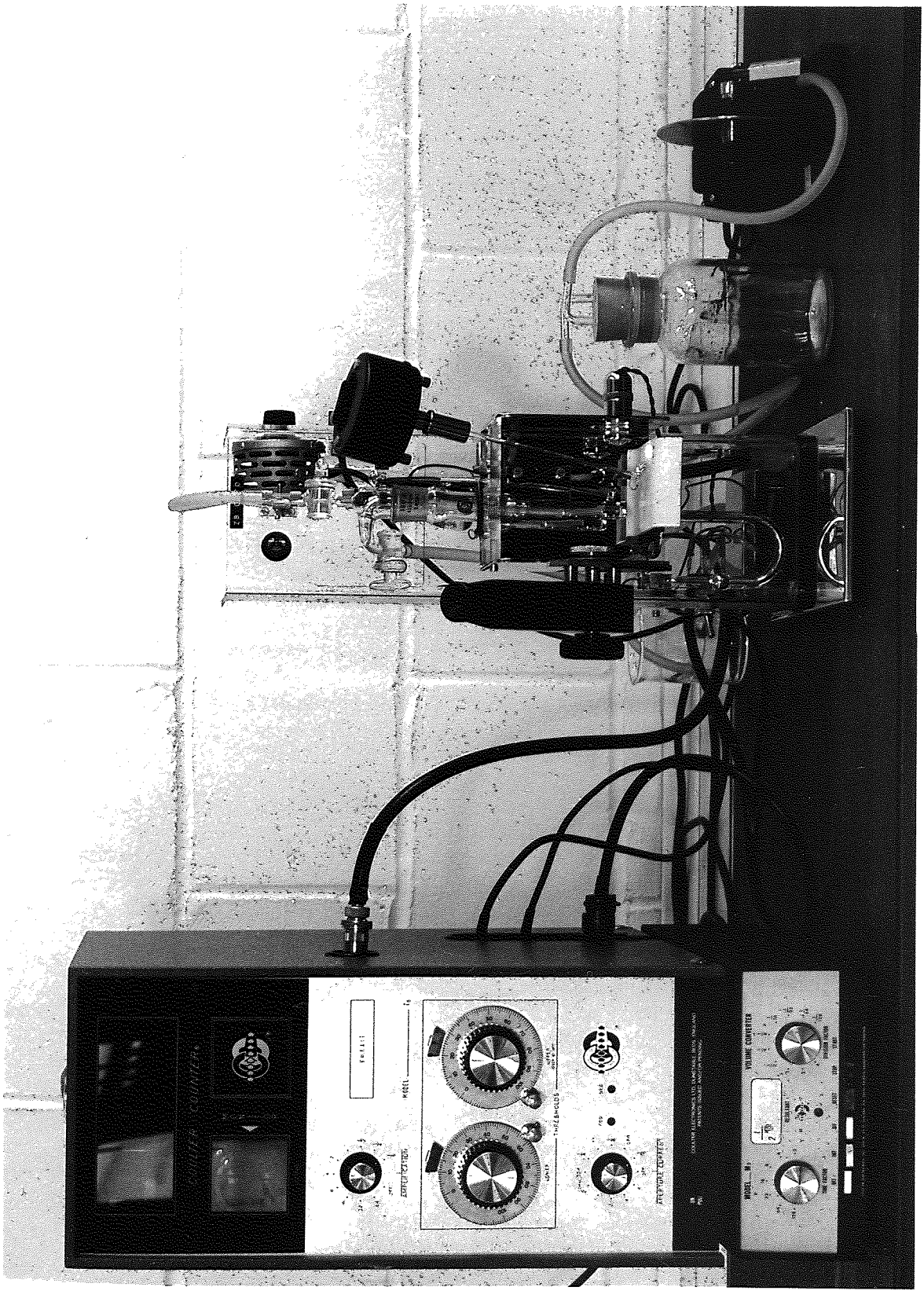

Figure 7.8. Coulter Counter Model ZB with M2 volume converter

Appendix A.

Samples for inlet drop size analysis were taken via the sampling valve positioned just before the dispersion entered the packing. Each sample was immediately stabilized to avoid coalescence prior to analysis; this involved direct transfer into a specially prepared solution of 0.9% sodium chloride and surfactant i.e. 3-5 drops Hyamine 2389. This electrically conductive solution was then analysed using the Coulter Counter, dilution with more electrolyte or concentration with more dispersion being made when necessary as discussed in Appendix A.

Unfortunately Coulter Counter application is limited to oil-in-water emulsions since the sample must be diluted with an electrolyte before examination. Therefore a microscopy technique was adapted for drop size analysis of water-in-oil emulsions. A sample of the emulsion was placed in the small depression in a glass slide. The slide was placed under a microscope and several photographs taken of various areas of the sample using a magnification of x 1000. A photograph was also taken of a calibrated graticule at an identical magnification. A full size analysis of drops was carried out using a Zeiss TG3 particle counter, as described for exit drop size analysis in Section 7.8.

7.8. EXIT DROP SIZE ANALYSIS

A metal rod of known diameter was suspended in the column near the exit of the packing and at a distance of 2×10^{-2} m from the column wall. Photographs of the outlet dispersion were then taken by focussing on the rod using a Nikkormat

still camera fitted with an f3.5, 55mm Nikkor lens. The film used was Kodak Trix-pan 35mm., 400 A.S.A. and a shutter speed of 0.5×10^{-3}s was found to give adequate definition. Illumination was provided from the rear of the column by light diffused through a 2mm polypropylene sheet to give uniformity. Negatives were printed on grade 4 'Bromesco' paper to give an overall magnification of about 3x. At least 300 drops were counted for each event, the magnification being determined from the dimensions of the suspended rod. A computer program was used to analyse the measurements as described in Appendix B.

Samples of outlet dispersions were also collected in a separating flask and the continuous layer was analysed on the Coulter Counter as discussed in Section 7.7., to determine whether secondary dispersion was present.

CHAPTER 8

Experimental techniques for the investigation of the separation mechanisms within the fibrous glass cell

CHAPTER 8

EXPERIMENTAL TECHNIQUES FOR THE INVESTIGATION OF THE SEPARATION MECHANISMS WITHIN THE FIBROUS GLASS CELL

The mechanisms of collection, coalescence and travel of droplets within a fibrous glass packing were studied using pilot scale equipment. Two novel procedures were adapted for this purpose, refractive index matching and an ultrasonic technique. The bases for these techniques are given in Chapter 6.

8.1. REFRACTIVE INDEX MATCHING TECHNIQUE

This involved arranging for the packing, which was originally white and opaque, to become transparent when a specific liquid-liquid dispersion was passed through it. This required a liquid-liquid-packing system in which each component had the same refractive index. The packing was fibrous glass with a fixed refractive index, therefore the choice of a liquid-liquid system to match it was limited.

8.1.1 EXPERIMENTAL EQUIPMENT

The equipment used to investigate separation mechanisms within the packing is shown in Figure 8.1. A flow diagram of the arrangement is shown in Figure 8.2. This was as described earlier, in Sections 7.1 and 7.2, with the following minor modifications:-

a) The continuous phase reservoir and transfer pump were not used and were isolated by a valve.

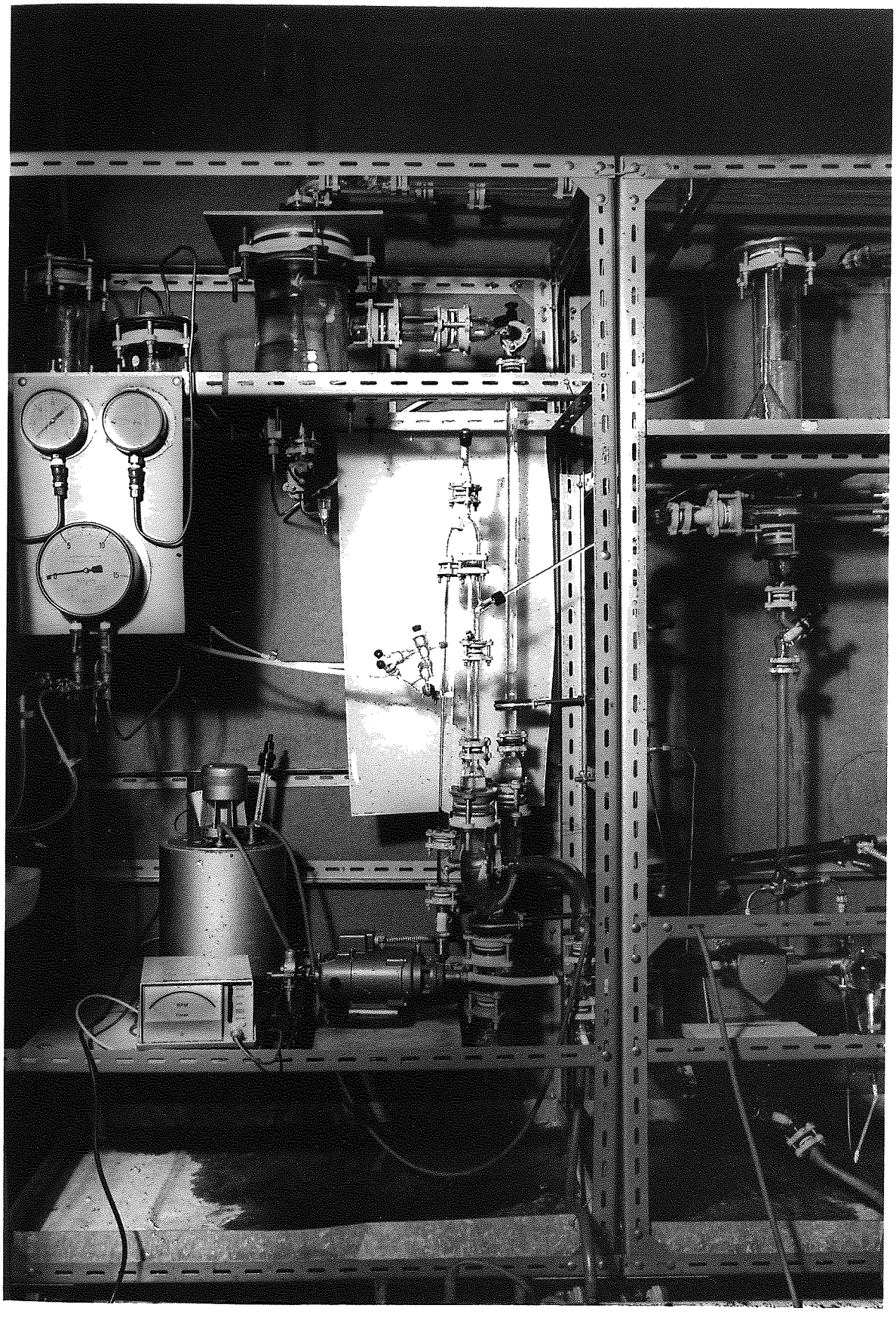

Figure 8.1. Part of the equipment used for Refractive Index matching

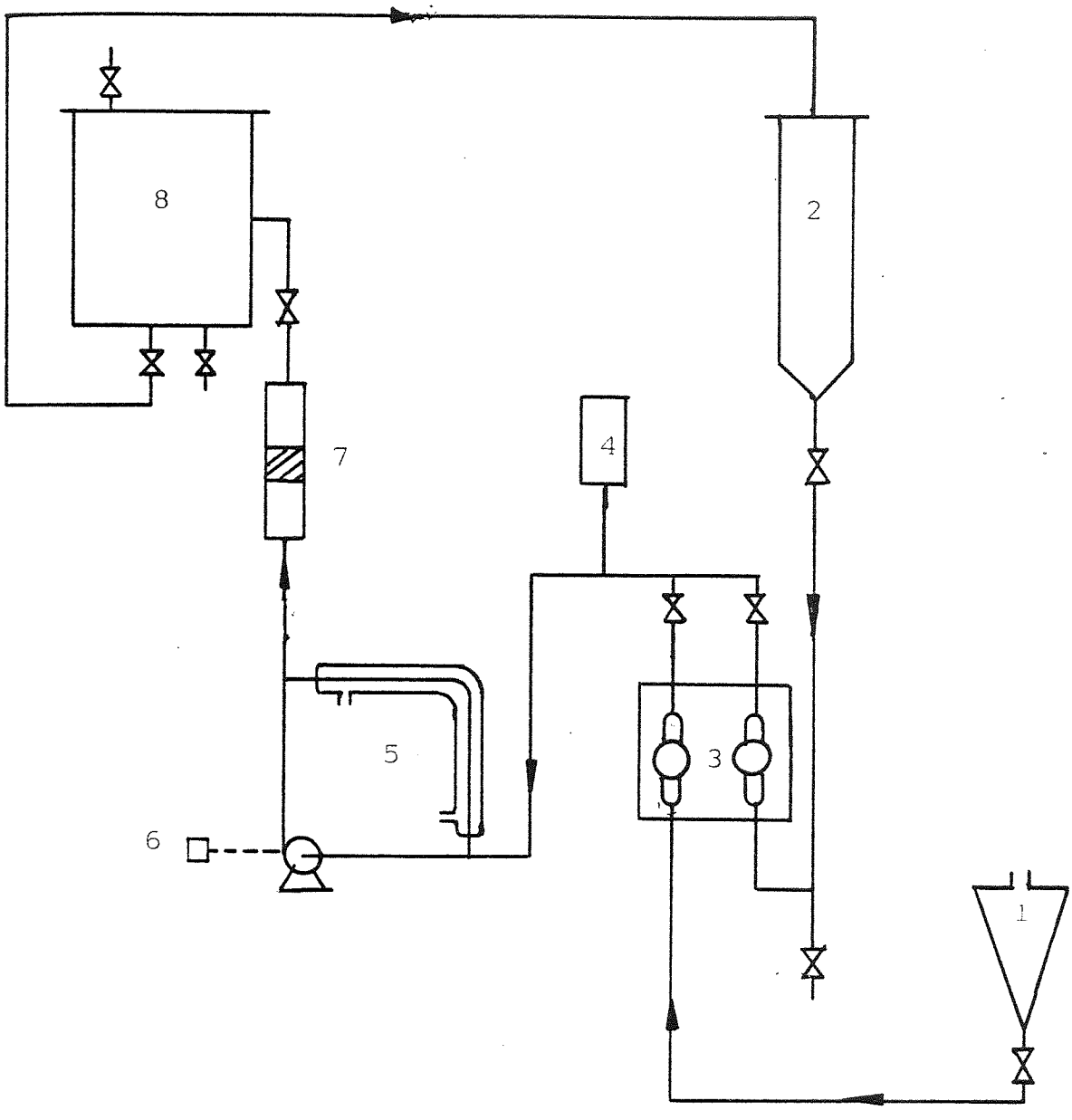

Figure 8.2. Flow diagram of flow system

1. Disperse phase reservoir
2. Continuous phase reservoir
3. Metering pump
4. Pulsation damper
5. Emulsification loop with a cooling jacket
6. Electronic tachometer
7. Coalescer cell
8. Settler

b) The larger of the two dispersed phase reservoirs described, in Section 7.2.3 was used for the continuous phase and the small reservoir for the dispersed phase. Both phases were transfered by the metering pump discussed in Section 7.2.3.

8.1.2 PACKING/PACKING HOLDER

Packing was prepared from pure glass wool with an average fibre diameter of 10 microns and manufactured by Regina Glass Fibre Ltd.

The packing holder was a standard piece of QVF industrial glass of 1.8×10^{-2}m diameter and 20×10^{-2}m long. The holder was weighed and the requisite height of the packing was built in by inserting fibrous glass in limited thicknesses, i.e., about 3mm each time. These were pushed together to ensure a reasonably constant voidage across the packing; this method was preferred since compression of a thicker section on insertion resulted in decreased average voidage at the inlet and outlet sides. The cell was then reweighed. This enabled the average packing voidage to be calculated.

8.1.3 LIQUID-LIQUID-PACKING SYSTEM

The approximate refractive index value of the glass was estimated as about 1.50 from the literature (149). To obtain a precise value, small quantities of the glass wool were placed in several beakers containing organic liquids with refractive indices in the range 1.49 to 1.51. The liquid in which the

packing was most transparent was chosen and its refractive index found using an Abbe refractometer and a sodium light source at a constant temperature of 23°C. Some of the organic liquids considered are listed in Table 8.1. Benzene with a refractive index of 1.501, and a 50% V/V mixture of O-xylene with xylene (Analar quality) both gave a perfect match. However due to the high toxcity of benzene (150) the xylene mixture was preferred as one phase in most experiments. For the second liquid phase, only one solution was found to be immiscible with the benzene or xylene and to match their refractive index. This was a solution of potassium thiocyanate in formamide; both of these materials were of Analar quality and their specifications are given in Table 8.2.

8.1.4. EXPERIMENTAL PROCEDURE

Any contamination, or the presence of any liquid with a different refractive index to the packing, would have reduced the packing transparency. Therefore the equipment was washed thoroughly with a solution of Decon 90, as described in Section 7.5., before placing the packing in position. After reflushing with hot distilled water it was left to drain for 24 hours. Filtered air was then blown through the flow line for 2 hours to remove any traces of water. (This was found necessary since if the packing was wetted by water it remained opaque even after contact with the matching liquid-liquid dispersion). The packing was then placed in position in the flow line. Both the continuous and the dispersed phase were metered to give the required phase ratio. The emulsification

TABLE 8.1. ORGANIC LIQUIDS CONSIDERED

Dispersed Phase	RI	Surface Tension $Nm^{-1}(x10^{-3})$	Density $Kgm^{-3}(x10^{3})$	Viscosity $Kgm^{-1}s^{-1}$ $x(10^{-3})$
*Benzene	1.5011	28.9	0.879	0.640 $20^{o}C$
*O-Xylene	1.5054	29.9	0.880	0.738 $26.54^{o}C$
P-Xylene	1.4954	28.3	0.861	0.639 $20.53^{o}C$
*Xylene Analar Grade	1.4972	28.1	0.866	0.710 $21.5^{o}C$
Pyridine	1.5102	38.0	0.983	0.945 $20^{o}C$
*Mixture of O-Xylene and Xylene Analar Grade(50% V/V)	1.5012	28.2	0.870	0.721 $21^{o}C$
*Toluene	1.4972	27.96	0.867	0.579 $20.6^{o}C$
Mixture of Turpentine and Ethylene Bromide or Clove Oil	1.480 1.535	-	-	-

* Chemicals used for experimentation.

TABLE 8.2. CONTINUOUS PHASE

Continuous Phase	Refractive Index	Density $Kgm^{-3}x10^{3}$	Viscosity $Kgm^{-1}s^{-1}$ $x(10^{-3})$
Potassium Thiocyanate	-	1.89	-
Formamide	1.447	1.13	3.95 $23^{o}C$
100ml. Formamide + 50ml. Potassium Thiocyanate	1.499	1.34	17.4 $23^{o}C$
100ml. Formamide + 60ml. Potassium Thiocyanate	1.501	1.38	25.1 $23^{o}C$

pump was then adjusted to produce the required inlet drop size distribution; this was determined by the microscopy method described in Section 7.7. The transparent emulsion so formed was passed through the packing. Figure 8.3 illustrates packing in the process of becoming transparent as flow passes through it.

Mechanisms of droplet coalescence within the packing were studied, and recorded photographically, after rendering the drops visible as described in Sections 8.1.4.2. The packing was then removed, flushed through with hot water and acetone, and left to dry at 40^{o}C in an oven. It was then filled with liquid Perpex and left to stand for about 10 days to dry. Parallel horizontal slices of the packing and holder were then cut using an electric diamond saw. The pieces were examined using microscopy and the Stereoscan to estimate the fibre pitch size distribution. A section of the packing encased in Perspex is shown in Figure 8.4.

8.1.4.1. DROP VISUALIZATION

Amongst several dyes tested for drop visualization, one phototropic dye was found most suitable. Only traces of it were required to bring an effective colour change, and it caused no change in the physical properties of the system. Furthermore as the photochemical reaction was reversible, the process could be repeated as many times as required without any effect on the transparency of the packing. The compound chosen was 1,3,3-Trimethylindolino-6'-nitrobenzopyrylospiran (TMINBS). This compound is not commercially available but was synthesized using the procedure of Berman et al (151) by refluxing a mixture

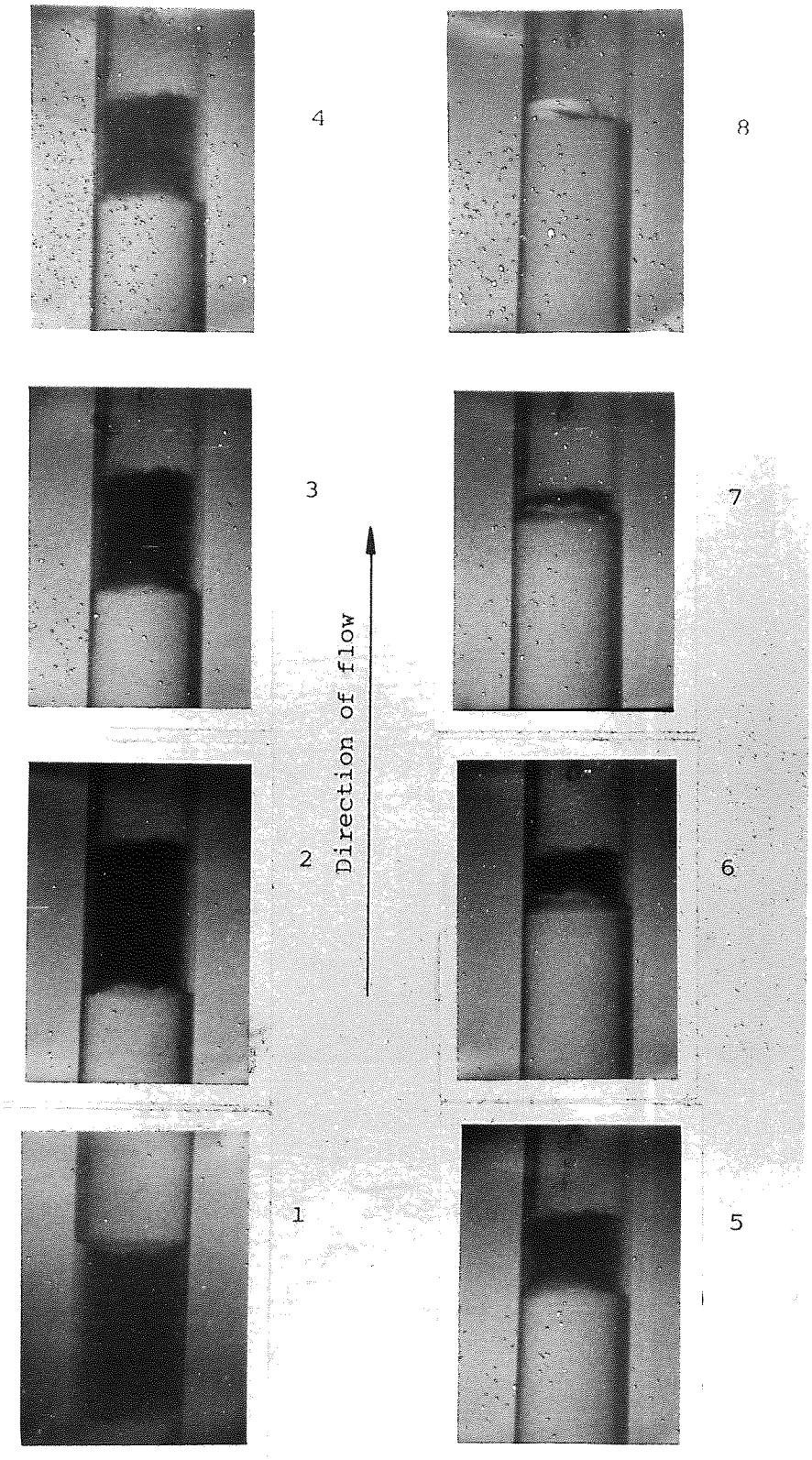

Figure 8.3 Fibrous glass packing, becoming transparent (1 to 8) by refractive index matching

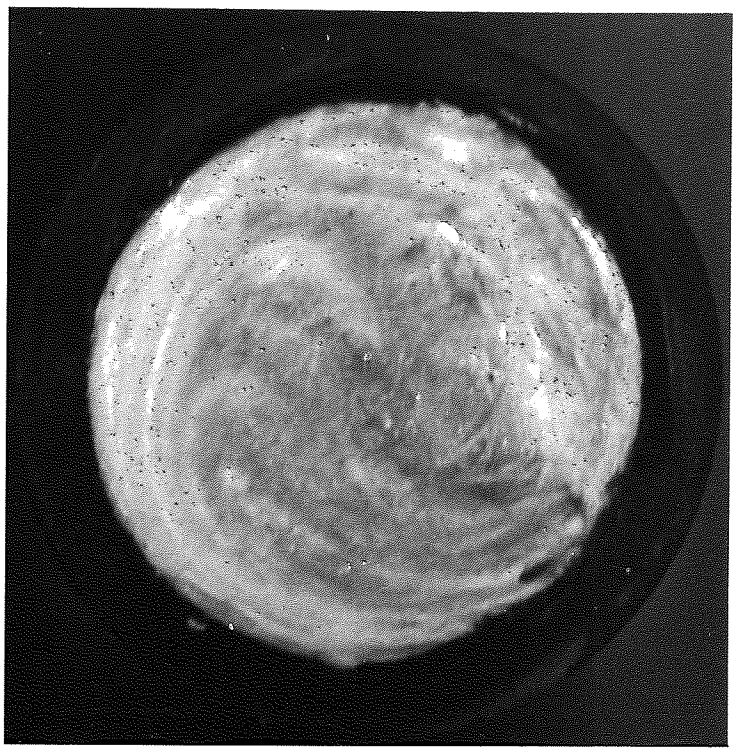

Figure 8.4. Loose glass wool packing section encased in Perpex

Magnification: x 3.9

of equimolar amounts of (5-Nitrosalicylaldehyde) and (2-Methylene-1,3,3-Trimethylindoline) in absolute ethanol in a steam bath for 5 hours. The resultant highly coloured mixture was cooled in an ice water bath, filtered, and washed with cold ethanol and recrystallized from the ethanol-water mixture. Just before experimentation about 2×10^{-3}% by weight of the dye was dissolved in the dispersed phase in the absence of direct light; this amount has been found to be a suitable quantity and non-surfactive (152,153). A mercury arc lamp fitted with an iris diaphragm was used as the source of the ultraviolet light to effect the colour change. The mercury arc lamp was placed at a distance of about 5×10^{-2}m from the packing, facing it and with the iris diaphragm closed. A short pulse of the mercury arc lamp via the iris diaphragm caused the drops in the path of the ultraviolet light to change colour. They formed a coloured layer of drops at the inlet of the bed and could be followed visually as they passed through it.

8.1.4.2. RECORDING

The phenomena within the packing were recorded by means of a television camera and video recorder, cine photography and still photography.

The small sizes of droplets, i.e. about 100 μm, required the use of high magnification lenses. Therefore lenses were used with extension tubes to give a magnification of up to 40 times.

The video equipment used was Sony monitor PV M200CE with a high density video tape V62 and a Sony Video camera AVC 3200CE.

The cine camera was a Beauleu number R16, giving a speed range of 2 to 64 frame/s; Ektachrome 7242 film for tungsten light 125 ASA, was used with side lighting using the ultraviolet source described in Section 8.1.4.1.

8.2. DEVELOPMENT OF AN ULTRASONIC TECHNIQUE

The basis of an ultrasonic technique for measurement of the volume fraction and the average drop size of the dispersed phase in a liquid-liquid dispersion was described in Chapter 6. This was developed further as part of this work but was not used extensively.

The transducers used were type LD25 manufactured by Celesco Industries Environmental Systems; they were originally coated with neoprene rubber on the sensing surface but this was not resistant to organic solvents. It was therefore removed and replaced by cementing on with a non-surfactive, non-reactive Araldite adhesive, a 0.2mm thick glass section cut from a glass rod with a diameter equal to that of the sensing surface; this surface was highly polished using 0.1 μm diamond paper. This treatment avoided any droplet of the dispersed phase adhering to the surface during the experimentation. The transducer manufacturer's specifications are given in Appendix E.

8.2.1. EXPERIMENTAL EQUIPMENT

The equipment used was as described earlier in Section 7.1. and 7.2. but incorporating the packing holder described in Section 8.2.3.

8.2.2. CIRCUIT CONNECTIONS

The circuit arrangement is shown in Figures 8.5 and 8.6. It consisted of a piezoelectric transducer acting as a transmitter, and a second transducer, acting as receiver, located in a special packing holder so as to face each other. The distance between the transducers was adjustable. They were interconnected to an oscilloscope and/or a phase indicator via the electronic hardware described in Appendix E.

8.2.3. PACKING/PACKING HOLDER

Packing was prepared from pure glass wool as described in Section 8.1.2.

The packing holder shown in Figure 8.7. was made from a standard QVF industrial glass section 1.8×10^{-2}m diameter and 15×10^{-2}m long. It was cut into two equal pieces and a standard QVF glass spacer of the same internal diameter and 2.0×10^{-2}m long was fused between them. This spacer had a thicker wall which enabled two 1.1×10^{-2}m diameter holes to be drilled in opposite sides using a diamond drill. A threaded stainless steel bush was then cemented into each hole using a non-surfactive, non-reactive Araldite adhesive (AV138 and HV998). The transducers could be moved inwards and/or outwards by rotating them in the bushes; hence the distance between the sensing surfaces could be varied.

8.2.4. EXPERIMENTAL PROCEDURE AND PRELIMINARY OBSERVATIONS

Continuous phase was passed through the packing with a

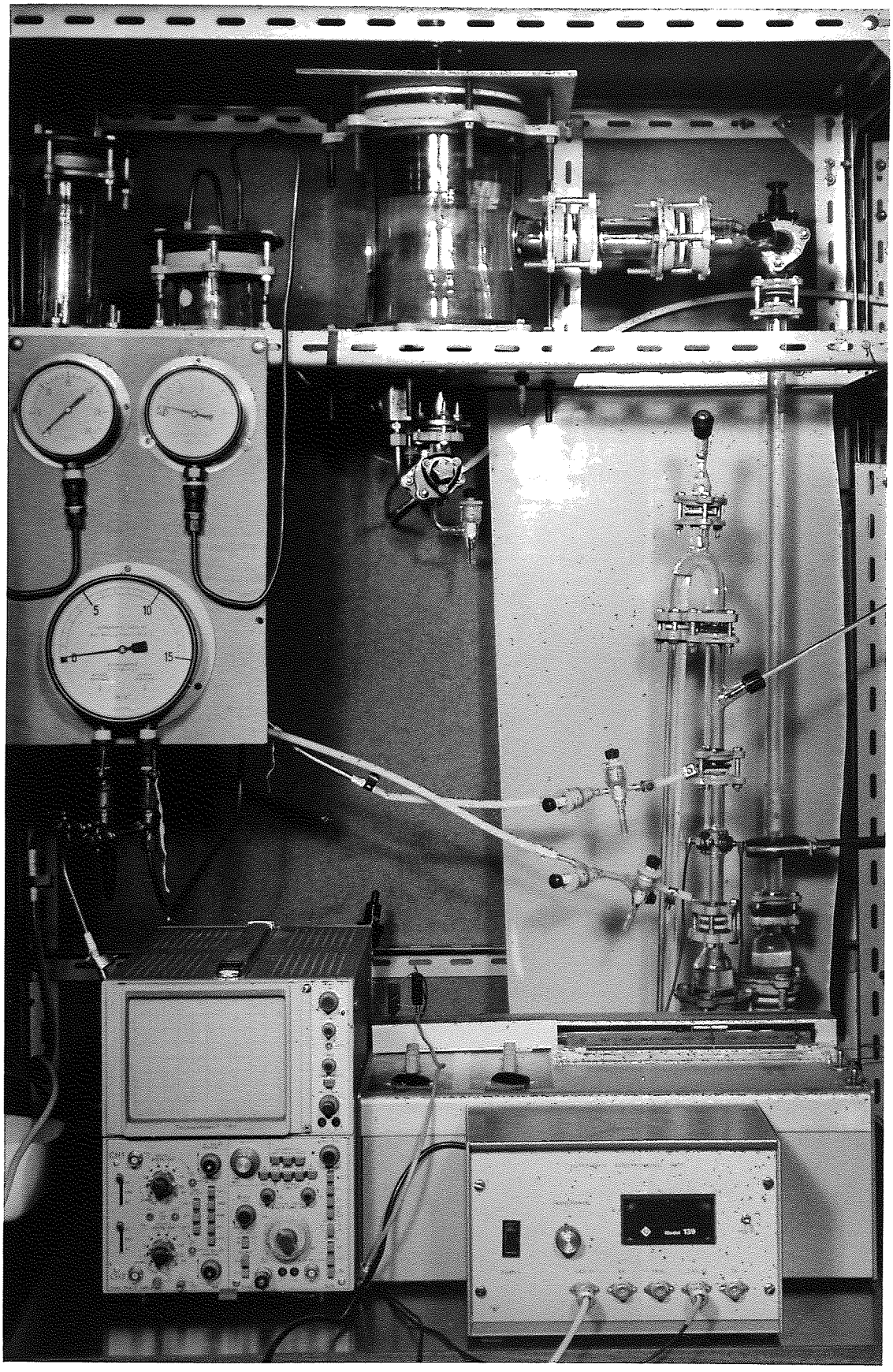

Figure 8.5. Arrangement for use of ultrasonic Technique.

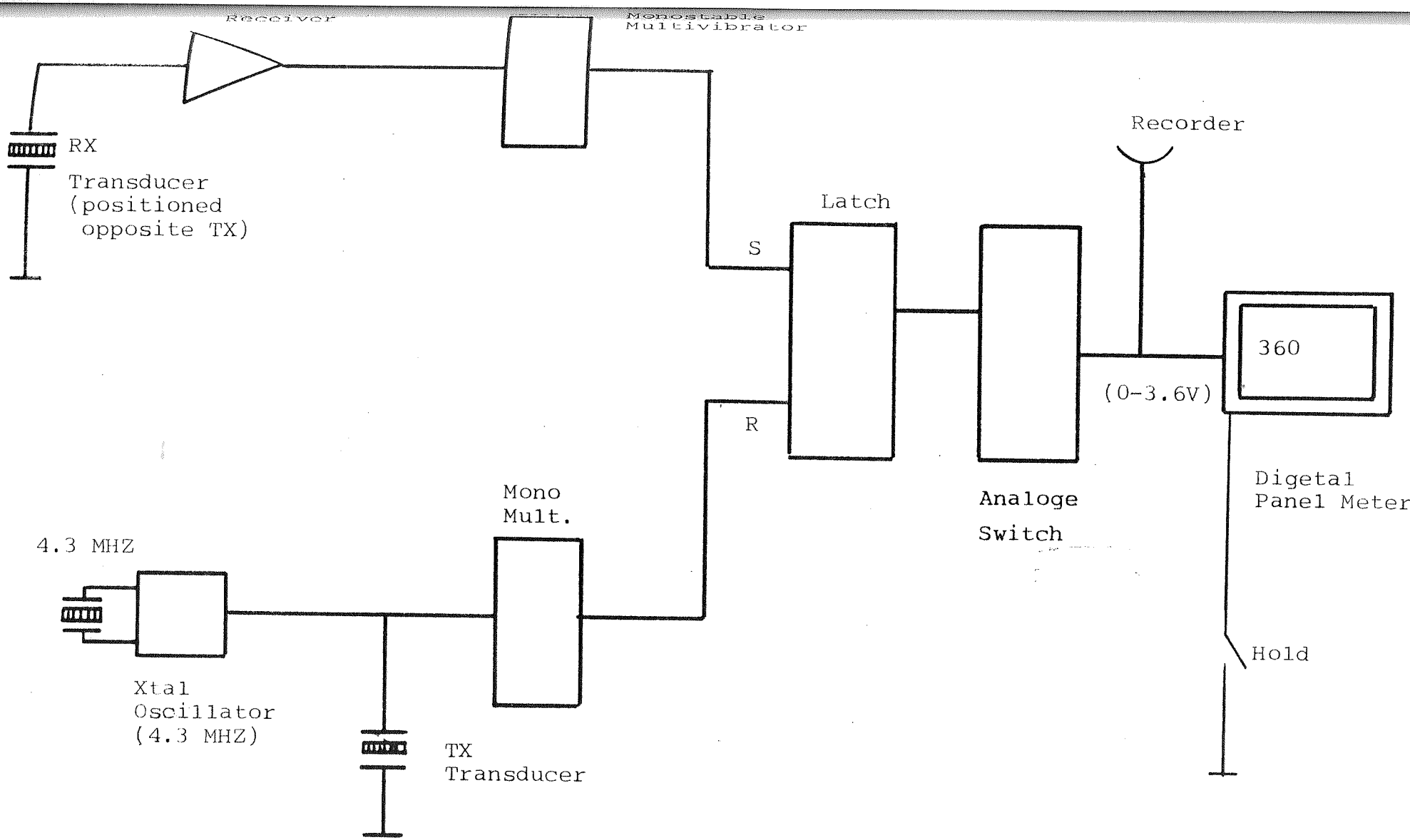

Figure 8.6. Circuit diagram - ultrasonic probe arrangement

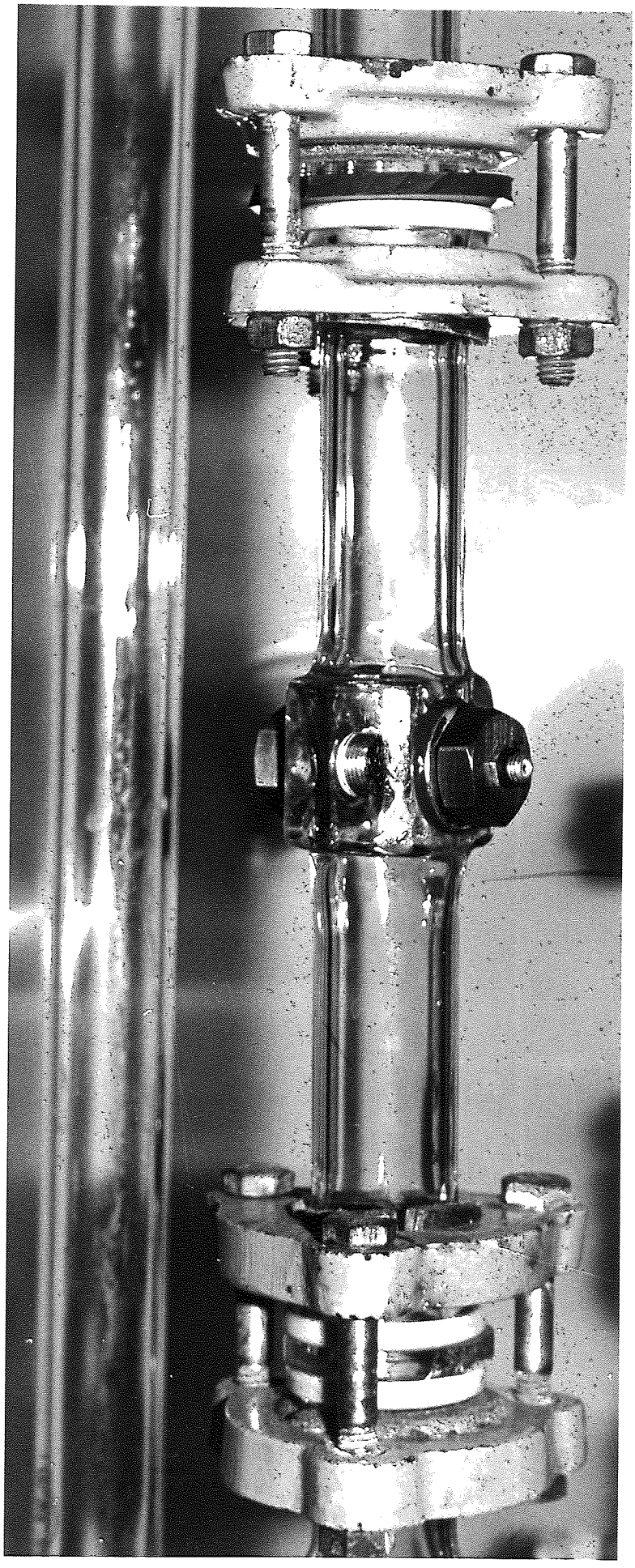

Figure 8.7. Packing holder
Transducers are screwed
in the stainless steel bush

known superficial velocity, originally $0.5 \times 10^{-2} ms^{-1}$. The oscilloscope signal produced by the transducer receiver was then adjusted to coincide with the standard signal by turning one of the transducers clockwise, or anticlockwise. An emulsion of a known phase ratio was then passed through at the same superficial velocity. A phase shift due to droplets in the dispersion was indicated on the oscilloscope; after about 5 minutes this phase shift remained unchanged indicating the attainment of steady state. This phase shift was measured on a metric scale placed on the oscilloscope screen. The superficial velocity was then changed keeping the phase ratio constant and the phase shift remeasured.

A small change in temperature of the dispersion, i.e. $0.5^{o}C$, was also found to affect the phase shift. Therefore the phase shift was calibrated against temperature, to allow for any small increase or decrease in the system temperature.

CHAPTER 9

Discussion of results

CHAPTER 9

DISCUSSION OF RESULTS

Prior to this work the selection and design of packings for the separation of secondary dispersions were based on trial and error. This was due to lack of information regarding the coalescence, travel and exit mechanisms of the droplets. Development of the techniques described in Chapter 6 enabled these mechanisms to be observed visually within the packing. These observations are described in Chapter 10, where the general mechanisms of operation are also defined.

Following observation of the various mechanisms within a glass fibrous packing, a novel knit-fibre glass packing was selected and a full study undertaken of its steady state operation for the separation of both oil/water and water/oil secondary dispersions. Parameters studied included the variation of single phase and two phase pressure drop with superficial velocity, the variation of exit drop size distribution with inlet drop distribution, the variation of exit drop size with superficial velocity and the variation of 'critical' velocity with bed depth and/or number of layers.

9.1. PRESSURE DROP

For any packing, the two phase flow pressure drop at a particular superficial velocity differs from that for single phase flow because the effective voidage of the packing is decreased due to hold-up of the dispersed phase within the packing.

In this work, depending on superficial velocity and packing thickness, ten to twenty minutes were required for a packing to reach its equilibrium pressure drop, that is for the bed hold-up to reach a steady state value. This is in agreement with the observations of Sherony (154) and Spielman (95) who found that as the dispersed phase accumulated in the bed, the pressure drop increased.

Graphs of two phase flow pressure drop against superficial velocity for four different oil/water and water/oil dispersions are shown in Figures 9.1 to 9.9. These graphs, are plotted on the same scale as those for single phase flow to aid comparison.

These plots demonstrate linear relationships and the slopes are independent of the system properties or packed height. However the slope for two phase flow differs from that for single phase flow. This arises because two phase flow pressure drop varies with drop size captured within the packing as well as with the bed hold-up, i.e. at low superficial velocity droplets grow within the bed to a larger size than for a higher superficial velocity as described in Section 9.4. It is easier for small drops to pass through any void or pores than large drops which block them. Therefore larger droplets, which contribute more to ΔP, reside in the bed at lower velocities; hence $\frac{d\Delta P}{dV}$ is less for two phase flow than single phase flow.

A linear relationship was also obtained for variation of single and two phase flow pressure drop with packing thickness as shown in Figures 9.10 to 9.13. These results confirm the validity of equations 9.3 and 9.4. By drawing an analogy between single phase and two phase flow, previous workers (95,120) have

packing thickness $= 0.5 \times 10^{-2}$ m
No. of layers = 5

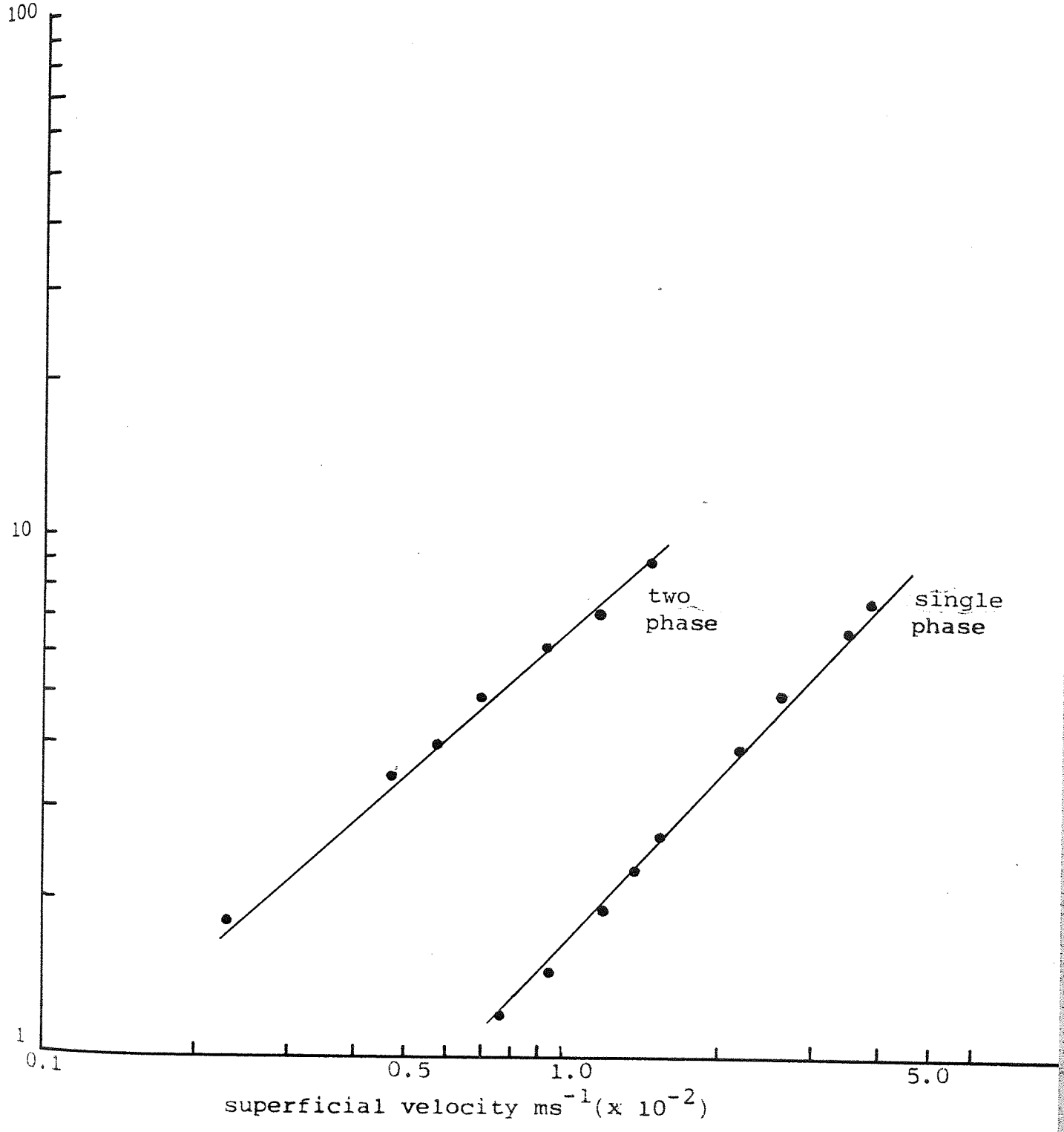

Figure 9.1 Pressure drop v's superficial velocity single phase and two phase flow

system: water- single phase
toluene/water- two phase

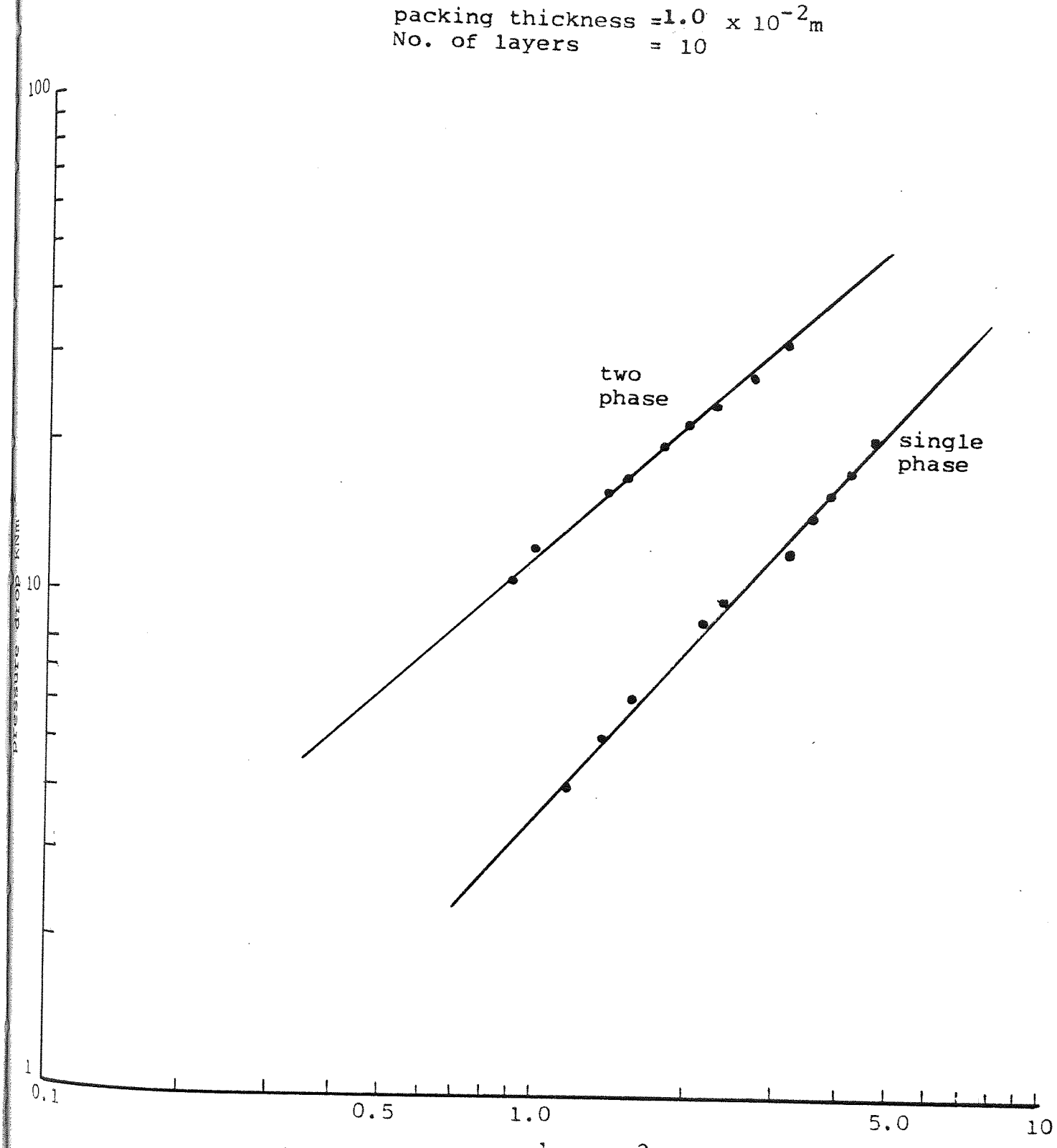

Figure 9.2 Pressure drop vs superficial velocity single phase and two phase flow

system: water- single phase
toluene/water- two phase

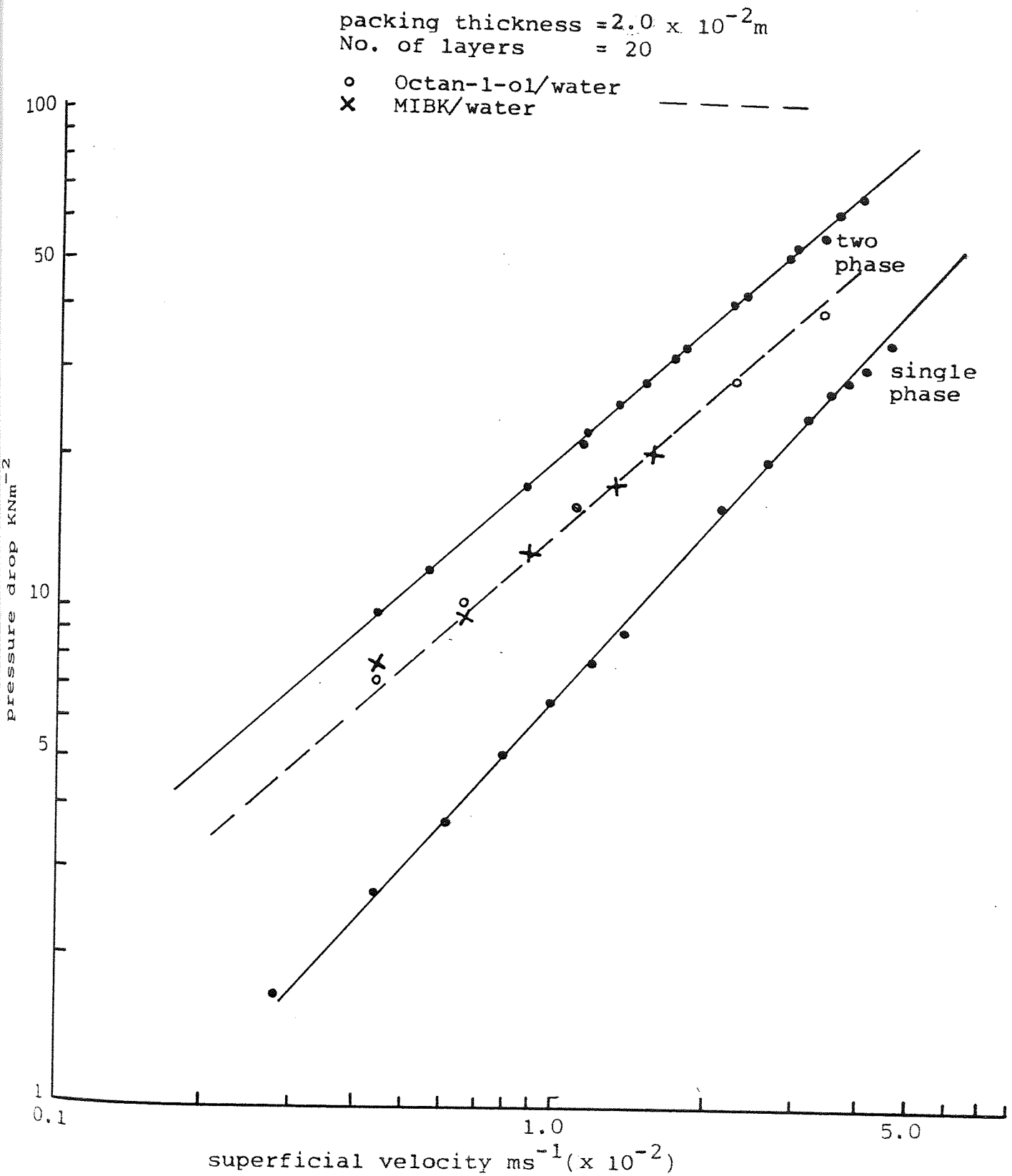

Figure 9.3 pressure drop vs superficial velocity single phase and two phase flow

system: • water- single phase
• toluene/water- two phase
MIBK/water - two phase
Octan-1-ol/water- two phase

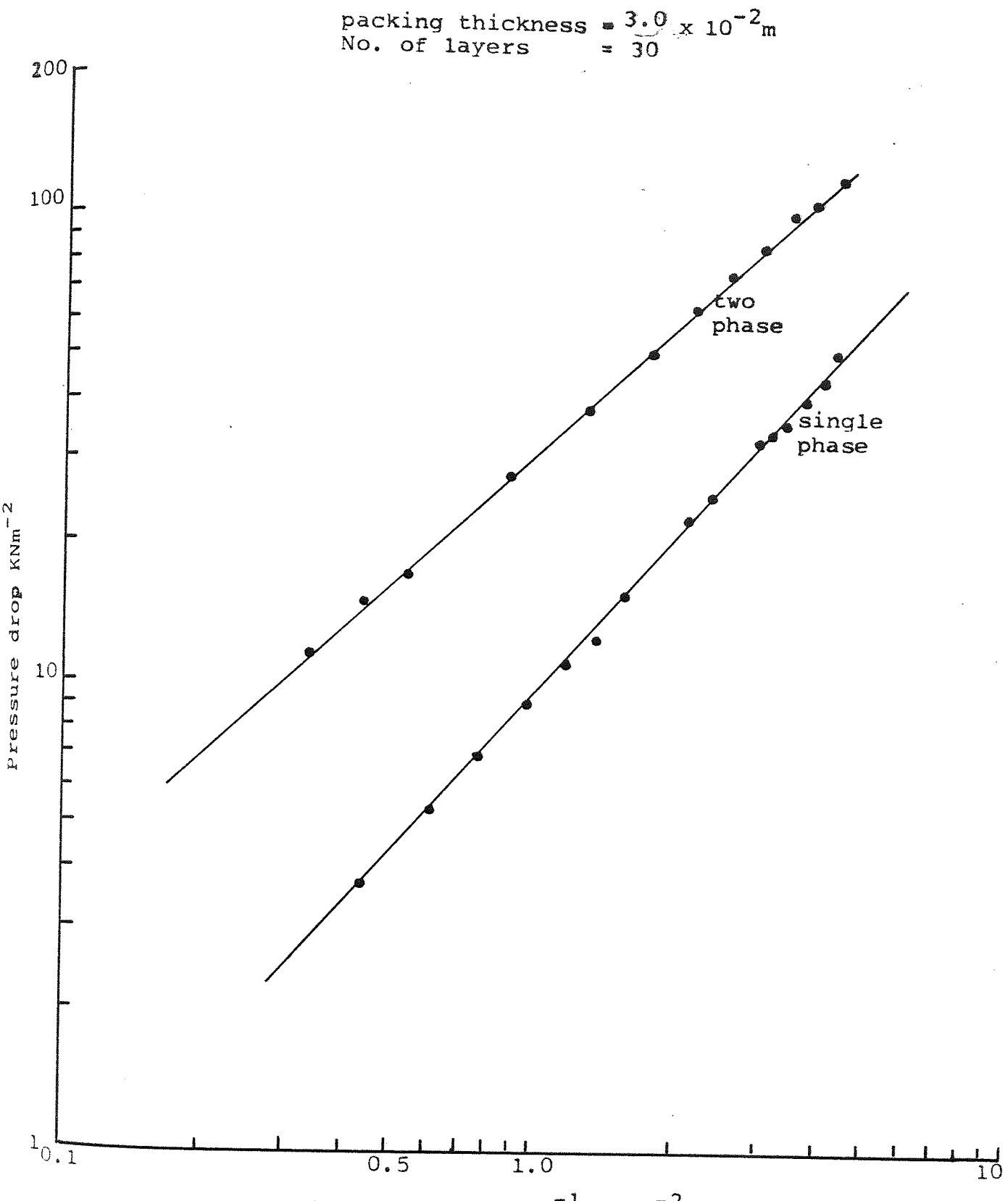

Figure 9.4 pressure drop vs superficial velocity single phase and two phase flow

system: water- single phase
toluene/water- two phase

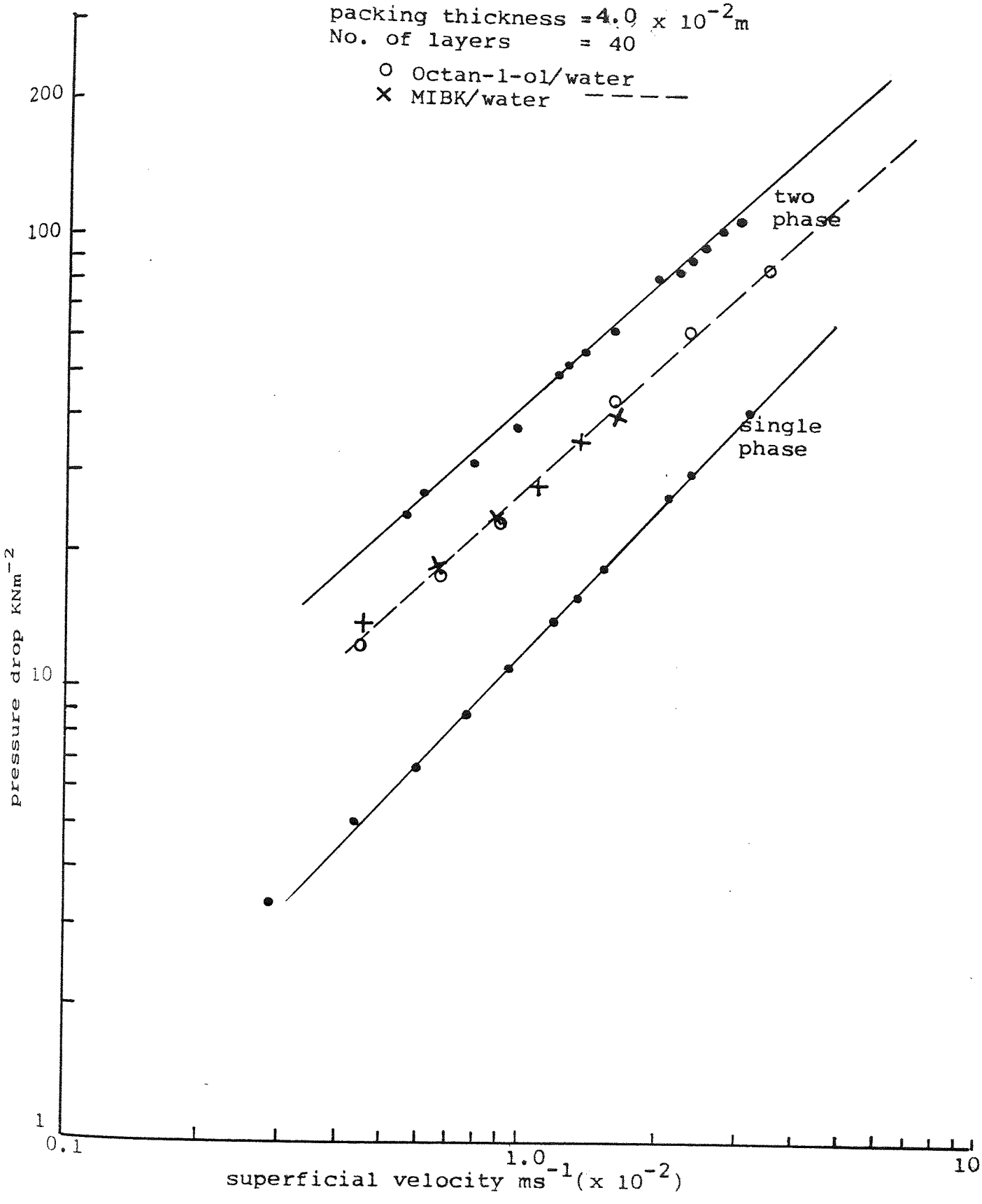

Figure 9.5 pressure drop vs superficial velocity single phase and two phase flow

system: • water- single phase
• toluene/water- two phase
MIBK/water - two phase
Octan-1-ol/water- two phase

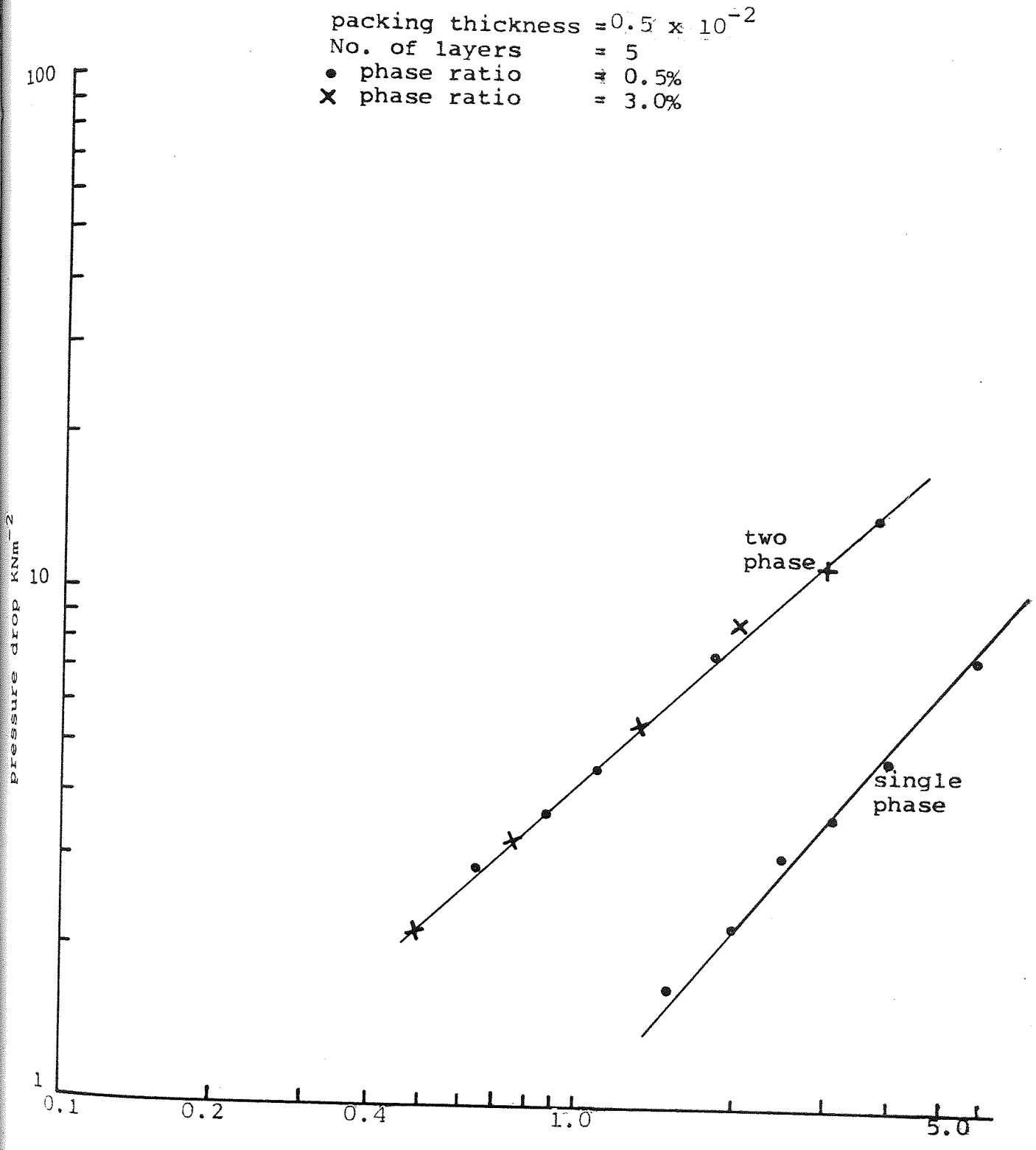

Figure 9.6 pressure drop vs superficial velocity single phase and two phase flow

system: toluene - single phase
water/toluene - two phase

packing thickness = 1.0×10^{-2}m
No. of layers = 10

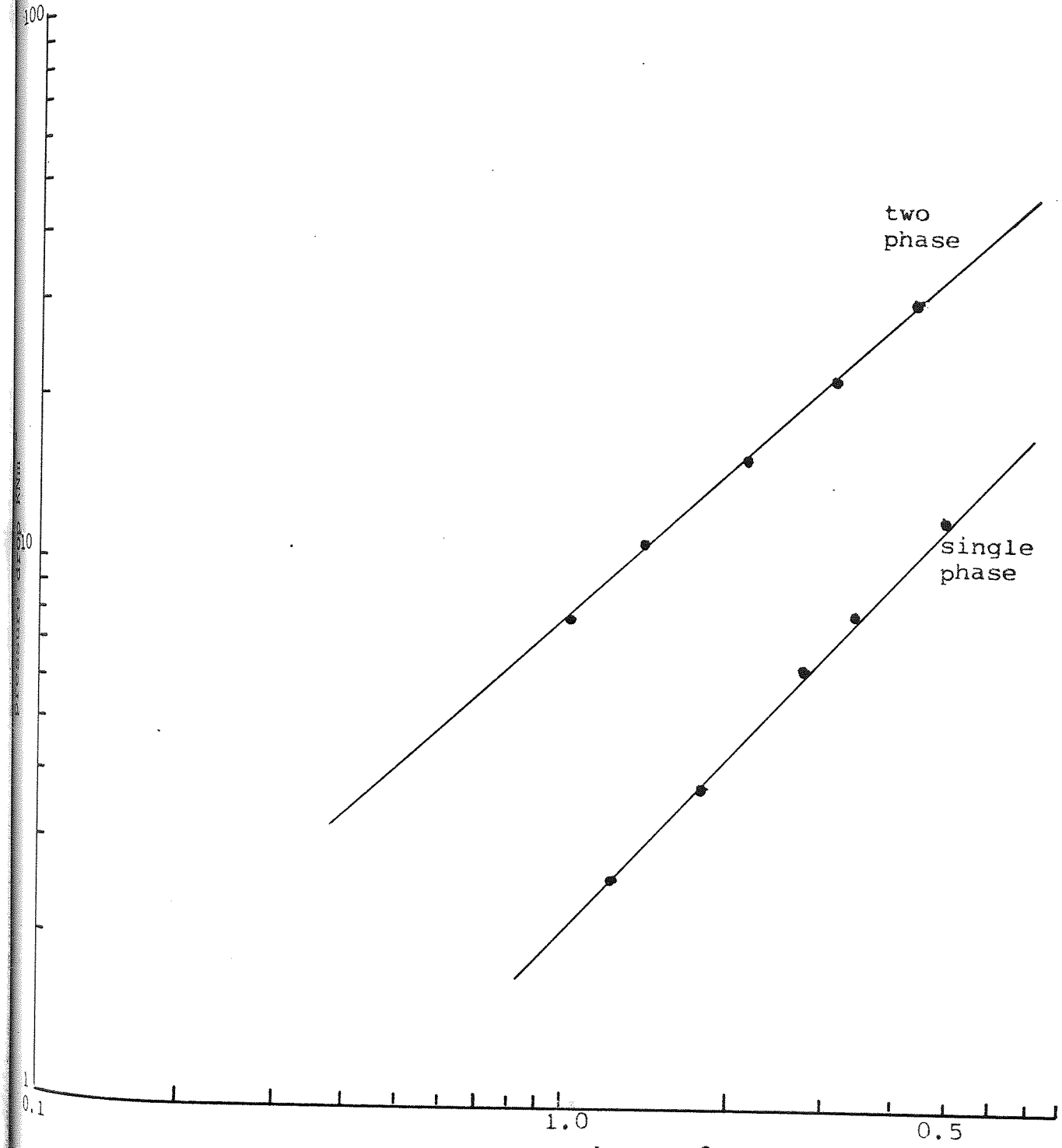

Figure 9.7 Pressure drop vs superficial velocity single and two phase flow

system: toluene - single phase
water/toluene - two phase

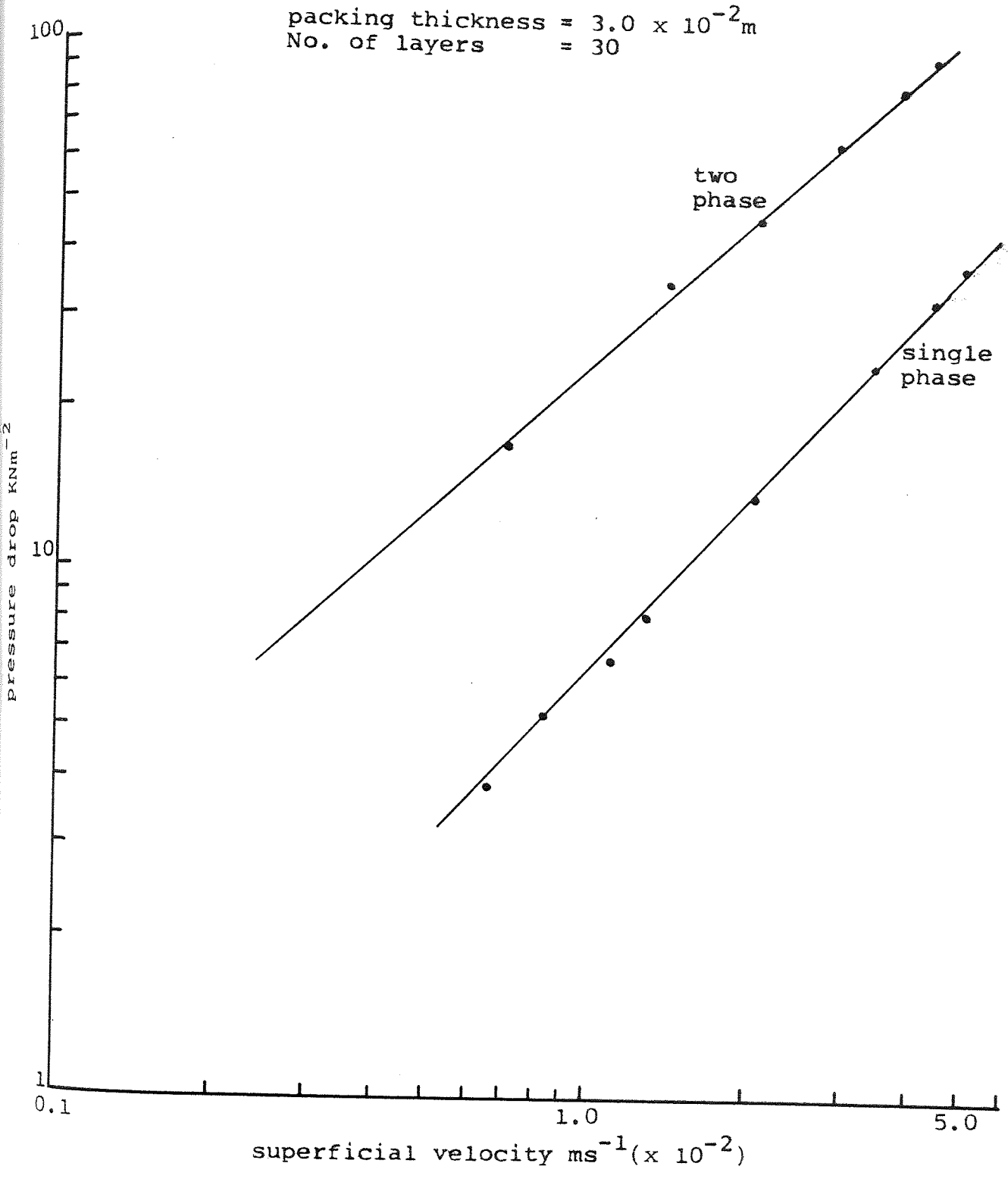

Figure 9.8 pressure drop vs superficial velocity single phase and two phase flow

system: toluene- single phase
water/toluene- two phase

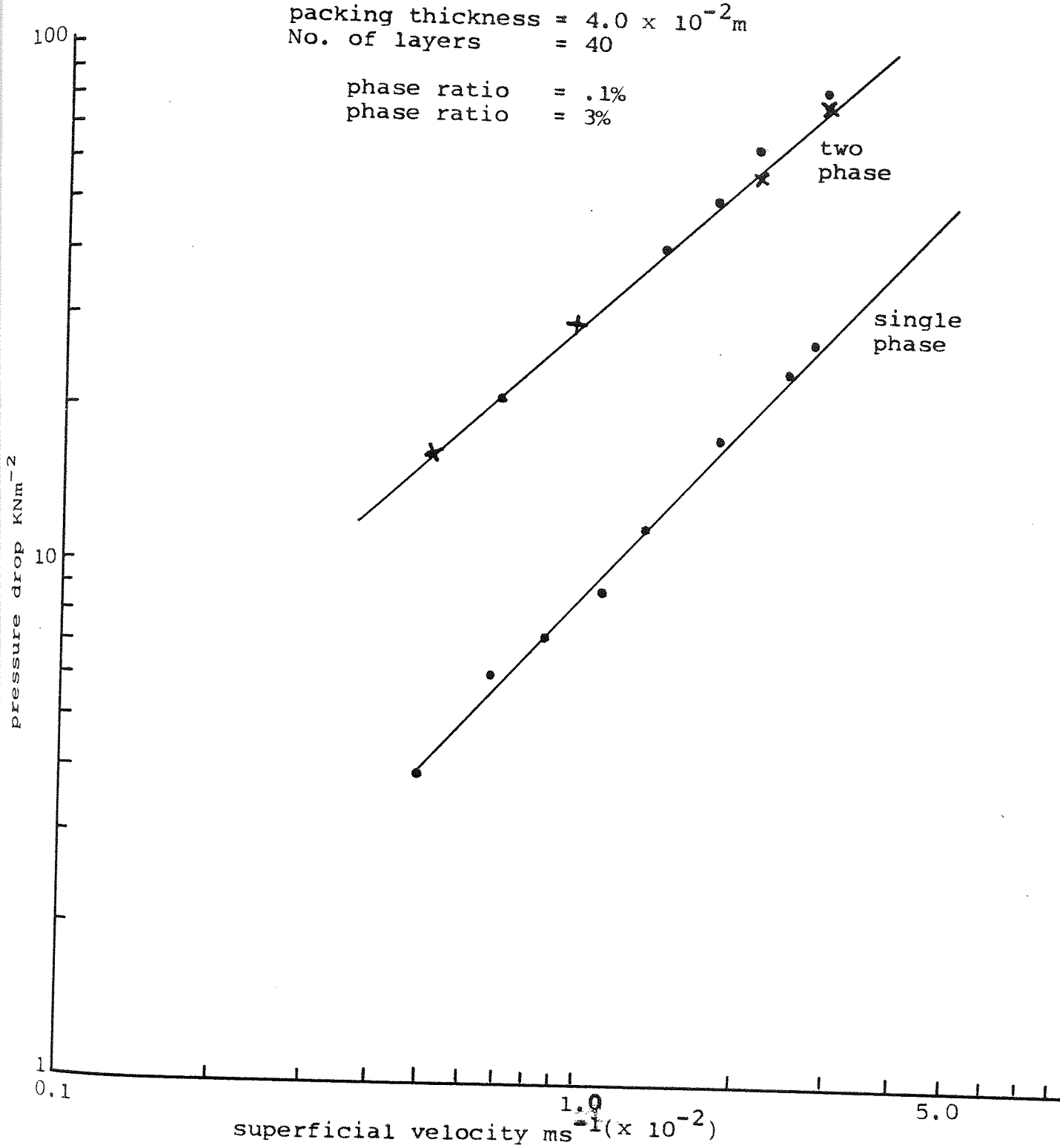

Figure 9.9 pressure drop vs superficial velocity single phase and two phase flow

system: toluene- single phase
water/toluene- two phase

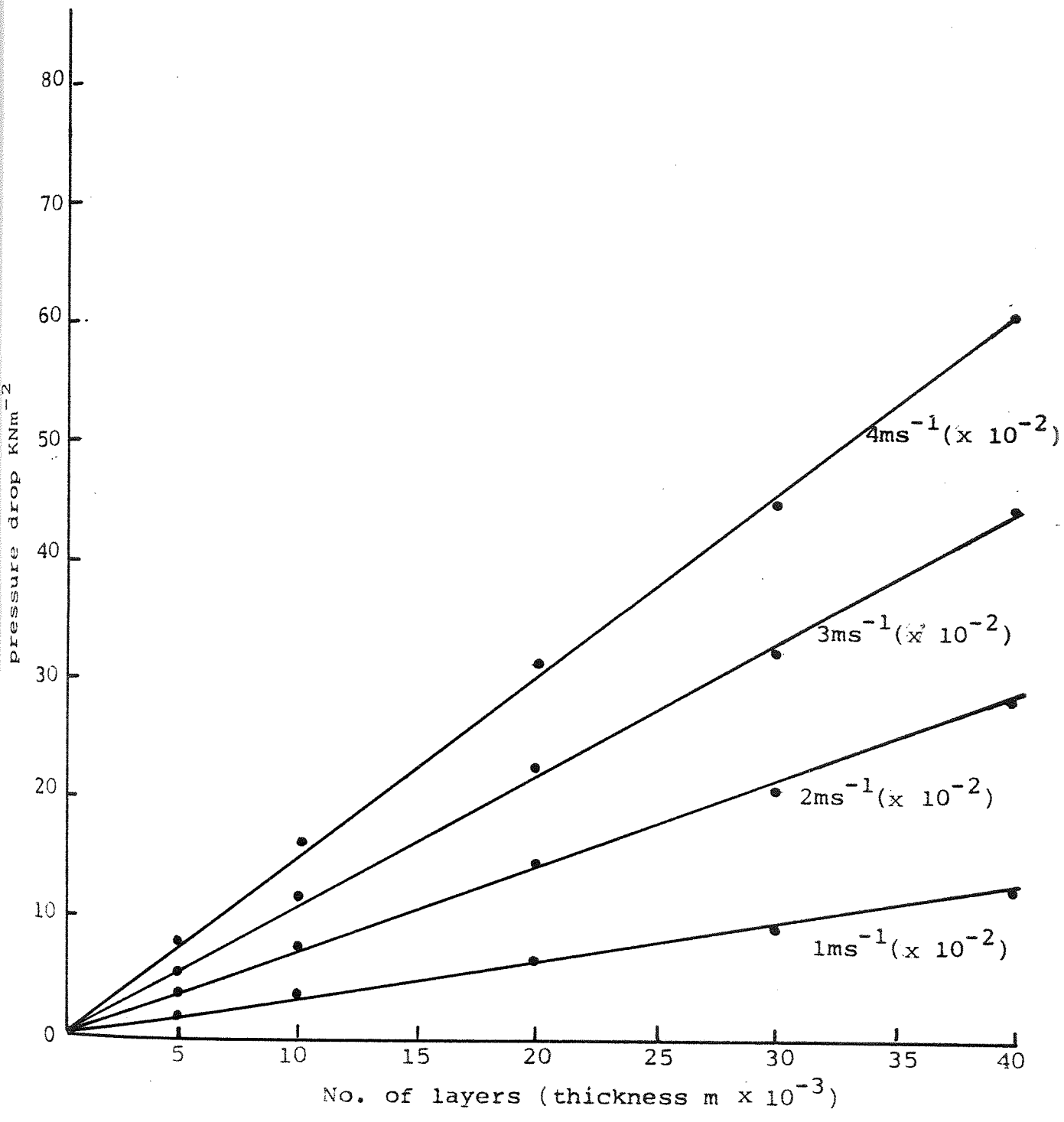

Figure 9.10 single phase flow pressure drop vs No. of layers at different superficial velocities of water

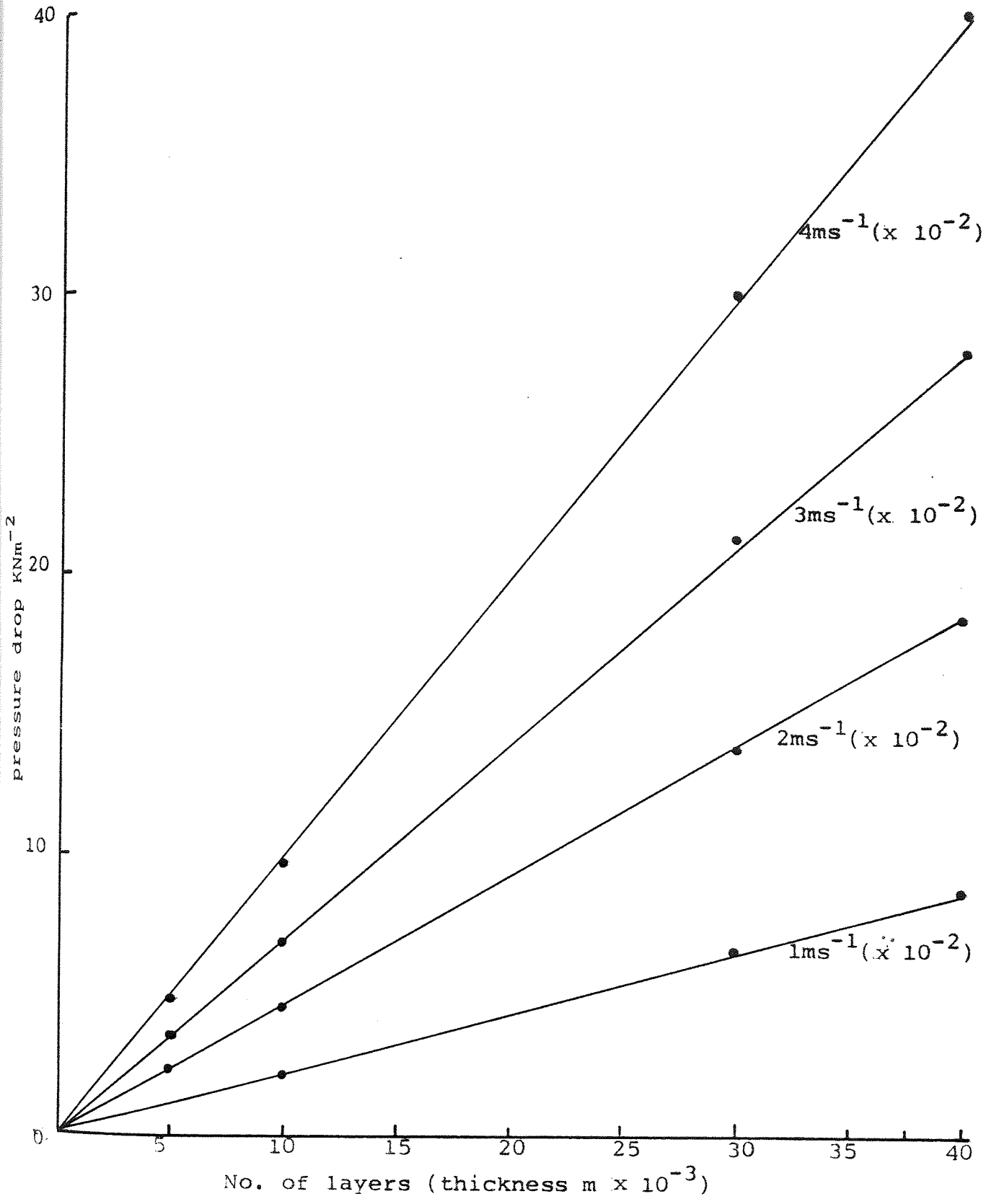

Figure 9.11 single phase flow pressure drop vs No. of layers at different superficial velocities of toluene

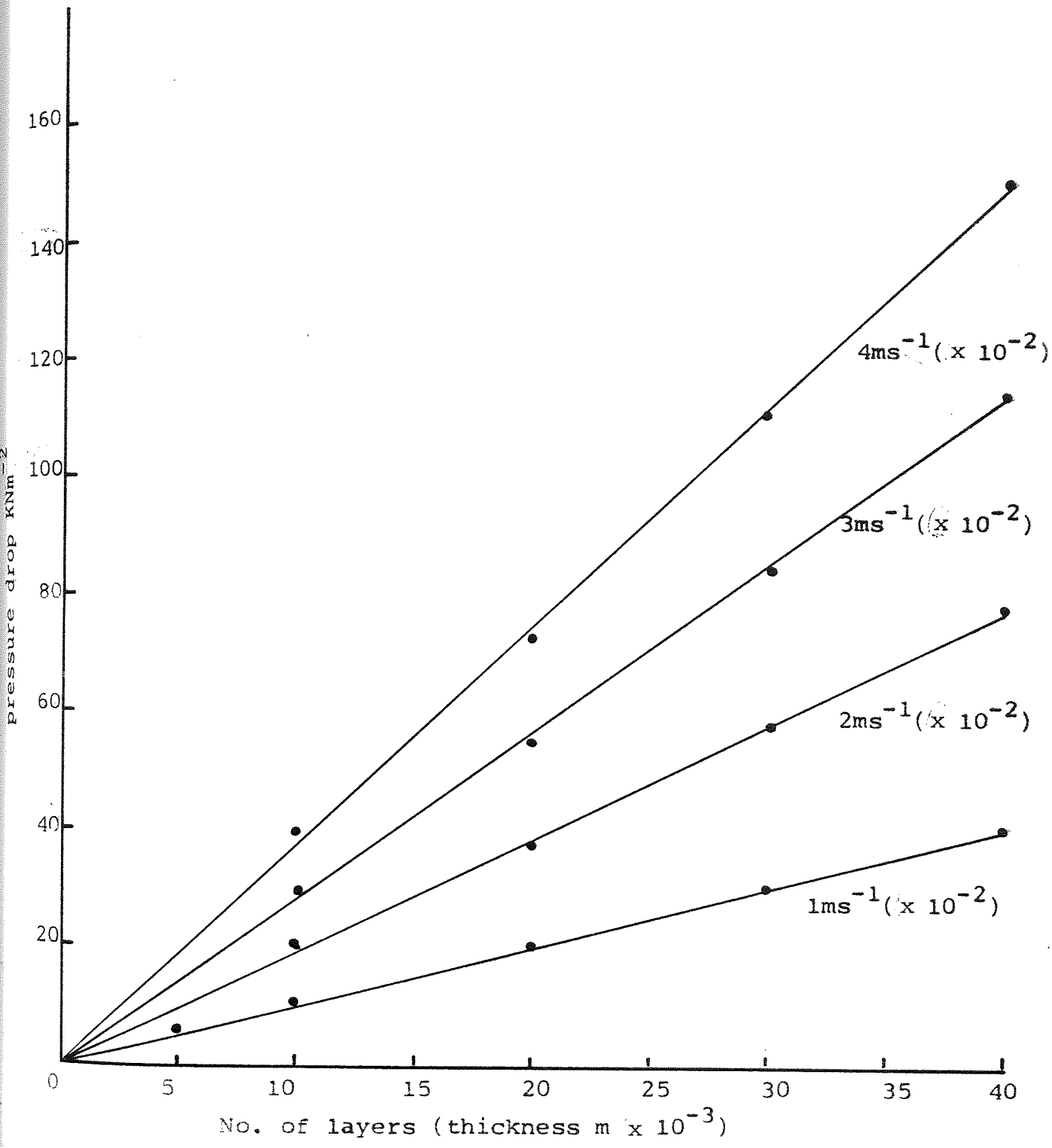

Figure 9.12 two phase flow pressure drop Vs thickness at different superficial velocity

system: toluene - water

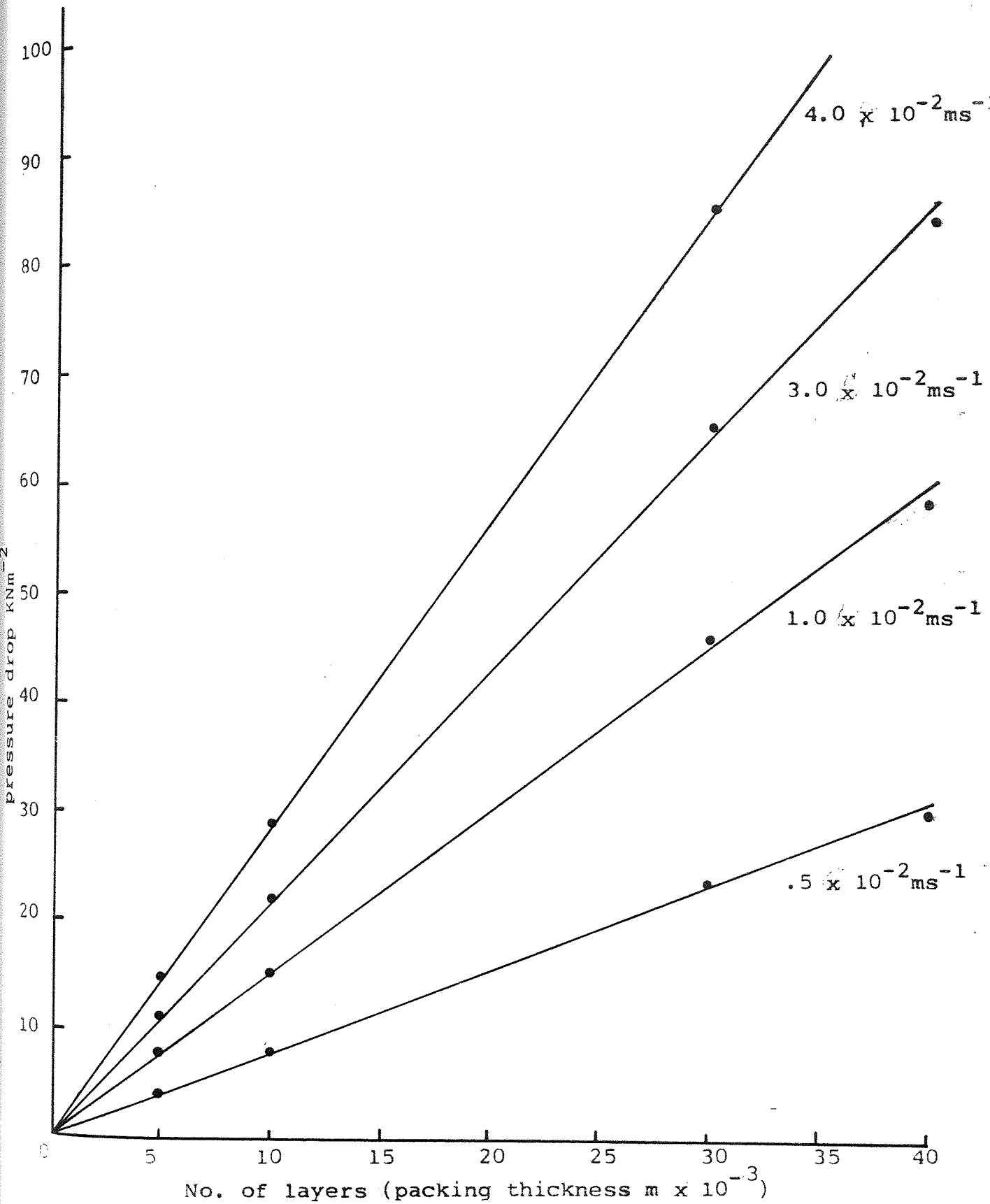

Figure 9.13 Two phase flow pressure drop vs thickness at different superficial velocity

System: Water - Toluene

correlated pressure drop in fibrous beds by a Blake-Kozeny equation in the form:

$$\Delta P = \frac{150\ \mu_c L}{g d_f^2} \times \frac{(1-E)^2}{E^3} \times V \quad \ldots\ldots\ldots\ldots\ldots\ldots 9.1$$

$$\text{OR} \quad \ell n \Delta P = \ell n V + \ell n \left(\frac{150\ \mu_c L}{g d_f^2}\right) \quad \ldots\ldots\ldots\ldots\ldots\ldots 9.2$$

In this work plots of $\ell n \Delta P$ vs $\ell n V$ did not give a gradient of unity. Therefore the Blake-Kozeny equation had to be modified.

Two modified versions of the Blake-Kozeny equation were developed, one for single phase flow and one for two phase flow in the form:-

for single phase flow at superficial velocity V_1

$$\Delta p_1 = \frac{K\ \mu_c\ L}{d_f^2} \times \frac{(1 - E_1)^2}{E_1^3} \times V_1^{1.09} \quad \ldots\ldots\ldots\ldots 9.3$$

and for two phase flow at superficial velocity V_2

$$\Delta P_2 = \frac{K\ \mu_c\ L}{d_f^2} \times \frac{(1 - E_2)^2}{E_2^3} \times V_2^{0.91} \quad \ldots\ldots\ldots\ldots 9.4$$

These two equations were applicable to all the systems studied. This indicates that, within the range studied, the dispersed phase acts merely to reduce the voidage. As might

be expected once the equilibrium hold-up is reached, depending on the interfacial tension and wetting characteristics of the dispersed droplets, the rate of increase in ΔP with throughput is independent of the nature of the dispersed phase.

The power for V_1 in equation 9.3 was found from the slope of the plot of ℓnP_1 vs ℓnV_1 for single phase flow of two liquids, toluene and water, and five different packing heights in the range 5×10^{-3}m to 40×10^{-3}m. Similarly the power for V_2 in equation 9.4 was obtained from plots of ℓnP_2 vs ℓnV_2 for four different oil/water and water/oil dispersions and the five different packing heights. Equation 9.3 applies for V_1 in the range 0 to $6 \times 10^{-2} ms^{-1}$ and equation 9.4 applies for V_2 from 0 to the appropriate critical velocity; at break-through $V_2 \longrightarrow V_1$ since the hold-up $\longrightarrow 0$.

Values for K were obtained from equation 9.3 and experimental results as tabulated in Tables 9.1 and 9.2. The average value for K for all bed heights was constant at about 20.7 $\pm$ 10%. Clearly K values, although independent of system physical properties, are some function of the operating voidage, and therefore will vary with packing type and structure.

9.2 INLET DROP SIZE DISTRIBUTION

The determination of drop size distribution is described in Appendix A and Section 7.7. A typical plot of drop diameter in micrometers versus cumulative weight percent over size, obtained at a phase ratio of 0.2% and a pump speed of 33.3 rps, is shown in Figure 9.14. The distribution was unimodal and the mean inlet drop diameter, that is the size which exceeded

Table 9.1. VALUES FOR K AT DIFFERENT SINGLE PHASE FLOW VELOCITIES; WATER

BED 5 LAYERS		BED 10 LAYERS		BED 20 LAYERS	
ms^{-1} V $\times 10^{-2}$	K	ms^{-1} V $\times 10^{-2}$	K	ms^{-1} V $\times 10^{-2}$	K
0.39	20.70	1.09	22.50	0.77	20.30
0.52	20.20	1.58	22.52	0.94	20.55
0.62	20.80	2.03	22.85	1.18	20.64
0.90	20.80	2.48	22.96	1.43	20.92
1.17	20.23	3.55	22.90	2.05	21.20
1.70	20.80	4.60	22.96	2.65	21.36
2.20	20.93			3.76	21.88
3.70	20.80			4.85	22.10
AVERAGE K = 20.7		AVERAGE K = 22.9		AVERAGE K = 21.1	

30 LAYERS		40 LAYERS		
ms^{-1} V $\times 10^{-2}$	K	ms^{-1} V $\times 10^{-2}$	K	
0.56	19.40	0.44	18.90	
0.66	19.40	0.51	19.30	
0.86	19.40	0.68	18.60	
1.05	19.50	0.84	18.40	
1.50	19.90	1.23	18.40	
1.92	20.20	1.60	18.50	
2.75	20.50	2.33	19.30	
3.60	20.40	3.00	18.60	
AVERAGE K = 19.8		AVERAGE K = 18.8		

Table 9.2. VALUES FOR K AT DIFFERENT SINGLE PHASE FLOW VELOCITIES; TOLUENE

BED 5 LAYERS		BED 10 LAYERS	
V $ms^{-1} \times 10^{-2}$	K	V $ms^{-1} \times 10^{-2}$	K
1.8	20.3	1.4	20.0
2.6	20.4	2.2	20.4
3.4	20.3	3.0	20.4
4.2	20.2	4.2	20.2
		6.0	20.5
AVERAGE K = 20.3		AVERAGE K = 20.3	

BED 30 LAYERS		BED 40 LAYERS	
V $ms^{-1} \times 10^{-2}$	K	V $ms^{-1} \times 10^{-2}$	K
0.80	20.5	0.60	21.0
1.08	20.7	0.81	21.2
1.52	20.3	1.13	21.1
2.20	20.4	1.63	21.2
2.82	20.7	2.12	21.2
4.10	20.7	2.12	21.2
5.30	20.9	3.05	21.4
AVERAGE K = 20.6		AVERAGE K = 21.2	

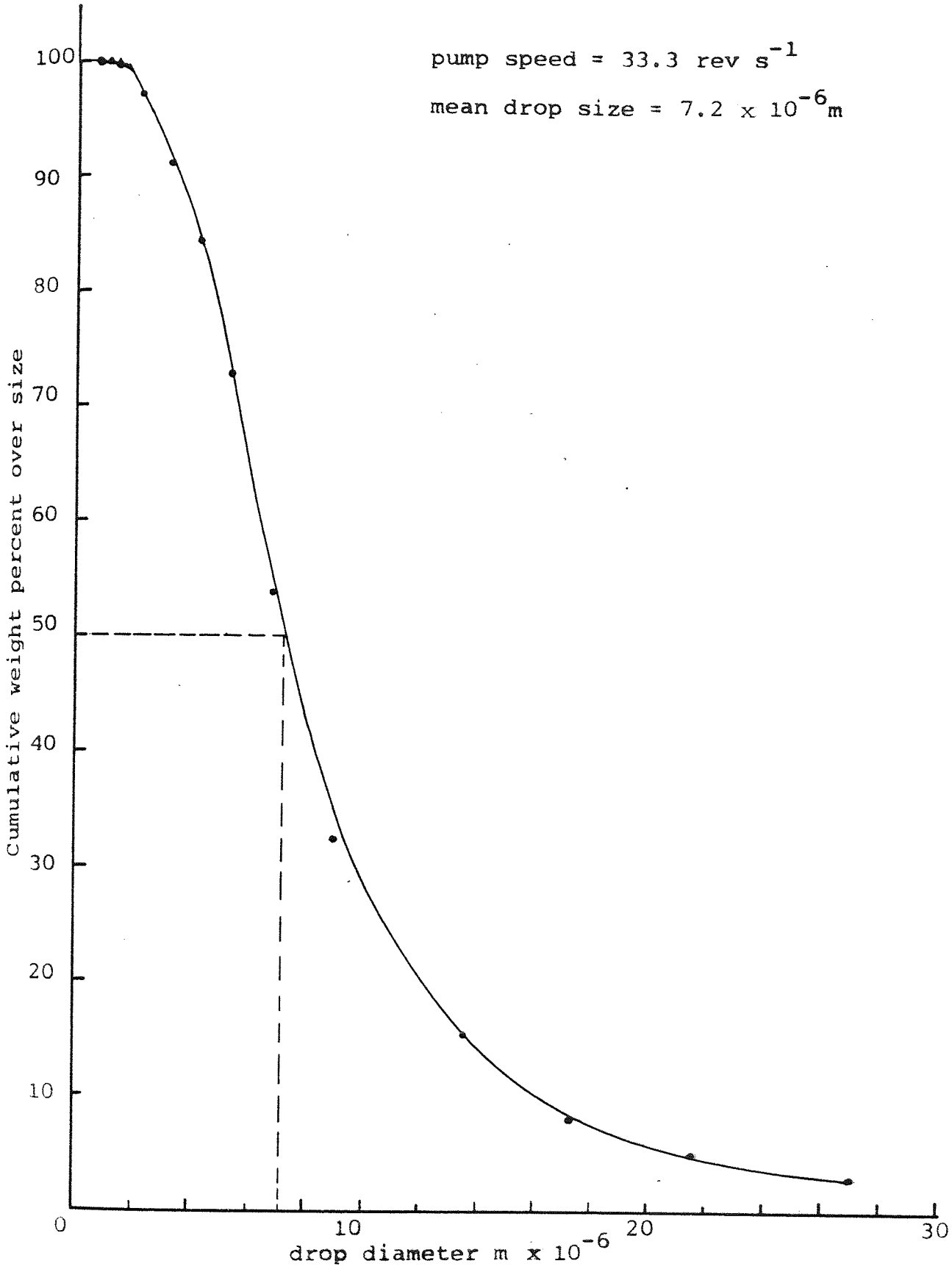

Figure 9.14 Inlet drop size analysis using Coulter Counter

Cumulative weight percent over size vs drop diamter

System: Octan-1-ol - Water

the diameter of 50% of droplets, was determined for each operating condition. The mean inlet drop size for any particular pump speed was found to be within ± 2 μm from up to 10 determinations over the phase ratios 0.1 to 3%. As would be expected, the mean drop size increased with a decrease in the pump speed. The change of mean inlet drop size with pump speed in the range 16.7 to 75 rev s^{-1} for octan-1-ol/water at phase ratio 0.2% is shown in Figure 9.15.

As described in Section 7.7 for water-oil dispersions the mean droplet size distribution for each operating condition was determined using a microscopic technique. A typical microscopic photograph of water droplets in toluene is shown in Figure 9.16a.

Mean drop size distributions were determined from similar photographs at pump speeds ranging from 16.7 to 75 rev s^{-1} as shown in Figure 9.16.

9.3. EFFECT OF INLET DROP SIZE ON TWO PHASE FLOW PRESSURE DROP

The effect of mean inlet drop size on two phase flow pressure drop over the range investigated, i.e., 8 to 40 μm, was found to be insignificant. Other investigators (93,95) using different systems have also observed that with small droplets, i.e.< 40 μm, pressure drop was independent of the inlet drop size.

In this work plots of steady state flow pressure drop against superficial velocity, shown in Figures 9.1 to 9.9, were independent of inlet drop size over the size range studied. Clearly this occurs because at the relatively low phase ratios

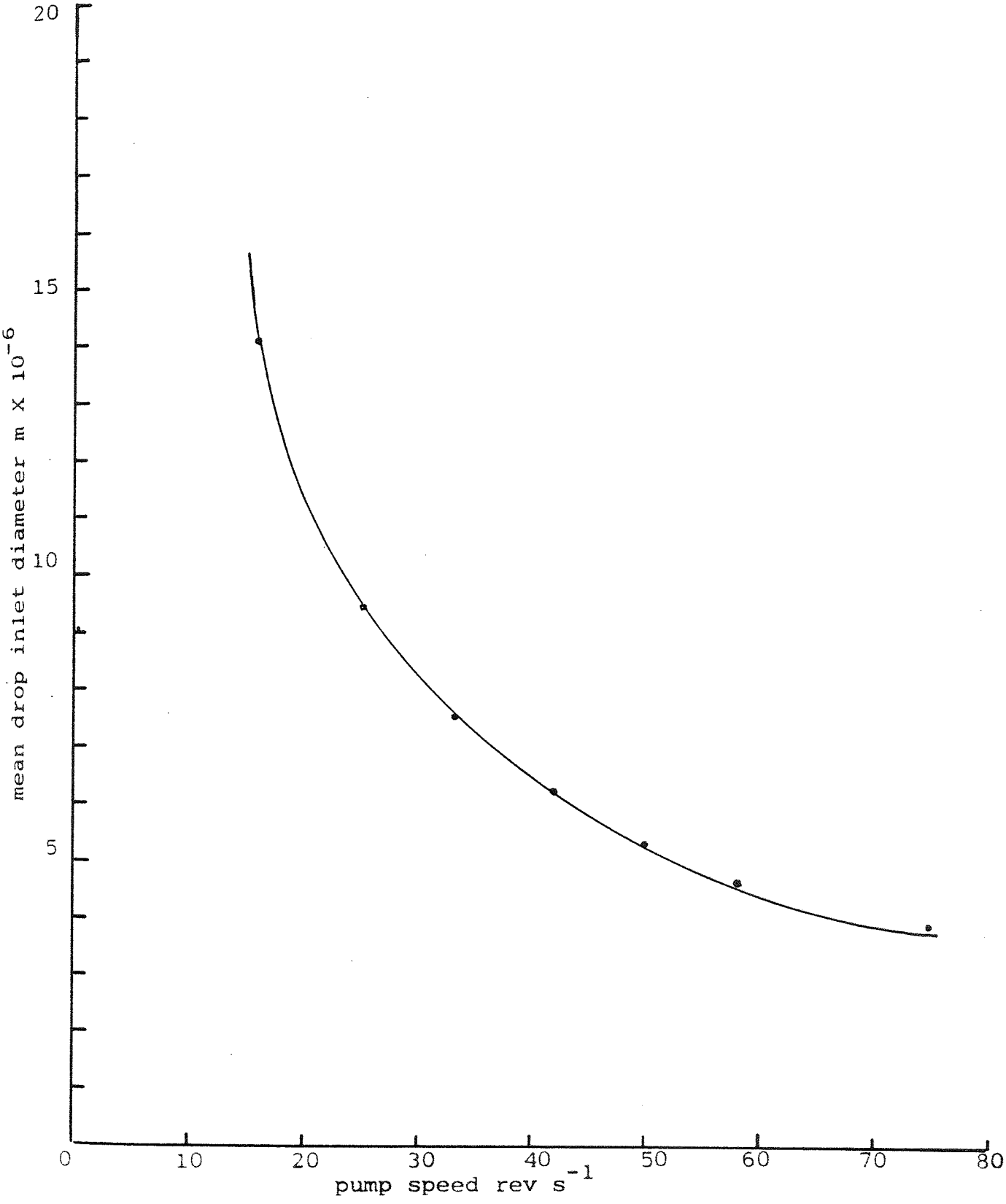

Figure 9.15 variation of mean inlet drop size with pump speed at phase ratio 0.2%

system : Octan-1-ol - Water

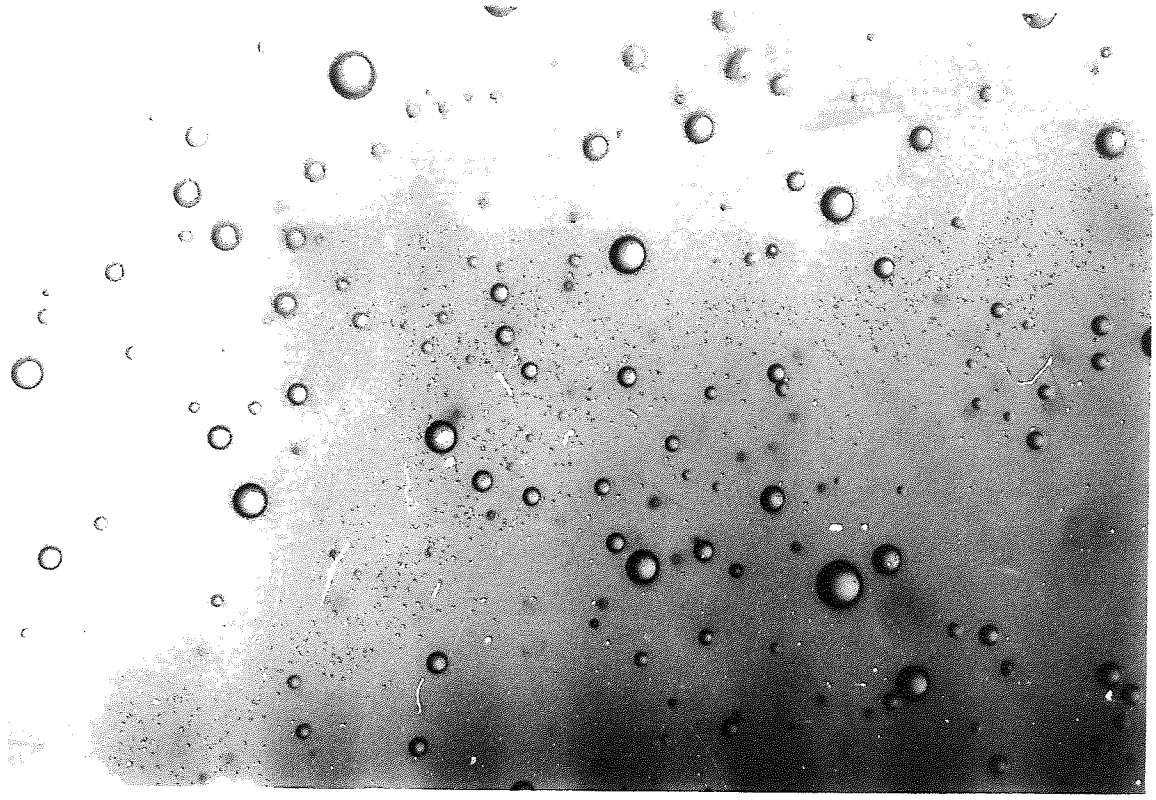

Figure 9.16a Microscopic photograph of inlet dispersion

Magnification = 1000 x

System: Toluene/Water

Phase Ratio: 2%

Pump Speed: 75 rev s^{-1}

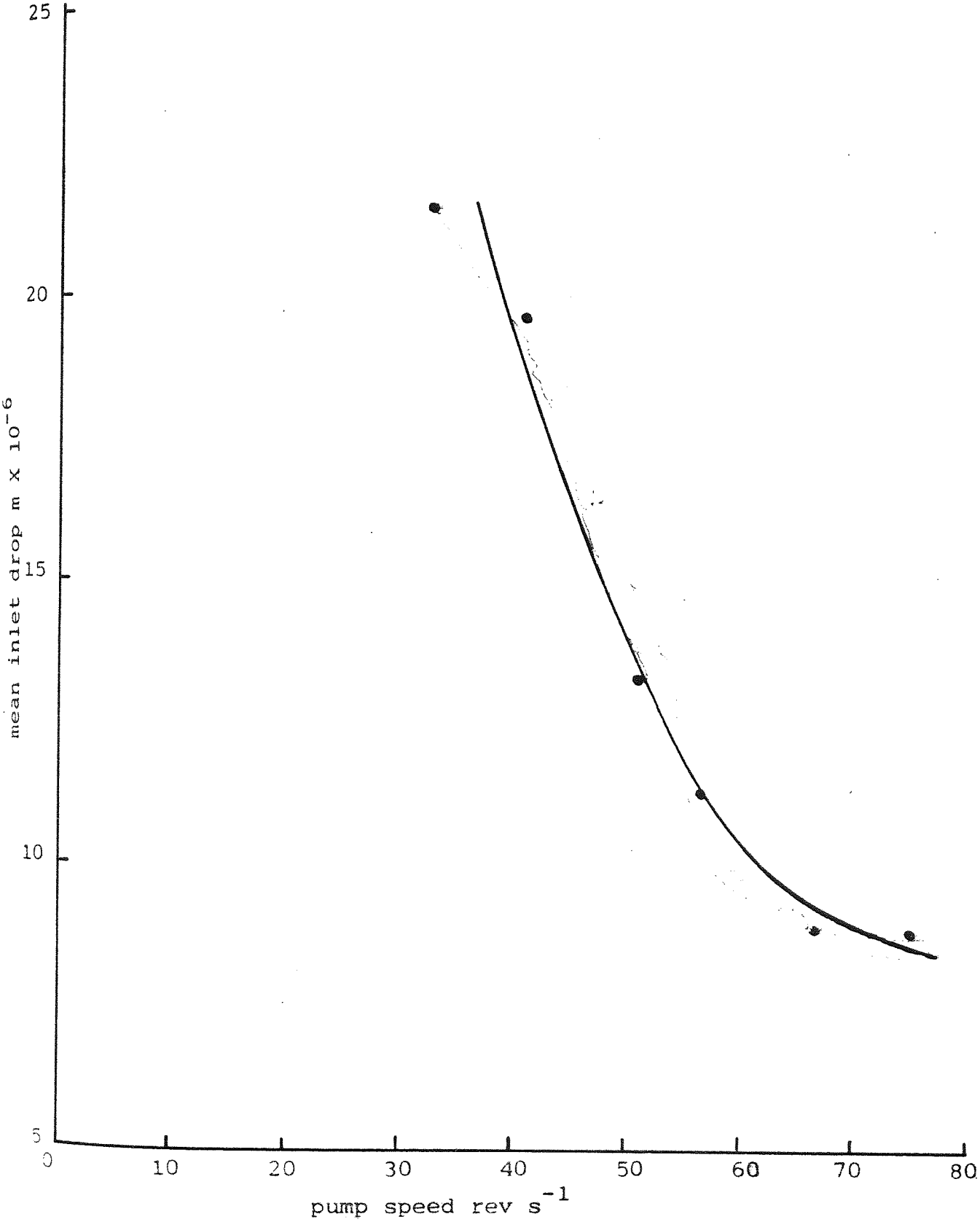

Figure 9.16 variation of mean inlet drop size with pump speed

Phase ratio: 2%

System : Water-Toluene

involved, the presence of the dispersed phase did not significantly affect the dispersion physical properties, in particular its viscosity.

9.4. EFFECT OF PHASE RATIO ON TWO PHASE FLOW PRESSURE DROP

Phase ratios in the range of 0.1 to 3% had no effect on pressure drop. Typical results for two different phase ratios 0.5 to 3% are plotted in Figure 9.6 and for phase ratios 0.1 and 3% in Figure 9.9. Thus the pressure drop data shown in Figures 9.1 to 9.9 represent up to five phase ratios investigated i.e., 0.1, 0.5, 1, 2 and 3 percent.

In previous studies, pressure drop was independent of phase ratios in the range 0.1 to 0.6%, (156) and in the range of 3 to 7% (93). In the first investigation the time to achieve the equilibrium pressure drop was reported to be up to one hour. This was due to the low packing voidage (0.92) and possibly the very small dilution of the dispersed phase necessitating a longer time for the hold-up to reach its equilibrium value. However in the latter investigation (93) up to twenty minutes was necessary.

In conclusion, the results discussed so far imply the presence of a constant bed hold-up independent of superficial velocity up to an appropriate critical velocity, and of inlet drop size and phase ratio.

9.5. EXIT DROP SIZE

Mean exit drop size was found to be dependent on the precise mechanism of release at the exit side of the packing

as well as packing thickness and the superficial velocity of the flow. However the mode of exit droplet release was the predominant factor affecting exit drop size for water/toluene separation.

Individual, and combinations of, release mechanisms are discussed in Chapter 10.

9.6. EFFECT OF SUPERFICIAL VELOCITY ON EXIT DROP SIZE

As superficial velocity increased the mean drop diameter decreased, as shown in Figure 9.17 for the system toluene/water and in Figure 9.18 for the system octan-1-ol/water. This is in agreement with the conclusion of other workers that the degree of coalescence decreased with increase in superficial velocity (93,95,154).

*Typical photographs of exit drops for four different systems at a similar magnification i.e. x 3.5, shown in Figures 9.6.1 to 9.6.8, indicate that a much larger mean drop size e.g. by a factor of ten was obtained for water/toluene than for any of the o/w systems. This arose because the mechanism of release, both within and at the exit from the bed, differed for water/toluene from those of o/w systems; these are discussed in Chapter 10.

* A complete set of photographs showing the range of exit drop sizes for all systems over all operating parameters has been deposited in the Departmental Library.

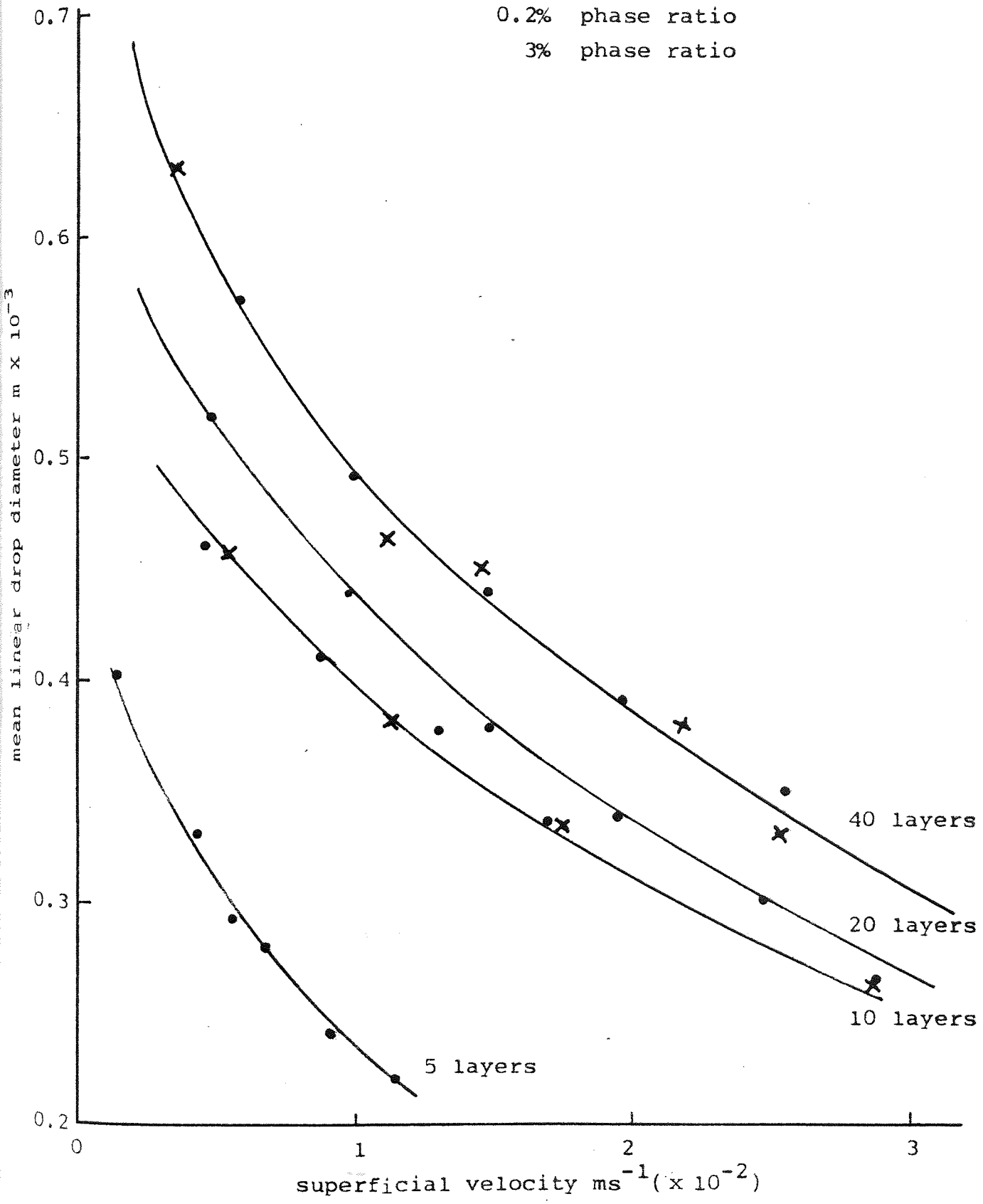

Figure 9.17 Exit drop diameter vs superficial velocity

System: Toluene - Water
Disp. Cont.

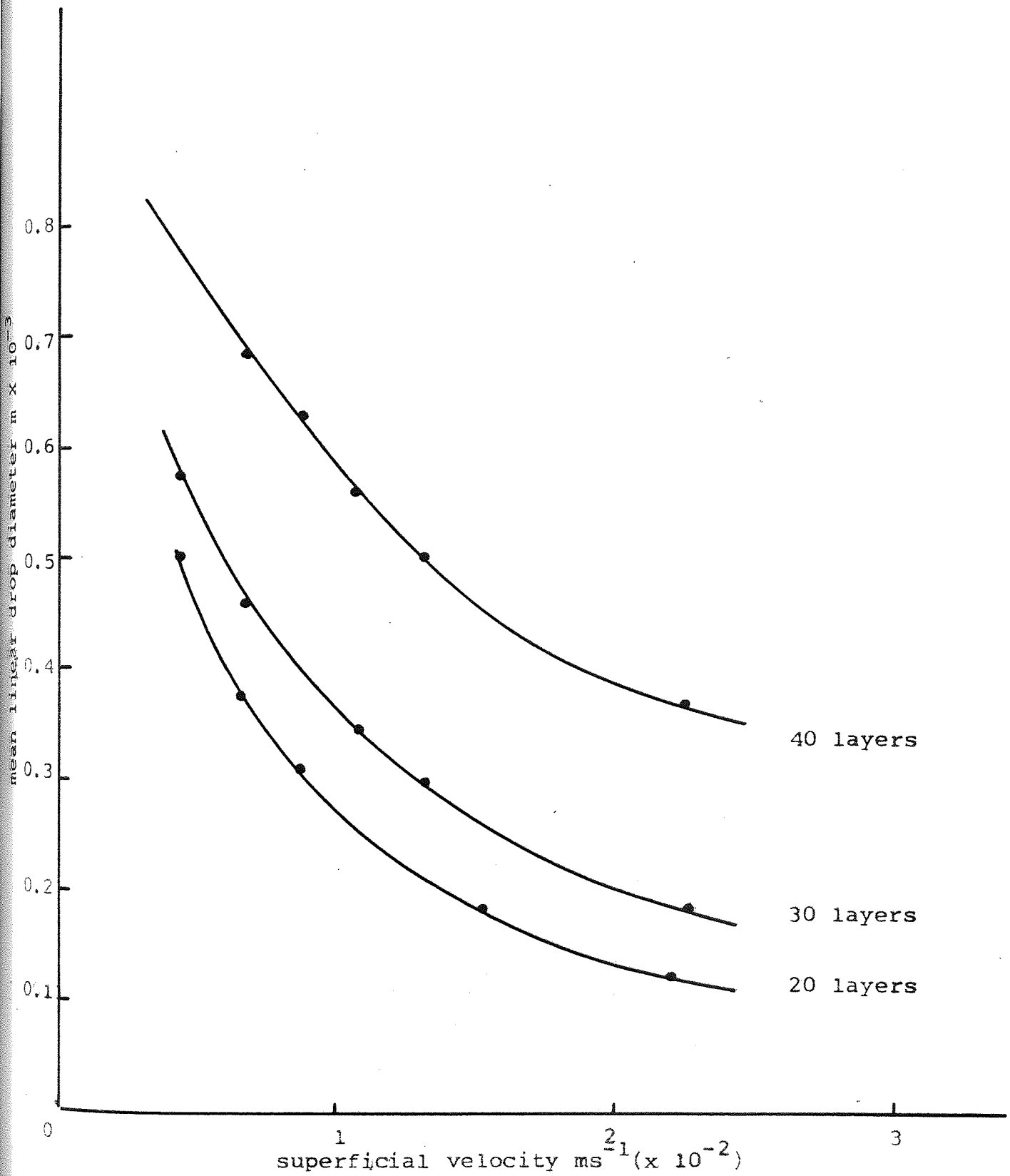

Figure 9.18 Exit drop diameter vs superficial velocity

System: Octan-1-ol - Water
Disp. Cont.

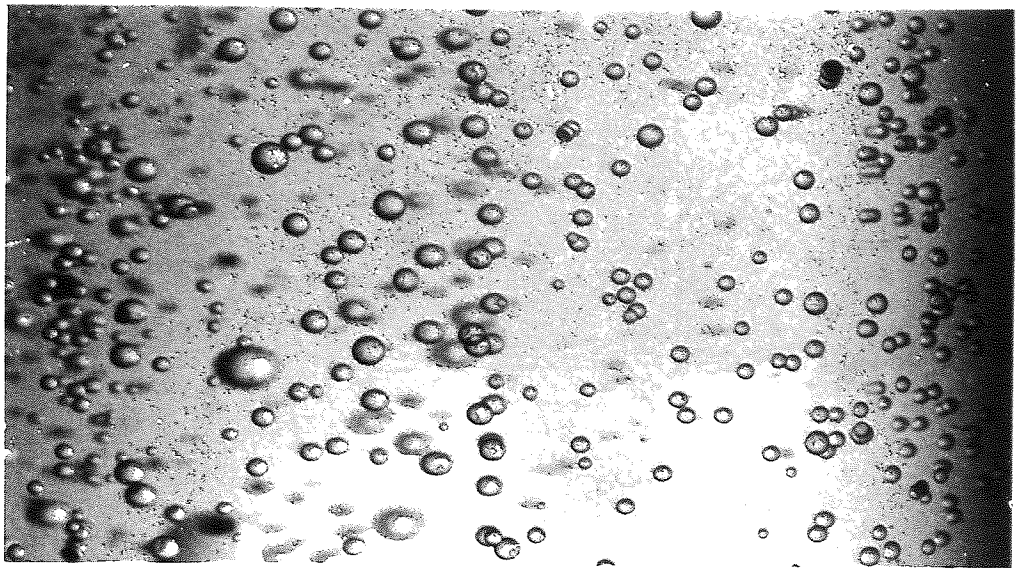

Figure 9.6.1 Exit drops Toluene/Water; 3% phase ratio

$V = 0.48 \times 10^{-2} ms^{-1}$

$d_{max} = 1.5 \times 10^{-3} m$

$d_{min} = 0.5 \times 10^{-3} m$

$h = 20 \times 10^{-3} m$

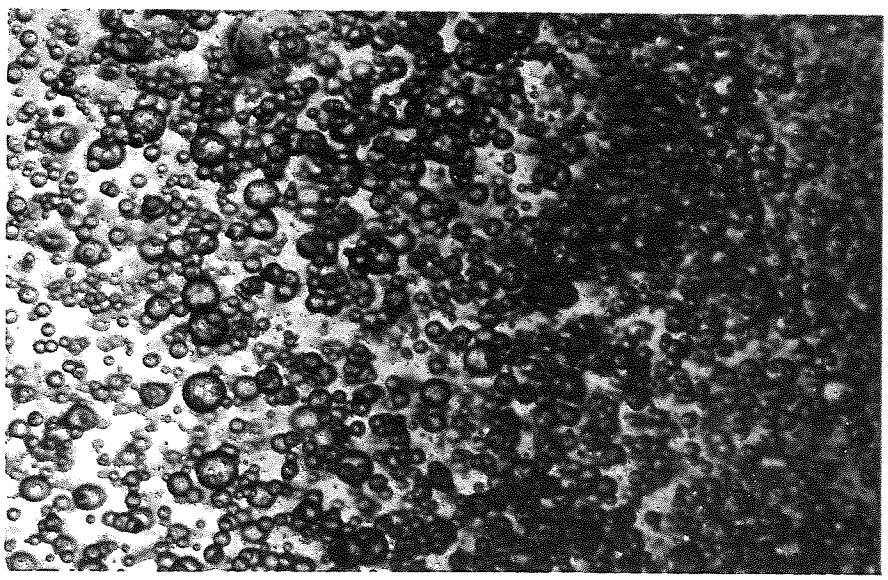

Figure 9.6.2 Exit drops Toluene/Water; 3% phase ratio

$V = 1.95 \times 10^{-2} ms^{-1}$

$d_{max} = 1.5 \times 10^{-3} m$

$d_{min} = 0.3 \times 10^{-3} m$ $\quad h = 20 \times 10^{-3} m$

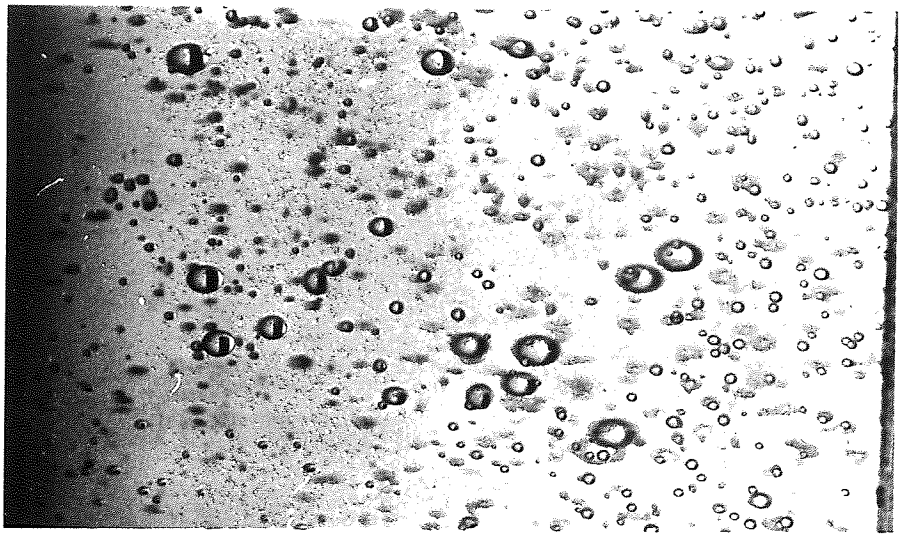

Figure 9.6.3 Exit drops Toluene/Water; 0.5% phase ratio

$V = 1.13 \times 10^{-2} ms^{-1}$

$d_{max} = 1.5 \times 10^{-3} m$

$d_{min} = 0.4 \times 10^{-3} m$

$h = 10 \times 10^{-3} m$

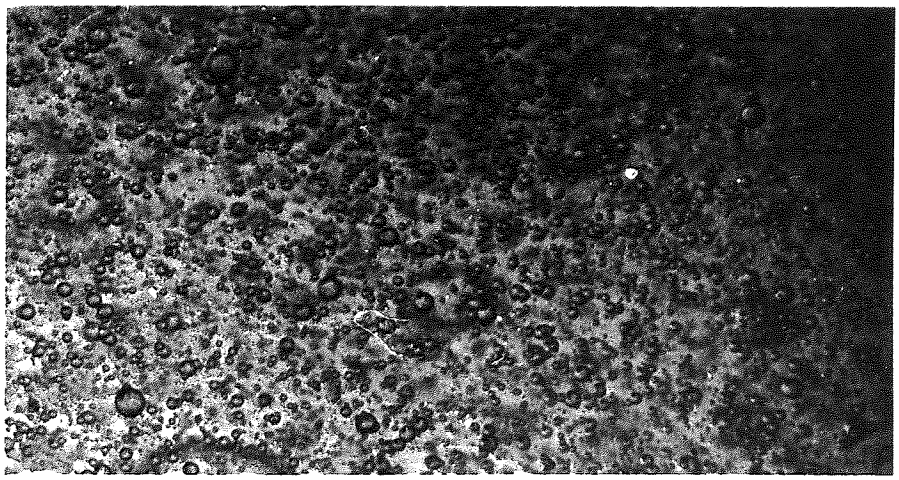

Figure 9.6.4 Exit drops Toluene/Water; 0.5% phase ratio

$V = 2.9 \times 10^{-2} ms^{-1}$

$d_{max} = 1.5 \times 10^{-3} m$

$d_{min} = 0.2 \times 10^{-3} m$

$h = 10 \times 10^{-3} m$

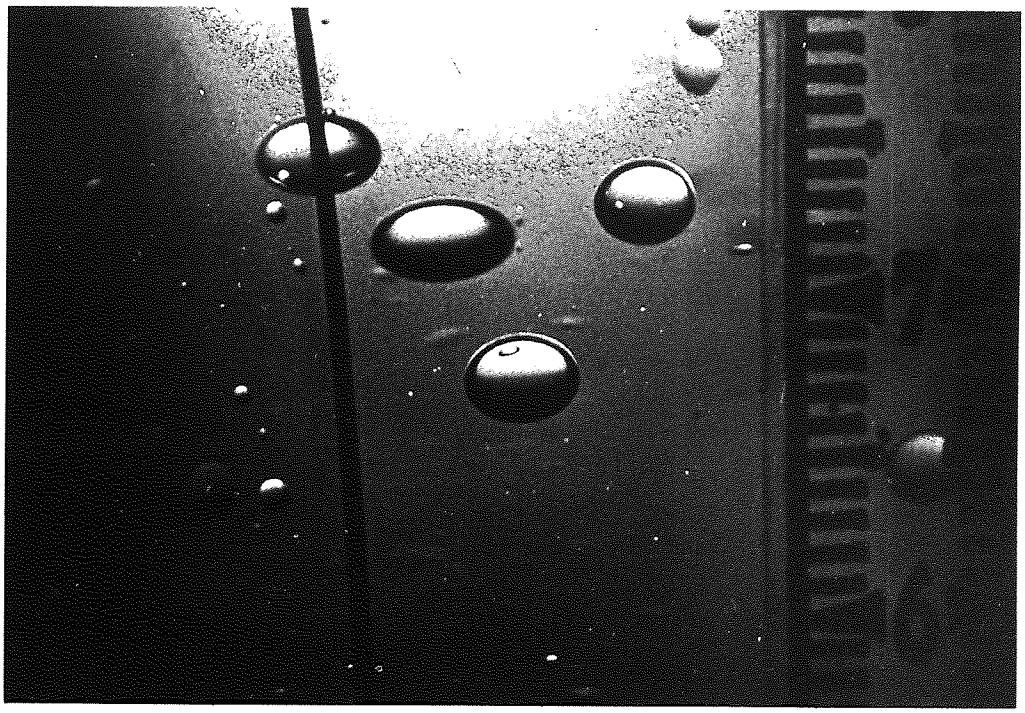

Figure 9.6.5 Exit drops Water/Toluene 2% phase ratio

$V = 1.5 \times 10^{-2} ms^{-1}$ $d_{max} = 5 \times 10^{-3} m$

$h = 30 \times 10^{-3} m$ $d_{min} = 0.3 \times 10^{-3} m$

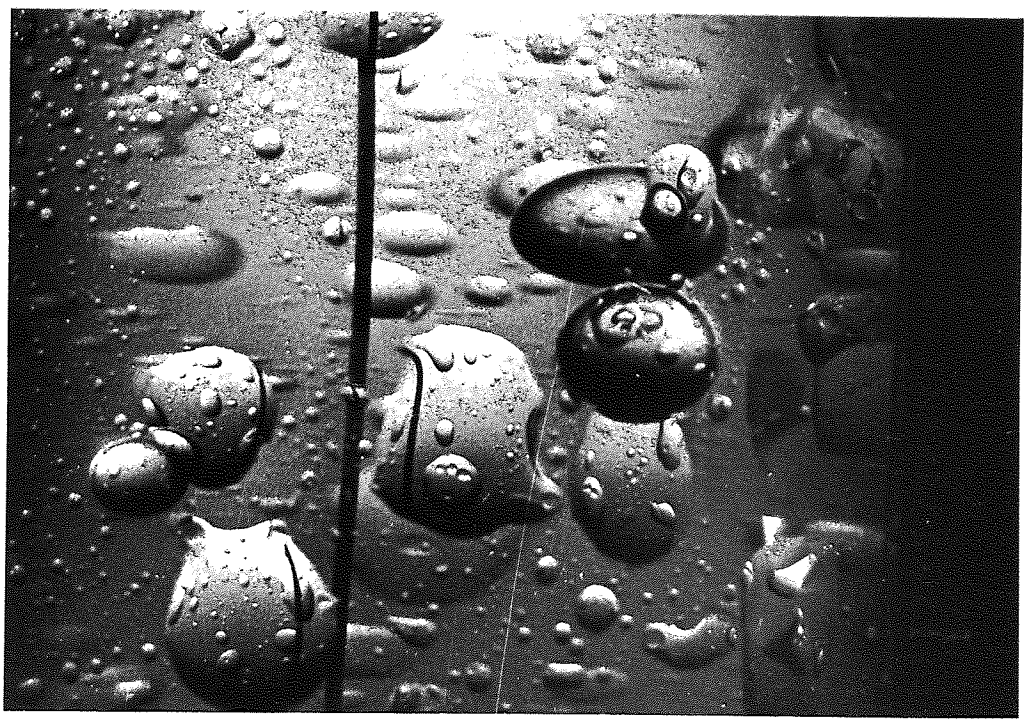

Figure 9.6.6 Exit drops Water/Toluene 2% phase ratio

$V = 5.2 \times 10^{-2} ms^{-1}$ $d_{max} = 7 \times 10^{-3} m$

$h = 30 \times 10^{-3} m$ $d_{min} = 0.2 \times 10^{-3} m$

Figure 9.6.7 Exit drops Octan-1-01/Water 0.2% phase ratio

$V = 0.5 \times 10^{-2} ms^{-1}$ $d_{max} = 1.5 \times 10^{-3} m$

$d_{min} = 0.2 \times 10^{-3} m$ $h = 20 \times 10^{-3} m$

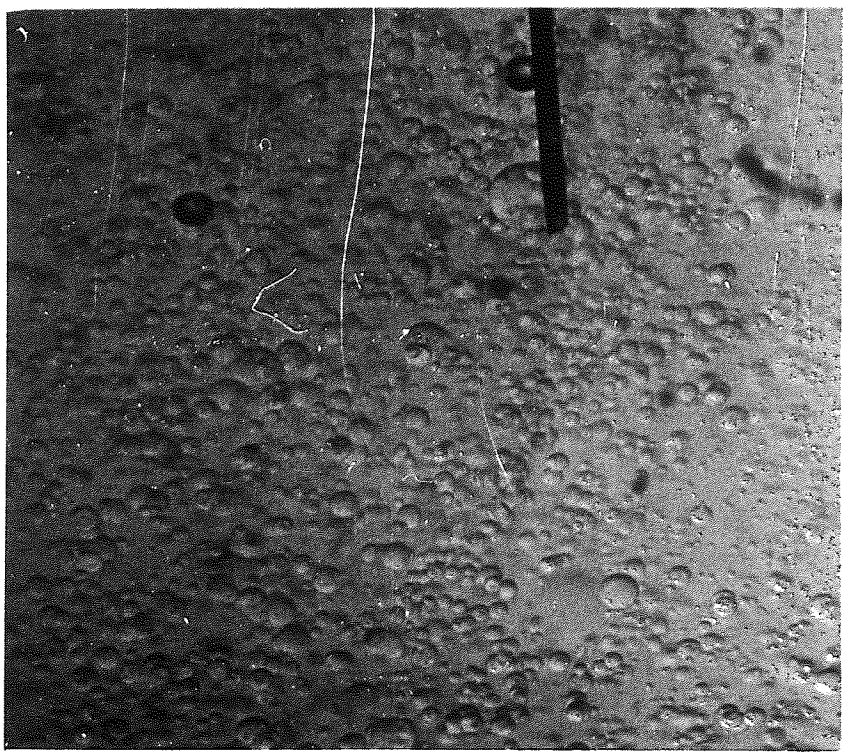

Figure 9.6.8 Exit drops MIBK/Water 2% phase ratio

$V = 0.5 \times 10^{-2} ms^{-1}$ $d_{max} = 1.5 \times 10^{-3} m$

$d_{min} = 0.2 \times 10^{-3} m$ $h = 20 \times 10^{-3} m$

9.7. "CRITICAL" VELOCITY

For each packing and any particular system there was a maximum dispersion superficial velocity flow above which either direct passage through the bed, or redispersion of drops held within it, or a combination of both occurred; this velocity is defined here as "critical" velocity i.e. the velocity for a specific system and packing arrangement, above which secondary droplets started to appear in the exit flow. Some secondary droplets were also produced by specific release mechanisms described in Section 10.2, but these were relatively insignificant.

The variation of "critical" velocity with packing thickness for three different liquid-liquid systems is shown in Figure 9.19. It is apparent that the "critical" velocity for any specific liquid-liquid system increases with an increase of bed thickness. For any one system the "critical" velocity reached a maximum value at which any increase in the number of layers of packing did not produce a corresponding increase in "critical" velocity. For the knitted fibre glass packing studied a 30 layer bed performed nearly as well as a 40 layer bed for all systems. For toluene/water and octan-1-ol/water dispersions a 20 layer bed approached the optimum performance. However for water/toluene even a 5 layer bed was efficient i.e. no break through occurred at velocities up to $5.5 \times 10^{-2} ms^{-1}$. This is explained by water, with a relatively high surface tension of $72.80 \times 10^{-3} Nm^{-1}$ compared with $27.96 \times 10^{-3} Nm^{-1}$ of toluene, having a greater force of adhesion (i.e. nearly 2.5 times). Hence there is a greater tendency for drop retention, and hence drop coalescence. Furthermore the viscous drag force on a water droplet in toluene

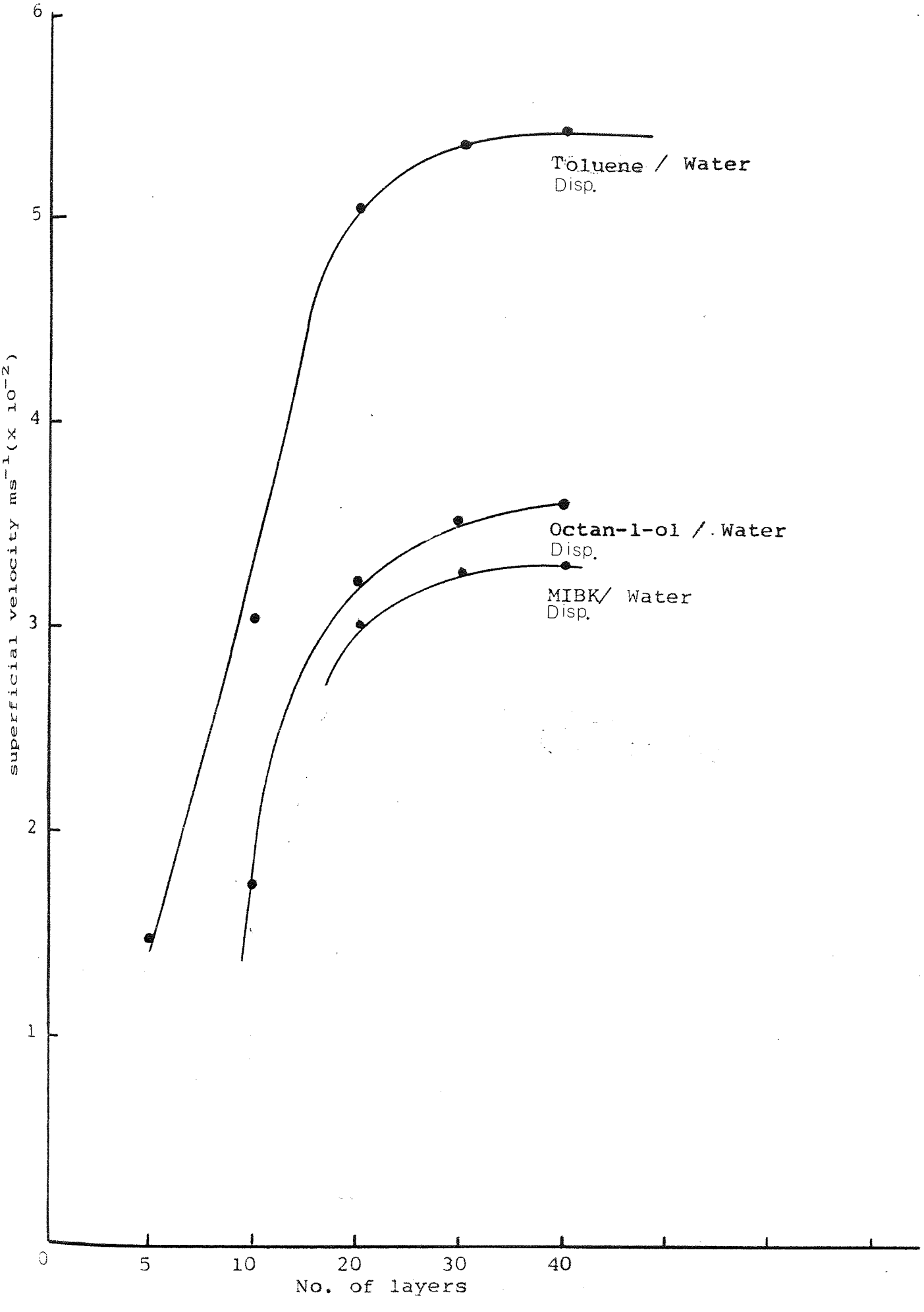

Figure 9.19 "Critical" superficial velocity vs Number of layers of the cell

is less than that on a toluene droplet in water i.e.toluene viscosity = 0.58 x $10^{-3}Kgs^{-1}m^{-1}$ compared with water viscosity = 0.98 x $10^{-3}Kgs^{-1}m^{-1}$. This means that at any particular continuous phase superficial velocity, the viscous drag force on a toluene droplet is about 1.7 times that on a water droplet of equivalent size. This contributes to the improved water drop retention and coalescence mechanisms. In addition the film drainage time discussed in Section 3.1. is directly proportional to the continuous phase viscosity, therefore a decrease in the continuous phase viscosity decreases the drainage time and hence increases the "critical" velocity.

For any particular thickness of packing the "critical" velocity for toluene/water was larger than for octan-1-ol/water although toluene and octan-1-ol have nearly the same surface tension of about 29 x $10^{-3}Nm^{-1}$, i.e. a similar force of adhesion, and both are in a continuum of water and therefore subjected to the same viscous drag force at any one superficial velocity. However the interfacial tension of octan-1-ol/water is 8.6 x $10^{-3}Nm^{-1}$ compared with 29.20 x $10^{-3}Nm^{-1}$ for toluene/water. Therefore the redispersion of octan-1-ol/ water is easier so that the formation of small droplets within the packing and at the exit would tend to be produced at lower velocities than with toluene/water.

The "critical" velocities for the systems MIBK/water and octan-1-ol/water were similar. These systems have very similar interfacial tensions but significally different dispersed phase viscosities i.e. octan-1-ol = 7.6 x $10^{-3}Kgs^{-1}m^{-1}$ and MIBK = 0.62 x $10^{-3}Kgs^{-1}m^{-1}$. This indicates that the effect of dispersed phase viscosity for the systems studied was negligible. A marginal change in "critical" velocity is attributable to the

differing surface tensions of the dispersed phase i.e. MIBK = 26 x $10^{-3}Nm^{-1}$, octan-1-ol = 29.5 x $10^{-3}Nm^{-1}$.

In conclusion, the most important factors affecting "critical" velocity for any particular packing height were interfacial tension of the system, the surface tension of the dispersed phase and the viscosity of the continuous phase. The viscosity of the dispersed phase was not a significant factor. This is in agreement with the observation of Vinson (94) who found only a slight increase in coalescence over a 30 fold increase in droplet viscosity.

9.8. EFFECT OF INLET DROP SIZE ON EXIT DROP SIZE

For any particular flow velocity below the "critical" value the exit drop size distribution was independent of inlet drop size distribution for the range investigated i.e. 8-40 μm. This was because each captured drop must grow to a size on each packing element involved until buoyancy and drag forces overcome the surface forces. These forces are only a function of superficial velocity for any particular packing and dispersion system.

9.9. EFFECT OF PHASE RATIO ON EXIT DROP SIZE

Under steady state conditions mean exit drop size was independent of phase ratio within the range 0.1 to 3% as shown in Figure 9.17. In parallel studies no changes in mean exit droplet size were observed at phase ratios between 0.1 to 0.6% (156) and 3 to 7% (93).

The degree of coalescence was clearly therefore independent of the ratio of dispersed phase entering the bed.

Although phase ratios less than 0.1% were not studied in this work, there is no reason in theory why these packings

should not function satisfactorily at very low phase ratios e.g. 0.01%. Indeed during washing operations using distilled water no secondary haze was formed at the exit. So far as an upper phase ratio is concerned a limited number of experiments demonstrated that 'flooding' as defined in Section 9.10, did not occur at inlet phase ratios up to 50%.

9.10. EFFECT OF PACKING THICKNESS ON EXIT DROP SIZE

Five different packing thicknesses in the range 5×10^{-3} to 40×10^{-3}m, with a constant voidage of 0.844, were investigated. An increase in packing thickness from 5×10^{-3} to 40×10^{-3}m led to an increase in exit drop size as well as in the "critical" velocity as shown in Figures 9.17 to 9.19. However, there was an optimum bed thickness after which any increase in thickness did not result in a corresponding increase in "critical" velocity; this is shown in Figure 9.19. This was in agreement with the observations of Sareen etal (81) who suggested that the degree of coalescence increased with bed depth up to a certain maximum bed thickness. Hence an optimum thickness existed for each application. This is because the velocity of any droplet within the packing decreases as it travels through the bed until after some distance the retention time is sufficient for film drainage to occur and hence for adherence of the droplet on a fibre; This is explained in Section 10.1. Therefore a greater depth of the packing is required at a larger drop velocity in order for coalescence to take place. However beyond the optimum packing thickness, after which the "critical" velocity discussed in Section 9.7 did not increase with increasing packing thickness,

the local viscous drag force predominates over the other forces and hence prevents droplet adherence to the fibre. For toluene/water the optimum thickness was about 30×10^{-3}m.

9.11. VOIDAGE DETERMINATION

The packing was of borosilicate crown fibrous glass with a known density of 2.50×10^{-3}Kg/m^3. It was used in sheets of constant thickness and weight per unit area, detailed specifications of the packing material are given in Section 7.3.1. A limited number of tests were made by pressing equal number of layers of packing into different heights. In this way the voidage and pore size distribution changed so that a preferred arrangement could be selected. 40 layers of packing pressed to make a 2×10^{-2}m bed resulted in some secondary dispersion at the exit for superficial velocities greater than 1.5×10^{-2}ms^{-1} possibly indicative of redispersion. At a phase ratio above 13% the same bed also exhibited poor release mechanisms i.e. foaming. (This type of release is defined here as "flooding" of the packing and is discussed in Section 10.2.5). The best performance was obtained by compressing a bed to allow 1×10^{-3}m height for each layer ; this gave a constant voidage of 0.844. Therefore the results shown in Figures 9.1 to 9.19 were obtained for the latter voidage. The packed bed prepared in this way did not flood for phase ratios as high as 50%.

Under two phase flow conditions a finite amount of the dispersed phase was retained in the bed thus decreasing its initial voidage. The two phase flow voidage of the cell was found using Equation 9.4 and is tabulated in Tables 9.3 to 9.5.

Table 9.3.1 EFFECT OF SUPERFICIAL VELOCITY ON VOIDAGE, HOLD UP AND SATURATION DETERMINATION, SYSTEM; TOLUENE/WATER

5 LAYERS				10 LAYERS			
$V_{ms^{-1} \times 10^{-2}}$	E_2	$\emptyset_H$	S	$V_{ms^{-1} \times 10^{-2}}$	E_2	$\emptyset_H$	S
0.272	0.745	0.635	0.117	0.460	0.752	0.590	0.109
0.425	0.745	0.635	0.117	0.550	0.752	0.590	0.109
0.580	0.745	0.635	0.117	0.730	0.752	0.590	0.109
0.750	0.745	0.635	0.117	1.30	0.753	0.583	0.108
0.915	0.745	0.635	0.117	2.30	0.754	0.577	0.107
1.07	0.745	0.635	0.117	3.35	0.755	0.571	0.105
AVERAGE E_2 = 0.745 AVERAGE $\emptyset_H$ = 0.635 AVERAGE S = 0.117				AVERAGE E_2 = 0.753 AVERAGE $\emptyset_H$ = 0.583 AVERAGE S = 0.108			

Table 9.3.2. EFFECT OF SUPERFICIAL VELOCITY ON VOIDAGE, HOLD UP AND SATURATION DETERMINATION, SYSTEM; TOLUENE/WATER

20 LAYERS				30 LAYERS			
V $ms^{-1} \times 10^{-2}$	E_2	$\emptyset_H$	S	V $ms^{-1} \times 10^{-2}$	E_2	$\emptyset_H$	S
0.305	0.765	0.506	0.094	0.295	0.766	0.50	0.092
0.460	0.766	0.500	0.092	0.630	0.766	0.50	0.092
0.723	0.766	0.500	0.092	0.980	0.766	0.51	0.094
1.00	0.767	0.494	0.091	1.34	0.766	0.51	0.092
2.17	0.768	0.487	0.090	2.45	0.765	0.51	0.094
3.45	0.769	0.481	0.090	3.22	0.766	0.51	0.094
4.10	0.769	0.481	0.089	4.00	0.764	0.51	0.095
AVERAGE E_2 = 0.767				AVERAGE E_2 = 0.765			
AVERAGE $\emptyset_H$ = 0.493				AVERAGE $\emptyset_H$ = 0.507			
AVERAGE S = 0.091				AVERAGE S = 0.093			

Table 9.3.3. CALCULATED AVERAGE VALUES FOR VOIDAGE, HOLD UP AND SATURATION FOR DIFFERENT PACKING HEIGHTS; TOLUENE/WATER

NO. OF LAYERS	AVERAGE E_2	AVERAGE $\emptyset_H$	AVERAGE S
5	0.745	0.635	0.117
10	0.753	0.583	0.108
20	0.767	0.493	0.091
30	0.765	0.507	0.093
40	0.764	0.513	0.095
AVERAGE	0.759	0.546	0.102

Table 9.4.1. EFFECT OF SUPERFICIAL VELOCITY ON VOIDAGE, HOLD UP, AND SATURATION DETERMINATION; MIBK/WATER

20 LAYERS				40 LAYERS			
V $ms^{-1} \times 10^{-2}$	E_2	$\emptyset_H$	S	V $ms^{-1} \times 10^{-2}$	E_2	$\emptyset_H$	S
0.44	0.784	0.380	0.070	0.44	0.790	0.346	0.064
0.66	0.793	0.330	0.061	0.66	0.794	0.320	0.059
0.88	0.790	0.346	0.064	0.88	0.793	0.327	0.060
1.31	0.790	0.346	0.064	1.08	0.790	0.346	0.064
1.53	0.794	0.320	0.059	1.31	0.792	0.333	0.062
				1.53	0.790	0.346	0.064
AVERAGE E_2 = 0.790 AVERAGE $\emptyset_H$ = 0.344 AVERAGE S = 0.064				AVERAGE E_2 = 0.792 AVERAGE $\emptyset_H$ = 0.336 AVERAGE S = 0.062			

Table 9.4.2. EFFECT OF SUPERFICIAL VELOCITY ON VOIDAGE, HOLD UP, AND SATURATION DETERMINATION; OCTAN-1-OL/WATER

20 LAYERS				40 LAYERS			
V $ms^{-1} \times 10^{-2}$	E_2	$\emptyset_H$	S	V $ms^{-1} \times 10^{-2}$	E_2	$\emptyset_H$	S
0.45	0.792	0.33	0.062	0.70	0.795	0.314	0.058
0.52	0.792	0.33	0.062	1.10	0.795	0.314	0.058
0.60	0.793	0.33	0.060	1.50	0.795	0.314	0.058
0.68	0.793	0.33	0.060	1.90	0.795	0.314	0.058
1.07	0.794	0.32	0.059	2.32	0.795	0.314	0.058
1.47	0.794	0.32	0.059	2.75	0.795	0.314	0.058
1.87	0.794	0.32	0.059	3.2	0.795	0.314	0.058
2.30	0.794	0.32	0.059	3.57	0.794	0.320	0.059
2.73	0.794	0.32	0.059	4.0	0.794	0.320	0.059
3.17	0.794	0.32	0.059				
AVERAGE E_2 = 0.793 AVERAGE $\emptyset_H$ = 0.324 AVERAGE S = 0.060				AVERAGE E_2 = 0.795 AVERAGE $\emptyset_H$ = 0.315 AVERAGE S = 0.058			

Allowing for experimental errors in the determination, the values for any particular system remained reasonably constant for all superficial velocities.

9.12. HOLD-UP DETERMINATION

Hold-up is expressed as the volume of liquid held per volume of solid and is given by,

$$\phi_H = \frac{E_1 - E_2}{1 - E_1} \qquad \ldots\ldots\ldots\ldots\ldots\ldots\ldots 9.5.$$

Calculated values, presented in Tables 9.3. to 9.6., indicated that over the range $0.3 \times 10^{-2} ms^{-1}$ to $5.0 \times 10^{-2} ms^{-1}$, bed hold-up was independent of superficial velocity. This is contrary to the work of Sherony (120) in which hold-up was concluded to decrease with increase in superficial velocity. This conclusion may have arisen due to the use of the Kozeny Equation 9.1. to calculate two phase flow voidage without any modification; reference to the original data (154) also shows that there was rather a wide scatter.

As already discussed two phase flow pressure drop was independent of inlet drop size distribution and phase ratio; also hold-up was independent of both. Thus an average hold-up value was determined for each liquid-liquid system used as shown in Table 9.6. The hold-up was apparently unaffected by viscosity of the dispersed phase i.e. the hold-up for MIBK-water with a viscosity $0.58 \times 10^{-3} Kgm^{-1}s^{-1}$, was the same as octan-1-ol/water with a viscosity $7.6 \times 10^{-3} Kgm^{-1}s^{-1}$. These systems had an almost equal interfacial tension of $9 \times 10^{-3} Nm^{-1}$. However hold-up increased with a decrease in viscosity of continuous phase i.e. with toluene/water

Table 9.5.1 EFFECT OF SUPERFICIAL VELOCITY ON VOIDAGE, HOLD UP, AND SATURATION DETERMINATION; WATER/TOLUENE

5 LAYERS				10 LAYERS			
V $ms^{-1} \times 10^{-2}$	E_2	$\emptyset_H$	S	V $ms^{-1} \times 10^{-2}$	E_2	$\emptyset_H$	S
1.2	0.760	0.540	0.099	0.60	0.750	0.60	0.111
1.73	0.760	0.540	0.099	0.86	0.749	0.61	0.112
2.55	0.760	0.540	0.099	2.00	0.750	0.60	0.111
4.00	0.760	0.540	0.099	2.70	0.748	0.61	0.114
5.00	0.760	0.540	0.099	4.30	0.747	0.62	0.115
AVERAGE E_2 = 0.760 AVERAGE $\emptyset_H$ = 0.540 AVERAGE S = 0.099				AVERAGE E_2 = 0.749 AVERAGE $\emptyset_H$ = 0.607 AVERAGE S = 0.112			

Table 9.5.2 EFFECT OF SUPERFICIAL VELOCITY ON VOIDAGE, HOLD UP, AND SATURATION DETERMINATION; WATER/TOLUENE

30 LAYERS				40 LAYERS			
V $ms^{-1} \times 10^{-2}$	E_2	$\emptyset_H$	S	V $ms^{-1} \times 10^{-2}$	E_2	$\emptyset_H$	S
0.38	0.748	0.615	0.114	0.64	0.753	0.580	0.108
0.80	0.747	0.620	0.115	1.00	0.753	0.580	0.108
1.25	0.747	0.620	0.115	1.35	0.752	0.590	0.109
1.70	0.746	0.630	0.116	1.75	0.753	0.580	0.108
2.65	0.746	0.630	0.116	2.10	0.752	0.590	0.109
3.65	0.746	0.630	0.116	2.50	0.752	0.590	0.109
4.65	0.746	0.630	0.116	3.30	0.752	0.590	0.109
				3.70	0.753	0.580	0.108
AVERAGE E_2 = 0.747 AVERAGE $\emptyset_H$ = 0.630 AVERAGE S = 0.116				AVERAGE E_2 = 0.752 AVERAGE $\emptyset_H$ = 0.590 AVERAGE S = 0.109			

dispersions the hold-up was lower than for water/toluene dispersions as shown in Table 9.6.

9.13. SATURATION DETERMINATION

The degree of saturation, defined as the fraction of pore space of the bed occupied by the dispersed phase, influenced both pressure drop and coalescence performance.

Saturation cannot be predicted from theory due to the difficulty of allowing for the effect of surface roughness (49,81) and the complexity of the process by which saturation occurs. However the method employed by Sherony (154) can be applied. It is assumed that the increased pressure drop associated with two phase flow is due solely to the decrease in void space because of the dispersed phase hold-up within the bed. This assumption is reasonable for small drops in a dilute system since, as in Section 9.4. they do not affect the bulk properties. The average saturation is therefore related to the average hold-up by:

$$S = \phi_H \left(\frac{1 - E_1}{E_1}\right) = 1 - \frac{E_2}{E_1} \quad \text{.....9.6}$$

Saturation S calculated from equation 9.6. gave a constant value for any particular system as shown in Tables 9.3 to 9.6. However the hold-up, and hence the saturation value, varied from system to system. The maximum average value was for the water/toluene system, which gave a value of 0.109, and the lowest was for octan-1-ol/water dispersion at 0.059. The disperse phase viscosity did not appear to have any significant effect on hold-up and/or degree of saturation i.e. MIBK

Table 9.6. AVERAGE VALUES FOR VOIDAGE, HOLD-UP AND SATURATION FOR DIFFERENT DISPERSION SYSTEMS

Dispersion Systems	Average E_2	Average $\emptyset_H$	Average S
Toluene/ water	0.759	0.546	0.102
MIBK/water	0.791	0.340	0.063
Octan-1-ol/ water	0.794	0.321	0.059
Water/ toluene	0.752	0.590	0.109

with a viscosity 0.62 x 10^{-3}Kgm^{-1}s^{-1} produced nearly an identical pressure drop line with octan-1-ol with a viscosity of 7.6 x 10^{-3}Kgm^{-1}s^{-1} and hence an identical hold-up and degree of saturation (Table 9.6.).

Spielman (95) did not measure the saturation values at various velocities, but only the final saturation after dismantling the bed. However Rosenfeld (130) used Spielman's pressure drop data to calculate the saturation at arbitrary velocities. Consideration was only given to those cases when the dispersed phase did not wet the fibre, it being assumed that when the dispersed phase wetted the fibre the drop release mechanism would be different. It was concluded that for velocities lower than 0.1 x 10^{-2}ms^{-1} saturation was independent of velocity.

In this study saturation was independent of superficial velocity over the range 0.5 x 10^{-2}ms^{-1} to 5 x 10^{-2}ms^{-1} since hold-up was constant. An average saturation was therefore calculated for each system as shown in Table 9.6.

CHAPTER 10

Mechanisms of collection, coalescence and release in a fibrous glass bed

CHAPTER 10

MECHANISMS OF COLLECTION, COALESCENCE AND RELEASE IN A FIBROUS GLASS BED

The novel refractive index matching technique described in Chapter 6 enabled the complete phenomena of drop collection/coalescence within the packing to be observed. It also aided the complete understanding of the release mechanisms described in Section 10.2.

10.1. FIBRE CATCHMENT/COALESCENCE

As discussed in Chapter 1 the settling velocity for secondary dispersion droplets is very low; therefore droplets enter the packing with a velocity equal to the continuous phase superficial velocity. However, due to repeated impaction with the fibres which obstruct their path, the mean droplet velocity decreases to less than the continuous phase superficial velocity. When a droplet reaches an appropriate velocity, i.e. it no longer rebounds following collision with the film of the continuous phase around a fibre, film thinning and drainage then occurs and the droplet adheres to the fibre. The droplet subsequently slides or rolls along the fibre in the direction of the pressure gradient until it meets another drop at an 'effective site'. An effective site generally coincides with fibre(s) intersections; as shown in Figure 10.1.1. Due to surface forces acting in random directions on a drop retained at an intersection, and under the influence of hydrodynamic forces of the continuous

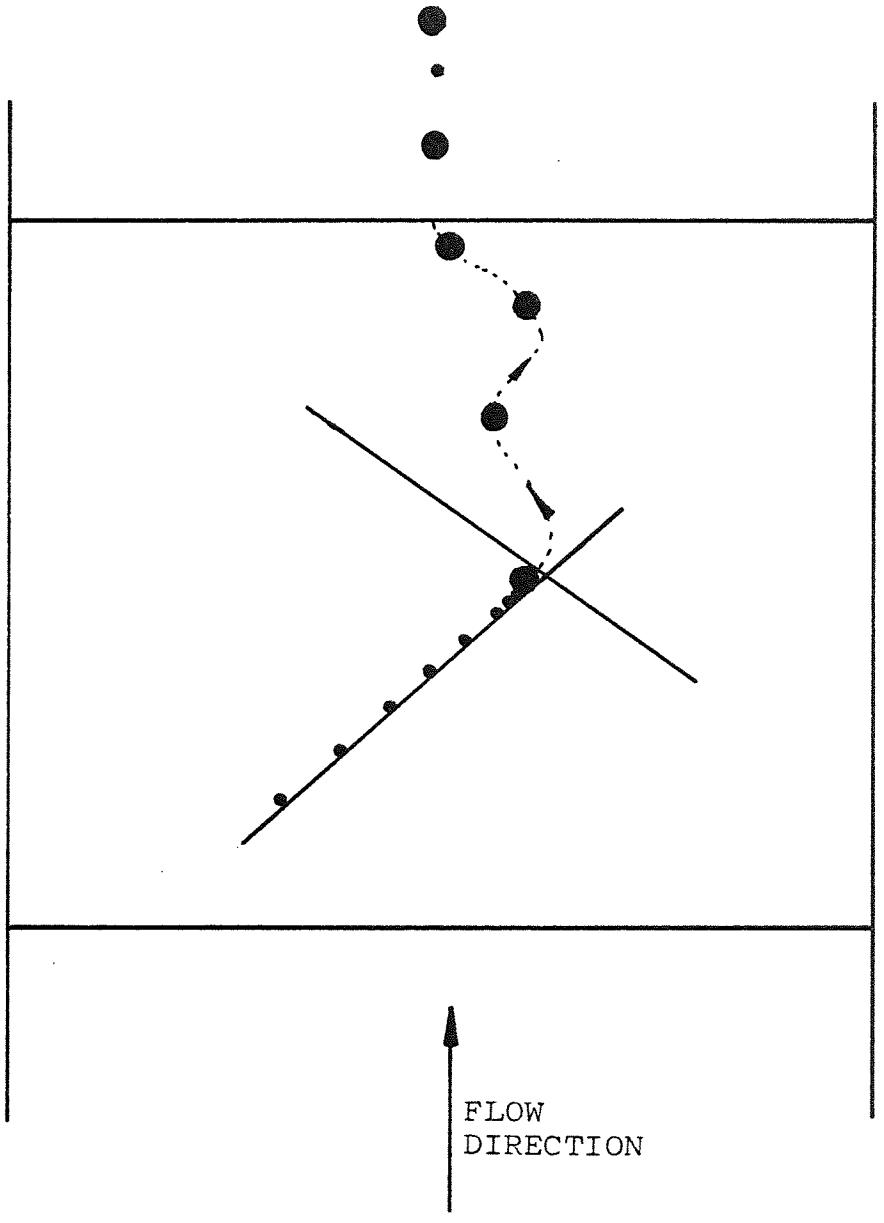

Figure 10.1.1. Mechanisms of collection/coalescence within the packing

Fibre intersection acts as an 'effective site'; droplets move along the fibre and are collected at the intersection.

phase, sphericity of the drop is partially lost. Distortion results in a loss of rigidity and therefore easier coalescence. Once coalescence has occurred, if the resultant droplet exceeds an equilibrium size it is swept off the fibre.

10.1.1. DROPLET VELOCITY WITHIN THE PACKING

Droplets exceeding the equilibrium size move in a tortuous path with a velocity dependent upon the droplet diameter and the continuous phase superficial velocity.

Table 10.1. lists vertically upward droplet velocities for several drop sizes and two superficial flow velocities. Clearly the velocities of the equilibrium drop size is far greater than the superficial flow velocities i.e. nearly 10 times larger. Therefore once the equilibrium drop size is attained the viscous drag force acts in opposition to the bouyancy force. However comparing these drop velocities with the settling velocities calculated from the Stoke's equation described in Chapter 1 for the case when no packing is present, the settling velocity for any given drop size is nearly 10 times greater. This would be expected because the droplets move in a tortuous path and also undergo repeated impactions within the bed which slows them down.

10.1.2. HOLD-UP DISTRIBUTION OF DISPERSED PHASE

Observations indicated that a constant hold-up was present throughout the packing.

Table 10.1. "MEAN" VELOCITY OF DROPLET TRAVEL WITHIN THE PACKING; 6% PHASE RATIO

System: Xylene/Potassium Thiocynide + Formamide

Packing Voidage = 0.92

a) Superficial flow velocity of $0.36 \times 10^{-2} ms^{-1}$

Drop Diameter $m \times 10^{-3}$	Settling Velocity according to Stoke's Law $ms^{-1} \times 10^{-2}$	'Mean' Velocity $ms^{-1} \times 10^{-2}$ within the bed	Observed 'Mean' Velocity $ms^{-1} \times 10^{-2}$	
			Min.	Max.
0.5	10.0	1.44	1.25	1.6
0.6	14.4	1.65	1.6	1.7
0.7	19.6	1.97	1.8	2.2
0.8	25.6	2.50	2.4	2.6
0.9	32.4	3.10	2.9	3.3
1.0	40.0	3.70	3.5	4.2

b) Superficial flow velocity $0.27 \times 10^{-2} ms^{-1}$

Drop Diameter $m \times 10^{-3}$	Settling Velocity according to Stoke's Law $ms^{-1} \times 10^{-2}$	'Mean' Velocity $ms^{-1} \times 10^{-2}$ within the bed	Observed 'Mean' Velocity $ms^{-1} \times 10^{-2}$	
			Min.	Max.
0.6	14.4	1.40	1.2	1.8
0.7	19.6	1.78	1.6	2.0
0.8	25.6	2.38	2.0	2.5
0.9	32.4	2.90	2.8	3.1
1.0	40.0	3.50	3.2	3.9

Figure 10.1.2 is a print from a *cine film. This demonstrates a constant hold-up distribution throughout the packing. Hold-up is concentrated at the fibre intersections i.e. 'effective sites' and no rivulets are apparent within the packing. This is contrary to the mechanisms described by Hazlett (97) and Shahloub (93) involving the formation of rivulets within the packing before the final release.

Finally the assumption of a constant hold-up throughout the bed for the calculations of the degree of saturation, discussed in Section 9.13, is clearly valid.

10.2. MECHANISMS OF RELEASE

Following repetitive capture and coalescence throughout the packing, enlarged droplets should ideally be released from the exit face with a minimum of redispersion or break up.

Prior to this work up to four kinds of exit droplet release mechanism had been reported; these are reviewed in Section 5.2.1. and illustrated in Figure 5.2.2. However due to the difficulty of observing the mechanisms of droplet coalescence and travel within the packing, no practical basis could be proposed for these mechanisms of release i.e. whether formation of a droplet took place entirely on the surface and/or the manner in which a drop was fed from underneath.

Throughout this study no less than 6 different mechanisms of drop release were observed. These are identified, and shown

* Cine films of the mechanisms of coalescence within the packing have been retained in the Department.

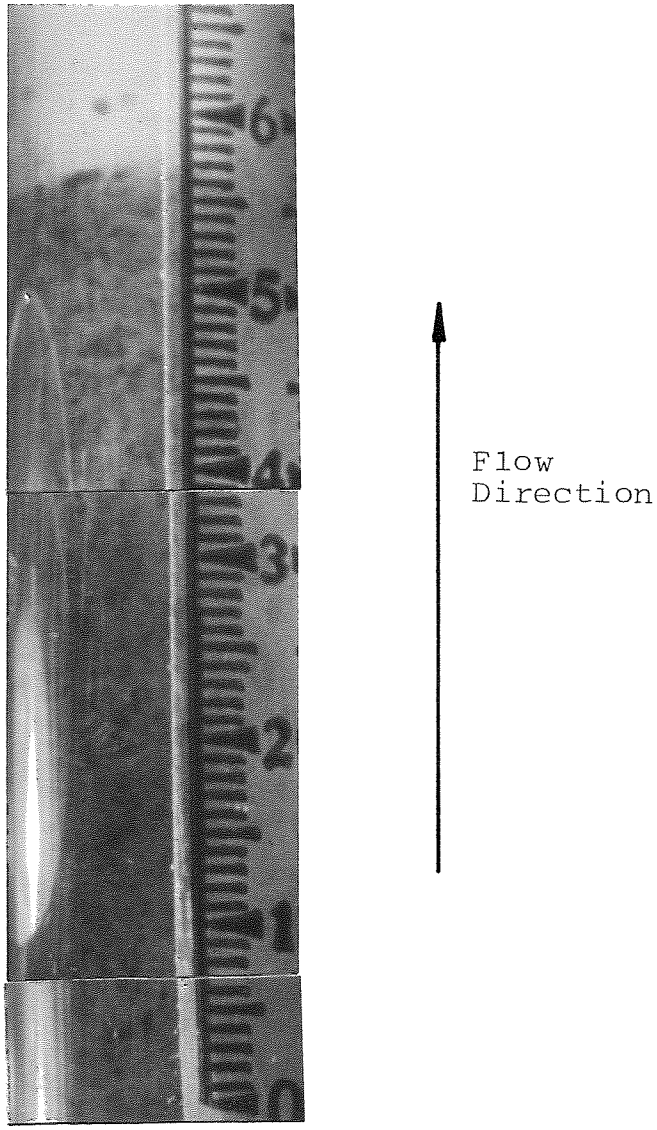

Figure 10.1.2. A print from a cine film

Showing the 'effective sites' and a constant hold-up within the packing.

1 small division on the scale = 1mm

(Film obtained using u.v. light to activate droplets containing phototropic dye)

diagramatically, in Figure 10.2.1. In most cases more than one type of drop release mechanism was observed for the same liquid-liquid packing system. A typical photograph of drop release from the outlet is shown in Figure 10.2.2; this indicates three different mechanisms of release occurring simultaneously. The individual mechanisms are discussed in Sections 10.2.1. to 10.2.6.

10.2.1. DRIP-POINT

Droplets of different sizes travelled within the packing at different velocities i.e. larger drops travelled quicker. As they approached the exit of a bed, depending on their velocity they either (a) passed through unchanged c.f. Section 10.2.2. or (b) resided on the exit surface of the packing where they were fed by other droplets following the same path, and probably originating from the same effective site. This is contrary to the suggestion by other workers (93,97) who postulated a thread feed for drops at the exit of the bed. The balloon-shaped drops grew and, when bouyancy and drag forces exceeded the surface forces, rupture occurred at the neck resulting in drip-point release. This kind of release is shown in Figure 10.2.3.

10.2.2. JETTING

A droplet with a high velocity entered a pore at the exit surface and passed through without any retention on the surface. (This is not to be confused with the mechanism observed by Polichronakis (125) which was jetting after break through, that

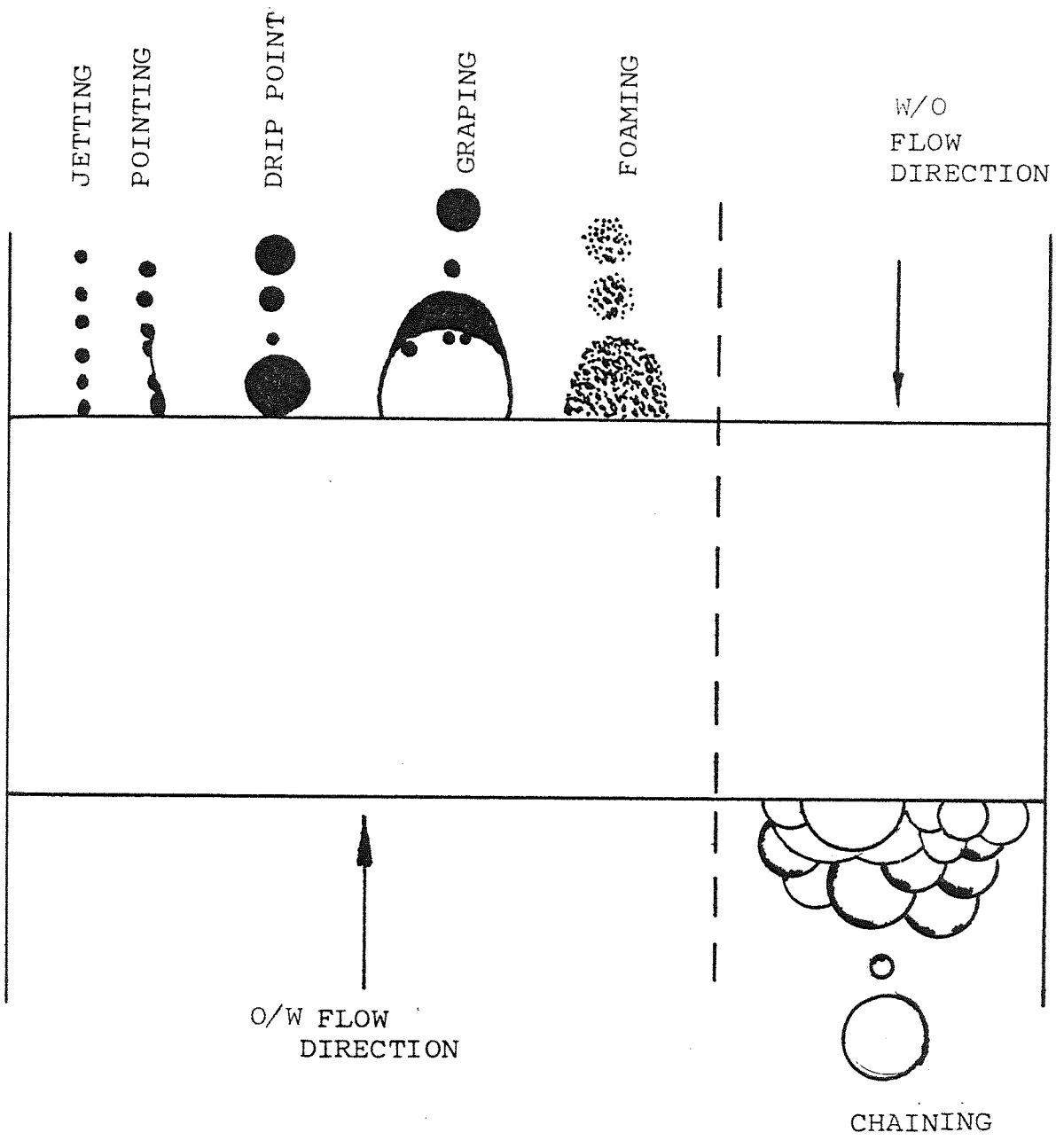

Figure 10.2.1. Various types of mechanisms of release

Figure 10.2.2. Mechanisms of release
"DRIP-POINT" + "JETTING" + "POINTING"

Magnification = 6 x

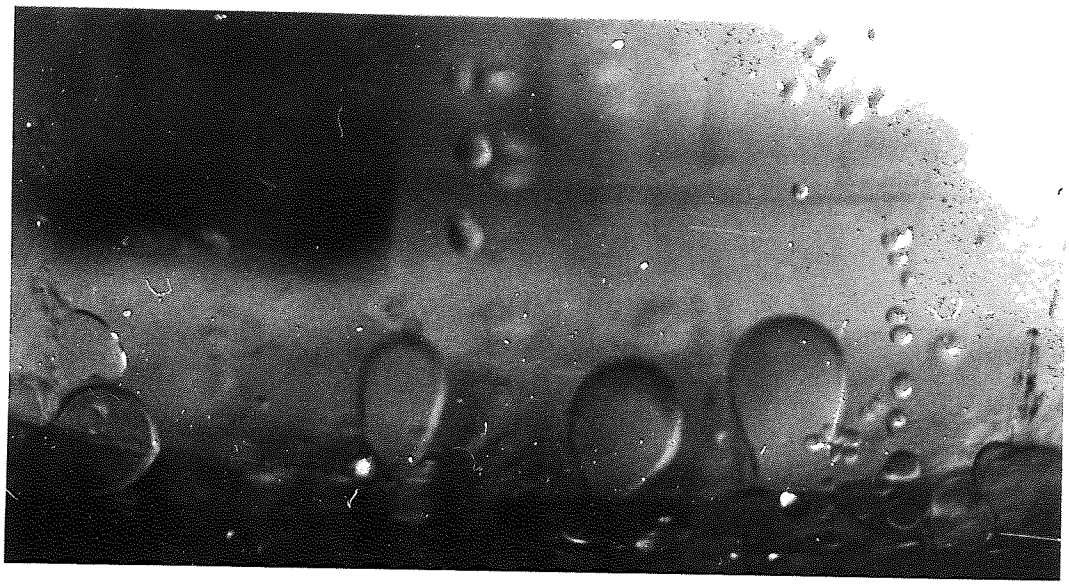

Figure 10.2.3 Mechanisms of release "DRIP POINT"

System: MIBK/WATER

Magnification = 3.5 x

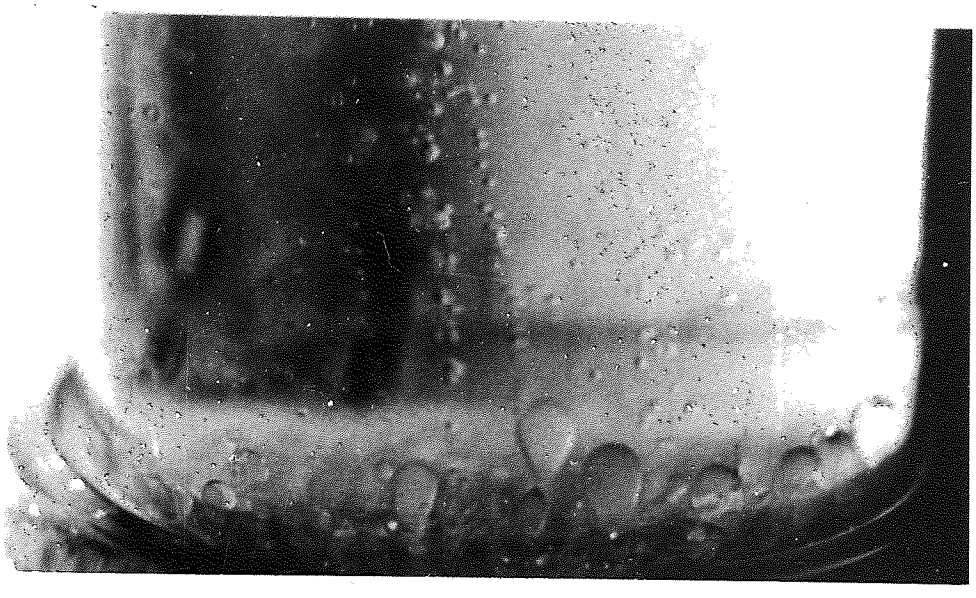

Figure 10.2.4 Mechanisms of release "DRIP POINT" + POINTING

System: MIBK/WATER

Magnification = 3 x

is when little or no collection was occurring). The mechanism of jetting as defined here involved formation of a primary drop within the packing and its acceleration out of the bed.

Jetting did not occur with water/oil dispersions since water droplets had a much larger force of adhesion and were therefore retained on the surface of the packing where they grew and left by drip-point with a transition to chaining as discussed in Section 10.2.6. The mechanisms of jetting are shown in Figure 10.2.5.

10.2.3. POINTING

In this mode of release droplets leaving from pores on the exit surface of the packing adhered to strands of fibre extending beyond the bed. These drops coalesced to produce an intermittent flow along an individual strand or collection of strands; they left the end of the strand(s) as drops of varying size, i.e. some were smaller than the size leaving from the bed proper. The size ranged from 0.2×10^{-3}m to 0.5×10^{-3}m depending on the combined strand diameter and the flow superficial velocity. Although the droplets resulting from pointing were quite small, they were primary size droplets and therefore acceptable. This mechanism of release was observed in most cases when the packing exit surface was unshaved. It is shown in Figures 10.2.5. and 10.2.6.

10.2.4. GRAPING

Graping was shown to depend upon the roughness of the exit

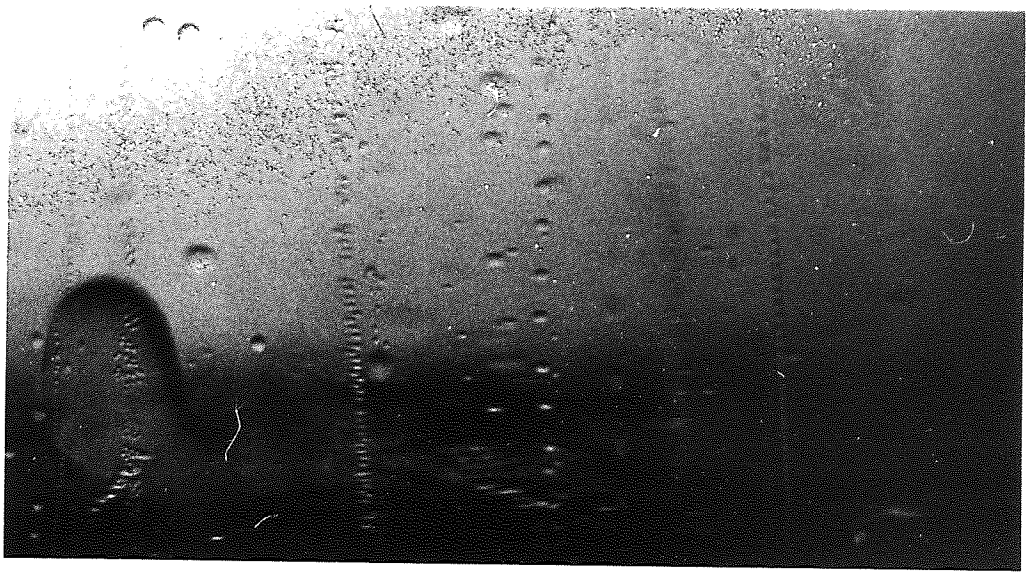

Figure 10.2.5 Mechanisms of release
"JETTING" + "POINTING"

System: Octan-1-ol/Water
Magnification = 3.5 x

Figure 10.2.6 Mechanisms of release
"JETTING" + "POINTING" + "DRIP POINT"

System: Octan-1-ol/water
Magnification = 3.5 x

face. By shaving off the strands from the exit face to make a smoother surface the phenomena of release for o/w dispersions were mostly due to graping. The complete mechanisms of grape formation and rupture are illustrated in Figure 10.2.7.

A film of dispersed phase blocked a few of the outlet pores and continuous phase pushed this film to form a "grape" filled with continuous phase. The top of this film thickened due to dispersed phase droplets coalescing underneath, and to a lesser extent into other areas of it, i.e. drop liquid interface coalescence. When the top was sufficiently thick the buoyancy and drag forces caused it to break from the top giving one or two satellite drops. The rest of the grape kept growing until it ruptured and produced one large drop and many smaller drops. The sizes were dependent on the superficial velocity of the flow. For superficial velocities up to 0.5×10^{-2}m/s graping was the predominant mechanism.

At the 3rd stage, (Figure 10.2.7.), i.e. before total breakage of the grape, drops in the size range 2×10^{-3}m to 5×10^{-3}m in diameter were released from the top of the grape, followed by up to three satellite drops of about 0.5×10^{-3}m. In the 4th and final stage, when the grape ruptured, one very large drop of about 7×10^{-3}m diameter and several very small drops, in the range 0.2×10^{-3}m to 0.5×10^{-3}m, were formed.

Clearly this type of release mechanism was not ideal since sudden rupture of the drop caused disruption of the flow pattern and some redispersion resulting in some drops with low settling velocities. Release by graping is shown in Figures 10.2.8. and 10.2.9.

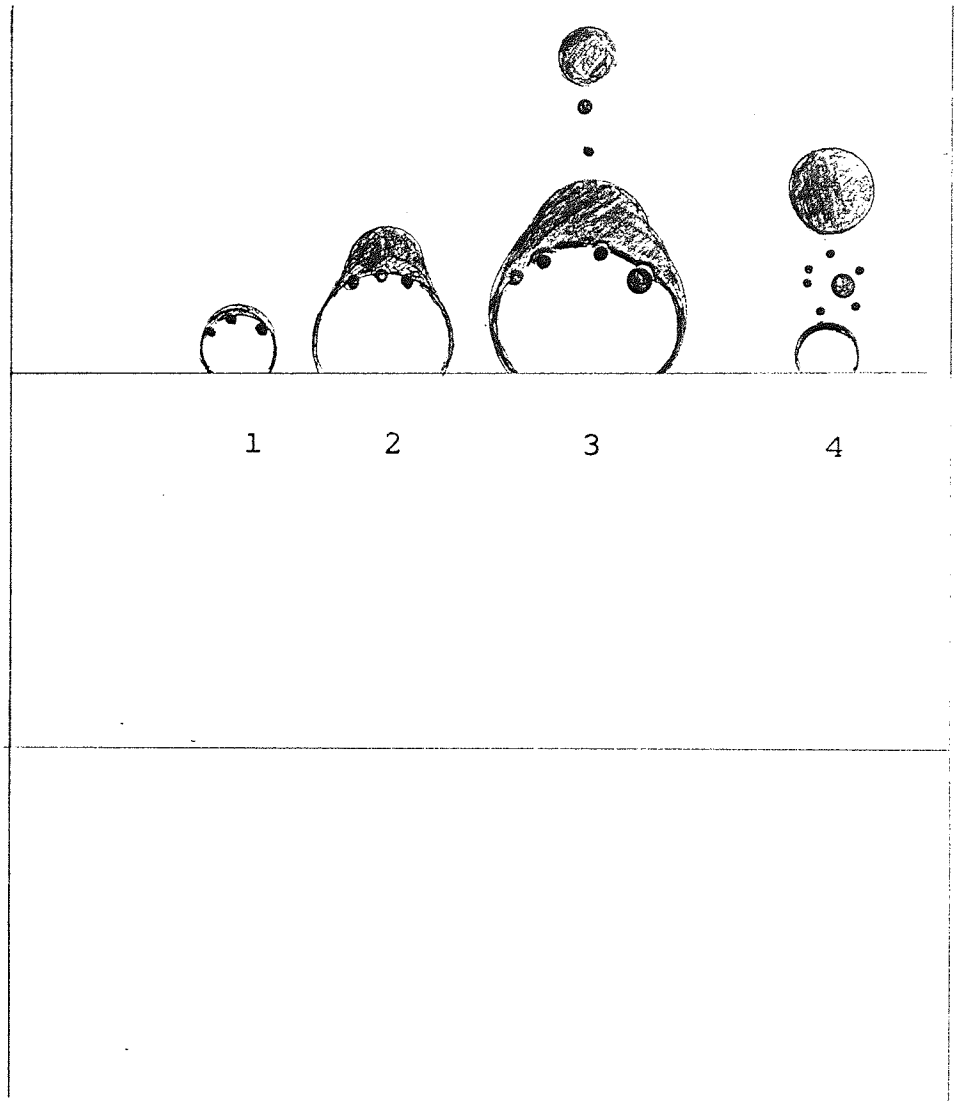

Figure 10.2.7 Mechanisms of "GRAPING"

1. Formation of the grape
2. Growth of the grape and thickening at the top
3. Breakage of part of the top leaving up to 3 secondary drops
4. Complete rupture of the grape and formation of a new grape

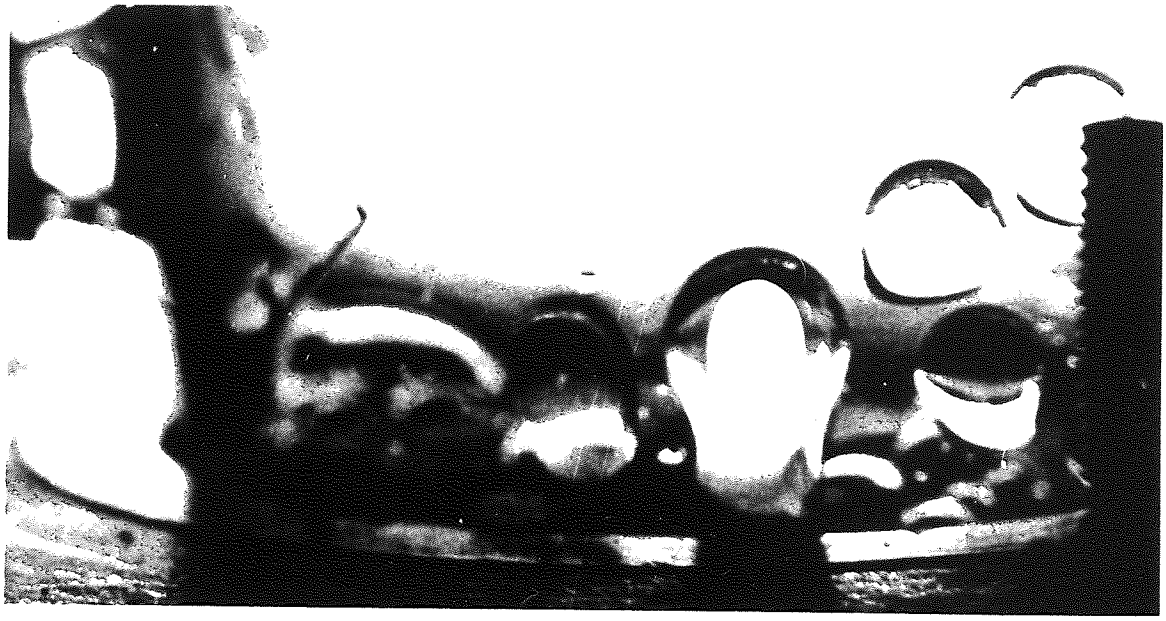

Figure 10.2.8 Mechanisms of release
"GRAPING" + "DRIP POINT"

System: Toluene/Water

Magnification = 3.5 x

strands of packing exit surface were shaved off.

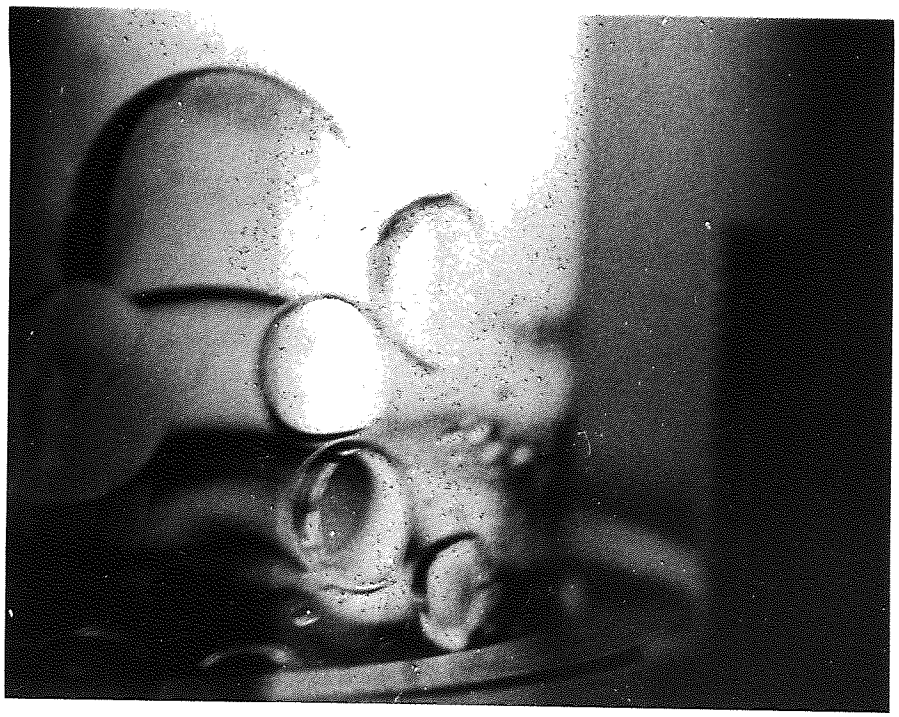

Figure 10.2.9 Mechanisms of release "GRAPING"

System: Toluene/Water

Magnification = 3.5 x

strands of packing exit surface shaved off.

10.2.5. FOAMING

This release mechanism was observed at high phase ratios in low voidage packing and is defined here as "Flooding" of the packing. For example with a packing of 40 layers pressed into a height of 20×10^{-3}m a white foam-like dispersion was formed at the exit at a phase ratio of 13% or greater as shown in Figure 10.2.10. This type of release was undesirable since it permitted capture of secondary haze within a film of dispersed phase; this resulted in low separation efficiency. It occurred with a system of low interfacial tension i.e. 10×10^{-3}Nm^{-2} and would be expected to predominate in systems containing surfactant. However for a packing made up of 1 layer compressed into 1×10^{-3}m thickness "foaming" did not take place even at phase ratios up to 50% i.e. this packing did not "flood" for phase ratios less than 50%.

10.2.6. CHAINING

This release mechanism was observed only with the water/toluene system and is shown in Figure 10.2.11. Drops grew on the exit surface of the packing and adhered together to form a large bunch of drops. This should not be confused with foaming described in Section 10.2.5; foam is formed mostly within the packing but a chain is formed on the exit face of the packing. Ultimate release of the drops in the case of chaining produced primary drops so that unlike foaming, this kind of release is acceptable. However release of the drops

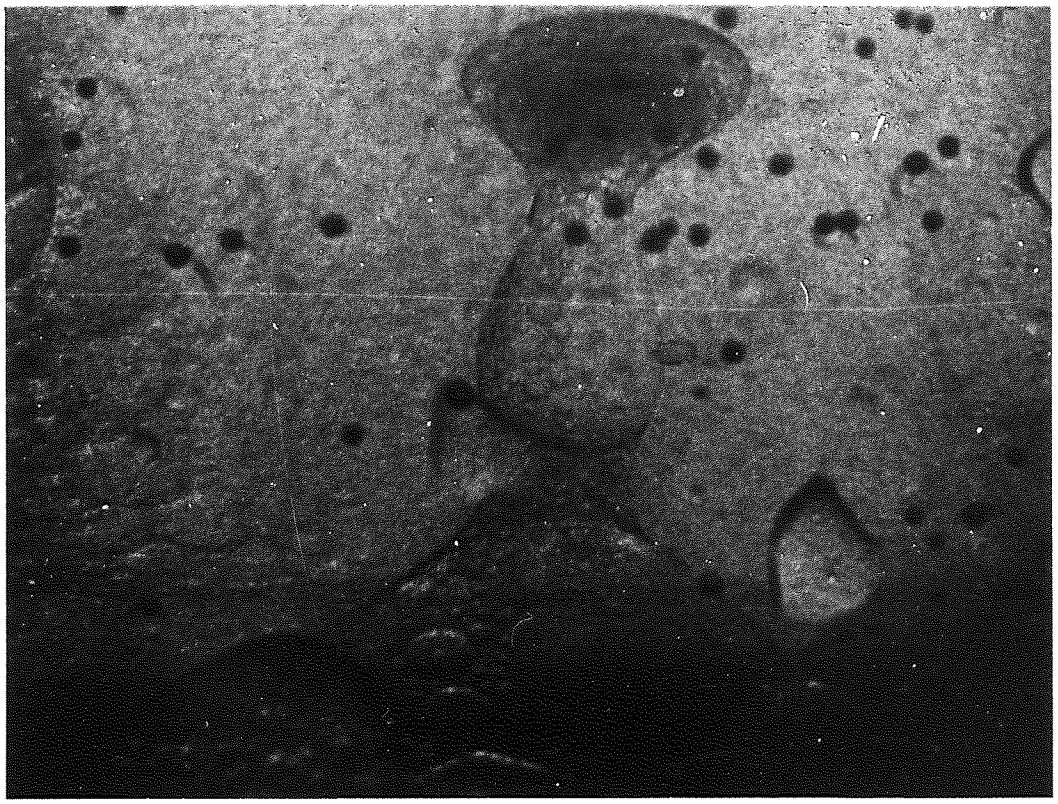

Figure 10. .10 Mechanisms of release "FOAMING"

Packing Voidage = 0.688 Magnification = 4.5 x

System: Octan-1.ol/Water

Phase Ratio = 13%

(The darker droplets are retained on the column wall)

Figure 10. .11 Mechanisms of release "CHAINING"

System: Water/Toluene

Magnification = 6x

caused a disturbance of the exit flow so that this kind of release cannot be considered ideal.

In conclusion from the above results, it is apparent that the exit surface properties of the packing critically affected the mode of the release mechanism and exit drop size.
A packing with the exit layer roughened was far superior to the smooth one i.e. the predominant mechanisms were drip-point and jetting for the roughened exit surface and graping for the smooth exit surface. Other factors determining the mode of drop release were packing voidage, system physical properties and superficial flow velocity.

CONCLUSIONS

The following main conclusions are drawn from this investigation :-

1. The use of refractive index matching in conjunction with a phototropic dye enabled the separation mechanisms within the packing to be observed visually. This enabled the mechanisms within the packing, and the modes of release, to be defined.

The mechanisms within the packing were (Section 10.1.)

i) drop adherence on the fibre(s)

ii) drop movement along the fibre(s)

iii) coalescence between drops at intersections between, or at other active sites on, the fibres

iv) release of an enlarged drop after attainment of the equilibrium size determined by a balance between the surface force and drag and bouyancy forces.

v) movement of the drop in a tortuous path with a velocity far greater than the superficial flow velocity.

Final release from the exit surface of the packing involved some combination of six distinct modes; these were dependent on the exit surface roughness of the packing, physical properties of the system and flow superficial velocity (Section 10.2.).

2. Hold-up was uniform throughout the packing; this also indicated that the packing was uniformly distributed i.e. of constant voidage.

3. The novel knitted fibrous glass packing selected (Section 7.3.1.) was 100% efficient for the separation of both o/w

and w/o secondary dispersions at velocities as high as $5.5 \times 10^{-2} ms^{-1}$. This was substantially higher than obtained for any other packing, the normal range being $0.01 \times 10^{-2} ms^{-1}$ to $3.0 \times 10^{-2} ms^{-1}$; this indicates that a packing with an ordered arrangement and a high number of intersections is far superior to loose fibrous packings.

4. With the knitted fibrous glass packing, pressure drop for single phase and two phase flow could be correlated by two modified Blake-Kozeny types equations for all the w/o and o/w systems studied (Section 9.1.).

5. With the knitted fibrous glass packing mean exit drop size was dependent on the precise mechanisms of release at the exit of the packing as well as packing thickness and superficial velocity of the flow. It decreased with increase in superficial velocity upto a critical velocity where break-through or redispersion occurred. As with other packings the outlet size was independent of both inlet drop size distribution and phase ratio.

The most important factors affecting "critical" velocity for any particular packing height were interfacial tension of the system, the surface tension of the dispersed phase and the viscosity of the continuous phase. The "critical" velocity increased with bed thickness, but there was a maximum thickness for any system.

6. Average bed hold-up, and hence the degree of saturation, were independent of drop size distribution, packing thickness and superficial flow velocity upto an appropriate "critical" velocity, but varied with the systems physical properties.

RECOMMENDATIONS FOR FURTHER WORK

The following areas are worthwhile for further investigation,

(1) The refractive index matching technique discussed in Chapters 6 and 8 could be adapted to investigate the coalescence mechanisms within particulate packings. Several packing materials with low refractive indices which could be used were discussed in Section 6.1. Calcium fluoride with a refractive index of 1.4338 is relatively insoluble, chemically inert, and has been proposed as a packing (136). Because of its relatively low refractive index several liquid/liquid systems could be employed to match the packing. However, the packing holder would require careful design to avoid interference with dispersion behaviour in the packing. A layer of similar surface energy knitted material and/or a mesh with pore diameter less than the smallest particle size could be used on either side of the packing in a glass tube. An alternative would be to avoid any extraneous effects due to coalescence of secondary dispersion at the packing support junctions, or on the supports, by creating the dispersion within the packing itself using an ultrasonic probe; care would be needed however to avoid packing disturbance.

(2) The ultrasonic technique discussed in Chapters 6 and 8 could be developed further using the same transducers and packing/holder design to measure mean drop size and hold-up within the packing. At least 3 pairs of

transducers of the type discussed in Appendix E would be required spaced along the packed height; these could be connected through suitable electronic circuits to digital counters to give comparable results.

(3) The study of release mechanisms in this work indicated that the roughness of the final layer of the packing, i.e. the exit surface, played an important role in the mode of release. This could be studied further by choosing different surface energy materials for the exit layer of the packing.

(4) In view of the observations (a) that most of the coalescence occurred at the intersections of the fibres and (b) the phenomena of the "junction" effect discussed in Section 3.4.3. and its effectiveness for coalescing secondary dispersions, a knitted fibrous material made up of two different surface energy materials for its weft and warp (e.g. p.t.f.e. and glass) could prove highly efficient. This could be investigated using the equipment and techniques described in Chapter 7.

APPENDIX A

COULTER COUNTER INSTRUCTIONS

APPENDIX A

COULTER COUNTER INSTRUCTIONS

The Coulter Counter Model ZB used in this work was designed to provide a drop size analysis over the range 0.6 - 400 μm using external glassware and a range of orifice tubes.

The instrument should preferably be located in a dust free room. However any bench can be used which is not subject to excessive airborne dust, strong vibrations, high intensity sound, or electrical noise, and such a bench was used in this work. The method of operation of the Coulter Counter for sizing secondary dispersions was adapted from the Manufacturer's Manual (157), and is described below. The controls are briefly explained to assist understanding.

A.1 COULTER COUNTER MODEL ZB CONTROLS

These are shown in Figures A.1 and A.2.

(a) Lower Threshold Dial t_L: Determined the size level above which the instrument counted pulses. All tips which reached this value were counted.

(b) Upper Threshold Dial t_u : Set the 'no count' level, so facilitating an 'in between' count.

(c) $\frac{1}{\text{Amplification}}$, Attenuation A: Set the amplifier sensitivity. Each clockwise step doubled the sensitivity and gain of the instrument and hence the pulse height, i.e. for any threshold setting the droplet size volume was halved for each successive switch position.

(d) $\frac{1}{\text{Aperture Current}}$ I : Controlled the amount of current flowing between the two electodes. Each consecutive clockwise interval increased the current by a factor of two or $\sqrt{2}$. Two lamps POS. NEG. indicated the polarity of the

external electrode which was automatically reversed to minimise electrochemical effects.

(e) Vacuum Regulator: Turning this control clockwise increased the vacuum available to the aperture tube.

(f) Microscope: When set correctly, the orifice appeared as a small circle in a bright disc. Any partial or complete blockage, which would cause incorrect counts, was detectable.

A.2 ELECTROLYTE FILTRATION

It was desirable for the electrolyte background count, discussed in Section A.3.1 to be as low as possible. This was achieved by careful filtration using a Sartorius Membrane filter to retain particles down to 0.1×10^{-6}m.

A.3 OPERATION

The orifice tube selected was such that the suspected largest droplet size occupied about 40% of the aperture diameter. After fitting this to the control piece, the manometer selector switch was set to the recommended position and the glassware filled with the filtered electrolyte. A clean two hundred and fifty millilitre beaker was then filled with this electrolyte and placed on the adjustable platform and the stirrer started. The controls t_L, t_u, I and A were set to 10, 110 (out), $\frac{1}{4}$ and $\frac{1}{8}$ respectively, and a blank count made.

A.3.1 Blank Count

When tap T shown in Figure A.2 was opened to vacuum the mercury came to rest below the start electrode; as shown in Figure A.3, the digital count display was automatically reset to zero, the oscilloscope lit-up and the aperture current was

initiated. When the tap was closed the instrument started to count as soon as the mercury touched the start electrode and stopped when it encountered one of the other electrodes, dependent upon the setting of the manometer volume switch. The count obtained represented the total number of particles in the blank electrolyte above a size level approximately 2% of the orifice diameter. For the desired accuracy this had to be within an acceptable range, e.g. for a fifty micrometer aperture tube at $0.05 \times 10^{-6} m^3$ manometer volume, the maximum blank count needed to be 300, although a lower count gave a better accuracy. If a higher count was obtained the beaker was rinsed and a fresh sample analysed. If it was still unacceptable the electrolyte was re-filtered. If the count continued to be high the possibility of external 'noise', interference, or a blocked orifice, was considered. Once acceptable, t_L, I and A were set to 20, 8 and 32 respectively, a size level 40% of the orifice diameter, and a count taken. One or two pulses generally appeared.

A.3.2 Calibration

Calibration was performed using Puff Ball Spores 'monosized' particles of 3.62 micrometre in diameter lying between 5% and 20% of the orifice diameter by the Half Count Technique.

A small sample of Puff Ball Spores powder was dispersed in a few drops of alcohol on a watch glass. Two hundred millilitres of electrolyte in a two hundred and fifty millilitre beaker was placed on the sample stand, the sample added and the stirrer started.

t_L, t_u, A and I were set to 1, 110, 1 and 1 respectively,

and tap T opened. Pulses appeared on the oscilloscope screen; A and I were then adjusted until the majority of these were about one and a half to two centimetres high. t_L was then increased until the shadow line coincided with the maximum height of the majority of the pulses. This was designated T. The control t_L was decreased to $\frac{T}{2}$, 2 to 4 counts taken, and the average designated N_1. t_L was then increased to $\frac{3T}{2}$ and the same procedure repeated to give N_2. N_3 was given by:

$$N_3 = \frac{N_1 + N_2}{2} \quad \text{.....A.3.2.1}$$

t_L was set back to T and a count taken. The setting was raised or lowered, to decrease or increase the count, until count N_3 was obtained as closely as possible. The final setting was designated t', If this value was more than 1 or 2 threshold divisions from T, the calibration procedure was repeated using t' as T. K, the calibration constant was calculated from:

$$K = 3\frac{d}{\sqrt{t' \times 1 \times A}} \quad \text{.....A.3.2.2}$$

Example: For a one hundred and forty micrometre orifice tube, $0.05 \times 10^{-6} m^3$ manometer volume, 0.2% sodium chloride solution and micrometre diameter Lycopodium powder.

$I = \frac{1}{4}$ $A = 2$ $T = 25$

$\frac{T}{2} = 12.5$ N = 6951, 6979, 6965, 6965. $N_1 = 6965$

$\frac{3T}{2} = 37.5$ N = 2387, 2296, 2204, 2296. $N_2 = 2296$

$$\therefore N_3 = \frac{6965 + 2296}{2} = 4630$$

At t' = 24 N = 4638, 4628, 4622, 4634. $N_{av} = 4631$

$\therefore$ I = ¼ A = 2 t' = 24 and d = 3.62

$$\therefore \quad K = \frac{3.62}{\sqrt[3]{24 \times \frac{1}{4} \times 2}} = 1.58$$

A.3.3 Analysis Technique

A sample of the dispersion was transferred to the electrolyte beaker as discussed in Section 7.7, the beaker placed on the platform and the stirrer started. t_L, I and A were set to 10, ¼, and 1/8 respectively, as discussed in Sections A.3 and A.3.1, and a count taken. The count had to be near to that denoted 10% 'coincidence' for the particular orifice tube and manometer volume. If a higher count was obtained, the dispersion was diluted with electrolyte; if it was lower a fresh, more concentrated suspension was prepared. When a satisfactory value had been achieved, t_L, I and A were set to 20, 8 and 32 respectively as discussed in Section A.3.1, and the count was arranged to be less than two as before. The intervals at which counts were taken depended upon the size range to be covered, but a full range of 16 points analysis was generally adopted with counts being taken at the levels shown in Table A.1.

A.4 MODEL M2 VOLUME CONVERTER CONTROLS

These are shown in Figure A.4.

(a) Off: Disconnected the M2 allowing the ZB to operate conventionally by manometer volume selection.

(b) Int. and Dif: Determined whether the ZB readout would be integral (cumulative) or differential (frequency) volume values.

(c) Stop: Cancelled the timer and prevented the pulses from feeding to the readout. In the event of an orifice blockage,

it was pressed, the blockage removed and the cycle recommenced in the Dif. mode.

(d) Start: Initiated the count cycle which switched on the count indicator light.

(e) Time Factor T: Set the sample analysis time from 128 to 2 seconds, over-riding the ZB manometer volume contacts.

(f) Division Factor U: Determined the computer division factor as part of volume conversion. 4 generated four pulses for each particle-generated pulse and $\frac{1}{128}$ generated one pulse for each 128 particle-generated pulses.

(g) Resultant: Confirmed the value used for computed volume conversion.

A.5 COMPLETE ANALYSIS USING M2 VOLUME CONVERTOR

A beaker filled with the electrolyte and sample was placed in counting position. The ZB controls were set to t_L = 20, t_u = 40, I = 8, A = 32, M2 controls to INT., T = 128, U = 4, and tap T opened. Reset on the M2 was pressed; pulse patterns appeared on the oscilloscope and the digital readout fell to zero. Start was pressed, the counting continued until the count indicator light went out. The readout value was then altered and start pressed until all the settings shown had been scanned. A blank count was then taken of the prefiltered electrolyte in a clean beaker using the same settings as the sample. Data handling is also shown in Table A.1.

A.6 COMMON SOURCES OF ERROR

Even with the established procedures just described there were practical sources of error. These could be identified and

eliminated as follows:

(a) A high blank count could be eliminated by proper electrolyte filtration as discussed in Section A.2.

(b) Orifice blockage would result in an increase in pulse height and counting time. These could be detected by a change in oscilloscope pattern and orifice observation through the microscope.

(c) Air bubbles in the sample and inside the orifice tube due to vigorous mixing. Slow mixing was used throughout to avoid vortex formation.

(d) Air leaks, breaks in the mercury column or dirty manometer.

(e) Cracked or damaged orifice tube.

(f) External interference from flickering or humming fluorescent lights, thermostats, motor brushes or power line noise.

TABLE A.1

COULTER COUNTER DATA AND WEIGHT CONVERSION

INDUSTRIAL MODEL ZB + VOLUME CONVERTER MODEL M2

Phase Ratio: 0.2% Pump Speed: 33.3 revs s^{-1} Electrolyte: 0.9% Sodium Chloride Date: 28. 2.1978

Aperture Diameter: 50×10^{-6} m Manometer Volume: $0.05 \times 10^{-6} m^3$ Calibration Data: □ I= ¼, A = 2 t = 24 Calibration Factor, K 1.58

Model ZB				Model M2			Model M2 Int. Mode			Cum. Wt. %
tL	tu	I	A	T	U	$d=K.\sqrt[3]{tL.I.A}$	Raw $\Sigma(\Delta n)\bar{V}$	B	$\Sigma(\Delta n)\bar{V}$-B	Oversize
20	40	8	32	128	4	27.0	601	0	601	3.2
20	40	8	16	64	4	27.5	1002	0	1002	5.4
20	40	8	8	32	4	17.2	1483	0	1483	8.0
20	40	8	4	16	4	13.6	1642	0	1642	8.9
20	40	8	2	8	4	10.8	2921	0	2921	15.8
20	40	8	1	8	2	8.6	6065	0	6065	32.7
20	40	4	1	8	1	6.8	10049	0	10049	54.0
20	40	2	1	8	½	5.4	13586	1	13585	73.0
20	40	1	1	8	¼	4.3	15734	2	15732	84.5
20	40	1	½	8	1/8	3.4	16844	3	16841	90.5
20	40	1	¼	8	1/16	2.7	17567	4	17563	94.3
20	40	1	1/8	8	1/32	2.1	17999	5	17994	96.6
20	40	½	1/8	8	1/64	1.7	18318	6	18312	98.4
20	40	¼	1/8	8	1/128	1.4	18538	7	18531	99.5
20	40	1/8	1/8	4	1/128	1.1	18624	8	18616	100.0
10	20	1/16	1/8	2	1/128	0.7	18627	8	18619	100.0

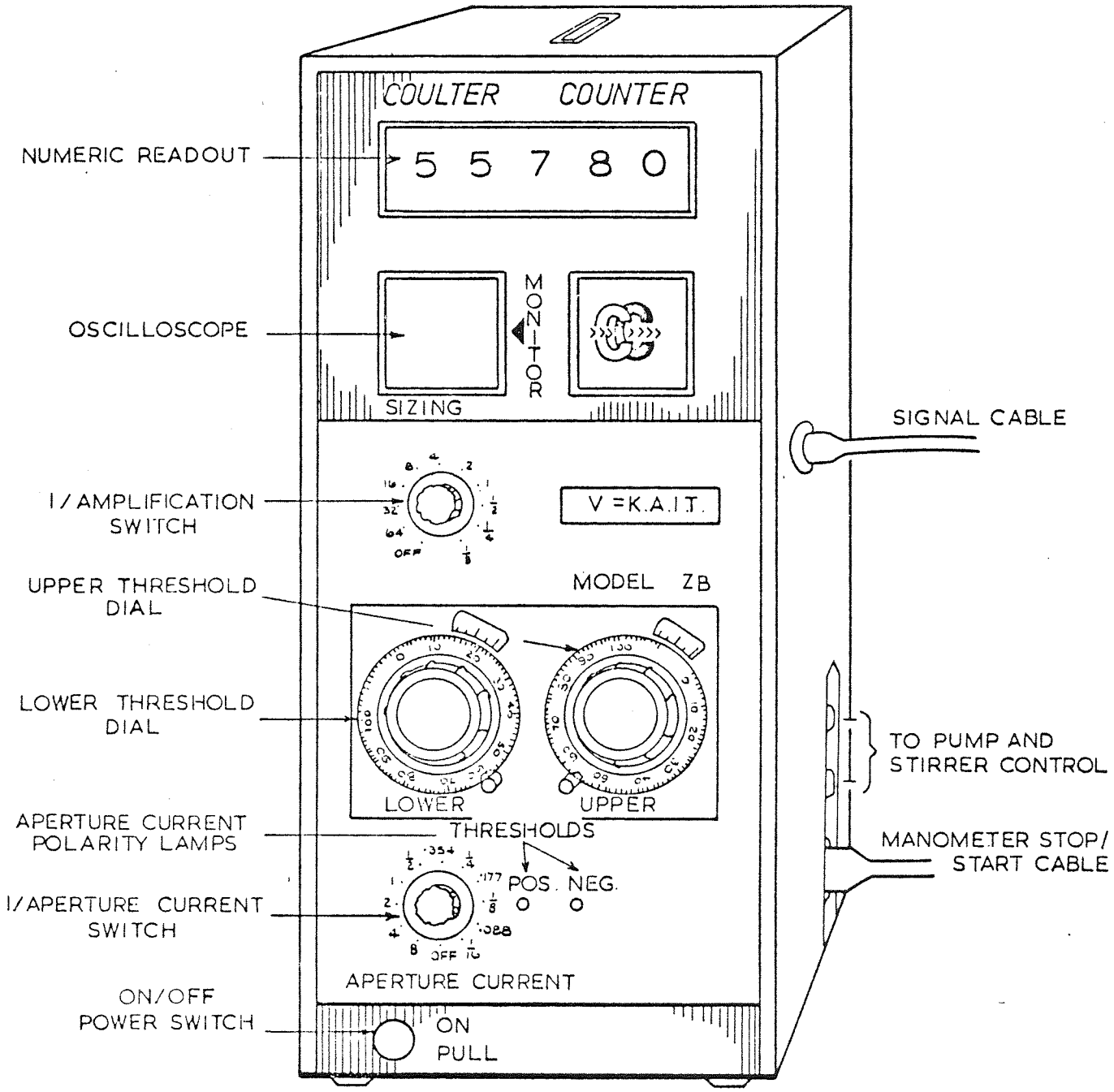

Figure A.1. Coulter Counter model ZB front panel

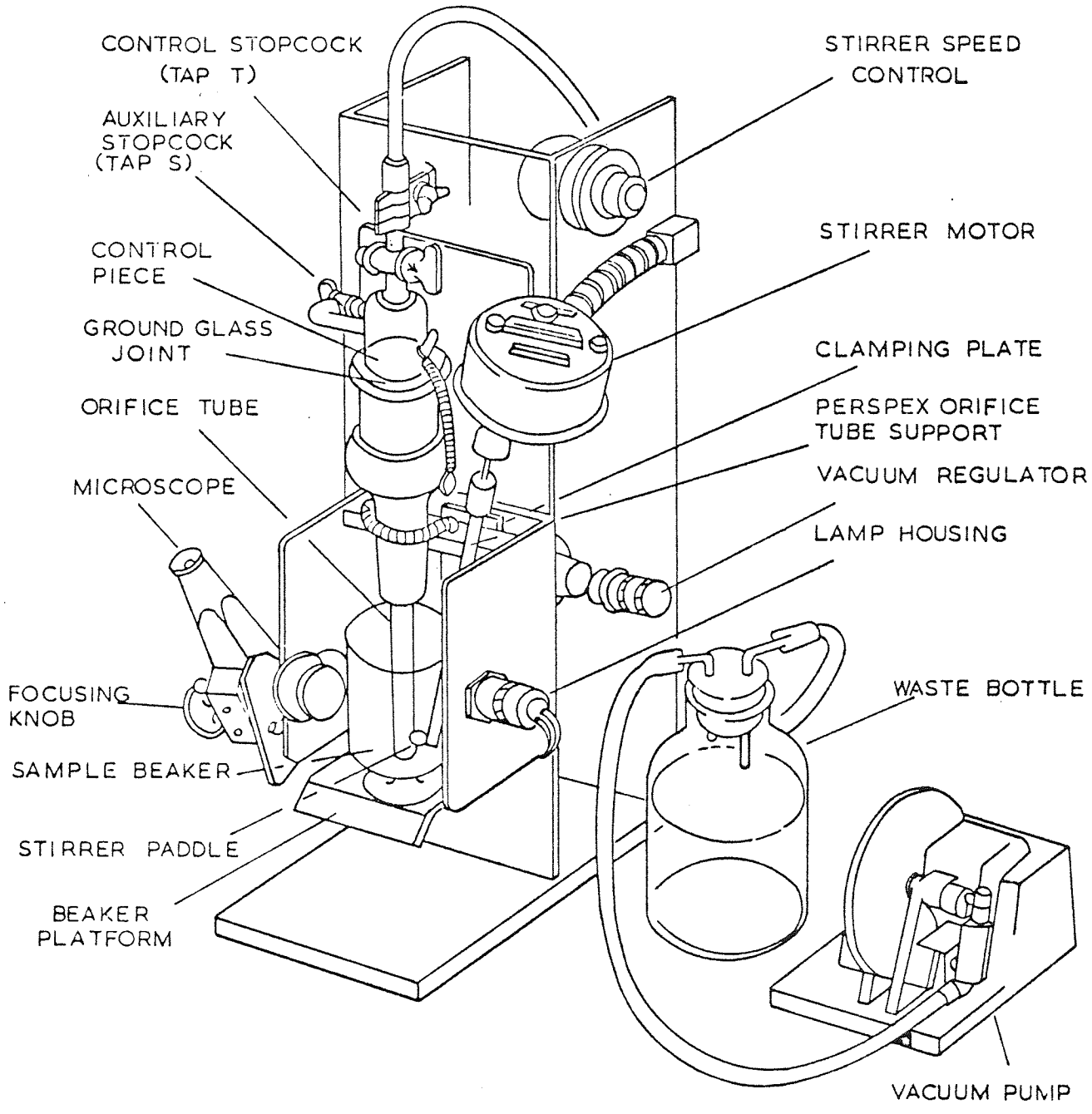

Figure A.2. Glassware stand assembly

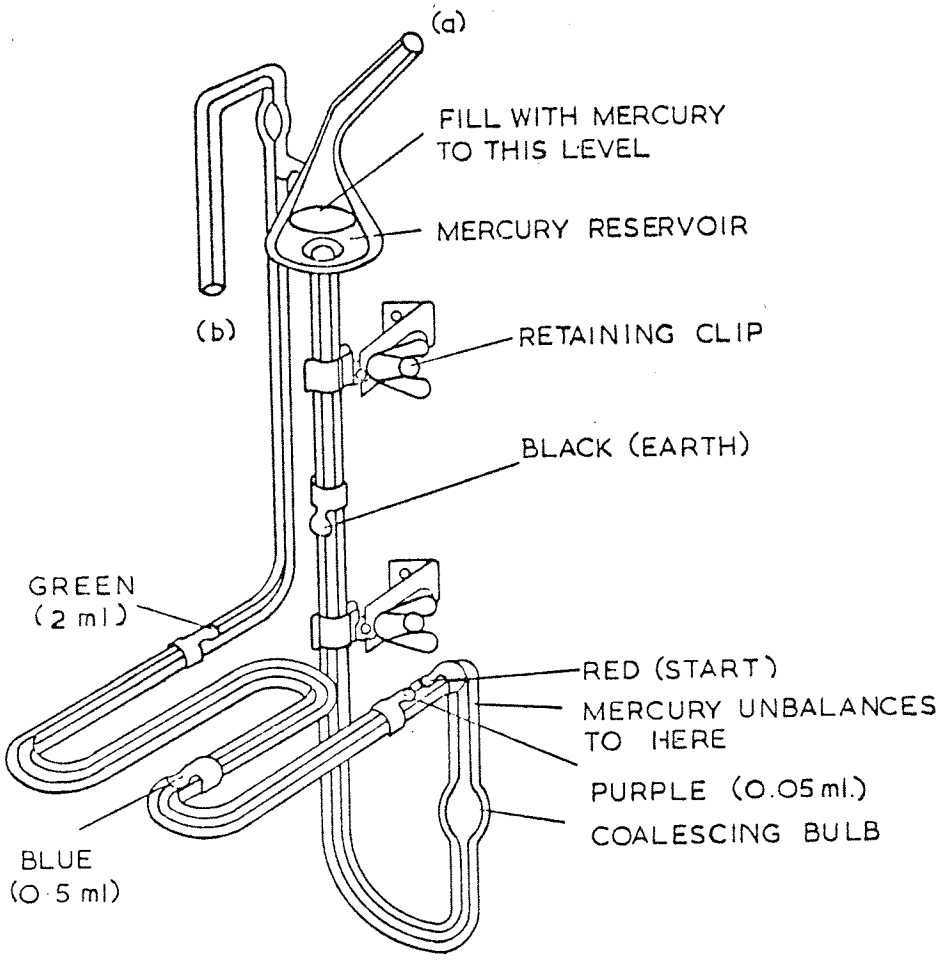

Figure A.3. Mercury manometer

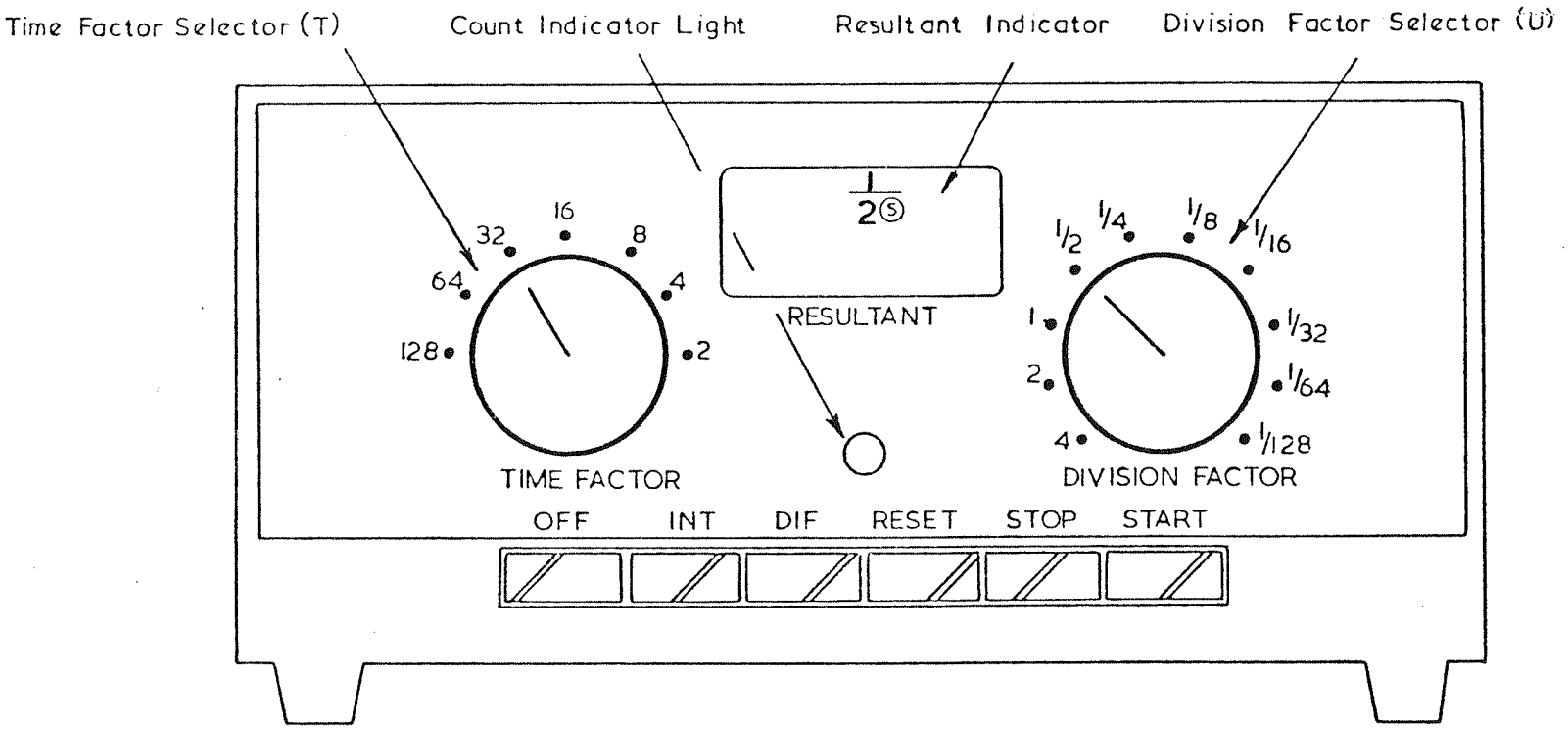

Figure A.4. Model M_2 volume converter

APPENDIX B

Programme to evaluate exit drop diameter using UAFORTRAN

Programme to evaluate exit drop diameter using UAFORTRAN

```
      LIST (LP)
      PROGRAM (FXXX)
      INPUT  1 = CR0
      INPUT  3 = TR0
      INPUT  5 = CR1
      OUTPUT 2 = LP0
      OUTPUT 6 = LP1
      COMPRESS INTEGER AND LOGICAL
      COMPACT PROGRAM
      EXTENDED DATA
      TRACE 2
      END



      TRACE 1
      MASTER ATTA
      REAL MF, ND1, ND2, ND3, MVD
      INTEGER K, I
C     MAGNEFING FACTER, MF
    5 READ(1,200)I,B,K,MF
  200 FORMAT(I5,F5.0,I5,F10.3)
      WRITE(2,201)I,B
  201 FORMAT(1H1,5X,'SERIALNO= ',I5,5X,'PHOT,NO= ',F5.0)
      WRITE(2,111)
  111 FORMAT(1H0,36X,'SAUTER MEAN DIAMETER AND ST.DEVIATION CALCULATION
     1)
      WRITE(2,112)
  112 FORMAT(24X,'DM',8X,'D',9X,'N',9X,'D2',8X,'D3',7X,'ND1',7X,'ND2',

     17X,'ND3')
      SUMD=0
      SUMN=0
      SUMND1=0
      SUMND2=0
      SUMND3=0
C     DROP MEAN DIAMETER,DM
C     NUMBER OF DROP,N
      DO 20J=1,K
      READ(1,114)DM,F
  114 FORMAT(F10.2,F10.0)
      D=DM/MF
      D2=D**2
      D3=D**3
      ND1=F*D
      ND2=F*D2
      ND3=F*D3
      SUMD=SUMD+D
      SUMN=SUMN+F
      SUMND1=SUMND1+ND1
      SUMND2=SUMND2+ND2
      SUMND3=SUMND3+ND3
   20 WRITE(2,115)DM,D,F,D2,D3,ND1,ND2,ND3
  115 FORMAT(22X,F5.2,3X,F9.5,4X,F3.0,4X,F9.5,1X,F8.4,2X,F9.4,2X,F9.4,
     11X,F9.4)
      GO TO 21
   21 WRITE(2,116)
  116 FORMAT(30X,'---------',4X,'---',24X,'---------',1X,'--------',2X
     1,'---------')
      WRITE(2,117)SUMD,SUMN,SUMND1,SUMND2,SUMND3
```

```
C       SAUTER MEAN DIAMETER ,SMD
C       ST,DEVIATION ,SD
        AMD=SUMND1/SUMN
        SMD=SUMND3/SUMND2
        SD=SQRT((SUMND2-(SUMN*AMD**2))/(SUMN-1))
        MVD=(SUMND3/SUMN)**0.3333
        WRITE(2,118)AMD
  118   FORMAT(20X,'ARITHMETIC MEAN DIA= ',F10.5)
        WRITE(2,119)SMD
  119   FORMAT(20X,'SAUTER MEAN DIA= ',F10.5)
        WRITE(2,120)SD
  120   FORMAT(20X,'STD.DEV= ',F10.6)
        WRITE(2,121)MVD
  121   FORMAT(20X,'MEAN VOLUME DIA= ',F10.5)
        IF(I-105)25,26,26
        I=I+1
   25   GO TO 5
   26   STOP
        END
```

Typical computer results for exit drop diameter

SAUTER MEAN DIAMETER AND ST.DEVIATIØN CALCULATIØN

DM	D	N	D2	D3	ND1	ND2	ND3
3.14	0.23004	3.	0.05292	0.0122	0.6901	0.1588	0.0365
3.70	0.27106	11.	0.07347	0.0199	2.9817	0.8082	0.2191
4.25	0.31136	36.	0.09694	0.0302	11.2088	3.4899	1.0866
4.80	0.35165	63.	0.12366	0.0435	22.1538	7.7904	2.7395
5.35	0.39194	41.	0.15362	0.0602	16.0696	6.2983	2.4686
5.90	0.43223	52.	0.18683	0.0808	22.4762	9.7150	4.1992
6.46	0.47326	32.	0.22398	0.1060	15.1443	7.1672	3.3920
7.01	0.51355	16.	0.26374	0.1354	8.2168	4.2198	2.1671
7.56	0.55385	21.	0.30675	0.1699	11.6308	6.4417	3.5677
8.11	0.59414	9.	0.35300	0.2097	5.3473	3.1770	1.8876
8.66	0.63443	7.	0.40250	0.2554	4.4410	2.8175	1.7875
9.22	0.67546	7.	0.45624	0.3082	4.7282	3.1937	2.1572
9.77	0.71575	4.	0.51230	0.3667	2.8630	2.0492	1.4667
10.32	0.75604	1.	0.57160	0.4322	0.7560	0.5716	0.4322
10.87	0.79634	3.	0.63415	0.5050	2.3890	1.9025	1.5150
11.98	0.87766	2.	0.77028	0.6760	1.7553	1.5406	1.3521
12.53	0.91795	2.	0.84263	0.7735	1.8359	1.6853	1.5470
13.08	0.95824	3.	0.91823	0.8799	2.8747	2.7547	2.6397
13.63	0.99853	2.	0.99707	0.9956	1.9971	1.9941	1.9912
14.13	1.03516	2.	1.07157	1.1092	2.0703	2.1431	2.2185
14.74	1.07985	4.	1.16608	1.2592	4.3194	4.6643	5.0368
15.84	1.16044	1.	1.34662	1.5627	1.1604	1.3466	1.5627
16.39	1.20073	3.	1.44176	1.7312	3.6022	4.3253	5.1935
16.94	1.24103	3.	1.54014	1.9114	3.7231	4.6204	5.7341
	17.17070	328.			154.4352	84.8752	56.3978

ARITHMETIC MEAN DIA= 0.47084
SAUTER MEAN DIA= 0.66448
STD.DEV= 0.192847
MEAN VØLUME DIA= 0.55610

APPENDIX C

PHYSICAL PROPERTIES OF LIQUID-LIQUID SYSTEMS

APPENDIX C

PHYSICAL PROPERTIES OF LIQUID-LIQUID SYSTEMS USED FOR EXPERIMENTATION DESCRIBED IN CHAPTER 7

Except for interfacial tension and surface tension which were measured by a Du Nuoy Tensiometer all the rest of the physical properties were from International Critical Table and/or manufacture specifications.

Interfacial Tension System	$Nm^{-1}(x\ 10^{-3})$	Temperature ^{o}C
Toluene-water	29.20	23
Octan-1-ol-water	8.6	23
M.I.B.K-water	9.8	20

Surface Tension	$Nm^{-1}(x\ 10^{-3})$	
Toluene	27.96	23
Octan-1-ol	29.50	23
M.I.B.K.	26.00	23
Water	72.80	20

Viscosity	$Kgm^{-1}s^{-1}(x\ 10^{-3})$	
Toluene	0.58	20.6
Octan-1-ol	7.60	20
M.I.B.K.	0.62	20.3
Water	0.98	20

Density	$Kgm^{-3}(x\ 10^{3})$	
Toluene	0.86	20

Density	$Kgm^{-3}(x\ 10^{3})$	Temperature ^{o}C
Octan-1-ol	0.86	20
M.I.B.K.	0.80	20
Water	1.00	20

APPENDIX D

ROTAMETERS AND PUMPS CALIBRATION CURVES

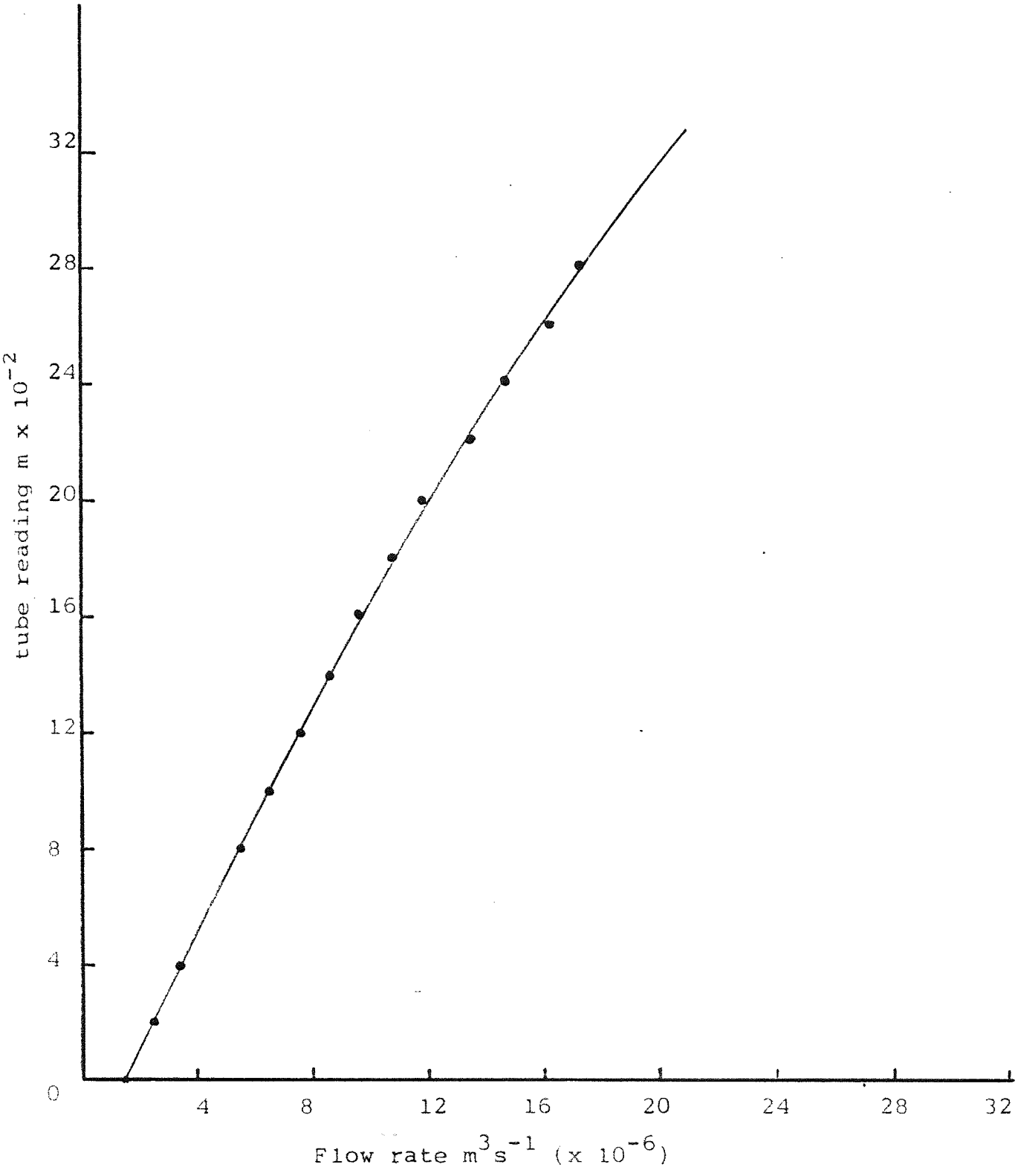

Figure D.1 Metric tube size 7 Rotameter Calibration

Water

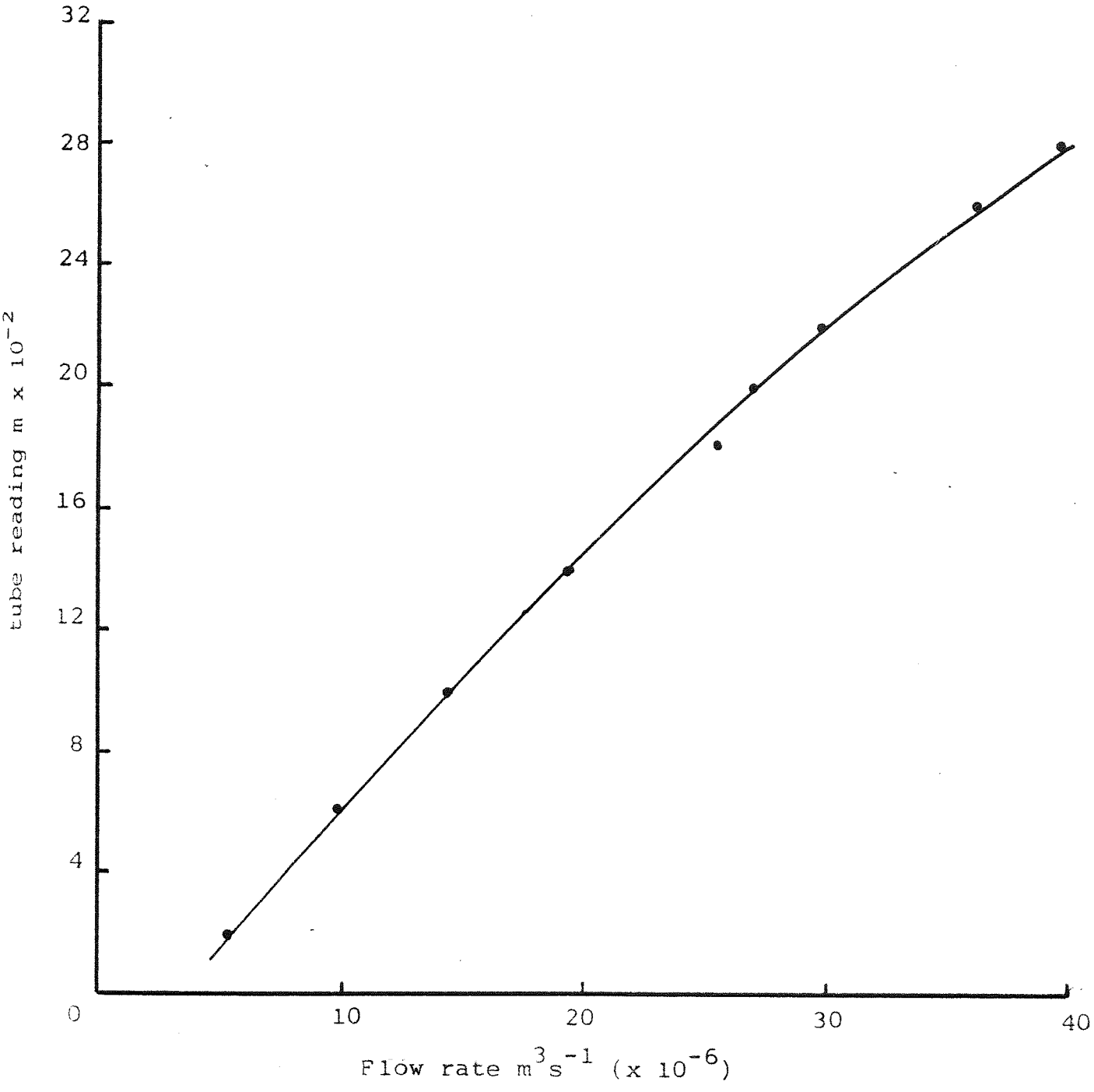

Figure D.2 Metric tube size K14 Rotameter Calibration

Water

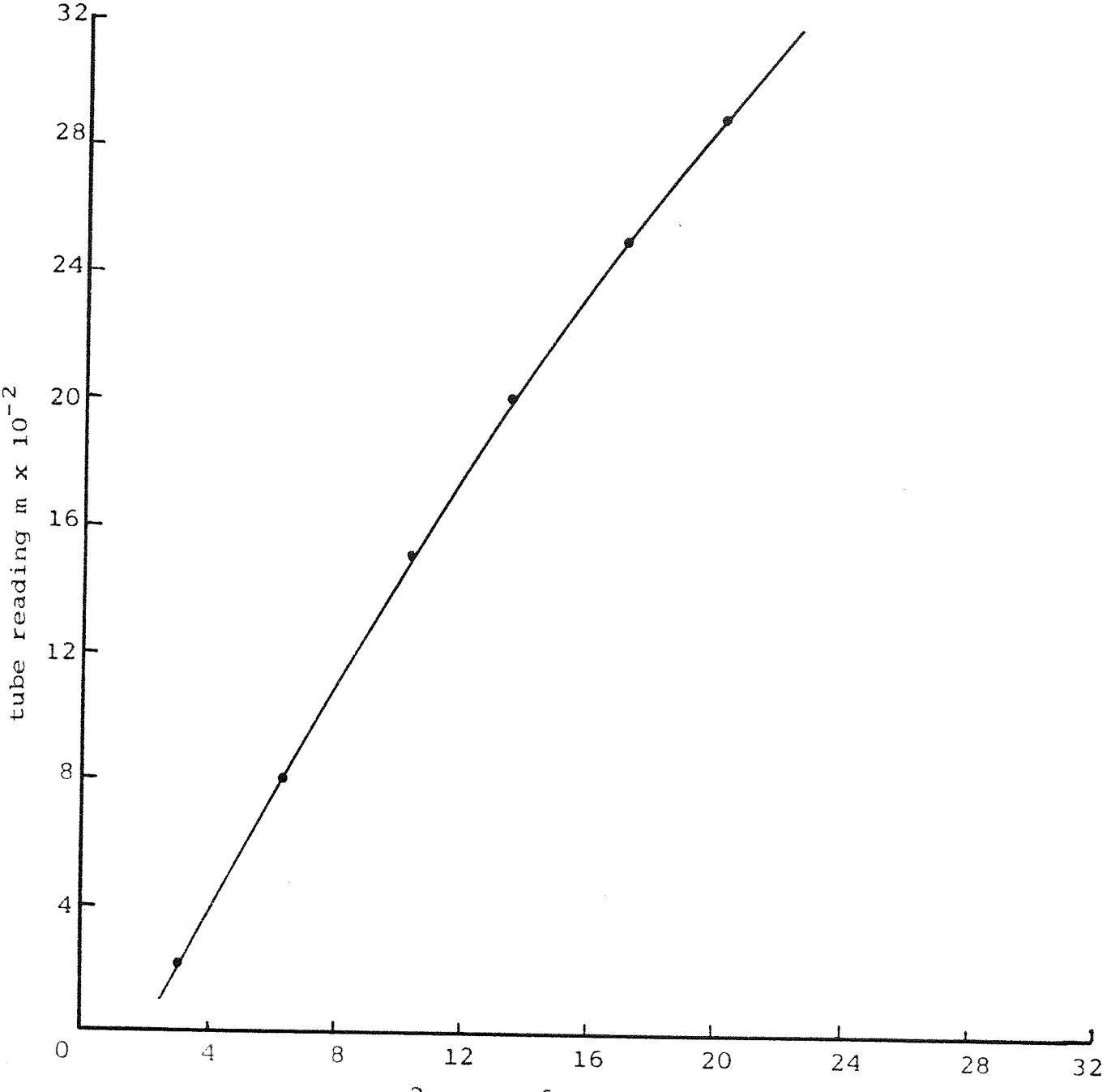

Figure D.3 Metric tube size 7 Rotameter Calibration

Toluene

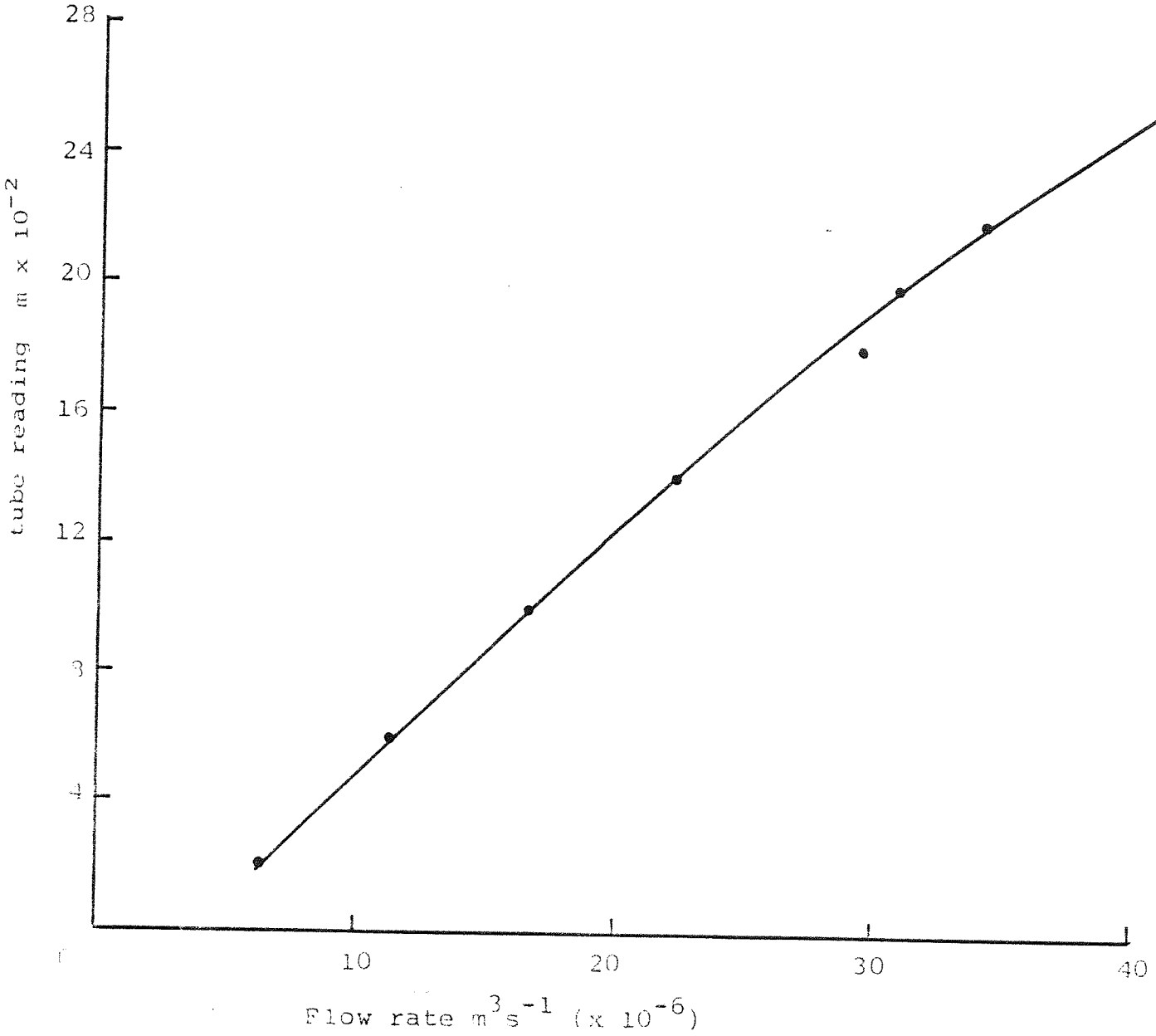

Figure D.4 Metric tube size 14 Rotameter Calibration

Toluene

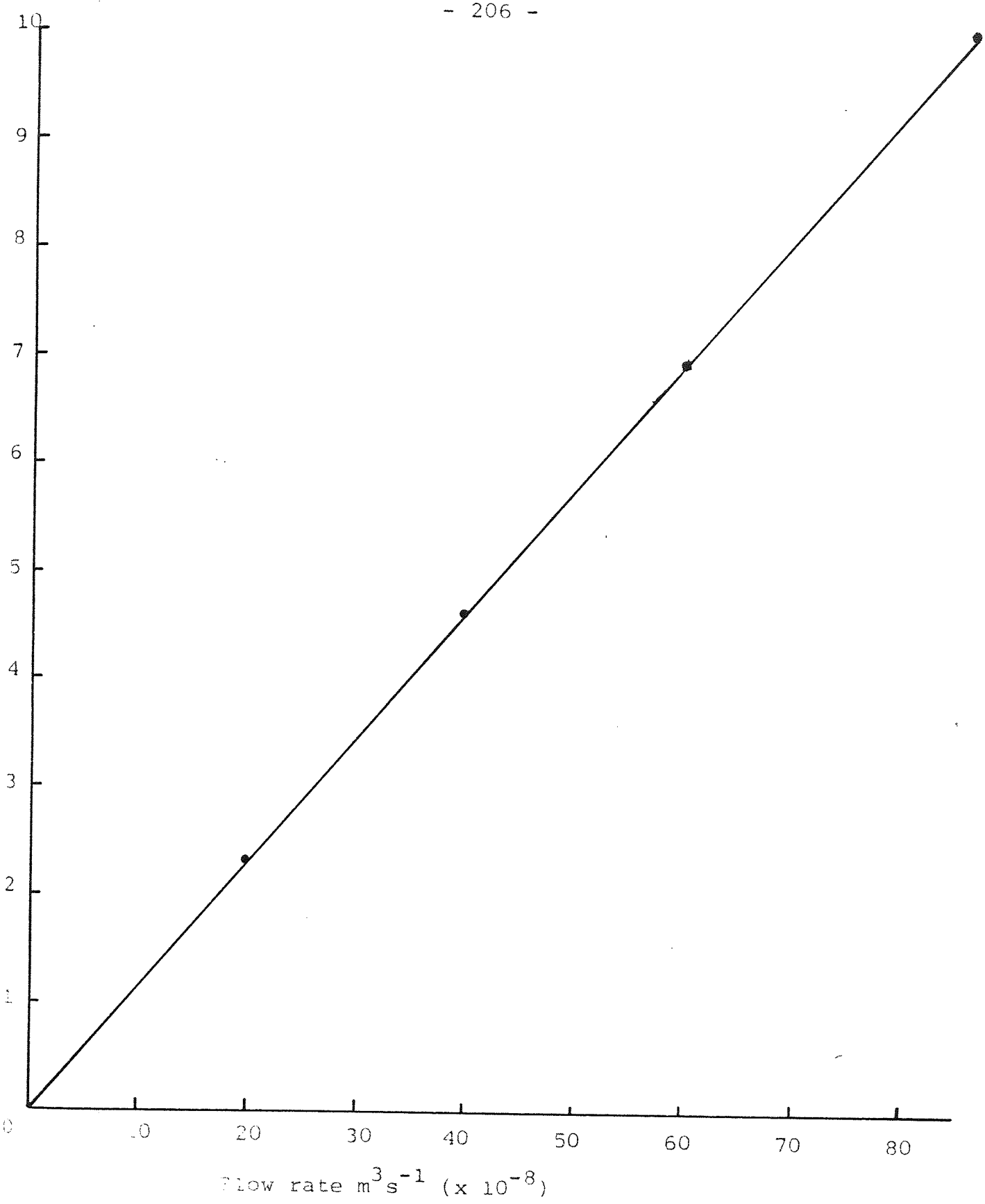

Figure D.5 Metering pump calibration
LONG STROKE MECHANISM
Water

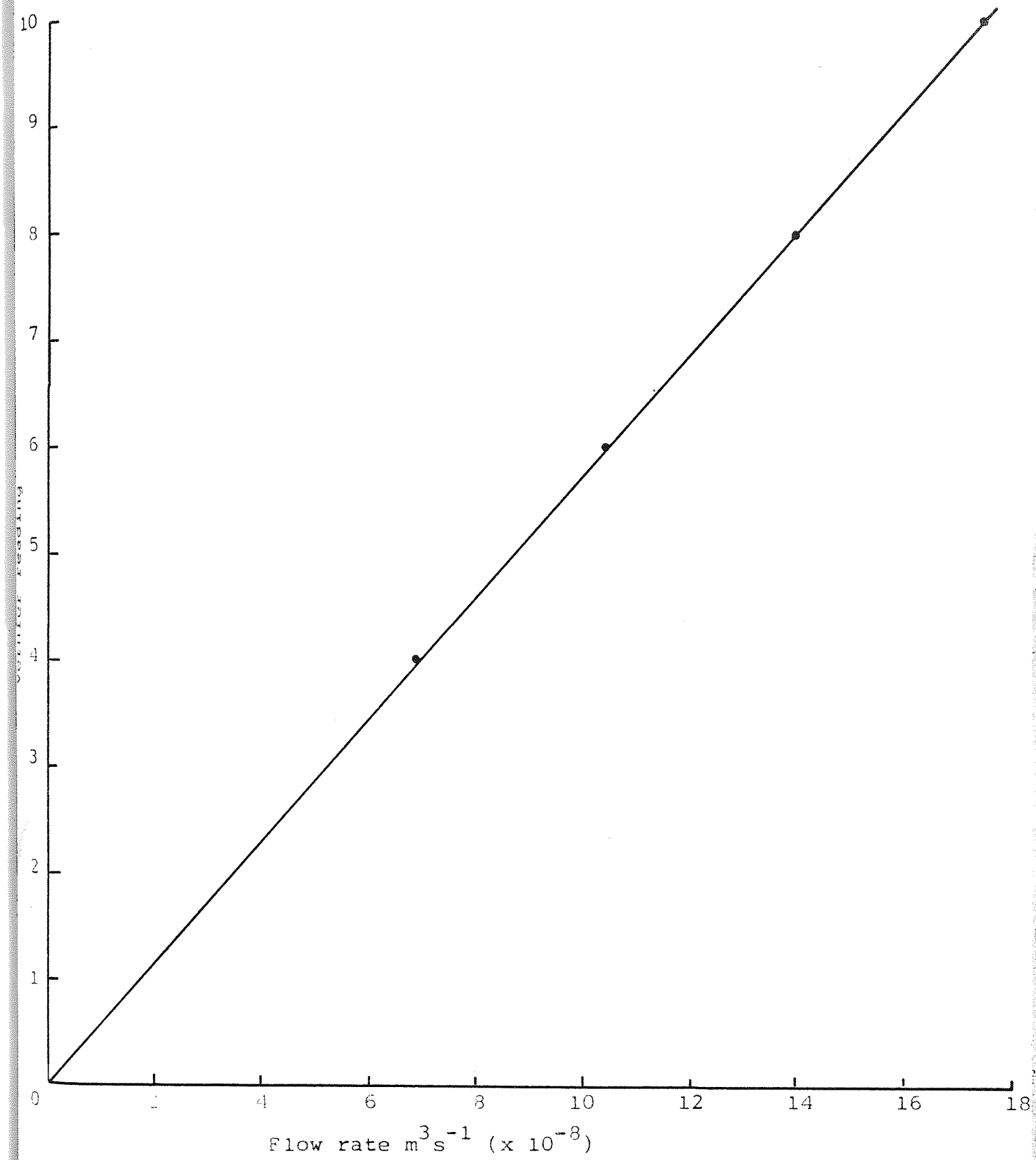

Figure D.6 Metering pump calibration

LONG STROKE MECHANISM + REDUCTION UNIT 5/1

Water

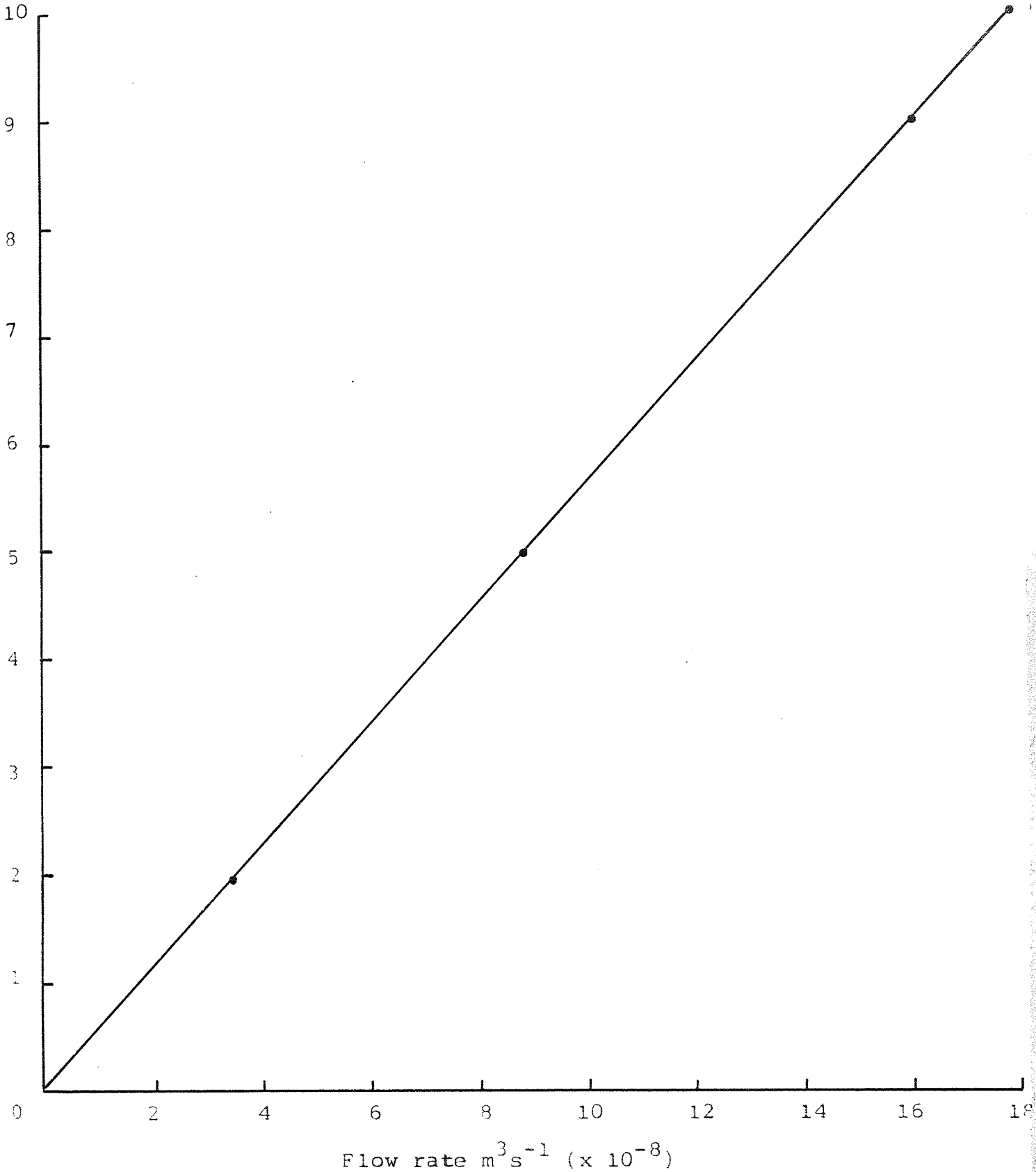

Figure D.7 Metering pump calibration

LONG STROKE MECHANISM + REDUCTION UNIT 5/1

Toluene

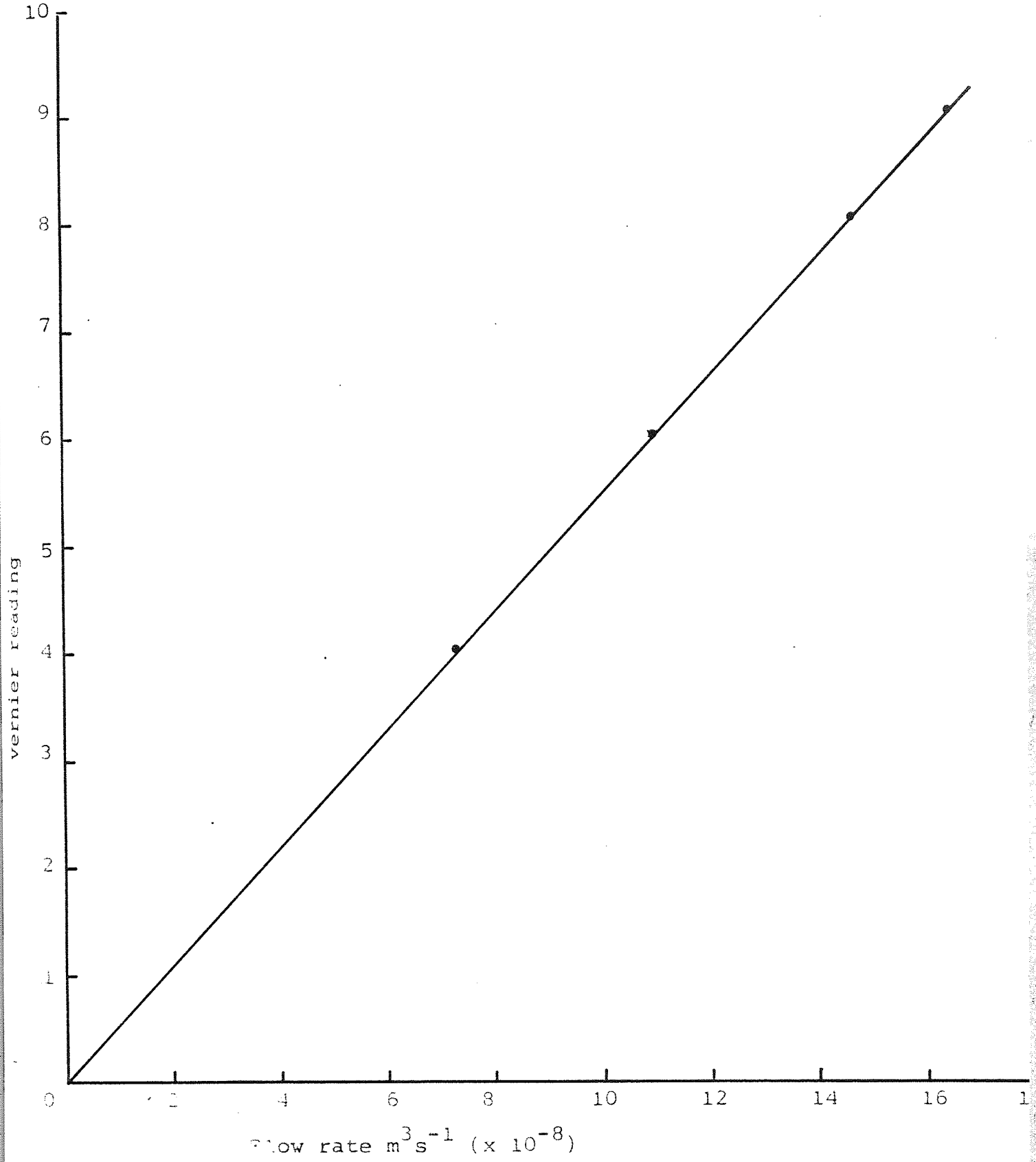

Figure D.8 Metering pump calibration

LONG STROKE MECHANISM + REDUCTION UNIT 5/1

Toluene

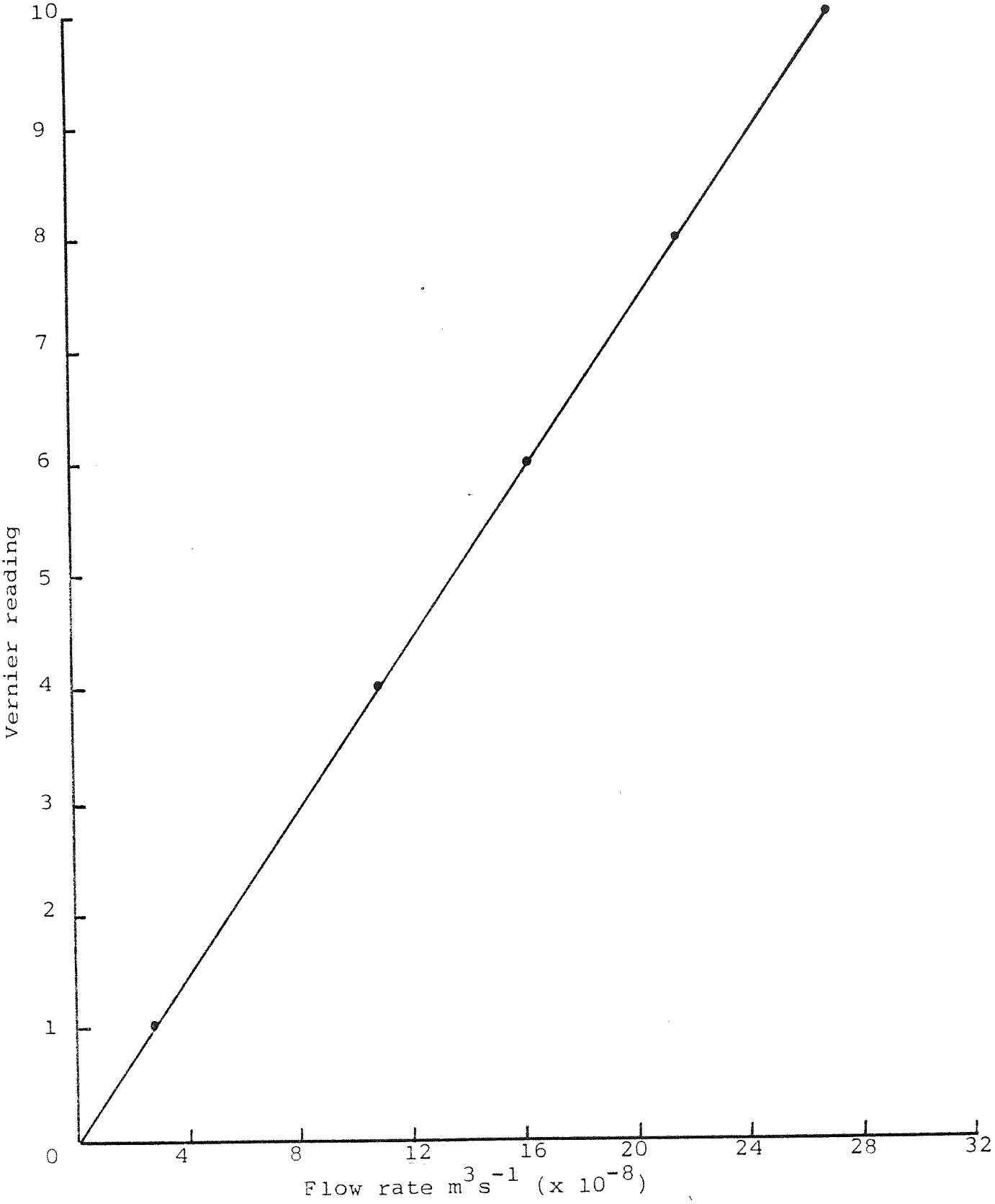

Figure D.9 Metering pump calibration

SHORT STROKE MECHANISM

Toluene

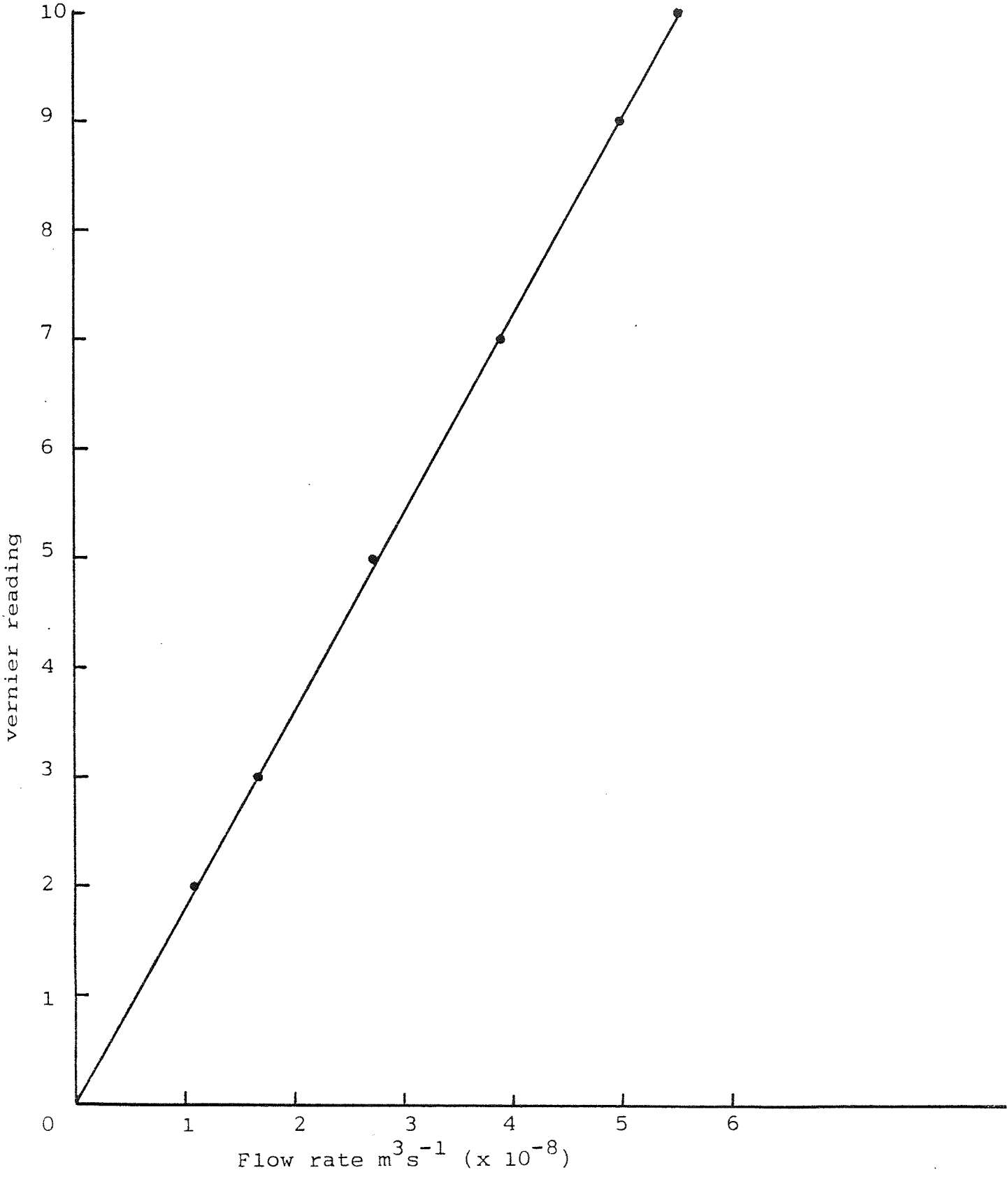

Figure D.10 Metering pump calibration

SHORT STROKE MECHANISM + REDUCTION UNIT 5/1

Toluene

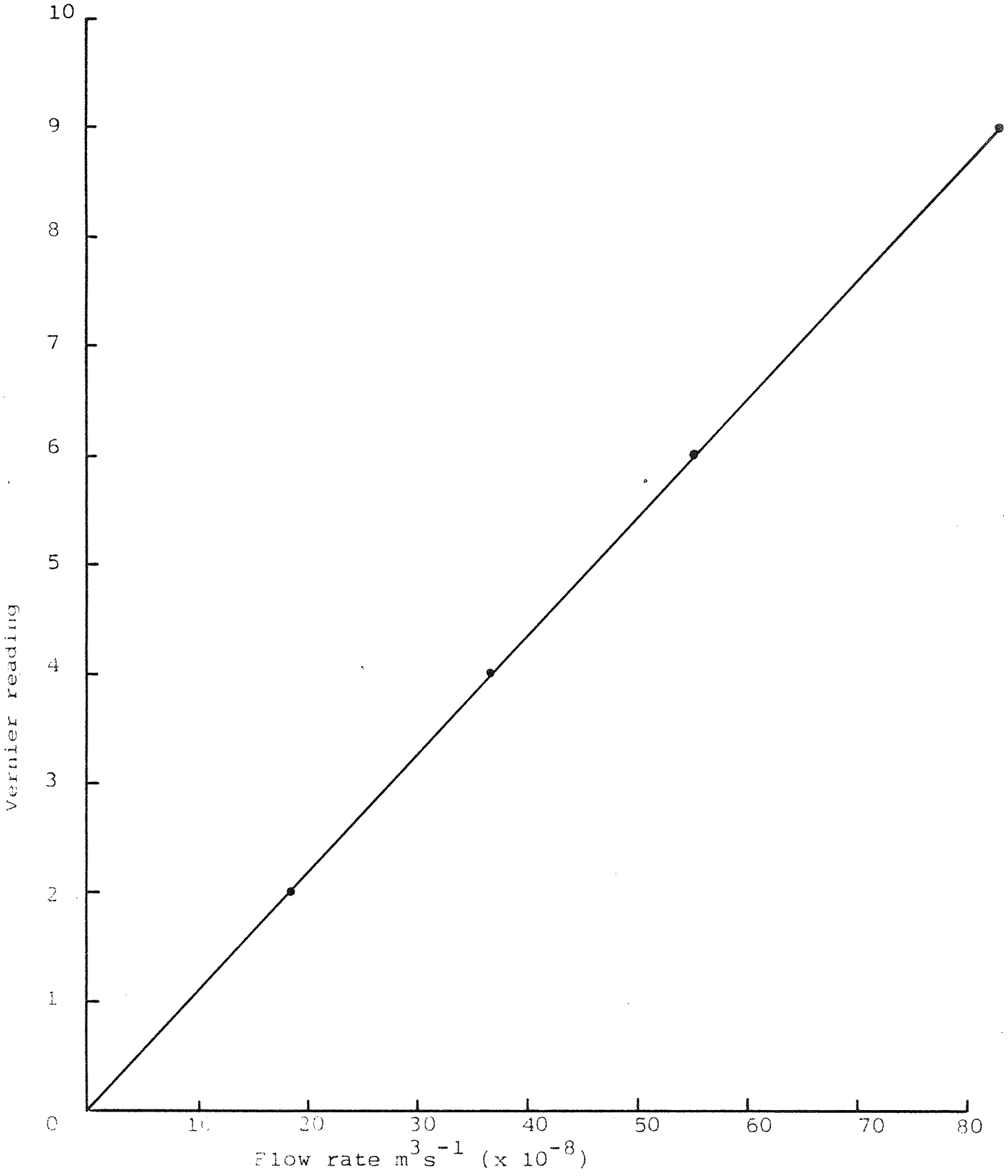

Figure D.11 Metering pump calibration

LONG STROKE MECHANISM

Octan-1-01

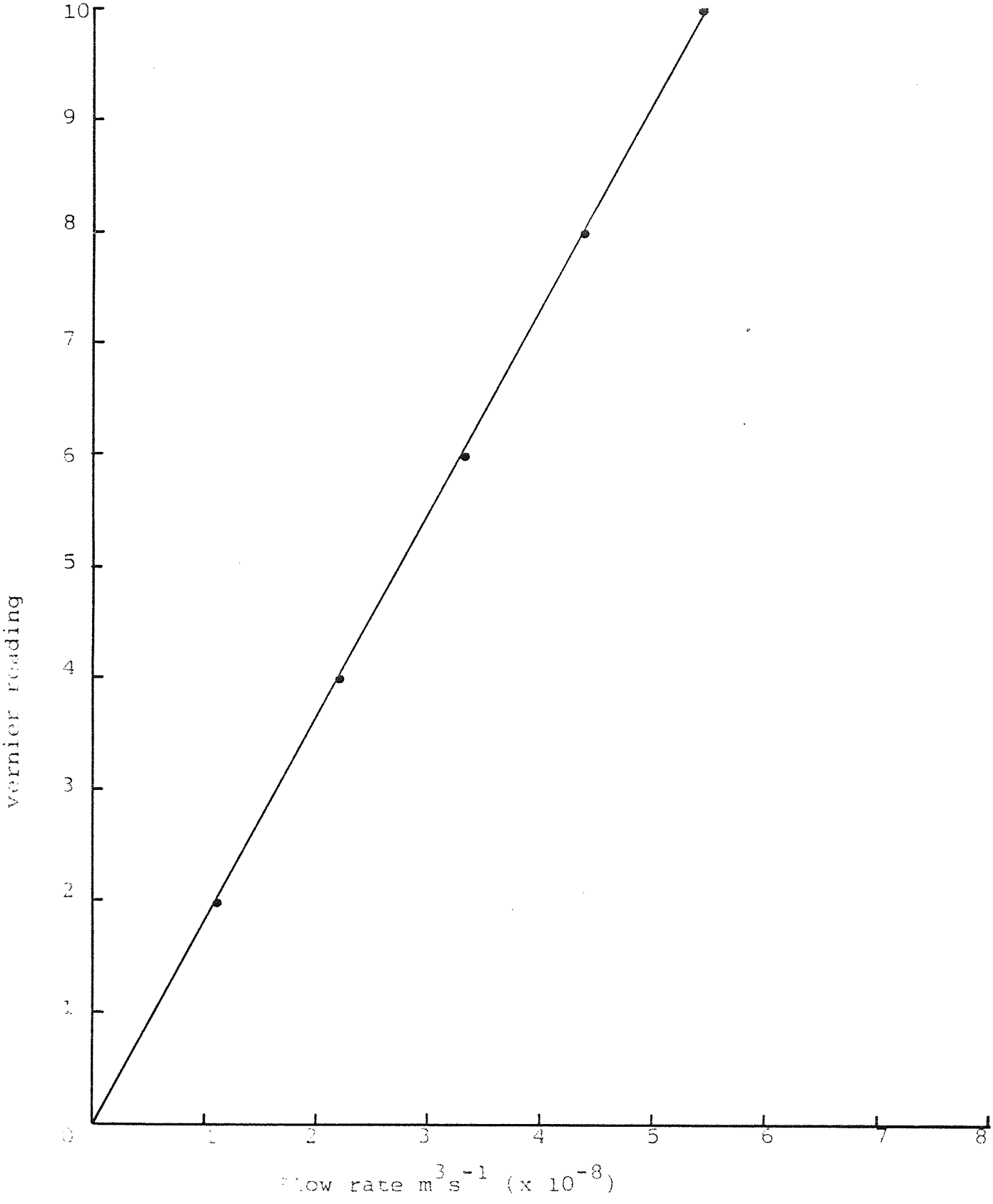

Figure D.12 Metering pump calibration

SHORT STROKE MECHANISM + REDUCTION UNIT 5/1

Octan-1-01

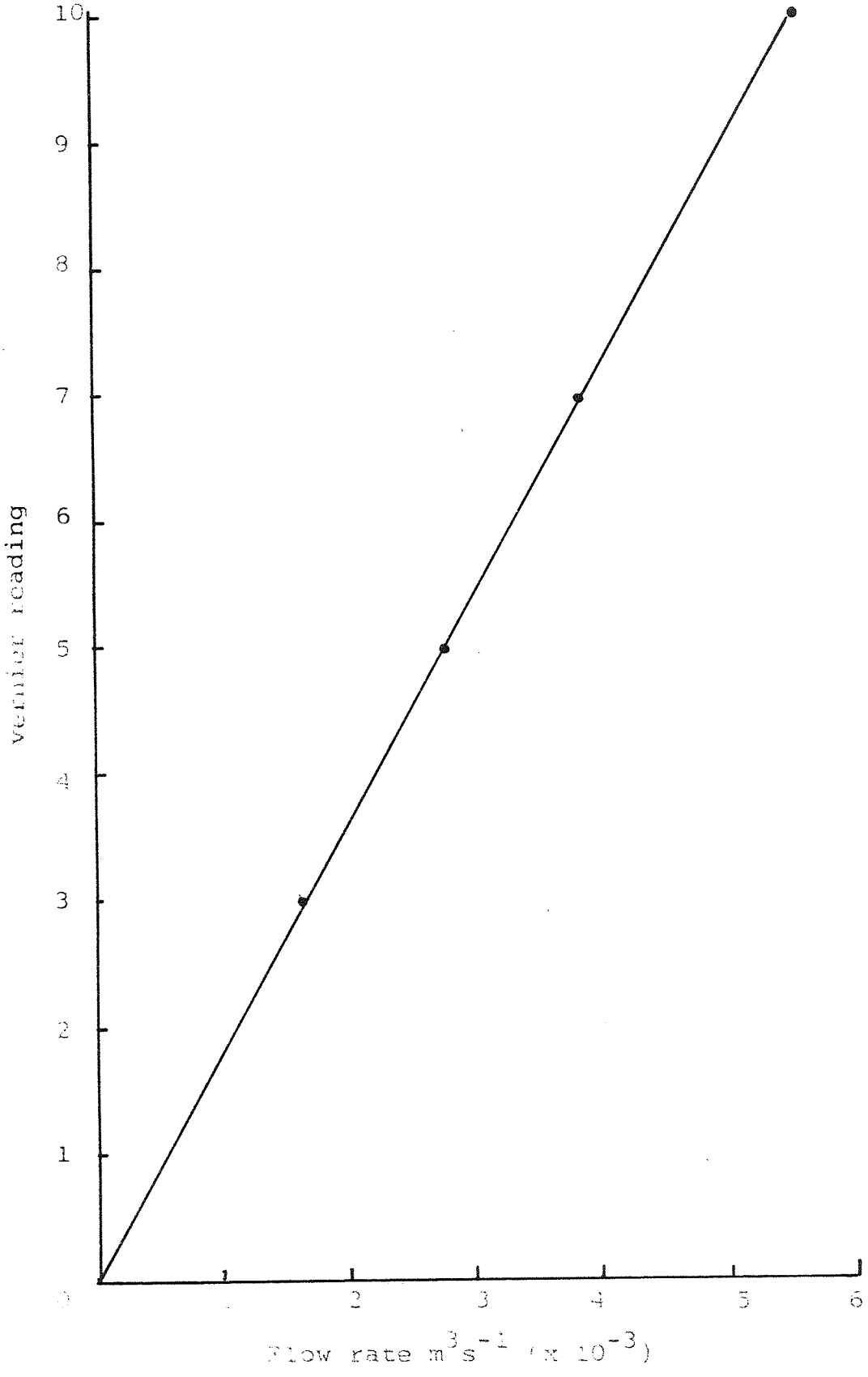

Figure D.13 Metering pump calibration

SHORT STROKE MECHANISM + REDUCTION UNIT 5/1

MIBK

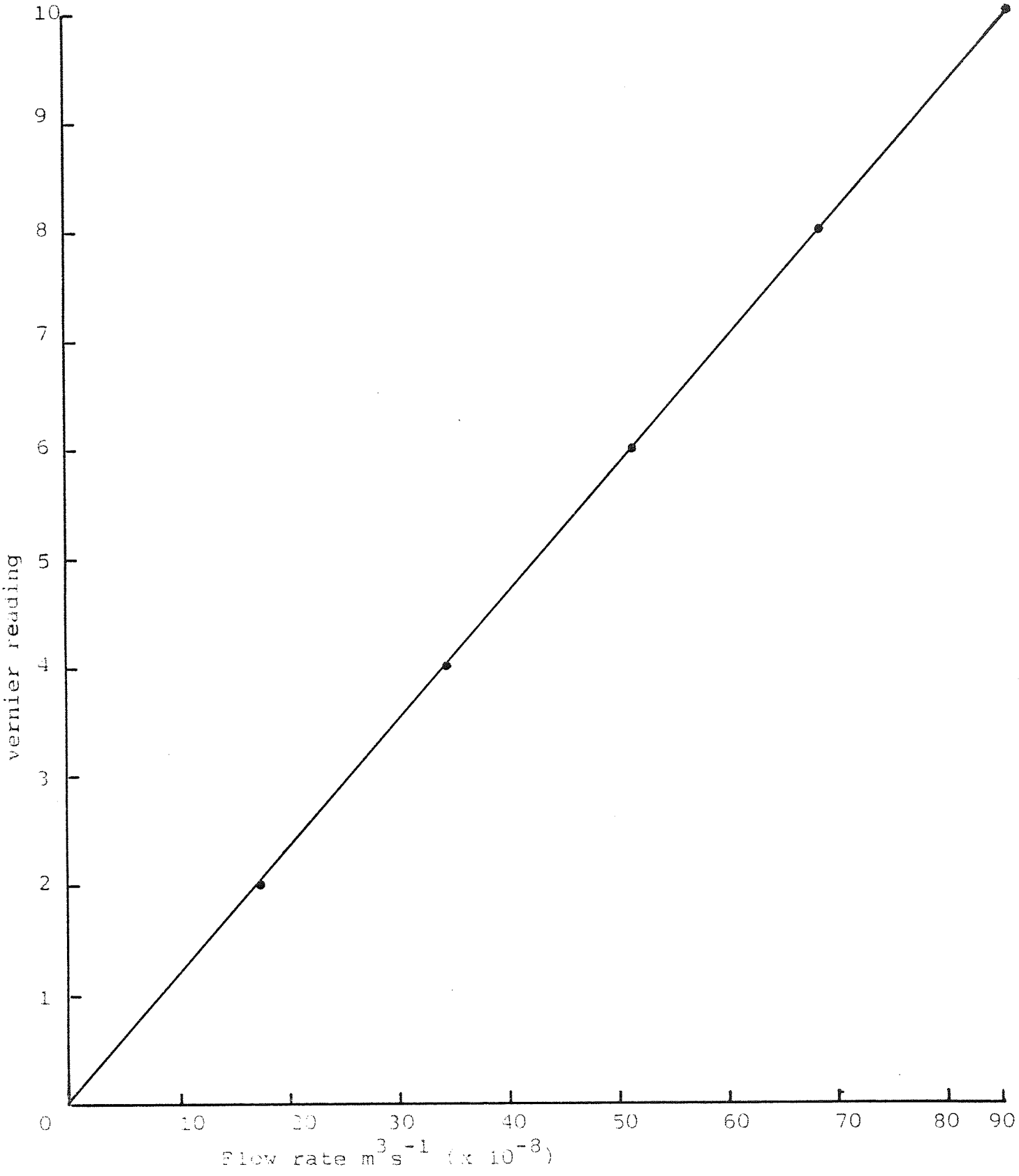

Figure D.14 Metering pump calibration

LONG STROKE MECHANISM

Potassium thocyanide + Formamide

APPENDIX E

Electronic arrangements and transducer specifications

APPENDIX E

ELECTRONIC ARRANGEMENTS AND TRANSDUCER SPECIFICATIONS

This oscillates at 4.34 MHZ close to resonance frequency of ultrasonic transducer. The out put is taken to the transducer which excites and causes the transducer to resonate at its natural frequency. The same waveform is applied to a Monostable Multivibrator which produces a fast pulse (30 n/s) from the symmetrical oscillator waveform and is fed to the set input of the latch.

E.2. TRANSDUCER RECEIVER

This high gain 3 stage receiver amplifies the out put from the receiver transducer to a signal level which is a T.T.L + 5V level (Transistor Transistor Logic) and is fed to Monostable identical to that of the oscillator which provides a fast pulse 30 n/s wide to a latch re-set imput.

E.3. LATCH

Variations in phase between the transducer and receiver transducer signal provides a proportional change in the resultant frequency from the latch out put.

E.4. ANALOGUE SWITCH

Out put from latch is applied to the analogue switch which

provides a proportional analogue voltage (0-3.6V) corresponding to the frequency of the applied imput signal.

E.5. DIGITAL PANEL METER

Contains a high impedance imput amplifier which is connected to the analog switch output to provide the level required to drive the digital panel meter display. Hold facility was also provided.

E.6. MANUFACTURERS SPECIFICATIONS FOR TRANSDUCERS (158)

TRANSDUCERS	DESCRIPTION	DIMENSIONS
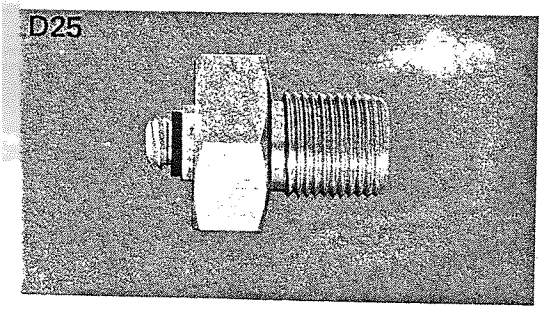	The flush-mounting transducer is the economy model for various measurements of dynamic pressure and acoustic phenomena. The low cost makes it ideal for expendable applications or simple triggering of photographic and recording apparatus. The LD-25 has been used in shock tunnels for high pressure transient to low pressure applications including underwater acoustics and flow measurements. The LD-25 is supplied uncalibrated for those utility requirements at a budget price.	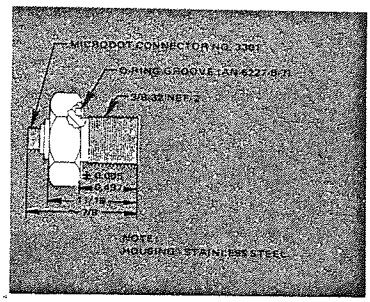

NOMINAL SPECIFICATIONS

Sensitivity: 0.15 V/psi
Sensitivity: -113 dB
Charge Sensitivity: 35pC/psi
Capacitance: 240pF
Maximum Pressure: 3,000 psi
Rise Time Face-On: 1 μ sec.
Polarity with Positive Pressure: Positive
D.C. Resistance (min): 500 MΩ
Operating Temperature Range: -40 to +200°F
Sensing Element: Lead zirconate titanate
Total Weight (max): 0.6 oz

NOMENCLATURE

Symbols have the following meanings except where specifically indicated in the text.

A = Ratio of viscous to surface tension forces (dimensionless)

b = Radius of undeformed drop (cm)

c_1 = Stabilizer concentration

d = Drop diameter (cm)

d_c = Diameter of critical packing size (cm)

d_f = Fibre diameter (cm)

d_{fe} = Effective fibre diameter which includes the influence of the retained drop (cm)

d_n = Nozzle diameter (cm)

d_{vs} = Sauter mean drop diameter at finite flow rate (cm)

d^o_{vs} = Sauter mean drop diameter at substantially zero flow rate (cm)

d_{10} = Average inlet drop size (cm)

E = Packing voidage (dimensionless)

E_s = Efficiency of collection by a single isolated fibre from a fluid stream of a width equal to the fibre diameter

F = Harkins - Brown factor (residual after drop detachment)

g = Acceleration due to gravity (cms^{-1})

G = Shear rate (s^{-1})

h = Height of packed section (cm)

h_1 = Film thickness before drainage commences (cm)

h_2 = Film thickness at rupture (cm)

k = Elastic modulus

K' = Constant dependent upon packing material

L = Fibrous bed thickness (cm)

n_i = Number of drops of diameter d_i

ΔP = Pressure drop (gcm^{-2})

R = Interception parameter d/d_f

R_e = Reynolds number $\rho V' d_f / u$

S = Average degree of saturation (dimensionless)

t = Coalescence time (s)

t_m = Mean coalescence time (s)

$t_{\frac{1}{2}}$ = Half life rest time (s)

T = System temperature (^oC)

u = Settling velocity (cms^{-1})

V = Superficial velocity (cms^{-1})

V' = Dispersion superficial velocity (cms^{-1})

$\bar{v}_o$ = Velocity of the dispersed phase relative to the continuous phase at substantially zero flow rate (cms^{-1})

V'_{cr} = Critical separating velocity. The velocity at which the filter coefficient begins to decrease (cms^{-1})

v = Linear efflux velocity (cms^{-1})

X = Fractional hold-up of dispersed phase (dimensionless) defined by equation 4.2.2.

Y = The ratio of outlet to inlet drop densities

GREEK LETTERS

α = Ratio of total number of particles striking a fibre to the total number approaching it

β = Fraction of collisions between drops that resulted in coalescence

γ = Interfacial tension ($dyncm^{-1}$)

λ_c = Filter coefficient (cm^{-1})

δ = Viscosity ratio (dimensionless)

ρ = Density (gcm^{-3})

$\Delta\rho$ = Density difference between the two phases (gcm^{-3})

η_c = Overall coefficient efficiency (dimensionless)

μ = Viscosity ($gcm^{-1}s^{-1}$)

μ_1 = Viscosity of dispersed phase ($gcm^{-1}s^{-1}$)

σ = Contact angle

ϕ_H = Dispersed phase hold-up in a fibrous bed

SUBSCRIPTS

c = Continuous phase

d = Dispersed phase

1 = Single phase flow

2 = Two phase flow

REFERENCES

1. Richardson, E.G.J. Colloid Sci. 5, 404 (1950).
2. Richardson, E.G., in Hermans, J.J. (ed.) Flow properties of disperse systems, "pp.42-46" New York, interscience publishers, 1953.
3. Taylor, G.I., Proc. Roy. Soc. (London) A138, 41 (1931) A146, 501 (1934).
4. Rumscheidt, F.D. and Mason, S.G., J.Colloid Sci. 16, 238 (1961).
5. Wood, R.W. and Loomis, A.L., Phil. Mag. (7) 4, 4, 417 (1927).
6. Roth, W., J. Soc. Cosmetic Chemists 7, 565 (1956).
7. Morrell, J.C. and Egloff, G., in Alexander, J. (ed), "colloid chemistry" III, P. 505, New York, Reinhold Publishing Corp., 1931.
8. Cordwell, F.G., U.S. pat. 987, 115, March 21, 1911.
9. Bonnet, C.F. (to American Cyanamid Co.), U.S. pat. 2, 260, 798, 609, Oct. (1940).
10. Bonnet, C.F. (to American Cyanamid Co.), U.S. pat. 2, 301, 609, November 1942.
11. Tranoski, P.T. and Uhlmann, E.H. U.S. pat. 2, 269, 134, Jan. 6, 1942.
12. Stagner, B.A., U.S. pat. 2, 284, 106, May 26, 1942.
13. Hanson G.B. (to Petrolite Corp. Ltd.,) U.S. pat. 2, 325, 850, Aug. 3, 1943.
14. Goodloe, P. M. and Berger, H.G. (to Socony - Vacuum Oil Co.) U.S. pat. 2,317,050 April 20, 1943; U.S. pat. 2,355,778, Aug. 15, 1944.
15. De Groote, M., Keiser, B., and Blair, C.M., Jr. (to Petrolite Corp. Ltd.,), U.S. pat. 2,216,312 Oct. 1, 1940.
16. De Groote, M. and Keiser, B. (to Petrolite Corp. Ltd.,), U.S. pat. 2,241,011, May 6, 1941.
17. Shashkin, P.I., Vostochnaya Neft 1940, No.5-6,59.

18. Magaril, R.Z., Novosti Neft. i Gaz. Tekhn., Neftepereabotka i Naftekhim. 1961, No.6,16, C.A. 58, 286b.

19. Small, A.D., U.S. pat. 2,420,687, May 20, 1947.

20. Passler, W. Oel V. Kohle 37, 194 (1941).

21. Monson, L.T. and Stenzel, R.W. in Alexander, J. (ed) "Colloid Chemistry", VI, p. 538, New York, Reinhold Publishing Corp., 1946.

22. Truter E.V., "Woolwax" p. 117-131, New York, Interscience Publishers, inc, 1956.

23. Bell, J.M. ED Proceedings of the 30th industrial waste conference. 1977 ISBN pp 611 ART BY JN CHIEU ANN ARBOR SCIENCE.

24. Jeffreys G.V. and Lawson, G.B.- Trans. Inst. Chem.Eng. -43- T294 - (1965).

25. Jeffreys G.V. and Davies, G.A. - Recent Advances in Liquid-Liquid Extraction. Edited by C. Hanson, Pergamon Press - Oxford, N.Y. etc (1971).

26. Davies, G.A. and Jeffreys, G.V. - Filt. and Sep. Sept/Oct. 546 - (1970).

27. Gillespie, T and Rideal, E.K. - Trans. Far. Soc. 52 -137 (1956).

28. Jeffreys, G.V. and Hawksley, J.L. - J. Appl. Chem. - 12 - 329 1962.

29. Hodgson, T.D.- Ph.D. Thesis - Univ. College of Wales (1966).

30. Hodgson, T.D., and Lee, J.C. J. of Coll. Sci., and interface science 30, 94 (1969).

31. Hitit, A., Ph.D. Thesis Univ. of Aston (1972).

32. Cockbain, E.G. and McRoberts, T.S. - J. Coll. Sci. 8-440 1953.

33. Elton, G.A. and Picknett, R. G. Proceeding of the 2nd International Congress on Surface Activity - Vol.1 288 - Butterworths - London (1957).

34. Charles, G.E. and Mason, S.G. J. Coll. Sci. 15, 105, 236 (1960).

35. Lawson, G.B. - Ph.D. Thesis - University of Manchester (1967).

36. Scheele, G.F., Leng, D.E., Chem.Eng.Sci., 26 1867 (1971).

37. Robinson, J., and Hartland, S., I.S.E.C. Paper No.56 (1971).

38. Malejicek, A., Sivokova, M., and Eichler, J., Collection Czech Chem. Commun. 36 35 (1971).

39. Kintner, R.C., Advance in Chem. Eng. 4 87 (1968). Academic Press, New York and London.

40. MacKay, G.D.M., and Mason, S.G., Cand. J. Chem. Eng. 41 203 (1963).

41. McAvoy, R.M. and Kintner, R.C., J. Colloid Sci., 20 188, (1965).

42. Charles, G.E. and Mason, S.G., J. Colloid Sci. 15 236 (1960).

43. Princen, H.M., J. Colloid Sci., 18 178 (1963).

44. Murdoch, P.G. and Leng, D.E., Chem. Eng. Sci. 24 1881 (1971).

45. Schwartz, A.M., Ind. Eng. Chem. 61 No.1 10 (1967).

46. Osipow, L.T., "Surface Chemistry" Reinhold Publishing Corporation (1952).

47. Young, T.H., Phil. Trans. 65 84 (1805).

48. Harkins, W.D., "The Physical Chemistry of Surface Films", Reinhold Publishing Corp., (1952).

49. Davies, G.A. and Jeffreys, G.V., Filtration and Separation, July/Aug. (1969).

50. Davies, G. A., Jeffreys G.V., Pryce Bayley D., British pa. No.1 409,045.

51. Al-Saadi A.N. M.Sc. Thesis University of Aston in Birmingham (1976).

52. Lewis, J.B., Jones, I., and Pratt, H.R.C., Trans.Instn. Chem. Engrs. 29, 136 (1951).

53. Dell F.R., and Pratt, H.R.C., Trans. Instn. Chem. Engrs. 29, 270 (1951).

54. Gayler R., Pratt, H.R.C., Trans Instn. Chem. Engrs. 31, 69, (1953).

55. Ramshaw, C. and Thornton, J.D. - Inst. Chem. Eng. Symp. Series No.26 - 80 - (1967).

56. Ramshaw, C. and Thornton, J.D. Ibid No.26 - 73 - (1967).

57. Thomas, R.J. and Mumford, C.J. - I.S.E.C. - Hague-Vol.1 400 - (1971).

58. Wilkinson, D. Mumford, C.J. and Jeffreys G.V., AICHE Journal Vol.21, No.5, page 910 Sep., (1975).

59. Perry, J.H., Chemical Engineering Handbook, 4th edn., New York; McGraw-Hill.

60. Scheibel, E.G., Chem. Eng. Prog. 44 681 (1948).

61. Honeykamp, J.R., and Burkhart, L.E., Ind.Eng.Chem. Proc. Des. Dev.1, 177 (1962).

62. Piper, H., M.Sc. Thesis, Univ. Manchester Inst. Science and Techol., (1965).

63. Slatter, M.A., M.Sc. Thesis, Univ. of Aston, (1968).

64. Juma, S.M., M.Sc. Thesis, Univ. Manchester Inst. Science and Technol., (1969).

65. Meister, B.J., and Scheele, G.F., A.I.Ch.E. J1, 1969, 14,15.

66. Wenzel, R.N. - J. Phys. Chem. - 53 - 1466 - (1949).

67. Elliott, C.E.P. and Riddiford, A.C., J. Coll. and Interface Sci., 23, 389 (1967).

68. Jeffreys, G.V. and Hawksley, J.L. - A.I.Ch.E.J. - 11, 413, (1965).

69. Neilson, L.E., Wall, R. and Adams, G. - J. Coll. Sci. 13, 441, (1958).

70. Smith, D.V. - M.Sc. Thesis, University of Manchester, (1966).

71. Lang, S.B. - Ph.D. Thesis - University of California, (1962).

72. Lang, S.B. and Wilke, G.R. - Ind. Eng. Chem. Fund., 10, 329, (1971).

73. Smith, D.V. - Ph.D. Thesis, University of Manchester, (1969).

74. Allan, R.S. and Mason, S.G. - Trans. Far. Soc.- 57, 2027, (1961).

75. Brown, A.H. and Hanson, C. - Trans. Far. Soc.- 61, 1754, (1965).

76. Hartland, S. - Trans. Inst. Chem. Eng., 46, T275, (1968).

77. MacCay, G.D.M. and Mason, S.G. - J.Coll. Sci. 18, 674, (1963).

78. Groothius, H. and Zwiderweg, F.J. - Chem. Eng. Sci. 12, 288, (1960).

79. Watanabe, T. and Kusui, M. , Bull. Chem. Soc. Japan, 31, 236, (1958).

80. Voyulskii, S.S., Kal'yanova, K.A. Panick, R., and Doiman,N., Dokl. Akad. Nauk SSSR, 91, 1155 (1953), CA, 49, 12053d (1955).

81. Sareen, S.S., et.al., A.I.Ch.E.Jnl, 12,6, (1966), 1045.

82. Burtis, T.A. and Kirkbride, C.G.- Trans. AI.Ch.E. 42 (3) 413 - (1946).

83. Hazlett, R.N. - I.E.C. Fund - 8 (4) - 625 - (1969).

84. Langdon, W.M. et al - Petro/Chem. Engng. - Nov. 34, (1963).

85. Farley, R. and Valentin, F.H.H., - A.I.Ch.E. Symp. Ser. No.1 - 39 - (1965).

86. Bird ,R.B. Stewart, W.E. and Lightfoot,'Transport Phenomena' J. Wiley and Sons - New York - (1960).

87. Graham, R.J., M.S. Thesis, Univ. of California, Lawrence Radiation Lab., Berkeley , Calif.,(1962).

88. Sweeney, W.F.,'Some observations on liq.liq. settling', M.S. Thesis, Ibid (1964).

89. Langdon, W.M. et al - Environmental Sci. and Technology - 6 (10) - 905 (1972).

90. Euzen, J.P. et al - I.S.E.C. - Lyon, France - Sept. (1974) Session 5 - paper 130.

91. Shah, B. Langdon, W. and Wasan, D. Environmental Science and Technology Volume 11, No.2, February (1977), 167.

92. Bitten, J.F. et al - J. Coll. Int. Sci. 37 (2) - 372 - (1971).

93. Shalhoub, N.G. Ph.D. Thesis University of Aston in Birmingham, (1975).

94. Vinson, C.G. and Churchill, S.W. The Chem.Eng.J. - 1 - 110, (1970).

95. Spielman, L.A. - Ph.D. Thesis, Univ. of California, Berkeley California (1969).

96. Bartle, J.W. Filt. and Sep.- 3 (5) - 404 (1966).

97. Hazlett R.N. and Homer W. Carhart Filt. and Sep. 6 July/Aug (1972) P. 456.

98. Lindenhofen, H.E. Filt. and Sep. Sept/Oct. - 567 - (1969).

99. Chieu John-Man et al, Proceedings of the 30th industrial waste conference 1977 ISBM 0250401630 pp 611 Art by JN Chier Ann ARBX Science.

100. Spielman, L.A., Goren, S.L., Ind. Eng. Chem. Fundam., 11, (1), pp 73 - 83, (1972).

101. Langdon, W.M. et al, Environmental Science and Technology, 6, (10), pp 905 - 910 (1972).

102. Ghosh, M.M., Brown, W.P.Jl. Water pollution control federation 47, (8), pp 2101 - 2113 (1975).

103. Ravault, Frank E.G.; Edwards, Bryan William (Foseco Int. Ltd.,) Ger. 2, 452, 387 (Cl. BOID) May (1975).

104. Vinson, C.G. 'Doctoral Dissertation' University of Michigan, Ann Arbor, Mich., 1965.

105. Rose P.R. , M.Sc. Thesis - I.I.T. Chicago, (1963).

106. Beatty, H.A., "Jet fuel decontamination studies", Interim Tech. Report Not GR 66 - 30. U.S. Army Engineer Research and Development Labs., for Belvoir, Virginia, July (1966).

107. Wasan, D.T. and V. Mohan paper at 81st National Meeting AIChE, Kansas City, April, (1976).

108. Wasan, D.T. et al paper at 81st National Meeting AIChE, Houston, Texas, March, (1977).

109. Jaisinghani, R.A. Filtration and Separation July/August (1977) pp 367 - 370.

110. Beatty, H.A. and C. Walcutt, Tech. Report No. GR. 65-1, U.S. Army Engineer Research and Development Labs. Fort Belovir, Virginia, March (1965).

111. Osterman, J.W., Filt. and Sep. March/April - 127 (1966).

112. Lindenhofen, H.E. - Filt. and Sep. July/Aug. - 317 - (1968).

113. Curtis BG Filt. and Sep. 1964 p 35-37 Jan/Feb (1964).

114. Border, L.E. - Chem.Met.Eng. 47 - 776 -(1940).

115. Douglas, E. and Elliott, I.G. - Trans. Inst. Marine Eng. 74 (5) - 164 - (1962).

116. Douglas, E. Brit. Patent - 972, 286 - (1960).

117. Garrison, M. and Van Loenen, W.F. - U.S. Patent - 1,947,709 - (1934).

118. Fowkes, F.M., Anderson, F.W. and Berger, J.E. - Env. Sci. and Tech. 4 (6) - 510 - (1970).

119. Krueger, Dennis L. (Minnesota Mining and Mfg. Co.) U.S. 3, 951, 814, (C1.210- 488; BOID 25/16). 20 April 1976, Appl. 407, 965, 19 Oct. 1973, 9pp. continuation of U.S. 3, 847, 821.

120. Sherony, D.F. et al con. J. Chem. Eng. 49, 321, (1971).

121. Voyutskii, S.S. et al, IZV. Vyssk. Ucked Zaved. Khim. Technol. 2 - 1970 - (1958). CA - 52 - 19266a - (1958).

122. Langmuir, I. - OSRD Rept. 865 - Sept. (1942).

123. Foseco Int. Lt. Ger. 2, 452, 387 (C1. BOID), 07 May (1975) Chem. Abst. 134270K.

124. Jeffreys, G.V., Mumford, C.J., 'The potential use of Foseco Reticulated Ceramic and Alumina - Silicate Products as Coalescers', October (1973).

125. Polichronakis, M.Sc. Thesis, University of Aston in Birmingham (1972).

126. Austin, D.G., Unpublished work, University of Aston in Birmingham (1976).

127. Hayes, J.E., Hays, L.A., and Woods, K.S., Chem. Eng. Prog., 45, 4, 1949, 235.

128. Redman, O., Chem. Eng. Prog., 59, (1963), 87.

129. Rosenfeld, J.I. and Wasan, D.T. - Can. J. Chem. Eng. - 52, 3 - (1974).

130. Rosenfeld, J.I. - Ph.D. Thesis - I.I.T. - Chicago, (1973).

131. Spielman, L.A. and Goren, S.L. - Env. Sci. Tech. - 1 (2) 135 - (1970).

132. Bitten, J.F. - J. Coll. Int. Sci. - 33 (2) - 265 - (1970).

133. Wasan, D.T. et al - I.S.E.C. - Lyon - France - (1974).

134. Spielman, L.A. and Goren, S.L. - Int. Eng. Chem. Fund - 11 (1) 66 - (1972).

135. De Josselin De Jong, G. Trans Am. Geog. Physical Union 39, 1160 (1958).

136. Heller, J.P., Rev. Sci. Instrum. 30, 1056 (1959).

137. Klarsfeld, S. et al, Applied Optics 12, No.2, 198, (1973).

138. Handley, D., Ph.D. Thesis University of Leeds, (1957).

139. Hummel, R.L. et al, Chem. Eng. Sci., 22, p.21, (1967).

140. Vignes, A., Chim. Ind. Gen. Chimique, 95, p.307, (1968).

141. Vigliecca, L., Ph.D. Thesis, University of Nancy, (1961).

142. Davies et al, A.I.Ch.E. National Meeting, New Orleans, (1974).

143. Exelby, R. and Grnler, R., Chem. Rev. 65, 2, 247 (1965) Eng.

144. Hummel, R. L. et al, Ind. Eng. Chem. Fund. 8, 1, 160 (1969).

145. Zolotrofe D.L., and Scheele, G.E., Ind. Eng. Chem. 9 No.2 293 (1970).

146. Smith, T.N., Chem. Engng. Sci. pp.583, 29, (1974).

147. Sherony, D.F., M.Sc. Thesis. Ill. Inst. of Tech., Chicago, Ill. (1965).

148. Cordes, R.A. - Ph.D. Thesis - University of California - Berkely - (1972).

149. Kaye, G.W.C. and Laby, T.H. Tables of physical and chemical constants.

150. Sax N.I. Dangerous properties of industrial materials.

151. Berman, Fox, Thompson, J. Am.Chem.Soc., 81, 5605 - 8 (1959).

152. Scheele, Zolotrofe: Ind. Eng. Ehem. Fund. 9, 2, 291-3 (1970).

153. Allak, A. Ph.D. Thesis, Chem. Eng. Aston University (1973).

154. Sherony, D.F. Ph.D. Thesis - I.I.T. Chicago- (1969).

155. Gudsen, R.C. M.Sc. Thesis - I.I.T. - Chicago - (1964).

156. Chiu, K.F. - Chem. Eng. Report - University of Aston in Birmingham (1975).

157. Coulter Electronics, Ltd., - Coulter Counter Model ZB- Instruction Manual - (1975) - Coulter Electronics Ltd., Dunstable, England.

158. Celesco Transducer Products, Inc., Division of Transducer Controls Corporation, 7800 Deering Ave., Canoga Park, California 91304.